A model for the regulation of lipopolysaccharide synthesis during outer membrane biogenesis in *Escherichia coli*

Akintunde Emiola

A thesis submitted in partial fulfilment of the requirements of the University of East London for a degree of Doctor of Philosophy

October 2015

ABSTRACT

The role of systems biology in the interpretation and analysis of important biological events is gaining rapid acceptance in a number of biological fields. Here a computational systems approach was applied to investigate the production and regulation of *Escherichia coli*'s (*E. coli*) outer membrane. The outer membrane comprises of phospholipids in the inner leaflet, and lipopolysaccharides (LPS) in the outer leaflet. LPS is an endotoxin that elicits a strong immune response from humans and its biosynthesis is in part, regulated via degradation of LpxC and WaaA enzymes by the protease FtsH. Despite a substantial amount of research conducted on LPS synthesis, there is remarkably little information on its regulation.

The model of the outer membrane synthesis was completed in two phases; firstly a model of lipid A (representing the LPS pathway) was constructed followed by an integrated pathway model which incorporated fatty acids biosynthesis pathway (representing phospholipid production). The parameters used to construct the model were derived from published datasets where available, and estimated when necessary prior to model fitting. Model validation was carried out using a combination of published datasets alongside subsequent experimental data from this research.

Model findings suggested that the FtsH-mediated LpxC degradation signal arises from levels of lipid A disaccharide, the substrate for LpxK. This was subsequently validated experimentally using an *lpxK* overexpression system. Analysis of the integrated model further refined this mechanism indicating the catalytic activity of LpxK appears to be dependent on the concentration of unsaturated fatty acids. This is biologically important because it assists in maintaining LPS/phospholipids homeostasis.

Further crosstalk between the fatty acids and lipid A biosynthetic pathways was revealed by experimental observations that LpxC is additionally regulated by an

unidentified protease whose activity is independent of lipid A disaccharide concentration, but could be induced *in vitro* by palmitic acid. The biological relevance of this acute mechanism is not obvious; however, experiments aimed at causing abrupt damage to the cell wall or membrane (by antimicrobials) suggest that under conditions which directly damage membrane structure, LPS regulation via this unidentified protease may be crucial.

Computational analysis into the regulation of WaaA suggested that its proteolytic regulation does not affect the LPS synthetic rate. Subsequent experimental analysis provided evidence that WaaA regulation is aimed at controlling the quality of LPS synthesized by preventing glycosylation of undesirable lipid acceptors. Overexpression of *waaA* resulted in increased levels of 3-deoxy-D-*manno*-oct-2-ulosonic acid (Kdo) sugar whereas, levels of heptose were not elevated in comparison to non-overexpressed cells. This implies that an uncontrolled production of WaaA does not increase LPS level but rather re-glycosylates lipid A precursors. This is the first time experimental data has been produced attempting to explain the regulation of WaaA.

Computation of flux coefficient indicates that LpxC is the rate-limiting step when pathway regulation is ignored, but LpxK becomes the limiting step if feedback regulation is included as it is *in vivo*. Thus, in contrast to LpxC, LpxK may represent a more appropriate target for novel drug development. Overall, the findings of this work provide novel insights into the complex biogenesis of the *E. coli* outer membrane.

DECLARATION

This thesis is a presentation of my original research work. Wherever contributions of others are involved, every effort is made to indicate this clearly, with due reference to the literature.

Akintunde Emiola

ACKNOWLEDGMENTS

First and foremost, I would like to appreciate Dr John George for his time-commitment, guidance and mentorship throughout the duration of my PhD. At the peak of my study, John made himself easily accessible even during weekends and public holidays. I couldn't have wished for a better director of study. Thanks for being a wonderful supervisor and a friend. My sincere gratitude also goes to Dr Joanne Tocher for her constant advice and immense support. Joanne always ensured that I had a conducive environment for optimal productivity. I also appreciate the contributions of Dr Paolo Falcarin on the computational aspects of my research.

I am very grateful to Dr Steven Andrews for his objective critiques, regular assistance and mentorship. I also appreciate Professor Franz Narberhaus for providing some of the materials utilized in this research. To all the bioscience academic and technical staff at UEL, I say thanks for all the support.

I will be eternally grateful to my parents Professor and Mrs A. Emiola for their undying love, sacrifices, and invaluable advice. A big thanks to all my siblings especially William for his love and care. Thank you Efe for all the moral support. And to Kolo, thanks for the sacrifices.

TABLE OF CONTENTS

LIST OF TABLES

LIST OF FIGURES

ABBREVIATIONS

°C	degree Celcius
α-L-Ara4N	4-amino-4-deoxy-α-$_{L}$-arabinose
µg	microgram
µl	microlitre
µM	micromolar
µmol	micromole
(p)ppGpp	guanosine pentaphosphate
A5P	arabinose-5-phosphate
ACP	acyl carrier protein
acyl-ACP	acyl-acyl carrier protein
ADP	adenosine diphosphate
AP	alkaline phosphatase
ATP	adenosine triphosphate
BSA	Bovine Serum Albumin
C14:0	myristic acid
C15:0	pentadecanoic acid
C16:0	palmitic acid
C16:1	palmitoleic acid

C18:0	stearic acid
C18:1	*cis*-vaccenic acid
CAMP	cationic antimicrobial peptides
CDP	cytidine diphosphate
CL	cardiolipin
CMP	cytidine monophosphate
CoA	Coenzyme A
core OS	core oligosaccharide
cyto	cytoplasm
DMSO	dimethyl sulfoxide
DNA	deoxyribonucleic acid
E. coli	*Escherichia coli*
EDTA	ethylenediaminetetraacetic acid
EI	electron ionization
eq.	equation
Fig.	Figure
g	gram
G3P	glycerol-3-phosphate
GCMS	gas chromatography-mass spectrometry

GFP	green fluorescent protein
h	hour
HGP	Human Genome Project
IM	inner membrane
IPTG	isopropyl β-D-1-thiogalactopyranoside
KAS	ketoacyl-ACP synthases
k_{cat}	turnover rate
K_d	dissociation constant
kDa	kilodalton
Kdo	3-deoxy-D-*manno*-oct-2-ulosonic acid
K_i	inhibition constant
K_m	Michaelis-Menten constant
L	litre
LB	Luria-Bertani
LPS	lipopolysaccharide
MCA	Metabolic Control Analysis
mg	milligram
MIC	minimum inhibitory concentration
min	minute

ml	millilitre
mM	millimolar
mRNA	messenger ribonucleic acid
MW	molecular weight
NADPH	Nicotinamide Adenine Dinucleotide Phosphate
nM	nanomolar
OD	optical density
ODE	ordinary differential equation
OM	outer membrane
PAGE	polyacrylamide gel electrophoresis
PBS	phosphate buffered saline
PE	phosphatidylethanolamine
PEG	polyethylene glycol
PG	phosphatidylglycerol
P_i	phosphate ion
PMSF	phenylmethanesulfonylfluoride
PVDF	polyvinylidene fluoride
rpm	revolutions per minute
s	second
SBML	Systems Biology Markup Language

SDS	sodium dodecyl sulphate
SFA	saturated fatty acid
SOB	Super Optimal Broth
TE	Tris-EDTA
TLR4	Toll-like receptor protein 4
ts	temperature-sensitive
TSS	Transformation Storage Solution
UDP	uridine diphosphate
UDP-GlcNAc	UDP-N-acetylglucosamine
UFA	unsaturated fatty acid
UMP	uridine monophosphate
v/v	volume/volume
V_{max}	maximum rate of reaction
WT	wild-type
x *g*	relative centrifugal force
XML	Extensible Markup Language

Chapter 1

Introduction

In 1976, the first complete genome sequence of an organism was published which in essence, opened up a new era for the biological sciences (Fiers *et al*, 1976). For the first time in human history, scientists could observe and analyse the complete nucleotide sequence of an organism and from this, determine and annotate the various genes which are present. These genome sets, of course, represent the blueprints which are responsible for producing a living organism. However, this data on its own is incapable of predicting or simulating an organism's behaviour. A major challenge of this century is to understand how the products of these genomes interact and form sophisticated biochemical networks which in turn produce a living organism. To accomplish this, much more data is required; in particular, precise information relating to each gene product. Most of this functional information is acquired through classical methods including *in vitro* experiments, cell culture analysis, and animal model studies (van Riel, 2006). Fortunately, a substantial amount of this data is available particularly for the prokaryotes, of which *Escherichia coli* is the best studied. Therefore, where sufficient information exists, the gene products can be assembled into specific groups carrying out specific tasks such as glucose metabolism, lipids biosynthesis or DNA synthesis. This results in the construction of metabolic pathways and also enables organisms to be studied as a 'whole' entity. Such an approach is commonly regarded as the "systems biology approach" (Ideker *et al.*, 2001).

1.1 SYSTEMS BIOLOGY AND ITS APPLICATION

Despite the acknowledgment and rapid acceptance of its importance in current-day biological interpretations, there is still no universally accepted definition for the term "systems biology" (Chuang *et al.,* 2010)**.** This thus gives an insight into the complexity of this relatively new area of discipline.

The mode and manner in which systems biology is viewed, perceived or defined differs amongst systems biology practitioners. However, O'Malley and Dupre (2005) are of the opinion that current definitions lack a precise explanation as to what constitutes a '*system'*. Perhaps, until a clear and coherent definition of a '*system'* exists, the definition of "systems biology" will remain ambiguous. Nevertheless, all proposed definitions centre around a fundamental understanding of biological systems based on individual modular components (Likic *et al.,* 2010). The word '*system'* in the context of "systems biology" depends largely on the research problem at hand, objectives of the study, and the methodological choices employed in its analysis (Likic *et al.,* 2010).

During the late 20th century, biological studies were greatly influenced by the so called '*reductionist'* approach which generally involved the creation of information regarding individual cellular components, their chemical composition, and most times, their biological functions (Palsson, 2006). Over the past decade, this process has been rapidly enhanced by the advent of genomics, largely resulting from the completion of the Human Genome Project (HGP) (Lander *et al.,* 2001)**.** Furthermore, the emergence of 'omics technologies such as transcriptomics, proteomics, and metabolomics has also accelerated this process (Schena *et al.,* 1995; Oliver *et al.,* 1998; Fiehn, 2001; Patterson and Aebersold 2003)**.** All aforementioned processes lead to the generation of a large array of data which enables cells to be viewed as systems. This is important because as informative as individual modular components may be, they only provide basic information such as the molecular and chemical constituents that make up cells, and when cells decide to utilize these components (Palsson, 2006). It is now generally accepted amongst biologists that the integrative exploration of multiple gene functions is important in the understanding of actual cellular behaviour. For instance, p53, sometimes referred to as the 'guardian of the genome' (Kitano, 2002) is a human protein of 393 amino acids that function as a tumour suppressor due to its positioning

within a network of transcriptional factors. However, its functional role as a tumour suppressor is reliant on the activities of other proteins. In particular, p53 alteration patterns such as phosphorylation, dephoshporylation, and action of proteases, lead to the activation, inhibition, and degradation of p53 protein respectively (Kitano, 2002). The resultant modification pattern to a large extent determines the selectivity of its target which highlights the complexity of this individual component. In other words, neither p53 nor other components of the network function as a tumour suppressor independently; instead, it is dependent on the collective state of the network. Therefore, in this scenario, cellular behaviour would be better characterized if studied as a system.

Integrative systems approaches also reveal complex and unexpected behaviours in what were originally assumed to be simple organisms. The bacterium *Mycoplasma pneumoniae* whose genome is relatively small, encoding for just 689 proteins lack most regulatory and transcriptional factors (Yus *et al.,* 2009). Yet, a co-ordinated and highly complex transcriptional response has been observed (Guell *et al.,* 2009). Despite its small genome, there is a substantial level of communication between various cellular components in which the proteome exhibits extensive reuse of functional components (Kuhner *et al.,* 2009). According to Likic *et al.* (2010), these observations do not indicate that *M. pneumoniae* is an unusual organism, rather they highlight and reveal potentially unknown regulatory machineries that operate across the transcriptome, proteome, and metabolome level. This only becomes obvious when studied as a '*system'*.

1.2 THE ROLE OF BIOINFORMATICS IN SYSTEMS BIOLOGY

It is practically unrealistic to interrogate the combined role of every individual component of a cell on observed cellular behaviour using the conventional

biochemical/experimental techniques (Breitling, 2010). However, these individual components can be assembled, analysed and used to predict cellular function using computational approaches (Breitling, 2010). As a result, bioinformatics has unarguably become an indispensable tool in systems biology (Kitano, 2002; May, 2004) and this is evidenced in a number of studies. In a number of modelling studies investigating yeast metabolism, a clear and coherent picture of the dynamic cellular behaviour becomes apparent only after mathematical modelling had been applied partly due to the complexity of the network (Tyson *et al.,* 2001; Chen *et al.,* 2004). The use of mathematical models also proved invaluable in the study of an *E. coli* inducible genetic switch by Roberts *et al.* (2011) in which the authors were able to interpret cellular behaviour in response to the presence of sugar in the external environment, and furthermore, elucidate the role of intracellular molecular crowding on sugar uptake. More recently, a whole-cell computational model of *Mycoplasma genitalium* has been developed which also has provided novel insights into previously unobserved cellular behaviours (Karr *et al.,* 2012).

In addition to producing novel findings, computational models are also being explored to represent our current understanding as regards biological entities. This entails replicating known biological behaviours using *in silico* models. Under these circumstances, model reliability is improved when models are capable of reproducing as many experimental data as possible. A reliable model thus enhances its predictive properties. Thus, computational or mathematical models also represent "concise summaries of our current knowledge of respective systems" (Likic *et al.,* 2010).

1.3 CONSTRUCTION OF IN SILICO MODELS

Generally, the construction of metabolic models follows four principal steps (Palsson, 2006). Firstly, the individual components that would be involved in the process are specified. These individual components could be enzymes which catalyse reactions in the pathway, transcription and regulatory proteins, or substrate molecules. Secondly, the interactions between these individual components are enumerated which invariably results in the construction of the network. In this regard, detailed information are obtained from the literature regarding the relationship between these individual components. Subsequently, a 'pseudo' network or algorithm is constructed based on such information. Thirdly, the constructed metabolic networks are represented mathematically and their properties analysed, resulting in a computational model. Finally, the models are used to interpret and analyse known biological events, and also to predict potential experimental outcomes.

In a broad sense, there are two modelling approaches being adopted in biological systems analysis (Smallbone *et al.,* 2007). These are *constraint-based modelling* (Beard *et al.,* 2002; Covert *et al*., 2003; Price *et al*., 2006; Kim *et al*., 2008) and *kinetic modelling* (Smallbone *et al.,* 2007; Resat *et al.,* 2009). Constraint-based modelling employs physiochemical constraints which include mass balance, energy balance, and flux limitations in the exploration of cellular behaviours (Smallbone *et al.,* 2007). In most cases, the basic biochemical architecture of metabolic pathways are known to some extent; hence, the stoichiometries of such a network can be inferred (Kim *et al.,* 2008; Orth *et al.,* 2010). Furthermore, when there is sufficient information about the network such as the reaction rate, the reaction flux through the network can be constrained (Orth *et al.,* 2010). The major advantage of constraint-based modelling approach lies in the minimal amount of biological data required to make quantitative

inference about the biochemical network (Smallbone *et al.,* 2007)**.** However, this approach does not provide a detailed picture of the network such as concentration of metabolites and regulatory patterns (Smallbone *et al.,* 2007).

In contrast, kinetic models are well detailed and they provide in-depth information about the system. Kinetic modelling aims to fully characterize how changes in a modular component (such as metabolites and enzymes) alter the local reaction rates (Smallbone *et al.,* 2007)**.** This approach usually involves a considerable amount of biological information to parameterize the model. As a result, kinetic models are computationally more expensive than constraint-based models. Obtaining the required parameters could be time-consuming and, in some cases, practically impossible to determine experimentally (Covert *et al.,* 2003). Since such parameters are required for the model, they are sometimes inferred or deduced from the available information. Such assumptions on the other hand, can result in biological interpretations that are highly speculative.

1.3.1 Modelling biological systems using kinetic approaches

Biological systems are typically modelled kinetically by using either deterministic methods, or stochastic methods, or a hybrid of both (Wilkinson, 2009; Lachor *et al.,* 2011)**.** The choice of methodology utilized is dependent on a number of factors as discussed below.

1.3.1.1 Deterministic kinetic models

The conventional approach to modelling chemical kinetics is to assume that the participating components (i.e. reactants) are present in high amounts, and have a level

measured on a continuous scale such as in units of concentration or particle numbers (Wilkinson, 2009). The deterministic approach is based on the hypothesis that since the population sizes of the reacting components are large, such models can be defined by the average population size (i.e. mean) of the reacting components (Szekely and Burrage, 2014). In addition, the changes in the concentration of the reacting species are assumed to occur in a continuous and predictable process (Wilkinson, 2009).

Deterministic models are particularly useful in the description of the evolution of bio-molecular populations (Lachor *et al.,* 2011). The reaction rates in these models are specified using equations that usually assume mass action kinetics or conventional enzyme kinetic laws such as Michaelis-Menten kinetics (Cornish-Bowden, 2004; Wilkinson, 2009). Under simplistic circumstances, deterministic models are relatively easy to use, and come at a low computational cost (Meng *et al.,* 2004).

On the other hand, there are certain limitations to the use of deterministic approaches in the study of biological systems. Firstly, it is inaccurate for systems that contain low level of reacting species. If the cellular concentrations of reacting species are low, representing this phenomenon by its 'population mean' can lead to erroneous model predictions, or may even alter the qualitative properties of the model (Lachor *et al.,* 2011). Secondly, when the behaviours of biological systems are being analysed for parameters close to diverging/branching points (for instance, in evolution studies), restriction to average values can again, as above, result in bypassing important features that are inherent to the system (Lachor *et al.,* 2011). Finally, deterministic models ignore noise and heterogeneity which are intrinsic components of certain biological events (Szekely and Burrage, 2014).

1.3.1.2 Stochastic kinetic models

Stochastic models are typically used to study the effects of random fluctuations in the numbers of reacting species on biological systems behaviour (Gillespie, 2007). As mentioned above, deterministic models may fail to capture cellular behaviours that arise from stochastic events or noise in the system. However, real biological systems will unarguably be influenced by factors that are not fully understood to biologists or impractical to model explicitly (Ditlevsen and Samson, 2013). For instance, it is well documented that a number of essential biochemical processes involve some element of randomness such as promoter binding events, mRNA transcription and degradation, protein translation and degradation, and protein-protein interactions (Ideker *et al.*, 2001). Ignoring these effects during modelling may affect the analysis of the biological system under investigation. These random events can be accounted for by utilizing stochastic approaches.

A stochastic approach treats the precise number of molecules in the system as a discrete quantity. The '*state'* which describes how many molecules of each type are present in the system changes discretely (Gibson and Mjolsness, 1999) and such changes are probabilistic. Specifically, the rate constants in stochastic equations represent the probability of a discrete event occurring per unit time (Gibson and Mjolsness, 1999). A popular approach used in modelling the dynamics of biological systems is the *Markov jump process* (Cox and Miller, 1977). In this case, an algorithm called the "stochastic simulation algorithm" (popularly referred to as Gillespie algorithm (Gillespie, 1977)), is used to generate 'runs' or 'exact realizations' of the *Markov jump process* (Gillespie, 1977). Starting from the initial state of the system, the algorithm produces time course trajectories over a given time period (Wilkinson, 2009). The '*runs'* or '*realizations'* are random; thus, they vary for each simulation. This variability over several runs

subsequently represents a benchmark for interpreting noise in the biological system being studied.

On the other hand, the computational cost of including stochasticity in models is high especially when analysing complex systems. Thus, the choice of modelling approach is dependent on the importance of noise and heterogeneity on the biological event being studied. In other words, a researcher would often compromise between computational time cost of the project, and the accuracy of the expected output (Lachor *et al.,* 2011). Nevertheless, when heterogeneity isn't particularly necessary, deterministic models would suffice.

1.4 TOOLS FOR SYSTEMS BIOLOGY ANALYSIS

The development and maintenance of modelling/software tools pose some significant challenges in systems analysis. In most cases, a specific tool is aimed at addressing only a specific need of systems biology. The specific need may include the development of data repositories, development of software tools for simulation and analysis, or creation of tools for the visualization of the systems component of biochemical networks (Likic *et al.,* 2010). As a result, biological systems analysis usually involves a combination of different bioinformatics tools.

In the early 2000s, the necessity for an effective platform for the exchange and distribution of quantitative systems biology models was recognized, and subsequently resulted in the development of the Systems Biology Mark-up Language (SBML) (Hucka *et al.,* 2003)**.** SBML is a free, open, XML-based format for representing reaction networks of biological systems. Currently, the SBML format is adopted in over 180

software tools which is testament to its importance (Likic *et al.* 2010). A good example is the COPASI software (Hoops *et al.,* 2006; Mendes *et al.,* 2009).

The COPASI software is one of the most common modelling tools used in metabolic pathway analysis (as at 2015, the first publication describing COPASI has been cited 1145 times which implies an average citation rate of 127 per year). COPASI is an independent, user-friendly, and widely accepted simulator of models encoded in SBML. It can be used to describe models based on ordinary differential equations (ODE), stochastic approaches, or a combination of both (i.e. hybrid)**.** Furthermore, COPASI provide tools for the visual analysis of simulation results, and also tools for conducting post-simulation analyses such as metabolic control analyses (MCA) (Mendes *et al.,* 2009)**.**

It has been acknowledged that modelling certain biological events by ignoring spatial localization (such as with COPASI) may be inadequate. This is because a number of cellular processes depend on intracellular location and collisions of the individual reacting molecules (Andrews *et al.,* 2010). For example, during cell signalling, signals are transmitted across substantial distance of length and across multiple intracellular membrane compartments (Andrews *et al.,* 2010). In this regard, software tools have been developed which incorporate spatial effect into simulations. These include MCell (Stiles *et al.,* 1996), Smoldyn (Andrews *et al.,* 2010), and MesoRD (Fange *et al.,* 2012). The importance of spatial localization in biological models was recently buttressed in Roberts *et al.* (2011). In the study, the authors observed that intracellular molecular crowding greatly influences the uptake of sugar from the environment and subsequent activation of the *lac* expression system.

In order to run computational simulations, input parameters are usually required. In the case of COPASI for instance, such input parameters could be enzyme turnover rate,

Michaelis-Menten constant (K_m), drug inhibition constant etc. Consequently, databases which incorporate biological information and parameters have been developed. A good example is the BRENDA database which represents a fairly comprehensive collection of enzyme and metabolic information (such as K_m values and turnover rates) obtained from the experimental literature (Schomburg *et al.*, 2004).

1.5 THE APPLICATION OF SYSTEMS BIOLOGY IN THE STUDY OF GRAM-NEGATIVE BACTERIA

A significant number of clinically relevant bacterial infections are caused by a group of bacteria known as 'Gram-negatives' (Quinn, 1998; Gaynes *et al.,* 2005; Paterson, 2006; Kumarasamy *et al.*, 2010). In particular, four of the most frequent hospital-acquired infections may be caused by this group of bacteria (Gaynes *et al.,* 2005). These are bloodstream infection, urinary tract infection, surgical site infection, and pneumonia. The rise in the incidence of antibiotic-resistant strains of bacteria especially amongst Gram-negatives has limited the scope of treatment of these common infections (Poole, 2001; Paterson, 2006). It is estimated that in the United States, approximately 2 million people become infected with bacteria that are resistant to antibiotics resulting in at least 23,000 deaths yearly (Centre for Disease Control, 2015a). Similarly, there has been significant increases in cases of multi-drug resistant bacterial infection in the United Kingdom (UK). For instance, between the years 2003 and 2009, the cases of bacterial resistance to carbapenems (often regarded as the antibiotic of last resort (Papp-Wallace *et al.,* 2011)) in the UK, has increased by approximately 14 folds (Kumarasamy *et al.,* 2010). Therefore, a proactive approach is required in tackling what has been regarded as one of the "*world's most pressing public health problems"* (Centre for Disease Control, 2015b).

In a broader sense, there are primarily two ways at tackling the problem of bacterial resistance (Bush *et al.,* 2011). Firstly, by enlightening patients on the importance of adhering to prescribed antibiotics regimen, and in addition, encouraging health practitioners to minimize the prescription of antibiotics. However, there are instances whereby the use of antibiotics are indispensable such as under surgical settings. Secondly, the development of new classes of antibiotics, especially those aimed at novel metabolic pathways. The importance of the latter option is readily acknowledged by both health researchers and governments (Bush *et al.,* 2011; Centre for Disease Control, 2015b). Therefore, there is a need to drive the development of novel antibiotics aimed at novel drug targets. An example of a biochemical pathway that would represent a suitable drug target is that which is involved in the synthesis of the outer membrane found in Gram-negatives. This is because the outer membrane is of importance to the survival of the bacteria and the enzymes involved in its biosynthesis have no orthologs in humans. Although, often underestimated, one of the difficulties in novel antimicrobial design is identifying the appropriate enzyme target within a pathway. This is important because bacteria tend to devise ways to counteract external perturbations when certain enzymes are being inhibited thereby resulting in a quick development to resistance (Brinster *et al.,* 2009). In order to elucidate suitable drug targets within pathways, it is essential to study, understand, investigate, and analyse the physiology and metabolism of these bacteria in the context of the specific pathway in question. As mentioned above, such detailed integrative analyses are only obtainable when a computational systems approach is employed. Furthermore, because the outer membrane of Gram-negatives is quite complex and consists of series of biosynthetic and regulatory machineries, development of a computational model of this pathway also represents a key step towards the creation of a whole-cell model.

1.6 THE OUTER MEMBRANE OF GRAM-NEGATIVE BACTERIA

The outer membrane of Gram-negative bacteria is composed of LPS in the outer leaflet, and phospholipids in the inner leaflet (Nikaido, 2003) (Fig. 1.1). Studies investigating bacterial membrane synthesis have been conducted primarily on *E. coli* (Raetz, 1978; Heath *et al.,* 2002)**.** This is partly because *E. coli* cells can be grown easily in the laboratory and can also be readily manipulated by the investigator (Heath *et al.,* 2002)**.** Perhaps, more importantly, their complete genome sequence is available (Blattner *et al.,* 1997) and thus, suitable for genetic manipulation (Heath *et al.,* 2002). Additionally, the outer membrane system of *E. coli* is structurally similar to those of some other Gram-negatives (Silhavy *et al.,* 2010). For these reasons, *E. coli* represents a suitable model organism for the study of outer membrane in Gram-negatives.

The outer membrane is an attractive drug target for a number of reasons. Firstly, it is decorated with a potent endotoxin (called lipid A) which plays a significant role in bacterial pathogenicity and immune evasion (Walker *et al.,* 2004)**.** Secondly, it acts as a physical barrier protecting the cell from chemical attack, and represents a significant obstacle for the effective delivery of numerous antimicrobial agents (Nikaido, 1996; Delcour, 2009). Being in direct contact with the environment, the outer membrane is a dynamic system continuously adapting its composition in response to chemical or physical pressures (Taneja *et al.,* 1979). Because surrounding conditions can vary rapidly, acute or fine control mechanisms aimed at optimising membrane composition are of importance for bacterial adaption and survival (Zhang and Rock, 2008).

.

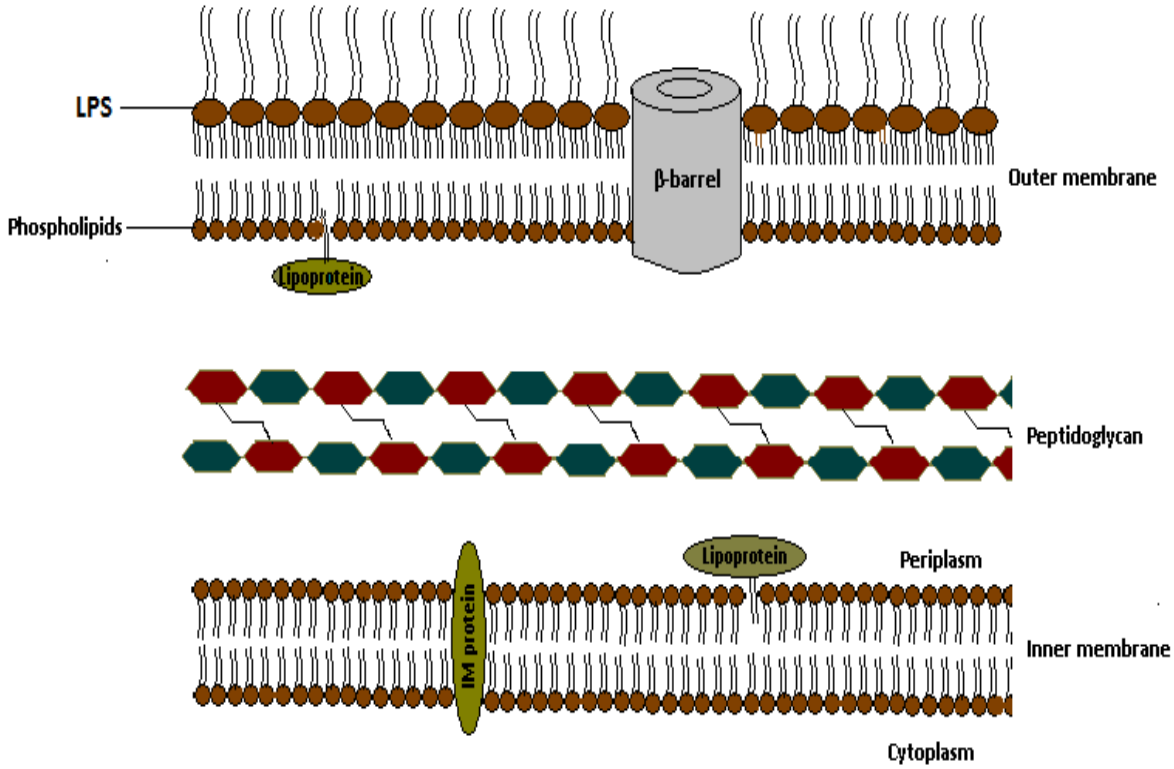

Figure 1.1 Structure of *E. coli* outer membrane. The bacterial cytoplasm is surrounded by a cell envelope which consists of an inner membrane (IM), periplasm, and outer membrane (OM). LPS occupy the outer leaflet of the OM while the inner leaflet comprises of phospholipids. The peptidoglycan layer is localized in the periplasmic space.

1.6.1 Lipopolysaccharide

LPS is a glycolipid that forms the major component of the outer leaflet and occurs with approximately 1 million copies in *E. coli* cells, covering about 75% of the cell surface area (Raetz *et al;* 2009; Whitfield and Trent, 2014). LPS helps stabilize these membranes, protects them from chemical attack, and promotes cell adhesion to various surfaces (Walker *et al.,* 2004). LPS comprises three components: lipid A, core oligosaccharide (core OS), and O-antigen (Fig. 1.2A) (Raetz and Whitfield, 2002; Raetz *et al.,* 2009). The lipid A component includes six hydrophobic acyl chains that reside in the outer leaflet of the bacterial outer membrane. These are connected together by a glucosamine and phosphate head group. In the majority of Gram-negative bacteria, including *E. coli*, this head group connects to a pair of 3-deoxy-D-*manno*-oct-2-ulosonic acid (Kdo) sugar residues (Raetz *et al.,* 2009). These Kdo residues connect to several additional sugar residues, and sometimes also to phosphate, pyrophosphorylethanolamine, or phosphorylcholine residues, which together form the core OS (Raetz and Whitfield, 2002). This core then connects to the O-antigen, which is a long polysaccharide that varies widely between different bacterial species and different strains within each species (Raetz and Whitfield, 2002).

LPS elicits a strong immune response in humans and other animals being detectable at picomolar levels by the innate immune system's Toll-like receptor 4 (TLR4) protein (Raetz *et al.,* 2009). In macrophages, the resulting activation of TLR4 by LPS stimulates the production of different inflammatory molecules, and drives the synthesis of co-stimulatory metabolites required for the adaptive immune response (Raetz and Whitfield, 2002). In mononuclear and endothelial cells, the presence of LPS stimulates tissue factor production (Drake *et al.,* 1993). Such stimulation events are normal, and are in fact, important in local infection (Raetz and Whitfield, 2002). However, when LPS drives the overproduction of these mediating and clotting factors (such as under

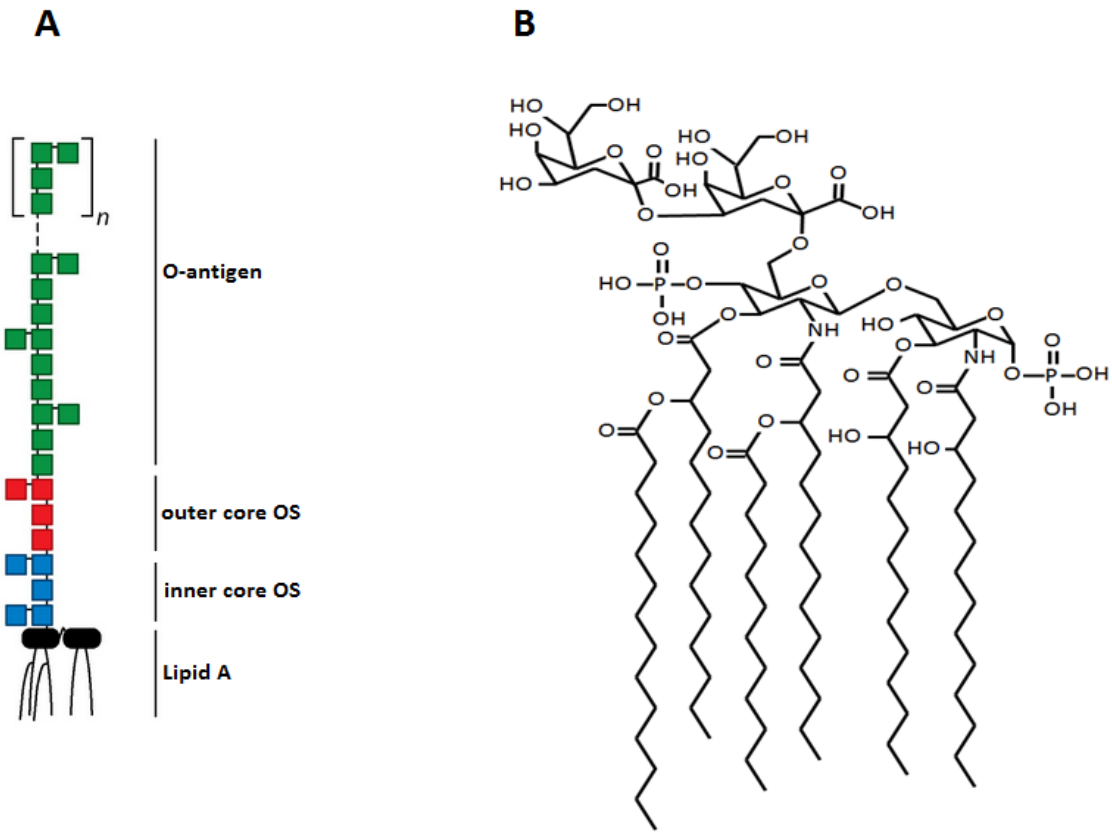

Figure 1.2. Structure of LPS and lipid A. (A) Figure was obtained from Whitfield and Trent (2014) with permission. LPS is comprised of lipid A, core OS, and O-antigen. The core OS can further be divided into inner and outer core OS. The number of polysaccharide repeats present in the O-antigen region is widely diverse and varies from strain to strain. (B) Structure of lipid A. The top two sugars are Kdo groups, which are part of the core OS, while the remainder of the structure represents the hexa-acylated lipid A moiety.

severe sepsis), they can destroy blood vessels, cause disseminated intravascular coagulation, and potentially result in organ failure (Parillo, 1993; Reatz and Whitfield, 2002). These attributes have made the study of LPS important to the fields of bacteriology and drug discovery (Raetz and Whitfield, 2002; Raetz *et al.,* 2007; Raetz *et al;* 2009; Wang and Quinn, 2010; Whitfield and Trent, 2014).

1.6.1.1 Lipid A

Of the three structural components of LPS, the lipid A moiety (Fig. 1.2B) is of particular interest because it is the only component that is essential for cell viability and is highly conserved (Raetz and Whitfield, 2002). In addition, the endotoxin component of LPS resides in the lipid A moeity. These also make its biosynthesis pathway an attractive target for new antibiotics (Onishi *et al.,* 1996; Jackman *et al.,* 2000). For these reasons also, this research would focus on the lipid A moiety of LPS.

The biosynthesis of *E. coli* lipid A proceeds through nine-enzyme catalysed steps (Fig. 1.3; Table 1.1) (Raetz *et al.,* 2009). Of these, the first seven enzymes (LpxA, LpxC, LpxD, LpxH, LpxB, LpxK, and WaaA) are essential for growth under optimum conditions (Raetz *et al.,* 2009)**.** Three of these essential enzymes are of interest due to certain characteristics. LpxA possesses a highly unfavourable equilibrium constant (Anderson *et al.,* 1993) which indicates the proceeding enzyme LpxC catalyses the pathway committed step. In addition, lipid A production is regulated in part through proteolysis of LpxC and WaaA proteins (Ogura *et al.,* 1999; Katz and Ron, 2008). The biosynthesis and regulatory processes of lipid A are described in great detail in Chapter 2.

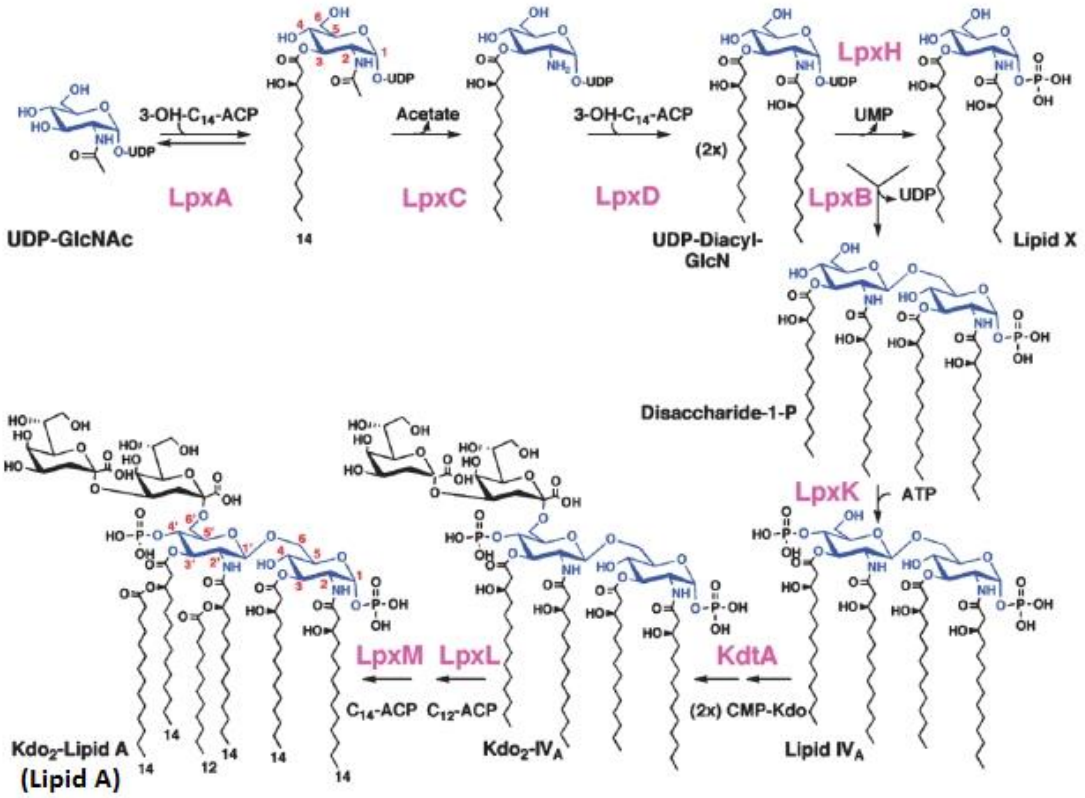

Figure 1.3. Biosynthesis of *E. coli* lipid A. Biosynthesis of lipid A commences by the acylation of UDP-N-acetylglucosamine (UDP-GlcNAc) with an acyl chain derived from β-hydroxymyristoyl-ACP (3-OH-C_{14}-ACP) catalysed by LpxA. This first reaction step is highly unfavourable. Subsequent steps are conducted by LpxC, LpxD, LpxH, LpxB, LpxK, WaaA (also known as KdtA), LpxL, and LpxM (Figure obtained from Raetz *et al.* (2009) with permission).

1.6.1.2 Core oligosaccharides (core OS)

The core OS can be divided into inner core OS and outer core OS (Fig. 1.2A). The inner core OS connects directly to the lipid A component. Although the lipid A moiety of LPS is highly conserved, the core OS exhibit some degree of variation albeit within the outer core (Wang and Quinn, 2010). This highlights an important role of inner core OS in outer membrane stability (Whitifield and Trent, 2014). Whilst the inner core OS typically consists of Kdo and L-*glycero*-D-*manno*-heptose (Wang and Quinn, 2010), the outer core can consist of a variety of sugars such as galactose and glucose. The diverse nature of the core OS is understandable given that it is exposed to the environment in most *E. coli* strains (i.e. strains lacking O-antigen), and thus, exposed to selective pressures of the host responses and environmental stress (Raetz and Whitfield, 2002). Biosynthesis of the core OS occurs at the cytoplasmic surface of the inner membrane and is conducted by membrane-associated gylcosyltransferases which utilizes nucleotide sugars as donors. This process is usually prompt and efficient which suggests that the glycosyltransferases function as a co-ordinated complex (Wang and Quinn, 2010).

After attachment of the core OS to the lipid A moiety, the core OS-lipid A complex is flipped by MsbA protein from the inner surface to the outer surface of the inner membrane (Fig. 1.4). An inactivation of MsbA results in the accumulation of precursor molecules of LPS in the inner membrane (Rees *et al.*, 2009) which indicates that MsbA plays a crucial role in LPS assembly. However, suppressor mutations in the *yhjD* gene has been observed to functionally replace MsbA under extreme conditions (Mamat *et al.*, 2008).

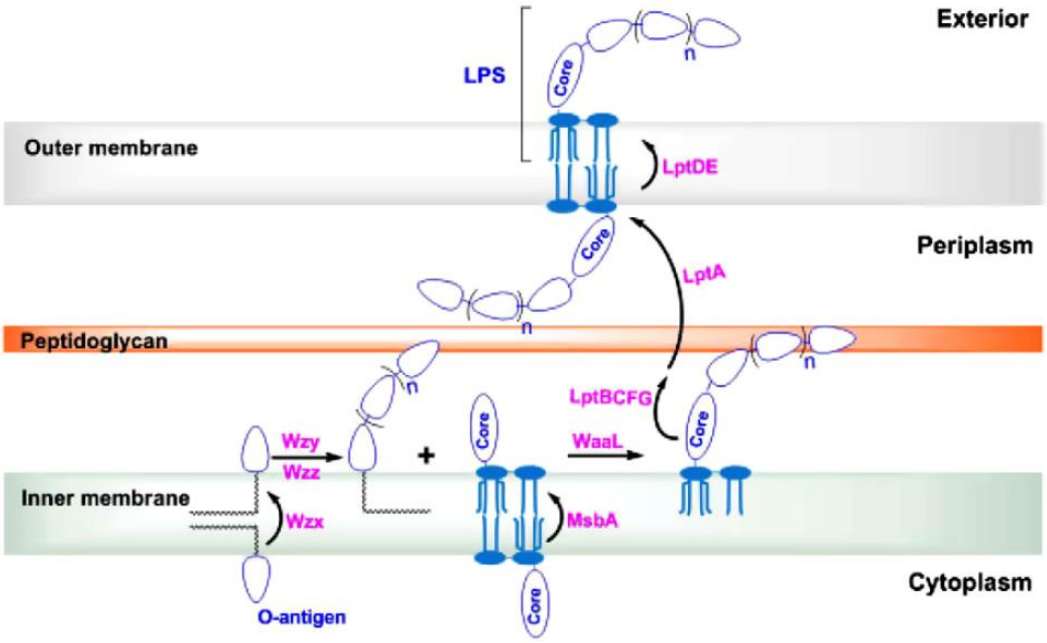

Figure 1.4. Assembly and transport of LPS in *E. coli*. MsbA flips the core OS-lipid A complex from the cytoplasmic face of the inner membrane to the outer surface of the inner membrane. Likewise, the O-antigen oligosaccharides are assembled and flipped from the inner surface to the outer surface of the inner membrane by the transporter Wzx. Polymerization subsequently occurs by Wzy and Wzz enzymes. The core OS-lipid A is then ligated with the polymerized O-antigen by WaaL. The nascent LPS is then shuttled to the periplasmic face of the outer membrane by LptA, LptB, LptC, LptF and LptG. Lastly, the outer membrane proteins LptD and LptE exports the LPS to the outer membrane (Figure obtained from Wang and Quinn (2010) with permission).

1.6.1.3 O-antigen

Most of the laboratory strains of *E. coli* such as K-12 lack the O-antigen moiety; nevertheless, O-antigen is present in virulent strains of *E. coli* and they help confer resistance to antibiotics (DebRoy *et al.,* 2011; Band and Weiss, 2015). The level of diversity in the O-antigen region is remarkable. Over 60 monosaccharides and 30 non-carbohydrate components have been elucidated (Raetz and Whitfield, 2002).

The O-antigen region is synthesized by glycosyltransferase enzymes in the cytoplasmic surface of the inner membrane similarly to core OS (Wang and Quinn, 2010). The *rfb* gene cluster encodes for enzymes which produce sugar-nucleotide precursors that are unique to O-antigen (Raetz and Whitfield, 2002; Wang and Quinn, 2010). The protein Wzx flips the O-antigen from the cytoplasmic face to the outer surface of the inner membrane in a similar pattern to that of core OS-lipid A with MsbA (Fig. 1.4) (Wang and Quinn, 2010).

1.6.1.4 LPS assembly and transport

Since LPS is localized within the outer membrane and its individual components are synthesized in the inner membrane, LPS must be assembled and subsequently transported to the outer surface. The core OS-lipid A complex together with the synthesized O-antigen are exported to the periplasmic face of the inner membrane where O-antigen is further polymerized by Wzy and Wzz (Wang and Quinn, 2010) and subsequently attached to the core OS-lipid A by the ligase WaaL (Abeyranthe *et al.,* 2005) (Fig. 1.4). The resulting structure is referred to as a “nascent LPS”.

Transportation of nascent LPS from the periplasmic face of the inner membrane to the inner leaflet of the outer membrane is performed by LptA, LptB, LptC, LptF, and LptG

proteins (Ruiz *et al.,* 2008; Sperandeo *et al.,* 2007; Sperandeo *et al.,* 2008). Subsequent translocation to the outer leaflet of the outer membrane are conducted by LptD and LptE (Bos *et al.,* 2004; Wu *et al.,* 2006; Ma *et al.,* 2008) (Fig. 1.4). Table 1.1 lists the enzymes involved in lipid A biosynthesis and LPS transport.

1.6.1.5 Structural modification of lipid A component of LPS

Some Gram-negative bacteria such as *E. coli* have evolved mechanisms to modify either the hydrophobic acyl chain region or hydrophilic disaccharide region of lipid A (Raetz *et al.,* 2007). Such modification assists the bacterium in evading recognition by the innate immune system, or to resist cationic antimicrobial peptides (CAMPs) synthesized by the host immune machinery (Whitfield and Trent, 2014).

A palmitate group obtained from phospholipids can be added to lipid A by the enzyme PagP resulting in a hepta-acylated structure (Hwang *et al.,* 2004). This modified form of lipid A is believed to play a major role in resistance to some CAMPs (Wang and Quinn, 2010). On the other hand, PagL is a lipase that removes 3-O-linked acyl group from lipid A (Rutten *et al.,* 2006). However, this play no role in resistance to CAMPs (Kawasaki *et al.,* 2004). Furthermore, the phosphate region on the hydrophilic region can be modified or removed. This structural modification is important because the *E. coli* lipid A usually contains 2 phosphate groups resulting in a negatively charged molecule which facilitate binding to positively charged CAMPs (Wang and Quinn, 2010). Common modification patterns involve the addition of amine-containing residues such as phosphoethanolamine and α-L-Ara4N which enable bacteria cells develop resistance to polymyxin B and CAMPs (Trent *et al.,* 2001; Lee *et al.,* 2004).

Table 1.1: Enzymes involved in lipid A biosynthesis and LPS transport in *E. coli*

Enzyme	Function
Lipid A biosynthesis	
LpxA	fatty acylation of UDP-GlcNAc using β-hydroxymyristoyl-ACP as donor
LpxC	catalyses the committed step in lipid A synthesis by deacetylation of the product of LpxA.
LpxD	adds a second acyl-chain using β-hydroxymyristoyl-ACP as donor
LpxH	cleaves the pyrophosphate linkage from the reaction product of LpxD to form lipid X
LpxB	condenses the product of LpxD with lipid X to produce lipid A disaccharide
LpxK	phosphorylates lipid A disaccharide to form lipid IV_A
WaaA	incorporates two Kdo residues to lipid IV_A resulting in the formation of Kdo-lipid IV_A
LpxL	adds a laurate acyl chain to Kdo-lipid IV_A.
LpxM	adds a myristoyl group resulting in a hexa-acylated mature lipid A (Kdo-lipid A).
LPS transport	
MsbA	exports core OS-lipid A from the cytoplasmic to periplasmic face of inner membrane
Wzx	exports O-antigen to the periplasmic face of inner membrane similarly to MsbA
LptA	periplasmic protein required for LPS transport across the periplasm
LptB	cytoplasmic protein required for LPS transport across the periplasm
LptC	also required for LPS transport across the periplasm
LptD	outer membrane protein required for LPS incorporation in the outer leaflet of outer membrane
LptE	lipoprotein required for LPS assembly in the outer leaflet of outer membrane
LptF	required for LPS transport across the periplasm
LptG	required for LPS transport across the periplasm

1.6.2 Phospholipids

Phospholipids make up of about 10% of the dry weight of the cell, and are a major and essential component of the bacterial outer membrane (Heath *et al.,* 2002). The biosynthesis of a single mole of lipid typically involves 32 moles of adenosine triphosphate (ATP) (Heath *et al.,* 2002). Therefore, the cell invests substantial resources in the production of phospholipids. Its biosynthesis involves a series of cytosolic and membrane-bound enzymes that differ from those found in mammals (Heath and Rock, 2004; Janßen *et al.,* 2014**).** For this reason also, these enzymes are an attractive target for novel antimicrobial design (Zhang *et al.,* 2006).

Each phospholipid molecule consists of a glycerol moiety, a phosphate group, and two fatty acids (except for cardiolipins) (Fig. 1.5). *E. coli* possesses only three types of phospholipids in its membrane; phosphatidylethanolamine (PE) which comprises the bulk (about 75%), phosphatidylglycerol (PG), and cardiolipin (CL) which represents 15 - 20% and 5 - 10% respectively (Heath *et al.,* 2002)**.**

The steps involved in the synthesis of phospholipids can be broadly divided into three stages (Heath *et al.,* 2002)**.** These are, (i) initiation of fatty acid biosynthesis; (ii) fatty acid elongation; and (iii) phospholipid synthesis.

1.6.2.1 Initiation of fatty acid biosynthesis

The fatty acids most commonly found in *E. coli* membranes are palmitic acid (C16:0), palmitoleic acid (C16:1), and *cis*-vaccenic acid (C18:1) (Raetz, 1978)**.** However, other fatty acid species can be present in significant numbers depending on the *E. coli* strain being studied, and environmental conditions (Raetz, 1978)**.** The fatty acids notation presented in parenthesis above describes the carbon-length of the fatty acid, and the

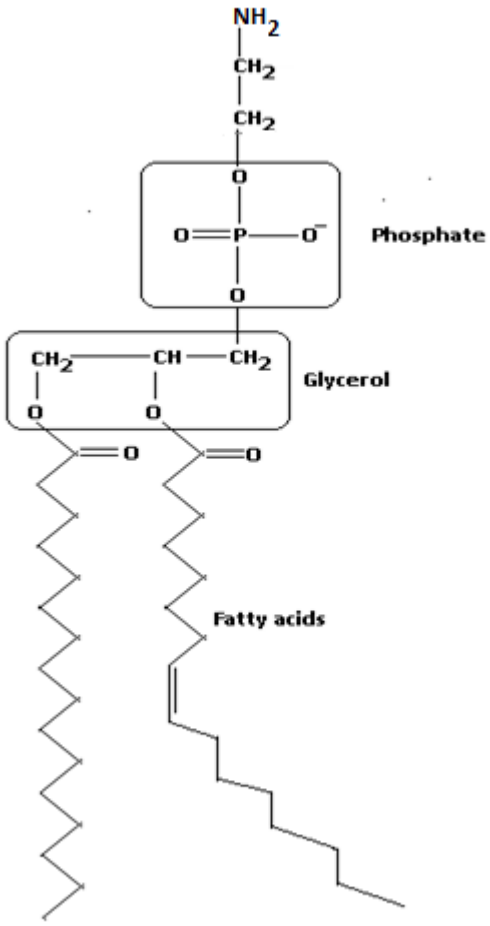

Figure 1.5. Structure of phospholipid. A schematic representation of a phospholipid molecule (PE in this case) with two acyl chains, a glycerol group and a phosphate group. Most times, the phosphate group is attached to a simple organic molecule.

presence or absence of a double bond. For instance, C16:1 indicates that the fatty acid consists of 16 carbons and also contains a double bond (i.e. unsaturated fatty acid (UFA)).

A schematic representation of fatty acids biosynthesis in *E. coli* is presented in Fig. 1.6. One of the key features of fatty acid biosynthesis is the presence of a small protein called "acyl carrier protein" (ACP) produced by the *acpP* gene (Heath *et al.,* 2002). It is one of the most abundant proteins found in *E. coli* comprising of about 60,000 copies per cell (Heath *et al.,* 2002). The intermediate acyl chain involved in fatty acid synthesis is attached to ACP via a thioester linkage (Majerus *et al.,* 1965)**.** An overproduction of ACP is generally toxic to the bacterial cell due the resulting high copies of *apo*-ACP (i.e. ACP not bound to an acyl group) (Keating *et al.,* 1995). Presumably, high levels of *apo*-ACP results in elevated levels of long-chain acyl-ACPs which inhibits cell growth (Keating *et al.,* 1995). However, *apo*-ACP are usually present at low copies in the cell (Ishihama *et al.,* 2008).

The first committed step in *de novo* fatty acid biosynthesis is catalysed by acetyl-CoA carboxylase (Janßen *et al.,* 2014) (Fig. 1.6). Acetyl-CoA carboxylase consists of four subunits which form a highly unstable complex (AccABCD); although this complex can be purified as two sub-complexes (Cronan and Waldrop, 2002; Choi-Rhee and Cronan, 2003)**.** The reaction requires ATP and two molecules of acetyl-CoA to produce malonyl-CoA. Malonyl-CoA in *E. coli* cells are consumed exclusively in the biosynthesis of fatty acids (Heath *et al.,* 2002). In addition to the requirement for ATP, each protein subunit must be produced in proportionate amounts. Thus, it is unsurprising that acetyl-CoA carboxylase is regulated at the level of transcription (Li and Cronan, 1993; James and Cronan, 2004)**.** Furthermore, acyl-acyl carrier protein (acyl-ACP) inhibits the carboxylase activity apparently to prevent an accumulation of

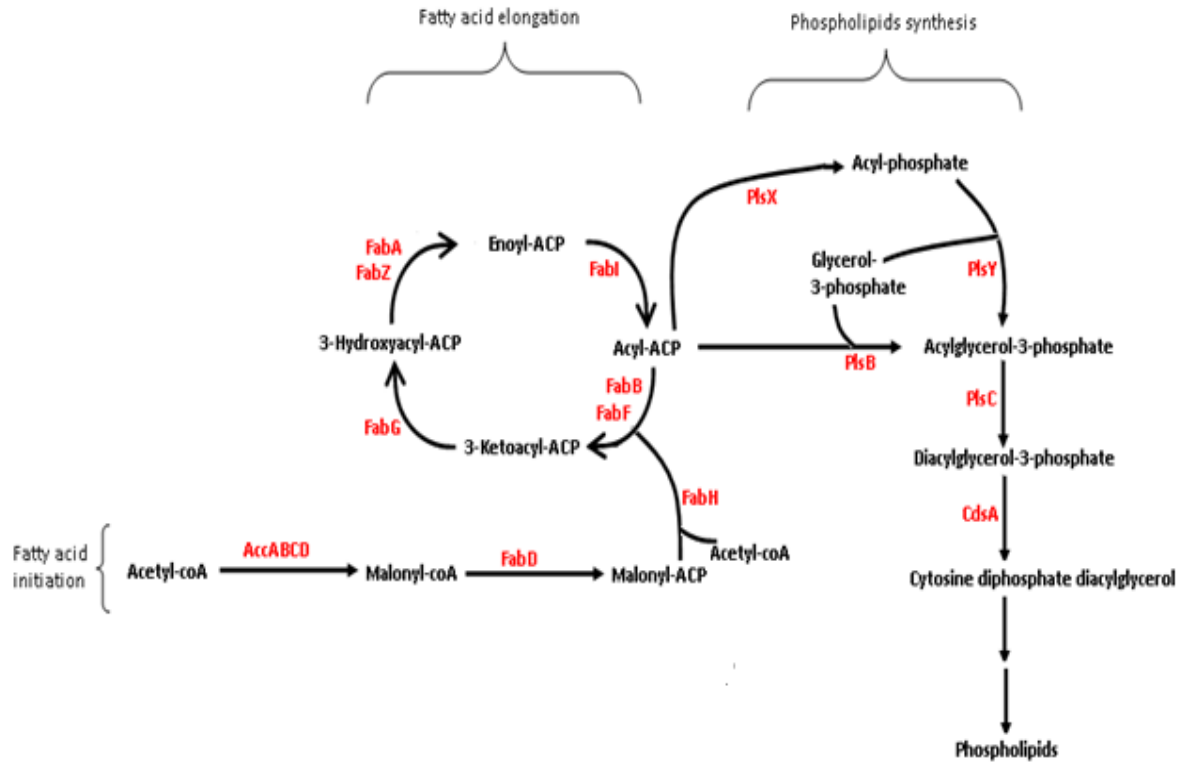

Figure 1.6. Schematic representation of phospholipids biosynthesis in *E. coli.* Fatty acids biosynthesis commences with the condensation of two molecules of acetyl-CoA to produce malonyl-CoA which is subsequently converted to malonyl-ACP by FabD. Malonyl-ACP is then condensed with acetyl-CoA by FabH to initiate fatty acids biosynthesis cycle. The role of FabH is solely restricted to fatty acids initiation step. The product of FabH is catalysed by FabG, FabZ/FabA, and FabI to complete a cycle. The next cycle begins with the condensation of malonyl-ACP with the growing acyl-chain which is catalysed by FabB/FabF.

excess acyl-ACPs that may not be required for fatty acid synthesis (Davis and Cronan, 2001).

Malonyl-CoA is converted to malonyl-ACP (3-carbon atom) by malonyl-CoA:ACP transacylase (FabD) (Fig. 1.6). FabD is specific for malonyl-CoA and is incapable of utilizing acetyl-CoA (Janßen *et al.,* 2014). Deletion of the *fabD* gene is lethal to the cell (Zhang and Cronan, 1998) whereas, overexpression of *fabD* results in decreased amount of palmitoleic acid (C16:1) and elevated levels of *cis*-vaccenic acid (C18:1) (Magnuson *et al.,* 1992). A possible explanation for this observation is that overexpressing *fabD* would enable malonyl-ACP which has a regulatory effect on FabF to accumulate, and thus, increase the activity of FabF (Magnuson *et al.,* 1992). This is because the elongation of palmitoleic acid to *cis*-vaccenic acid is performed exclusively by FabF (Garwin *et al.,* 1980a).

The malonyl-ACP produced is condensed with acyl-ACPs for fatty acid elongation by the 3-ketoacyl-ACP synthases (Fig. 1.6) (Janßen *et al.,* 2014). There are three 3-ketoacyl-ACP synthases in *E. coli;* FabB, FabF, and FabH (KASI, KASII, and KASIII) and they are all functionally distinctive (Heath *et al.,* 2002; Janßen *et al.,* 2014). The initial condensation of malonyl-ACP requires acetyl-CoA (2-carbon atom) and this reaction is performed solely by FabH (Heath and Rock, 1996a) (Fig. 1.6)**.** Further condensation reactions are conducted exclusively by FabB and FabF which involves the addition of 2-carbon atoms derived from malonyl-ACP to the growing acyl-chain to produce a ketoester (Janßen *et al.,* 2014)**.** The catalytic activities of FabH towards acetyl-CoA and propionyl-CoA (3-carbon atoms) are similar and hence, reactions with the latter substrate results in the formation of fatty acids with an uneven number of carbon atoms (Heath and Rock, 1996a)**.**

1.6.2.2 Fatty acids elongation

The resulting ketoesters produced by 3-ketoacyl-ACP synthases are reduced by an NADPH-dependent 3-ketoacyl ACP reductase (FabG) (Toomey and Wakil, 1966). The FabG product is further dehydrated by β-hydroxyacyl-ACP dehydratase (FabA and FabZ) (Heath and Rock, 1996b). The final step in the elongation cycle is conducted by enoyl-ACP reductase (FabI) which catalyses the reduction of reaction products of FabA and FabZ to form an acyl-ACP (Heath and Rock, 1995). This acyl-ACP in turn, serves as substrate for another condensation reaction with malonyl-ACP (Fig. 1.6). In addition to its dehydratase role, FabA possesses an isomerase catalytic activity which is involved in the first step of UFAs synthesis (Janßen *et al.,* 2014).

A detailed description of the fatty acid elongation pathway is presented in Chapter 3.

1.6.2.3 Phospholipids synthesis

Usually, when the growing acyl-ACP chain reaches 16 or 18 carbons, they serve as substrates for the synthesis of phospholipids (Heath *et al.,* 2002). As an alternative, exogenous fatty acids can be utilized in the synthesis of phospholipids following esterification to CoA (co-enzyme A) (Janßen *et al.,* 2014). Table 1.2 lists the enzymes involved in fatty acids and phospholipids synthesis.

Phospholipids synthesis using acyl-ACP can occur via two different routes (Janßen *et al.,* 2014). Firstly, the long acyl-ACPs can be activated with an inorganic phosphate molecule to produce an acyl-phosphate under the influence of the enzyme PlsX. This acyl-phosphate is then added to a glycerol-3-molecule by the enzyme PlsY (Janßen *et al.,* 2014). Alternatively, and secondly, the acyl-ACP can be condensed directly with glycerol-3-phosphate to produce acylglycerol-3-phosphate by the action of PlsB (Fig.

1.6) (Janßen *et al.,* 2014). The activity of PlsB is inhibited in the presence of elevated (p)ppGpp which occurs under stringent conditions (Heath *et al.,* 1994). Despite the presence of two routes leading to phospholipids production (i.e. PlsX/PlsY or PlsB), one synthetic route cannot compensate for the complete loss of the other (Yoshimura *et al.,* 2007). However, overexpression of *plsX* and *plsY* does not increase the catalytic activity of the reaction step (Larson *et al.,* 1984). Next, an acyl chain is attached to acylglycerol-3-phosphate resulting in the formation of diacylglycerol-3-phosphate in a reaction catalysed by PlsC (Janßen *et al.,* 2014**).** The product of the PlsC reaction is catalysed by the enzyme CdsA to produce cytosine diphosphate diacylglycerol (CDP diacylglycerol) (Fig. 1.6) (Janßen *et al.,* 2014). This then acts as substrate for the formation of the various forms of phospholipids found in *E. coli* (i.e. PE, PG, and CL).

A serine residue can be condensed with CDP diacylglycerol by PssA and subsequently decarboxylated by Psd leading to the production of PE. Cells deficient in PE production are only viable when the culture medium is supplemented with divalent metal ions and are characterized with disruptions in permeases activity, electron transport, and motility (Heath *et al.,* 2002). Alternatively, PgsA condenses glycerol phosphate with CDP diacylglycerol and the reaction product is dephosphorylated by either PgpA, PgpB, or PgpC resulting in the formation of PG (Icho and Raetz, 1983; Funk *et al.,* 1992). A triple mutant of *pgpA*, *pgpB*, and *pgpC* is non-viable; however, cells are viable at low temperatures with one of each functional gene (Lu *et al.,* 2011). PG is essential for the translocation of proteins across the membrane and is also required for channel activity of bacterial colicins (Heath *et al.,* 2002). Furthermore, cell division proteins depend on PG for their activities (Erez *et al.,* 2010). On the other hand, CL is formed by the condensation of two molecules of PG by the action of CL synthases. CL has been found to accumulate in cells at the stationary growth phase and it is required for prolonged

bacteria survival (Heath *et al.,* 2002). Expectedly, *E. coli* mutants deficient in the production of CL lose viability at the stationary phase (Heath *et al.*, 2002).

1.6.2.4 Fatty acids degradation

When exogenous fatty acids are present in the growth medium, they can be utilized in the synthesis of membrane phospholipids by PlsB and PlsC (Janßen *et al.,* 2014). Alternatively, they can act as the sole carbon source for growth (Nunn and Simons, 1978). The intake of fatty acids containing 10 or more carbons from the environment requires a transporter protein known as FadL (Kumar and Black, 1991) while shorter chain fatty acids are presumed to diffuse through the membrane (Maloy *et al.,* 1981). Fatty acids bound to FadL are transported into the periplasmic space and thereafter enters the cytosol in the form of acyl-CoA through the action of FadD (Fig. 1.7) (Weimar *et al.,* 2002). The esterification of free fatty acids to CoA is crucial because accumulation of free fatty acids in the cytosol are toxic to the cell (Lennen *et al.,* 2011). Additionally, FadD is capable of utilizing fatty acids that are cleaved from membrane lipids in which the resultant acyl-CoA is consumed via the β-oxidation pathway (Fig. 1.7) (Janßen *et al.*, 2014).

In simplistic terms, β-oxidation is a process whereby fatty acids (i.e. acyl CoA) are degraded to generate acetyl-CoA (i.e. carbon source). The β-oxidation process occurs through repeated cycles involving a gradual reduction of acyl-CoAs in which a single unit of acetyl-CoA is produced per cycle (Fig. 1.7). In other words, it is essentially the reverse process of fatty acids biosynthesis (Heath *et al.,* 2002). Whilst β-oxidation utilizes fatty acids bound to CoA, fatty acids biosynthesis involves acyl-ACPs as substrates (Heath *et al.,* 2002). Acyl-CoA is oxidized by FadE to enoyl-CoA and subsequently hydrated by FadB to produce a 3-hydroxyacyl-CoA, and further oxidized

again by FadB to form a 3-ketoacyl-CoA (Janßen *et al.*, 2014). The final step in the cycle is catalysed by FadA in which case, acetyl-CoA is released from acyl-CoA (Feigenbaum and Schulz, 1975).

1.6.2.5 Regulation of fatty acids biosynthesis

Due to the high energy requirement involved in the production of fatty acids, some of the biosynthesis enzymes are regulated at the transcriptional or post-translational level as discussed below (Janßen *et al.*, 2014).

Although FadR is a known *repressor* of enzymes involved in the β-oxidation cycle under high levels of intracellular acyl-CoAs (Fujita *et al.,* 2007), its role in fatty acids synthesis became apparent when it was discovered that FadR also *activates* the transcription of *fabA* and *fabB* genes (Nunn *et al.,* 1983). The activation by FadR is intended to increase the rate of UFAs synthesis (Feng and Cronan, 2012) which indicates that FabA and FabB are key enzymes in UFAs production (discussed in more detail in Chapter 3). However, the homologous overexpression of *fadR* in *E. coli* can increase both saturated fatty acids (SFAs) and UFAs (Zhang *et al.*, 2012). More recently, FadR has been identified as an activator of *fabH*, *fabD*, and *fabG* transcription in the absence of long chain fatty acids (My *et al.,* 2013). This implies that in addition to its role at boosting UFAs levels, FadR also plays a crucial role at initiating fatty acids biosynthesis.

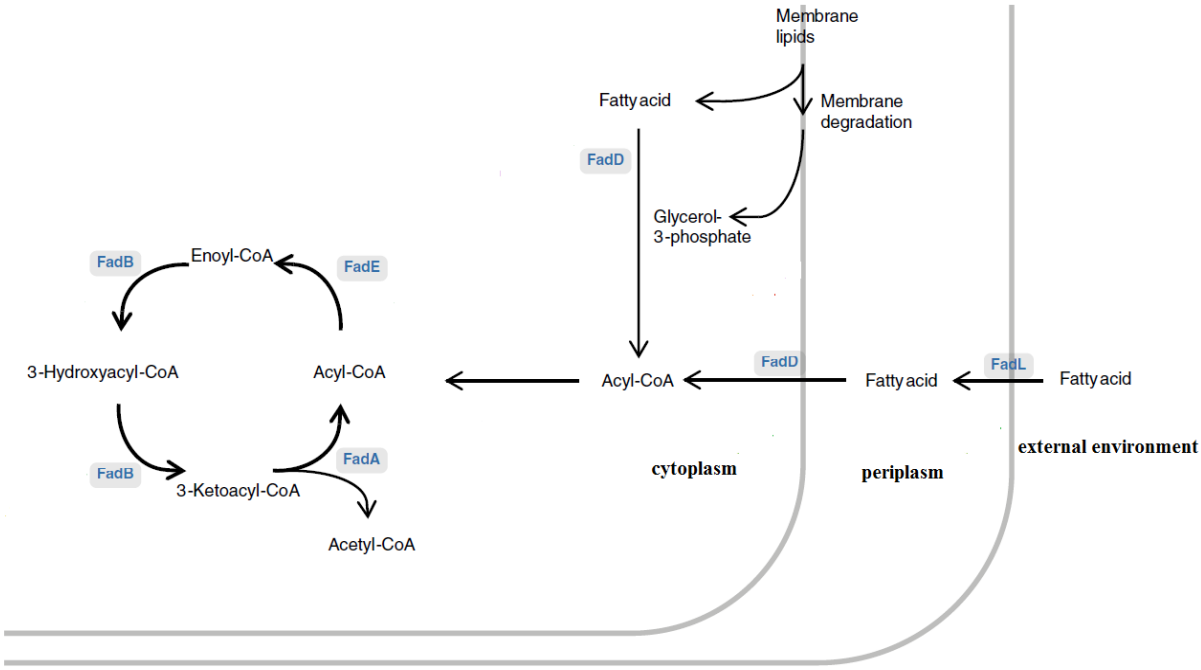

Figure 1.7. Fatty acids degradation in *E. coli.* Long chain exogenous fatty acids are transported across the outer membrane into the periplasmic space by FadL, and subsequently converted to an acyl-CoA by FadD prior to being translocated to the cytoplasm. Further reaction steps by FadE, FadB, and FadA completes a cycle in the β-oxidation process with the release of acetyl-CoA (Figure obtained and modified from Janßen *et al.* (2014) with permission).

Table 1.2: Enzymes involved in fatty acids and phospholipids biosynthesis in *E. coli*

Enzyme	Function
Fatty acids biosynthesis	
AccABCD	the AccABCD complex directs acetyl-CoA towards fatty acids synthesis
FabD	catalyses the transfer of the malonyl-moiety to ACP
FabH	it is involved only in the first cycle of fatty acids synthesis and catalyses the formation of ketoacyl-ACP by condensation of fatty acetyl-CoA with malonyl-ACP.
FabB	condenses fatty acyl-ACP with malonyl-ACP to form ketoacyl-ACP
FabF	condenses fatty acyl-ACP with malonyl-ACP to form ketoacyl-ACP
FabG	catalyses the reduction of ketoacyl-ACP to hydroxyacyl-ACP
FabA	possesses dual function. It dehydrates hydroxyacyl-ACP to produce an enoyl-ACP. It also isomerizes 10-carbon enoyl-ACP which represents the first step in UFAs synthesis
FabZ	dehydration of hydroxyacyl-ACP to produce an enoyl-ACP.
FabI	reduces an enoyl-ACP to complete a cycle in fatty acids biosynthesis
Phospholipids biosynthesis	
PlsX	catalyses the conversion of acyl-ACP to an acyl-phosphate
PlsY	addition of acyl-phosphate to glycerol-3-phosphate (G3P) to form acylglycerol-3-phosphate
PlsB	direct condensation of acyl-ACP with G3P to produce acylglycerol-3-phosphate
PlsC	condensation acyl-ACP with acylglyerol-3-phosphate to produce diacylglycerol-3-phosphate
CdsA	catalyses the conversion of diacylglycerol-3-phosphate to CDP-diacylglycerol
PssA	catalyses the condensation of CDP-diacylglycerol to produce phosphatidylserine
Psd	decarboxylates phosphatidylserine to form phosphatidylethanolamine (PE)
PgsA	condenses glycerol-phosphate with CDP-diacylglycerol to form phosphatidylglycerolphosphate
PgpABC	PgpA, PgpB and PgpC dephosphorylates phosphatidylglycerophosphate to produce phosphatidylglycerol (PG)
ClsA	condenses to PG molecules to produce cardiolipin (CL)

Furthermore, *fabA* and *fabB* are under the regulation of FabR which represses gene transcription (Feng and Cronan, 2011). Both unsaturated and saturated acyl substrates can bind to FabR; however, only FabR bound to saturated acyl substrates promotes gene repression (Zhu *et al.*, 2009). Thus, it has been suggested that FabR senses the ratio of SFAs and UFAs and accordingly, regulates the expression of *fabA* and *fabB* in order to balance the SFAs and UFAs moiety (Zhu *et al.*, 2009).

The catalytic activities of FabH, FabI are further inhibited by long chain intracellular acyl-ACPs (Heath and Rock, 1996a; Heath and Rock, 1996c). The inhibitory effect of long chain acyl-ACPs on other fatty acids biosynthetic enzymes has not been investigated; therefore, there is a possibility that more fatty acid enzymes may be regulated at the substrate level as well. Furthermore, long chain acyl-CoA induces a strong inhibitory effect on FabI (Bergler *et al.*, 1996). This mode of regulation enables the cell to conserve energy required for the synthesis of fatty acids under conditions in which cells can obtain membrane precursor molecules from the external environment (Janßen *et al.*, 2014).

1.6.2.6. Structural modification of membrane phospholipids

During stationary growth phase, fatty acids that are present in membrane phospholipids can be converted to cyclopropane derivatives by the action of CFA synthase (also known as CdfA) (Heath *et al.*, 2002). The cyclopropane derivatives are obtained as a result of methylenation of UFAs (Taylor and Cronan, 1979). *E. coli* mutant strains with deficient CFA synthase activity are more susceptible to freeze-thaw cycles and acid-shock (Grogan and Cronan, 1986; Chang and Cronan, 1999). Thus, it has been suggested that the cyclopropane derivatives help to protect the reactive double bond from adverse reactions during stationary growth phase (Heath *et al.*, 2002). However,

such mutants do not exhibit observable phenotypic defects under a wide range of conditions (Taylor and Cronan, 1976).

1.7 SCOPE OF RESEARCH

Despite a large of amount of research being carried out on either LPS or phospholipids synthesis, very little information exists regarding the behaviour of the integrated system. This would appear valuable as the synthesis of these molecules have to be synchronised in order to ensure a proper balance of membrane components are maintained. The studies of the bacterial outer membrane so far have mainly focused on individual components of enzymic reactions primarily due to the complex architecture of its biosynthesis. In order to investigate the 'combined' role of these individual components during membrane biogenesis, a whole '*systems'* approach is essential.

Furthermore, available research on the *E. coli* outer membrane has received remarkably little quantitative analysis, which is essential for testing the internal consistency of models and for investigating pathway regulatory mechanisms. In one modelling study, Kenanov *et al*. (2010) investigated the elementary flux modes (unbranched paths through the metabolic chemical reaction network, not including regulatory interactions) for the biosynthesis of all *E. coli* lipids. Since their model does not include regulatory interactions, a large and essential gap still exists in the understanding of the biosynthesis and regulation of the bacterial membrane.

This research aims to build a reasonably large and complex model of the *E. coli* outer membrane which will address a sizeable fraction of the *E. coli* metabolic reactions. Such a model could substantiate the proposed mechanism for the outer membrane synthesis as well as providing new insights into this complex and important microbial

pathway. Further expansion of the model will eventually lead to a whole-cell model. In addition, the findings could prove invaluable towards the identification of suitable therapeutic agents.

The specific questions to be addressed and aims of this research are highlighted in detail at the commencement of each Chapter. However, the proposed objectives of this study can broadly be divided into two; *(i)* developing a computational kinetic model of the *E. coli* outer membrane, and *(ii)* testing the model findings experimentally.

The development of the model would entail the integrative analysis of published datasets, and estimating relevant parameters when necessary. The constructed model would subsequently be used to interrogate the regulatory machinery involved in outer membrane biosynthesis, which thus far, is poorly understood. The predictive power of the model would be examined to provide insight into this complex and sophisticated network.

Chapter 2

A complete pathway model for lipid A biosynthesis in *E. coli*

2.1 OVERVIEW

E.coli LPS is comprised of three components; lipid A, core OS, and O-antigen. Of these, the lipid A moiety is the only essential component and it is highly conserved across the Gram-negatives. Because the core OS and O-antigen are dispensable and absent in some strains of *E. coli* (Raetz and Whitfield, 2002), studies investigating lipid A biosynthesis can be used as an indirect indicator of LPS synthesis.

Biochemical studies of the lipid A pathway have proved difficult for a number of reasons. Firstly, some of the reactions occur within the cytoplasm whilst subsequent steps occur within the membrane (Raetz and Whitfield, 2002). Secondly, a number of these enzymes have been difficult to purify (Garrett *et al.,* 1997) presumably due to stability problems and finally, the substrates and products of some of these reactions are difficult to assay for (Belunis and Raetz, 1992). Therefore, an *in silico* metabolic model of this pathway would prove extremely useful for a complete understanding of both the synthesis and regulation of lipid A.

A number of studies have investigated the biosynthesis and regulatory processes involved in the production of lipid A (Raetz and Whitfield, 2002; Reatz *et al.,* 2009). However, there remains a number of unresolved issues which require investigation. The first reaction step catalysed by LpxA is characterized with a highly unfavourable equilibrium constant *in vitro* (Anderson *et al.,* 1993). Such large unfavourable thermodynamics exist for other enzymes such as creatine kinase which solve the energetics by either coupling the reaction to an energetically favourable one or by interacting directly with subsequent proteins (Shih and Whitesides, 1977). However, there is no evidence of either of these mechanisms occurring for LpxA and to date, there have been no studies aimed at examining the impact of this unfavourable reaction in context of subsequent lipid A metabolism. Furthermore, the pathway is regulated in

part, through the proteolytic degradation of an essential enzyme LpxC by the protease FtsH (Ogura *et al.*, 1999; Fuhrer *et al.*, 2006). Yet, the regulatory feedback source remains unknown. In addition to LpxC regulation, WaaA is also degraded by FtsH and the rationale for this regulation is poorly understood (Katz and Ron, 2008).

This chapter aims to develop a complete computational model for lipid A biosynthesis. The model is specific to *E. coli* because this organism has been the subject of most lipid A research. However, the lipid A biosynthesis pathway is well conserved across Gram-negative bacteria (Raetz and Whitfield, 2002), so the model may be applicable to other Gram-negative bacteria.

2.2 MODEL CONSTRUCTION/ARCHITECTURE

2.2.1 Lipid A biosynthesis pathway

E. coli lipid A (or Kdo_2-lipid A) biosynthesis proceeds through nine enzyme-catalysed steps, which are sometimes referred to as the Raetz pathway (Wang and Quinn, 2010; Whitfield and Trent, 2014) (Fig. 2.1). All of these enzymes are constitutively expressed under optimum conditions (Raetz and Whitfield, 2002).

Lipid A biosynthesis begins with the UDP-N-acetylglucosamine (UDP-GlcNAc) and β-hydroxymyristoyl-ACP substrates. Both substrates are consumed in other metabolic pathways as well (Yokoyama *et al.*, 2008): UDP-GlcNAc is a substrate in peptidoglycan synthesis (Mengin-Lecreulx *et al.*, 1983; Anderson *et al.*, 1987) and β-hydroxymyristoyl-ACP is a precursor for phospholipid metabolism (Mohan *et al.*, 1994; Heath and Rock, 1996b; Gronow and Brade, 2001).

Figure 2.1. Model of the *E. coli* Kdo_2-lipid A biosynthesis pathway. The figure herein is displayed on the next page. Enzymes and metabolites are displayed with three text styles: upright bold indicates that these concentrations are fixed, upright plain indicates that these concentrations vary, and italics indicates that these species are not included in the model explicitly. Black arrows with barbed heads represent chemical reactions in which reactants are converted to products. Red arrows with closed heads represent enzymatic influences on chemical reaction rates, and red arrows with T-bar heads represent inhibitory influences. Variables represent model parameters. Numbers next to black arrows for bi-substrate reactions indicate which substrate is designated number 1 and number 2.

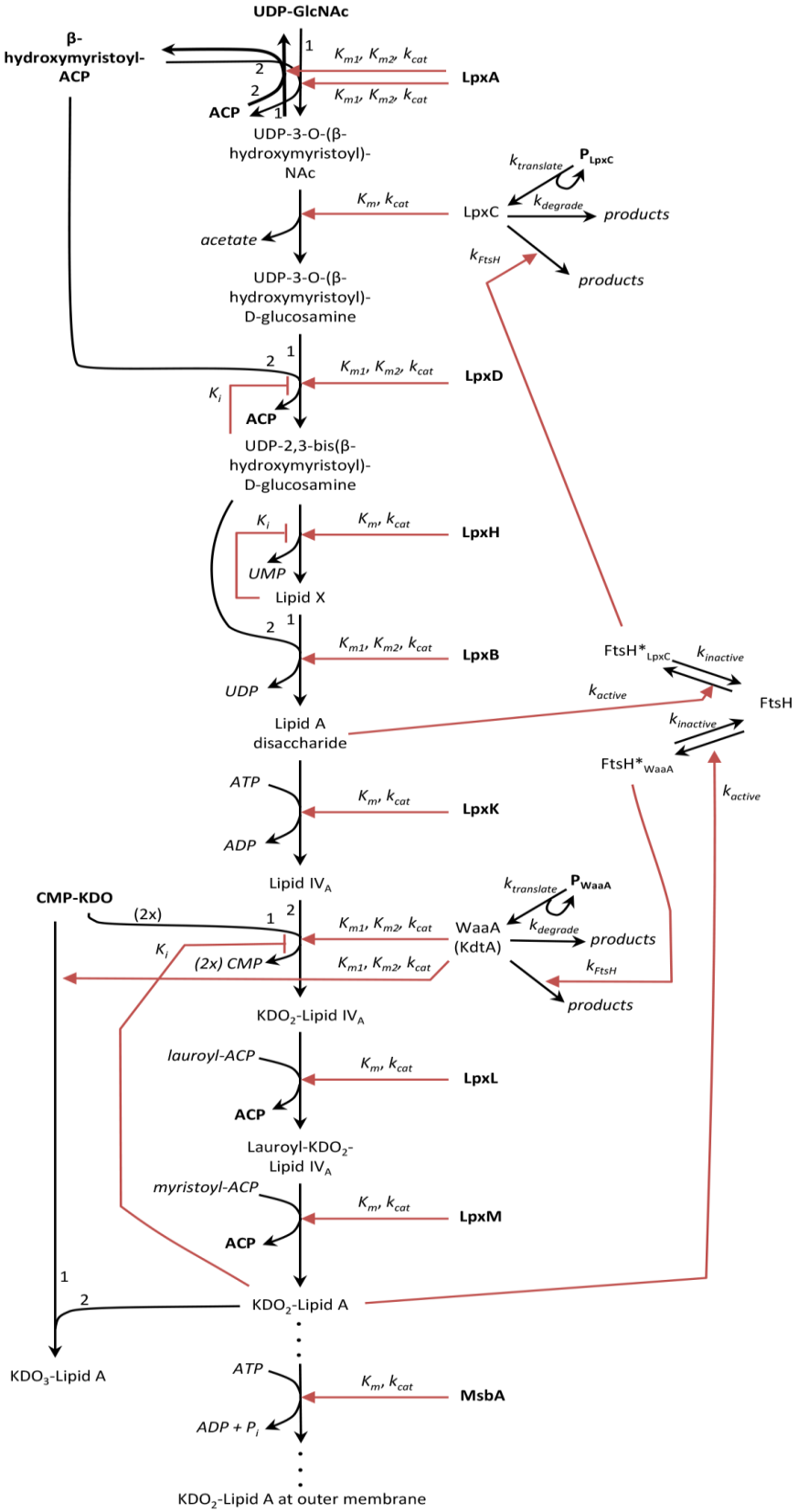
UDP-GlcNAc
β-hydroxymyristoyl-ACP
ACP
K_{m1}, K_{m2}, k_{cat}
LpxA
UDP-3-O-(β-hydroxymyristoyl)-NAc
$k_{translate}$
P_{LpxC}
$k_{degrade}$
K_m, k_{cat}
LpxC
products
acetate
k_{FtsH}
products
UDP-3-O-(β-hydroxymyristoyl)-D-glucosamine
LpxD
K_i
UDP-2,3-bis(β-hydroxymyristoyl)-D-glucosamine
LpxH
UMP
Lipid X
LpxB
UDP
FtsH*$_{LpxC}$
$k_{inactive}$
k_{active}
FtsH
Lipid A disaccharide
FtsH*$_{WaaA}$
ATP
ADP
LpxK
Lipid IV_A
CMP-KDO
(2x)
P_{WaaA}
WaaA (KdtA)
(2x) CMP
products
KDO_2-Lipid IV_A
lauroyl-ACP
LpxL
Lauroyl-KDO_2-Lipid IV_A
myristoyl-ACP
LpxM
KDO_2-Lipid A
KDO_3-Lipid A
MsbA
ADP + P_i
KDO_2-Lipid A at outer membrane

The initial three steps of the lipid A pathway occur in the cytoplasm. First, LpxA acylates UDP-GlcNAc with β-hydroxymyristoyl-ACP. This reaction has an unfavourable equilibrium constant of 0.01 *in vitro* (Anderson *et al.,* 1993), suggesting that the reaction products are not committed to proceed on through the lipid A pathway but may instead revert back into the pathway as substrates. The product is then deacetylated by LpxC in an essentially irreversible reaction, making this the first committed pathway step (Anderson *et al.,* 1988; Young *et al.,* 1995; Sorensen *et al.,* 1996; Barb and Zhou, 2008). For this and other reasons, LpxC is likely to be a primary biosynthesis control point (Anderson *et al.,* 1993) and has been of interest as a drug target. The third pathway enzyme, LpxD incorporates a second hydroxymyristate moiety onto the lipid A precursor (Kelly *et al.,* 1993; Bartling and Raetz, 2008). LpxD is similar to LpxA in that they are acyltransferases and consume the same β-hydroxymyristoyl-ACP substrate (Bartling and Raetz, 2008). Both LpxD reaction products inhibit the LpxD reaction, acting as either competitive or non-competitive inhibitors against each substrate (Bartling and Raetz, 2008). This was simplified in the model by only including non-competitive inhibition by UDP-2,3-bis(β-hydroxymyristoyl)-D-glucosamine. Ignoring inhibition by ACP had minimal effect on the results because its concentration was fixed.

The fourth and fifth lipid A biosynthesis steps are catalysed by the peripheral membrane proteins LpxH (Babinski *et al.,* 2002) and LpxB (Radika and Raetz, 1988). LpxH cleaves most of the UDP moiety to leave just a single phosphate on the remaining lipid portion, which is called lipid X. Then, LpxB combines lipid X with the preceding lipid metabolite, UDP-2,3-bis(β-hydroxymyristoyl)-D-glucosamine, to form lipid A disaccharide (Radika and Raetz, 1988).

The remaining four steps of lipid A biosynthesis are catalysed by integral membrane enzymes. LpxK is a kinase that phosphorylates lipid A disaccharide to produce lipid IV_A (Ray and Raetz, 1987; Garrett *et al.,* 1997). Remarkably, Lipid IV_A has been reported to be an endotoxin agonist in mouse cells and an endotoxin *antagonist* in human cells (Golenbock *et al.,* 1991). Next, WaaA (previously called KdtA), sequentially transfers two Kdo sugar residues to lipid IV_A to produce Kdo_2-lipid IV_A (Brozek *et al.,* 1989; Clementz and Raetz, 1991; Belunis and Raetz, 1992). WaaA has low substrate specificity, with the result that Kdo_2-lipid A can act as an inhibitor for this reaction (Belunis and Raetz, 1992), or as another possible WaaA substrate (Brozek *et al.,* 1989; Belunis and Raetz, 1992); in the latter case, the reaction produces "alternate lipid A", which the model defines as having more than 2 Kdo sugar residues. In addition, the WaaA reaction has been discovered to be reversible, based on the finding that *in vitro* combinations of the reaction products (enzyme, cytidine monophosphate (CMP), and Kdo_2-lipid IV_A) led to detectible concentrations of the Kdo-lipid IV_A intermediate (Belunis and Raetz, 1992). However, the authors only observed trace quantities of lipid IV_A even after prolonged incubations, thus, the forward reaction is likely to be strongly thermodynamically favourable, in which case, the *in vivo* back-reaction rate is probably negligible. For this reason, the model treats WaaA catalysis as being irreversible. Finally, the "late acyltransferases," LpxL (Clementz *et al.,* 1996) and LpxM (Brozek and Raetz, 1990; Clementz *et al.*, 1997), incorporate lauroyl and myristoyl chains to the Kdo_2-lipid IV_A, thus giving the final Kdo_2-lipid A product six acyl chains. Cells are still viable without LpxM, or without LpxL and with overexpressed LpxM (Vorachek-Warren *et al.,* 2002a). In cold-adapted *E. coli*, the LpxL function is replaced by LpxP, which incorporates a palmitoleate instead of the laurate, presumably as a way of adjusting membrane fluidity (Vorachek-Warren *et al.,* 2002b).

After synthesis, Kdo_2-lipid A is joined to core OS and then flipped from the inner leaflet of the inner membrane to the outer leaflet of the inner membrane by MsbA, an ABC transporter (Zhou *et al.,* 1998; Whitfield and Trent, 2014). Next, several enzymes add the O-antigen to form LPS, and then transport the LPS to the outer leaflet of the outer membrane (Wang and Quinn, 2010).

2.2.2 Lipid A biosynthesis regulation

Lipid A synthesis is regulated, at least in part, through controlled degradation of LpxC (Ogura *et al.,* 1999; Fuhrer *et al.,* 2006; Fuhrer *et al.,* 2007) and WaaA (Katz and Ron, 2008), both performed by FtsH. FtsH is an integral membrane AAA-type metalloprotease that degrades a wide variety of proteins. These include heat shock transcription factor RpoH (σ^{32}), phage λ proteins CII and CIII, and many misfolded proteins (Narberhaus *et al.,* 2009; Langklotz *et al.,* 2012). FtsH is an essential protein due to its role in regulating LpxC (Ogura *et al.,* 1999; Jayasekera *et al.,* 2000). Lipid A biosynthesis regulation is less well established than is the synthetic pathway, so these aspects of the model are described in great detail.

The model assumes that FtsH can reversibly convert between an inactive state, an active state for degrading LpxC, and a different active state for degrading WaaA (denoted FtsH, FtsH*$_{LpxC}$, and FtsH*$_{WaaA}$, respectively). This assumption of substrate-specific FtsH activation is supported by several findings: (*i*) FtsH degradation of RpoH and λ CII is substrate-specific, accomplished through separate adapter proteins (Ito and Akiyama, 2005; Langklotz *et al.,* 2012), (*ii*) neither increased nor decreased FtsH degradation of LpxC have a significant effect on the intracellular concentration of RpoH (Ogura *et al.,* 1999) or the activity of WaaA (Sorensen *et al.,* 1996), and (*iii*) LpxC is degraded more slowly at higher temperatures whereas WaaA is degraded more rapidly

at higher temperatures (Katz and Ron, 2008; Schakermann *et al.,* 2013). Substrate-specific activation of FtsH for LpxC may occur through YciM acting as an LpxC adapter protein (Mahalakshmi *et al.,* 2014).

The model also assumes that the regulatory signal that directs FtsH degradation of LpxC arises from the concentration of lipid A disaccharide. Again, this is based on several findings. Firstly, *E. coli* strains that have decreased LpxA, LpxC, or LpxD function, whether through temperature-sensitive mutants or chemical inhibition, exhibit decreased lipid A content and reduced LpxC degradation (Galloway and Raetz, 1990; Anderson *et al.,* 1993; Onishi *et al.,* 1996; Sorensen *et al.,* 1996). These suggest that the feedback source is downstream of LpxD. Secondly, chemically inhibiting CMP-Kdo production (Goldman *et al.,* 1987) blocks the lipid A biosynthesis pathway at the WaaA point. This was found to cause lipid IV_A accumulation but did not affect LpxC activity (Sorensen *et al.,* 1996). This suggests that the feedback source is upstream of lipid IV_A. Three metabolites fit these two criteria, UDP-2,3-bis(β-hydroxymyristoyl)-D-glucosamine, lipid X, and lipid A disaccharide. Of these, UDP-2,3-bis(β-hydroxymyristoyl)-D-glucosamine was already regulated by product inhibition (Bartling and Raetz, 2008), which makes its concentration a poor indicator of pathway flux and hence a poor candidate. Preliminary simulations that represented *ftsH* knock-out mutants, and hence did not include FtsH regulation, exhibited lipid A disaccharide accumulation (Fig. 2.2). This suggested that the feedback source for FtsH-mediated LpxC degradation is lipid A disaccharide.

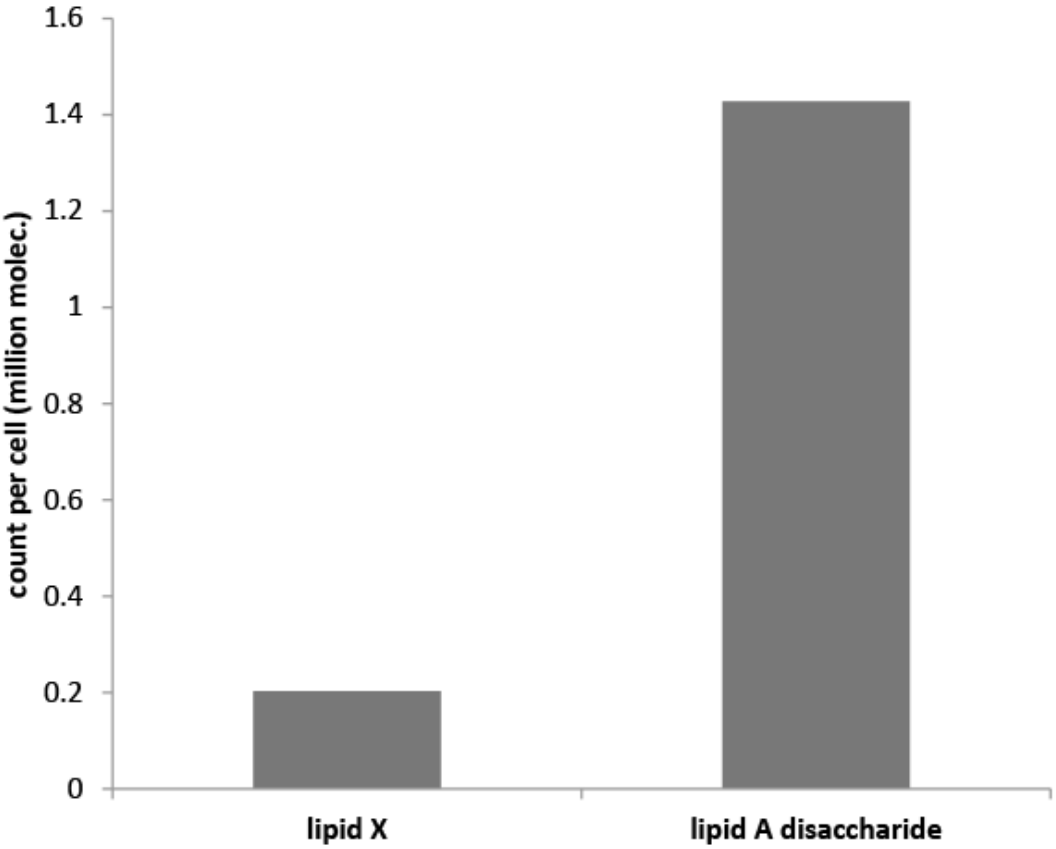

Figure 2.2. Lipid A disaccharide accumulation in an *in silico ftsH* mutant. Bars represent intracellular counts of lipid X and lipid A disaccharide at the end of a single cell generation (30 min) from preliminary model results. The model used the scheme presented in Fig. 2.1 and parameters listed in Table 2.1, with the exceptions: the FtsH count was set to zero, the LpxC and WaaA counts were set to their steady-state levels in the absence of FtsH degradation (1540 and 978, respectively and described below), and all metabolites were started with zero molecules. Although not displayed here, the lipid X count had stabilised at a constant level, while the lipid A disaccharide count was increasing at a constant rate of 924 molecules/s.

Finally, the model assumes that the regulatory signal for FtsH degradation of WaaA arises from Kdo_2-lipid A that is inside the inner membrane. The model utilized Kdo_2-lipid A rather than its precursors because the two enzymes downstream of WaaA, which are LpxL and LpxM, are non-essential (Vorachek-Warren *et al.*, 2002a), making their substrates unlikely activators. Also, Kdo_2-lipid A was chosen before it has been transported to the outer membrane, rather than afterwards, because bacterial cells are known to regulate excess lipid A in their outer membrane by shedding it into the environment (Mattsby-Baltzer *et al.*, 1991).

Other regulatory signals impinge upon the lipid A biosynthesis pathway as well but are outside of the scope of this chapter. In particular, modifications to the FabZ and FabI enzyme levels, used for phospholipid synthesis, have been reported to affect the concentration of LpxC and hence affect the rate of lipid A production (this was investigated and reported in Chapter 3 and the findings therein only supplements the results presented in this chapter) (Mohan *et al.*, 1994; Ogura *et al.*, 1999; Zeng *et al.*, 2013). Thus, by assuming that FabZ and FabI are maintained at wild-type conditions, and that there are no feedback processes from the lipid A pathway that affect the FabZ or FabI regions of the phospholipid pathway, the model can legitimately ignore these additional regulatory signals in this chapter.

2.3 MODEL ASSUMPTIONS, EQUATIONS AND PARAMETERS

The interactions of individual substrates and enzymes for a single *E. coli* cell were modelled at steady state based on Michaelis-Menten and mass action kinetics. It was assumed that the volume of a cell is 6.7×10^{-16} litres (Cayley *et al.*, 1991) (thus 1 molecule represents 2.5 nM, 1000 molecules represents 2.5 µM, and 10^6 molecules represents 2.5 mM). Unless specified otherwise, the model assumes a 30 minute (1800

s) doubling time, which is the experimental value in rich media (Plank and Harvey, 1979; Mackie, 2013). For the most part, the model did not account for protein synthesis, protein degradation, or cell volume growth during a cell generation. These approximations are legitimate because metabolic enzyme concentrations for constitutive enzymes likely remain constant over the course of the cell cycle. Table 2.1 lists all model parameters, along with the relevant data sources.

2.3.1 Substrate concentrations

Lipid A metabolism was investigated with either excess or limiting concentrations of the UDP-GlcNAc, β-hydroxymyristoyl-ACP, and CMP-Kdo substrates. The stoichiometric ratios of these substrates to lipid A are 2:1, 4:1, and 2:1, respectively, due to consumption of multiple copies and/or lipid dimerization by LpxB. The first two of these substrates are also precursors for other biosynthetic pathways (Mengin-Lecreulx *et al.*, 1983; Anderson *et al.*, 1987; Heath and Rock, 1996b; Yokoyama *et al.*, 2008), so their relative concentrations are controlled by factors outside of the model simulations. To this regard, their levels were kept constant at 2 million molecules (5 mM) throughout most simulations, which led to substrate saturation conditions. Additionally, the ACP level was fixed to 1024 molecules, based on proteomic results (Ishihama *et al.*, 2008).

2.3.2 Enzyme abundance

The LpxA, LpxD, WaaA, MsbA, and FtsH protein copy numbers used for simulations were derived from mass spectrometry proteomic data collected on *E. coli* cytosolic fractions (Ishihama *et al.*, 2008). Several of these are integral membrane proteins, so their experimental protein counts are likely to be lower limits for their true counts in a cell.

Table 2.1: Abundance and kinetic parameters used in the lipid A biosynthesis model.

Species	Location	Abundance (molec./cell)	K_m or K_{m1} (mM)	K_{m2} (mM)	k_{cat} (s^{-1})	Notes and other Parameters
UDP-GlcNAc		2,000,000[a]				excess concentration
β-hydroxymyristoyl-ACP		2,000,000[a]				excess concentration
CMP-Kdo		2,000,000[a]				excess concentration
ACP		1024[b]				actual concentration
LpxA	cyto.	664[b]	0.82[f]	0.0016[m]	7.17[f]	
			0.82	0.0016	717	back reaction
LpxC	cyto.	385	0.00019[g]		3.3[l]	$k_{translate}$ = 0.148 s^{-1} $k_{degrade}$ = 9.62×10^{-5} s^{-1}
LpxD	cyto.	453[b]	0.0025[h]	0.0032[h]	23[h]	K_i = 0.0094 mM[h]
LpxH	p.m.	177[c]	0.0617[c]		47	K_i = 0.015 mM
LpxB	p.m.	384[d]	0.287[d]	0.381[d]	129	
LpxK	i.m.	432	0.04[i]		2.1	
WaaA	i.m.	153[b]	0.088[j]	0.052[j]	16.7	K_i = 0.0317 mM $k_{translate}$ = 0.176 s^{-1} $k_{degrade}$ = 1.8×10^{-4} s^{-1}
			0.088[j]	0.052[j]	1.9	substrate is Kdo_2-lipid A
LpxL	i.m.	928[e]	0.015[k]		131[k]	
LpxM	i.m.	3720	0.00275		0.6	
MsbA	i.m.	206[b]	0.021		166	
FtsH	i.m.	579[b]				
$FtsH^*_{LpxC}$	i.m.	-	k_{FtsH} = 2.0 $mM^{-1}s^{-1}$			k_{active} = 0.14 $mM^{-1}s^{-1}$ $k_{inactive}$ = 0.1 s^{-1}
$FtsH^*_{WaaA}$	i.m.	-	k_{FtsH} = 6.8 $mM^{-1}s^{-1}$			k_{active} = 32.3 $mM^{-1}s^{-1}$ $k_{inactive}$ = 0.1 s^{-1}

These values are for *E. coli* cells in rich media. Location abbreviations are: cyto. for cytoplasm, p.m. for peripheral membrane, and i.m. for integral membrane (locations are not part of the model). Data estimation methods are presented in the main text. Data are from: **(a)** substrate molecules **(b)** Ishihama *et al.* (2008), **(c)** Babinski *et al.* (2002), **(d)** Metzger and Raetz (2009), **(e)** Clementz *et al.* (1996), **(f)** Wyckoff and Raetz (1999), **(g)** Hernick *et al.* (2005), **(h)** Bartling and Raetz (2008), **(i)** Fig. 5 in Ray and Raetz (1987), **(j)** Belunis and Raetz (1992), **(k)** Six *et al.* (2008), **(l)** Jackman *et al.* (1999), **(m)** Anderson *et al.* (1993). Parameters that do not have citations are discussed in the main text.

The same proteomic data source from Ishihama *et al.* (2008) was initially used for the copy number of LpxM, another integral membrane protein, but then had to be increased by 20-fold as described below. The LpxC, LpxH, and LpxB protein counts were calculated from protein purification data (Hyland *et al.*, 1997; Babinski *et al.*, 2002; Metzger and Raetz, 2009) along with the assumption that an average *E. coli* cytoplasm contains approximately 1.9 million protein molecules (Sundararaj *et al.*, 2004). For instance, when *lpxC* gene from *Pseudomonas aeruginosa* was cloned via a plasmid vector in an *E. coli* host (Hyland *et al.*, 1997), it was reported to be overexpressed between 900 and 1000 fold representing 3.7 mg (14% yield) of 130 mg of total protein in membrane-free crude lysate. By assuming that the protein was expressed 950 folds, this indicates that LpxC comprise of about 0.02% of cytoplasmic proteins given that there are about 1.9 million proteins present in the cytoplasm of *E. coli* (Sundararaj *et al.*, 2004). Similarly, the LpxL protein count was calculated from protein purification experiments (Clementz *et al.*, 1996) and the estimate that an *E. coli* membrane contains 580,000 proteins (Sundararaj *et al.*, 2004).

The LpxK protein count was estimated using information about MsbA. These proteins are co-transcribed (Garrett *et al.*, 1998) implying that their transcripts are synthesized at similar rates. Thus, differences in their expression rates depend on the relative stability of their transcripts and on the translation rates for individual proteins. The MsbA and LpxK transcript half-lives have been reported as 3.2 min and 3.8 min respectively (Bernstein *et al.*, 2002) from which their mean lifetimes were calculated as 277 s and 329 s. Given that the average translation rate is 20 amino acids per second (Alberts *et al.*, 2002), and that they comprise 582 (Karow and Georgopoulos, 1993) and 328 amino acids respectively (Garrett *et al.*, 1997), it should take about 29 s and 16 s for their translations. This means that about 9.6 MsbA proteins and 20 LpxK proteins are translated over the lifetimes of their respective mRNAs. Thus, LpxK is likely to be

synthesized about 2.1 times faster than MsbA. Both LpxK and MsbA are membrane proteins, so it was assumed that they had similar degradation rates (Akiyama, 2009). This meant that the synthesis rate ratio also represented the protein concentration ratio. MsbA has an abundance of about 206 molecules per *E. coli* cell (Ishihama *et al.*, 2008), from which it was calculated that the LpxK abundance is about 432 molecules.

2.3.3 Enzyme kinetics

All pathway reactions were modelled using single-substrate or bi-substrate Michaelis-Menten mechanisms. In most cases, reversibility of reactions were ignored. This can lead to misleading results in metabolic models because it ignores feedback effects that arise from product inhibition and hence can prevent models from attaining a steady-state (Fell, 1971; Fell and Sauro, 1985). However, it was legitimate here because the model included regulatory feedbacks that extend over most of the pathway length. These are alternative ways to enable models attain steady-state and, in fact, are typically more effective than reversible reactions (Cornish-Bowden and Cardenas, 2001). Also, most of the lipid A reactions are likely to be nearly irreversible, due to either favourable energetics or much more abundant substrates than products (e.g. the phosphorylation reaction catalysed by LpxK is effectively irreversible because ATP is abundant in cells whereas ADP is not).

Single-substrate Michaelis-Menten kinetics were employed for the LpxC, LpxK, LpxL, LpxM, and MsbA steps. Here, the metabolite flux is

$$\frac{d[\mathrm{P}]}{dt} = -\frac{d[\mathrm{S}]}{dt} = \frac{k_{cat}[\mathrm{E}][\mathrm{S}]}{K_m + [\mathrm{S}]} \qquad (1)$$

where [S] is the substrate concentration, [P] is the product concentration, [E] is the total enzyme concentration, k_{cat} is the enzyme catalytic rate constant, and K_m is the Michaelis constant. Most of these k_{cat} and K_m values have been published using data from *in vitro* experiments (Table 2.1), although some of them had to be estimated. (*i*) The specific activity of LpxK in crude *E. coli* membrane extract was estimated to be 22 nmol/min/mg in a plasmid-containing strain but 7-fold lower in wild type (Garrett *et al.*, 1998). There are about 432 LpxK molecules per cell and *E. coli* membranes include about 580,000 individual proteins (Sundararaj *et al.*, 2004) so, the LpxK purity in crude membrane is about 0.074%. Thus, the pure wild-type specific activity is about 4 µmol/min/mg, from which k_{cat} is about 2.1 s^{-1}. Furthermore, the LpxK K_m value was derived as 40 µM from Fig. 5 in Ray and Raetz (1987). Although K_m estimations from crude samples are prone to inaccuracies when the substrate can be catalysed by other enzymes in the lysates, there is no evidence of such competition for the LpxK substrate. (*ii*) The LpxM catalytic rate constant, k_{cat}, was estimated as 0.6 s^{-1} from the specific activity of the enzyme in crude lysates (Brozek and Raetz, 1990), much as was conducted for LpxK. The LpxM K_m value was also estimated from data presented in Fig. 6 of Clementz *et al.* (1997). To do this, it was necessary to simulate Clementz *et al.*'s experiment using COPASI (Mendes *et al.*, 2009), with the same enzyme and substrate concentrations that they used (0.1 µg/mL and 25 µM for protein and Kdo_2-lipid IV_A respectively in a 20 µL reaction mixture), from which the K_m value that corresponded to their figure results at a time of 30 minutes was identified. (*iii*) The MsbA catalysed translocation of Kdo_2-lipid A across the inner membrane was modelled as another Michaelis-Menten process, setting its K_m value to 0.021 mM and its k_{cat} value to 166 s^{-1} based on data provided in Fig. 6 of Doerrler and Raetz (2002).

Single-substrate Michaelis-Menten kinetics with inhibition was employed for the LpxH enzyme. In this case, the metabolite flux is

$$\frac{d[\mathrm{P}]}{dt} = -\frac{d[\mathrm{S}]}{dt} = \frac{k_{cat}[\mathrm{E}][\mathrm{S}]}{\left(K_m + [\mathrm{S}]\right)\left(1 + \frac{[\mathrm{P}]}{K_i}\right)} \quad (2)$$

where K_i is the inhibition constant and the other parameters are the same as in eq. 1. Assays conducted on LpxH purified to 60% homogeneity displayed a specific activity of 63.2 µmol/min/mg (Babinski *et al.*, 2002). This implies that the pure enzyme specific activity is about 105 µmol/min/mg, which is combined with the LpxH molecular weight of 26.8 kDa (Babinski *et al.*, 2002) to yield its k_{cat} as about 47 s^{-1}. The estimation of the K_i value is discussed below.

Bi-substrate Michaelis-Menten kinetics was used for the forward LpxA, reverse LpxA, LpxB, and WaaA catalysis of Kdo_2-lipid A steps. Treating the forward and reverse LpxA reactions as independent irreversible reactions is legitimate in non-spatial models, such as this, because doing so does not introduce any new approximations (although, this is not true for spatial models (Andrews and Bray, 2004)). Most bi-substrate enzymatic reactions follow either a sequential or ping-pong mechanism (Marangoni, 2003). In the sequential mechanism, the enzyme forms a ternary complex with both substrates before catalysing the reaction. In the ping-pong mechanism, the enzyme binds one substrate, forms one product, and then binds the second substrate and forms the second product. The only bi-substrate reactions in the lipid A pathway that have been investigated in sufficient detail to determine mechanisms are the steps catalysed by LpxA (Wyckoff and Raetz, 1999) and LpxD (Bartling and Raetz, 2008), both of which were found to follow the sequential mechanism. Lacking further experimental evidence, the model assumed sequential mechanisms for the other bi-substrate reactions in the lipid A pathway as well. The sequential mechanism metabolite flux is

$$\frac{d[\mathrm{P}]}{dt} = -\frac{d[\mathrm{S}_1]}{dt} = -\frac{d[\mathrm{S}_2]}{dt} = \frac{k_{cat}[\mathrm{E}][\mathrm{S}_1][\mathrm{S}_2]}{\left(K_{m_1} + [\mathrm{S}_1]\right)\left(K_{m_2} + [\mathrm{S}_2]\right)} \quad (3)$$

where $[S_1]$ and $[S_2]$ are the two substrate concentrations with respective Michaelis-Menten constants K_{m1} and K_{m2}. In some cases, these parameters needed to be estimated. (*i*) The LpxA kinetic parameters were determined previously for the forward reaction (Anderson *et al.,* 1993; Wyckoff and Raetz, 1999)**,** but not for the reverse reaction. Thus, the model assumed the same K_m values for the reverse reaction as for the forward reaction (the K_m of ACP was set to that for β-hydroxymyristoyl-ACP, and K_m of UDP-3-O-[β-hydroxymyristoyl]-NAc to that for UDP-GlcNAc) based upon the likelihood that the enzyme binding affinities are not substantially affected by the acyl group transfer. However, the reverse reaction k_{cat} value was set to 100 times that of the forward reaction to account for the reaction's unfavourable equilibrium constant of approximately 0.01 (Anderson *et al.,* 1993). (*ii*) The LpxB k_{cat} value was estimated from the specific activity of LpxB purified to near homogeneity (Metzger and Raetz, 2009) much as was done for LpxH, which resulted in a k_{cat} value of 129 s^{-1}. (*iii*) The WaaA specificity for Kdo_2-lipid A is 8.7 fold lower than for lipid IV_A (Belunis and Raetz, 1992). To account for this, the k_{cat} value for the former reaction was reduced by 8.7 fold while keeping other reaction constants the same.

Finally, the model utilized bi-substrate Michaelis-Menten kinetics with inhibition for the LpxD and WaaA steps. Assuming the sequential mechanism again, which was the correct mechanism for LpxD, the metabolite flux is

$$\frac{d[\mathrm{P}]}{dt} = -\frac{d[\mathrm{S}_1]}{dt} = -\frac{d[\mathrm{S}_2]}{dt} = \frac{k_{cat}[\mathrm{E}][\mathrm{S}_1][\mathrm{S}_2]}{\left(K_{m_1}+[\mathrm{S}_1]\right)\left(K_{m_2}+[\mathrm{S}_2]\right)\left(1+\frac{[\mathrm{P}]}{K_i}\right)} \qquad (4)$$

The WaaA k_{cat} value was computed as 16.7 s^{-1} from the specific activity of the purified protein much as was done for LpxH (Belunis and Raetz, 1992). The WaaA inhibition constant was computed from results by Belunis and Raetz (1992) which indicated that 100 µM of lipid A inhibited the WaaA reaction by 24.1% *in vitro*. Their experimental

conditions involved purified enzyme and substrates, thus excluding the possibility of FtsH playing a role in the inhibition. Whilst assuming a non-competitive inhibition (eq. 4), in which case K_m is constant, it was derived that at 100 μM of inhibitor and excess CMP-Kdo, a 24.1% reduction in the reaction rate implies that K_i is about 0.315 mM.

2.3.4 LpxC and WaaA synthesis and degradation

The model included translation and degradation reactions for LpxC and WaaA in order to explore the effects of their regulation via FtsH proteolysis. As in the rest of the model, the model accounted for degradative protein turnover within cells, but not protein loss through sequestration into daughter cells or the translation that is required to replace those proteins.

LpxC and WaaA synthesis were modelled with zero order reaction kinetics in which the production rate is constant. This approach combines transcription, translation, and any translocation into a single reaction step. The degradation of these proteins were also modelled with a first order reaction for degradation that is not catalysed by FtsH, and also an independent reaction obeying mass action kinetics for degradation that is catalysed by FtsH (Michaelis-Menten kinetics might be more appropriate, but those parameters cannot be computed from available data). Together, these processes combine to give the net production rate for each of these proteins as

$$\frac{d[\mathrm{P}]}{dt} = k_{translate} - k_{degrade}[\mathrm{P}] - k_{FtsH}[\mathrm{FtsH^*}][\mathrm{P}] \qquad (5)$$

where [P] is the concentration of the LpxC or WaaA protein, $k_{translate}$ is the production rate constant, $k_{degrade}$ is the rate constant for uncatalysed degradation, and k_{FtsH} is the rate constant for FtsH degradation.

To determine the production and degradation parameters for LpxC, initial analyses were conducted on results presented in Schakermann *et al* (2013) which indicated that LpxC in wild-type *E. coli* can have a half-life of 120 minutes under nutrient and temperature conditions that lead to rapid growth. Thus, it was assumed that the long LpxC half-life arose because FtsH was essentially inactive under these conditions. This implies that the uncatalysed LpxC degradation has a half-life of about 120 minutes and $k_{degrade}$ is about 9.62×10^{-5} s^{-1}. Separately, it has been reported that cells with inhibited FtsH activity using a temperature sensitive mutant, exhibit 4-fold elevated LpxC concentrations (Ogura *et al.,* 1999) thus, increasing LpxC counts from about 385 molecules to about 1540 molecules. Combining this molecule count with the $k_{degrade}$ value and the assumption that [FtsH*$_{LpxC}$] equals zero in this mutant, enables eq. 5 to be solved for steady-state conditions to give a $k_{translate}$ value of about 0.148 molecules/s. Next, combining the $k_{degrade}$, $k_{translate}$, and the wild-type LpxC count of 385 molecules enables eq. 5 to solved for steady-state to give that k_{FtsH}[FtsH*$_{LpxC}$] is 2.89×10^{-4} s^{-1}. It is impossible to solve for k_{FtsH} by itself from the available information, but the rationale for its estimation are presented below.

The WaaA synthesis and degradation parameters were computed similarly. First, a mutant without FtsH maintained about 72% of its WaaA concentration after 30 minutes (Katz and Ron, 2008), from which it was derived that $k_{degrade}$ is about 1.8×10^{-4} s^{-1}. Next, the half-life of WaaA in wild-type cells under optimal growth conditions is about 10 minutes (Katz and Ron, 2008). This gives the combined degradation rate constant, $k_{degrade}$ + k_{FtsH}[FtsH*$_{WaaA}$], as approximately 1.15×10^{-3} s^{-1}, implying that the catalysed degradation rate constant is about 9.8×10^{-4} s^{-1}. Combining the total degradation rate with the wild-type WaaA abundance of 153 molecules per cell gives the protein translation rate, $k_{translate}$, as 0.176 molecules/s.

2.3.5 FtsH activation and inactivation

The model treats FtsH activation in a substrate-specific manner, but with the constraint that the total FtsH count per cell is conserved at 579 molecules (Ishihama *et al.,* 2008). Furthermore, the model did not account for FtsH sequestration through activation for other degradation targets, such as RpoH or misfolded proteins. FtsH activation and inactivation were modelled with mass action kinetics, meaning that net FtsH activation towards a specific substrate was modelled according to

$$\frac{d[\text{FtsH*}]}{dt} = k_{active}[\text{activator}][\text{FtsH}] - k_{inactive}[\text{FtsH*}] \quad (6)$$

where [FtsH*] represents the concentration of a substrate-specific active form of FtsH, [activator] represents the concentration of the substrate-specific activator (lipid A disaccharide for the LpxC substrate and Kdo_2-lipid A for the WaaA substrate), and [FtsH] represents the concentration of inactive FtsH. The first term on the right hand side represents the activation rate and the second represents the inactivation rate.

The FtsH proteolysis rate, for either LpxC or WaaA, depends on three parameters, k_{active}, $k_{inactive}$, and k_{FtsH}. However, the available experimental data only enabled the quantification of the product k_{FtsH}[FtsH*], for each substrate, with values given above. Thus, the system is underdetermined, with multiple possible combinations of parameters that are each equally good at agreeing with the available data. This was addressed by making a few assumptions. First, it was assumed that during growth on rich media, 10% of the total FtsH is activated for degradation of LpxC, 10% is activated for degradation of WaaA, and 80% is inactive (i.e. there are 58 copies of $FtsH^*_{LpxC}$, 58 copies of $FtsH^*_{WaaA}$, and 463 copies of inactive FtsH). This is intuitively sensible

because it assumes a reasonably large reservoir of inactive FtsH to allow for strong regulatory control and other proteolysis tasks. Combining this assumption with the prior values for the k_{FtsH}[FtsH*] products yield k_{FtsH} of 2.0 $mM^{-1}s^{-1}$ for LpxC and k_{FtsH} of 6.8 $mM^{-1}s^{-1}$ for WaaA. Secondly, it was assumed that both $k_{inactive}$ values equal 0.1 s^{-1}. This gives the active states a 10 s lifetime, which is fast enough to enable rapid control. Next, the k_{active} was derived from the steady-state version of eq. 6, while substituting in this inactivation rate constant, the assumed FtsH* and FtsH concentrations, and the steady-state activator concentrations that arose from simulations in which the LpxC and WaaA enzyme counts were fixed to the values listed in Table 2.1 (activator counts were 35,600 and 155 molecules, respectively). The results are that k_{active} is 0.14 $mM^{-1}s^{-1}$ for LpxC and 32.3 $mM^{-1}s^{-1}$ for WaaA. It should be noted that the assumptions made here do not affect the model's steady-state condition at all. In other words, the estimates are necessary for running simulations but do not affect the results that are presented below.

2.4 METHODS

2.4.1 Simulations

Simulations were performed with non-spatial deterministic methods using the COPASI software (Mendes *et al.,* 2009). This level of detail was determined to be adequate because preliminary simulations using spatial stochastic simulations (with Smoldyn (Andrews *et al.,* 2010) and non-spatial stochastic simulations (with StochKit (Sanft *et al.,* 2011) yielded essentially identical results. It was assumed that the volume of a cell is 6.7×10^{-16} litres (Cayley *et al.,* 1991) and a cell generation time equal 30 min.

2.4.2 Experimental procedures

2.4.2.1 Bacterial strain and growth conditions

An *E. coli* K-12 strain AG1 (*recA1, endA1, gyrA96, thi-1, hsdR17*(r_K^- m_K^+)*, supE44, relA1*) containing a plasmid (pCA24N) (Kitagawa *et al.,* 2005) bearing *E. coli* LpxK-GFP gene fusion (to the C-terminus) was obtained from the National BioResource Project (NIG) Japan. Cells were grown at 30°C in Luria-Bertani (LB) (10 g tryptone, 5 g yeast extract, 5 g NaCl per litre) containing 20 µg/ml of chloramphenicol and when required, protein expression was induced using varying concentrations of IPTG (Sigma, UK).

2.4.2.2 Preparation of cell extracts

Cell extracts were prepared as described previously (Sorensen *et al.,* 1996; Zeng *et al.,* 2013). Briefly, an overnight culture was inoculated into fresh LB containing different concentrations of IPTG at an OD_{600} of 0.05 and grown to mid-log phase (OD_{600} = 0.5). The respective cultures were normalized to the same OD_{600} of 0.5. 3 ml of normalized culture was centrifuged using a benchtop centrifuge at maximum speed (13,000 rpm) for 1 min, and the cell pellets re-suspended in 100 µl of 2x Laemmli sample buffer (Sigma, UK). The samples were heated at 99°C for 10 min prior to centrifugation for 5 min. The supernatants were collected for Western blot analysis.

2.4.2.3 Western blot

20 µl of each sample were loaded onto a 10% SDS-polyacrylamide gel. Following electrophoresis, proteins were transferred to a PVDF membrane using the Bio-Rad Trans-Blot Turbo system. An LpxC antiserum generated in rabbit (a generous gift from

Prof. Franz Narberhaus) and a secondary anti-rabbit peroxidase-linked antibody (Sigma, UK) were used for immunodetection at dilutions of 1:20000 and 1:10000 respectively. Blots were developed using the ECL chemiluminiscent reagents (Bio-Rad) and the signals detected using the ChemiDoc MP system (Bio-Rad).

2.5 MODEL RESULTS

2.5.1 Model adjustment

The initial model, defined using literature parameter values where available, exhibited a lipid A production rate that was too low. Also, several internal metabolite concentrations accumulated to very high levels. These problems were addressed with two model adjustments.

2.5.1.1 LpxM enzyme count

Initial model simulations only produced about 20% of the 1 million lipid A molecules that *E. coli* cells actually produce per generation. This did not change even if the FtsH degradation of LpxC and WaaA and all negative feedbacks were removed. This slow production rate arose from LpxM acting as a bottleneck in the pathway as seen by its substrate increasing linearly over time, rather than stabilizing at a steady-state level. This may indicate that cells have more than the 186 LpxM proteins that proteomic research on the cell cytoplasm indicated (Ishihama *et al.,* 2008), which would not be surprising because LpxM is an integral membrane protein. Alternatively, it may be that other enzymes acylate LpxM's substrate in parallel to LpxM; in particular, LpxL and LpxP can catalyse essentially the same lipid A synthesis reaction (Clementz *et al.,* 1997; Vorachek-Warren *et al.,* 2002b). Whilst assuming the former explanation, the LpxM

molecule count in the model was increased by 20 fold, from 186 to 3720. This removed substrate accumulation upstream of LpxM and caused the model to produce lipid A at about 1 million molecules per generation.

2.5.1.2 LpxH product inhibition

Initial simulations also resulted in high lipid X concentrations which rose over the course of several cell generations and stabilized at about 400,000 copies. In contrast, 2000 copies were observed *in vivo* (Takayama *et al.,* 1983). From observations, this accumulation arose because LpxH rapidly diverted UDP-2,3-bis(β-hydroxymyristoyl)-D-glucosamine towards lipid X, while LpxB only consumed lipid X in a 1:1 ratio with UDP-2,3-bis(β-hydroxymyristoyl)-D-glucosamine. For this reason, it was assumed that LpxH is regulated through product inhibition, as described above. The experimental lipid X count was reproduced when the K_i value was set to 0.2 μM; however, this value is unusually small and it created a bottleneck in the pathway resulting in an accumulation of the LpxC product and decreased lipid A production (negative feedback at LpxD prevents accumulation of its product, backing the accumulation up to the LpxC product instead). Thus, it was imperative to decrease the LpxH inhibition by increasing K_i.

As mentioned above, mutants with inactive FtsH exhibit 4-fold increased LpxC concentrations (Ogura *et al.,* 1999); they were also reported to produce 32% more lipid A (Table 1 of Ogura *et al.* (1999), comparing their AR3317 at 30°C vs. 42°C, or their AR3289 vs. AR3291). The LpxH inhibition constant was set so that the model would reproduce this result, which turned out to be a K_i value of 0.015 mM. This value was large enough that it did not cause the LpxC product to accumulate in wild-type cells. However, the LpxC product still accumulated in cells without FtsH due to the higher

metabolite flux through the LpxC step and the lack of product inhibition at this step. This K_i value caused the steady-state lipid X concentration to be about 22,000 molecules in either wild-type or FtsH mutant cells, which is much larger than the 2000 that were observed experimentally (Takayama *et al.*, 1983). Further investigation indicated that this difference cannot be eliminated simply by adjusting enzyme kinetic parameters without creating large metabolite accumulations, which suggests that this region of the biosynthesis pathway includes dynamics that are not in the model. For example, the difference could arise from metabolic channelling between the LpxH and LpxB enzymes.

2.5.2 Comparison of model with experiment

2.5.2.1 Mutant with defective LpxA

Anderson *et al*. (1993) reported that cells with defective LpxA, which have at least 150-fold lower LpxA specific activities, have 5- to 10-fold increased LpxC concentrations and an LPS content that is reduced by approximately 30% (their strain SM101 at 30°C). This perturbation was simulated with the model by decreasing the LpxA k_{cat} value by 150 fold to 0.048 s^{-1}. The simulation resulted in a 3.9 fold increase in LpxC levels, in reasonably close agreement with experiment. This is essentially the maximum LpxC increase that the model can produce under any condition, arising from model assumption that cells with completely inactive FtsH exhibit 4-fold higher LpxC concentrations (Ogura *et al.*, 1999). However, the model only produced 24,000 lipid A molecules per generation rather than the 1.1 million molecules that it produces with the standard parameters (Table 2.1), which is a reduction of 98%. These results were unaffected irrespective of a decrement in the LpxA reverse reaction k_{cat} value or not, or even if the reverse reaction was removed altogether. This limitation is clarified by

noting that the reaction velocity of the LpxA step is simply k_{cat}[LpxA] in these conditions from eq. 1, which works out to 57,000 product molecules per generation; these need to dimerize to form lipid A, meaning that the LpxA step limits lipid A production to only 29,000 molecules per generation, in close agreement with the model result. Thus, Anderson *et al.*'s observation that LpxA in the SM101 strain exhibits a 150-fold reduced k_{cat} value but reduces the lipid A production rate by only 30%, is not compatible with the model. This is because their results cannot arise from the assumed LpxA protein count or k_{cat} parameters. The disagreement implies that these parameters are incorrect by more than an order of magnitude which seems unlikely, or potentially, there is an alternate biosynthetic pathway; for example, perhaps LpxD can catalyse what is normally the LpxA step since they both utilize β-hydroxymyristoyl-ACP as substrate.

2.5.2.2 Inhibition of LpxC

CHIR-090 is a powerful antibiotic that controls *E. coli* and *P. aeruginosa* growth with efficacy that is similar to the clinically-relevant drug ciprofloxacin (Barb and Zhou, 2008). Its minimum inhibitory concentration (MIC) on *E. coli*, meaning the lowest drug concentration required to inhibit visible growth, is between 0.20 and 0.25 μg/ml (Barb *et al.,* 2007; Zeng *et al.,* 2013). Barb *et al.* reported that CHIR-090 acts by inhibiting LpxC through the two-step mechanism (Barb *et al.,* 2007)

$$\mathrm{LpxC} + \mathrm{I} \underset{k_4}{\overset{k_3}{\rightleftharpoons}} \mathrm{LpxC\text{-}I} \underset{k_6}{\overset{k_5}{\rightleftharpoons}} \mathrm{LpxC\text{-}I^*} \qquad (7)$$

where LpxC-I represents a complex between LpxC and the CHIR-090 inhibitor, and I* represents an enzyme/inhibitor isomer. They reported the reaction parameters as k_4/k_3 = 4 nM, k_5 = 1.9 min^{-1}, and k_6 = 0.18 min^{-1} (Barb *et al.,* 2007). They did not report separate parameters for k_3 and k_4, but their results only becomes logical if this

complexation reaction comes to equilibrium reasonably quickly. Thus, it was assumed here that $k_4 = 0.1\ s^{-1}$, from which k_3 was computed as 25000 $mM^{-1}s^{-1}$. This mechanism was added to the model to see if it would exhibit the same inhibitory effect. Firstly, it was observed that fixing the free inhibitor concentration to a constant value does not affect the steady-state biosynthesis pathway at all. This seems reasonable because the LpxC count is not fixed in the model, but arises from the LpxC translation and degradation rates, which the inhibitor does not affect (the reversibility of inhibitor binding implies that, at steady-state, LpxC is sequestered into and released from complexes at the same rate). On the other hand, the inhibitor induces a very strong transient effect. Fig. 2.3A represents the amount of lipid A produced by the model over the course of 30 minutes, in which all metabolite concentrations started at steady-state and then CHIR-090 was added at time 0. The CHIR-090 MIC was assumed to correspond to the inhibitor concentration that reduces lipid A production by 50%, based on results that reported that this is when cells become non-viable (Onishi *et al.,* 1996). From the data presented in Fig. 2.3A, model cells became non-viable when the free intracellular CHIR-090 concentration exceeds 0.31 molecules/cell, which is 0.76 nM. Clearly, molecule counts are discrete, implying that these are time-averaged quantities. This MIC corresponds closely with the *in vitro* inhibition constant of CHIR-090 (K_i*) which is 0.5 nM (Barb *et al.,* 2007). Taking the *in vivo* MIC as 0.25 µg/ml, and using the CHIR-090 molecular weight of 437.4 g/mol, indicates that the MIC is 570 nM of extracellular CHIR-090. Combining this with the intracellular MIC suggests that the intracellular CHIR-090 concentration is about 1000 fold lower than the extracellular concentration.

Figure 2.3. Comparison of model with experiment. The figure herein is displayed on the next page. (A) Effect of CHIR-090 antibiotic on lipid A production. The model (Fig. 2.1 plus eq. 7) was started with all metabolites at their steady-state concentrations without CHIR-090. Then, antibiotic was added and the total amount of lipid A produced over the following 30 minutes was quantified, indicated with the solid black line. The free antibiotic concentration, quantified as the average number of uncomplexed CHIR-090 molecules/cell was kept constant. The black dashed line represents model estimate of the MIC for the intracellular antibiotic concentration and the red dashed line represents the antibiotic inhibition constant (Barb *et al.*, 2007) (B) Correlation between LpxC half-life and cell generation time. The experimental data (red circles) are from Schakermann *et al.* (2013), who varied generation times using different growth conditions and then quantified LpxC half-lives. The model data (black diamonds) were collected by varying the LpxC half-lives (and LpxC k_{cat}) and then quantifying the generation times, defined here as the time required to produce 1 million lipid A molecules. Lines are least-difference best-fits to the data using the function $y = c_1/x + c_2$, primarily to guide the eye. (C) Effect of overexpressing LpxC on the LpxC half-life (black curve, left axis) and on the lipid A production rate, measured relative to the wild-type production rate (blue curve, right axis). The dashed line represents the wild-type condition using the LpxC translation rate from Table 2.1.

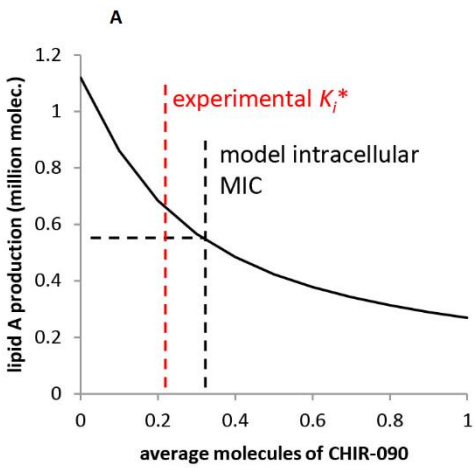
A
lipid A production (million molec.)
1.2
1
0.8
0.6
0.4
0.2
0
experimental K_i*
model intracellular
MIC
0
0.2
0.4
0.6
0.8
1
average molecules of CHIR-090

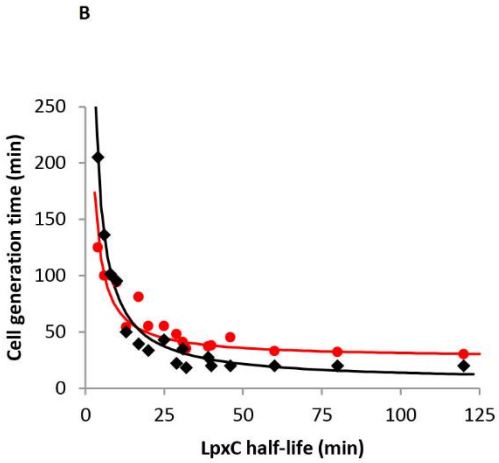
B
Cell generation time (min)
250
200
150
100
50
0
0
25
50
75
100
125
LpxC half-life (min)

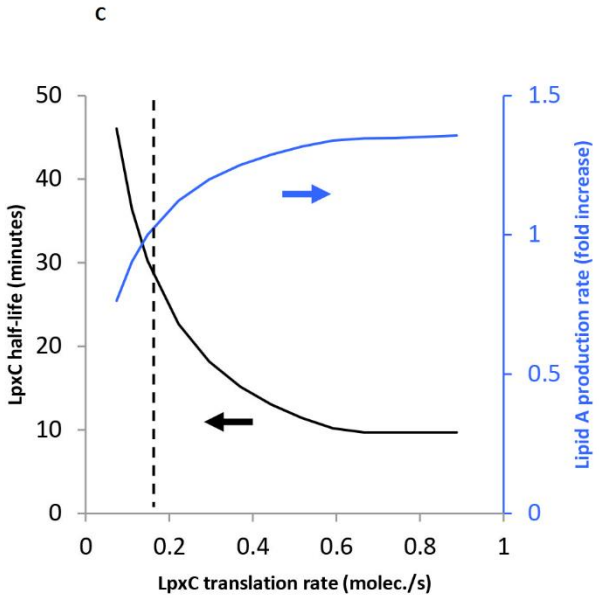
C
LpxC half-life (minutes)
50
40
30
20
10
0
1.5
1
0.5
0
Lipid A production rate (fold increase)
0
0.2
0.4
0.6
0.8
1
LpxC translation rate (molec./s)

2.5.2.3 Correlation between LpxC half-life and cell generation time

Schakermann *et al.* (2013) reported that faster growing cells, such as those grown in rich media and/or at higher temperatures, stabilize LpxC more rapidly than slow-growing cells. These experiments were simulated as a way of validating the model. Schakermann *et al*.'s results for rich medium were only considered because all of the model parameters were estimated from experiments performed with rich medium. For each LpxC half-life value from Table 2 of Schakermann *et al.* (2013), eq. 5 was used to compute the concentration of $FtsH^*_{LpxC}$ that would produce it (here, $k_{translate}$ was 0, and $k_{degrade}$ and k_{FtsH} were the values from Table 2.1). Next, the standard model was changed in two ways: the LpxC k_{cat} value was adjusted to account for the given growth temperature according to data presented in Fig. 2 of Jackman *et al.* (2000), and the rate of FtsH activation for LpxC degradation, k_{active}, was adjusted until the model exhibited the desired $FtsH^*_{LpxC}$ concentration. The rationale for the latter change is that cells might regulate LpxC half-lives by altering the FtsH activation rate. Finally, the cell generation time was computed from the steady-state lipid A production rate in this adjusted model, under the assumption that a generation time is determined by how long a cell requires to produce 1 million lipid A molecules. Fig. 2.3B indicate that the model results agree reasonably well with the experimental results, which supports the model. It is suspected that the model underestimates cell generation times with long LpxC half-lives because it does not account for other cell processes which may limit cell division rates at these fast growth rates.

2.5.2.4 Overexpression of lpxC

Fuhrer and co-workers cloned the *lpxC* gene into an inducible expression vector and then induced with 0.01% or 0.1% arabinose, which overexpressed the LpxC enzyme

(Fuhrer *et al.,* 2006; Fuhrer *et al.,* 2007). They did not quantify the extent of overexpression, but comparable cells increased protein expression by 100 to 200 fold with 0.01% arabinose induction (Guzman *et al.,* 1995). Fuhrer *et al.* found that LpxC overexpression increased LPS amounts by about 1.27 fold and 1.7 fold in cells induced with 0.01% and 0.1% arabinose respectively (this was estimated from Fig. 4 of Fuhrer *et al.* (2007)). They also found that overexpressing LpxC with 0.01% arabinose resulted in a protein half-life of about 11 minutes (Fuhrer *et al.,* 2006).

This arabinose induction was simulated by increasing the model's LpxC translation rate constant and observing its effect on the lipid A production rate and LpxC half-life (Fig. 2.3C). As in the experiment, overexpressing LpxC led to increased lipid A production and shorter LpxC half-lives. However, these effects stopped changing once LpxC was overexpressed about 4-fold, in contrast to the 100 to 200 fold overexpression that the experiments may have produced. At higher than 4-fold overexpression, the LpxC product accumulated in the model because LpxD became a bottleneck; this prevented further changes to the LpxC lifetime and lipid A production rate. Nevertheless, if one assumes a more modest experimental overexpression, then the model results agree well with the 0.01% arabinose induction experiment. In particular, at 2.8 fold overexpression, the model observed a 1.27 fold increase of lipid A production and a 14 minute LpxC half-life, which is reasonably close to the 11 minutes that Fuhrer *et al.* observed (Fuhrer *et al.,* 2006). The 0.1% arabinose induction experiment is harder to match because this resulted in 1.7 fold more LPS, whereas LpxC overexpression could not produce more than 1.36 fold more lipid A in the model due to LpxD acting as a bottleneck. A possible explanation for this difference is that Fuhrer *et al.* found that LpxC overexpression led to longer cell generation times (Fuhrer *et al.,* 2006) in addition to the effects mentioned above. Thus, it may be that cells produce lipid A only 36% faster than normal, but they take twice as long to divide, leading to 1.7 fold more LPS in

cells. Together, these results indicate that the model agrees qualitatively with Fuhrer *et al*.'s LpxC overexpression experiments, and it could agree quantitatively as well; but this cannot be assessed currently with the available experimental data.

2.5.2.5 Substrate limitation

It is well known that organisms grow more slowly when nutrients are limited. For example, Taniguchi *et al.* (2010) observed that *E. coli* grown on minimal medium had a 150 minute generation time. Replicating this in the model was straightforward. As above, it was assumed that a cell generation is the time that the model takes to produce 1 million lipid A molecules. The model reproduces the 150 minute generation time when any one substrate limits the lipid A production rate with 16,000 UDP-GlcNAc molecules, or 43 β-hydroxymyristoyl-ACP molecules, or 510 CMP-Kdo molecules. It also reproduces the 150 minute generation time when all three substrates are partially limiting with 80,000 UDP-GlcNAc, 210 β-hydroxymyristoyl-ACP, and 2400 CMP-Kdo molecules (about 5 times the prior numbers). Thus, substrate limitation does increase generation times in the model as expected.

However, these results disagree with those of Schakermann *et al.* (2013) in that the low substrate concentrations in the model led to decreased lipid A disaccharide counts which caused slower LpxC degradation whereas, Schakermann *et al.* reported that substrate limitation leads to a more rapid LpxC degradation. They found that growth in minimal medium leads to an LpxC half-life of about 10 minutes. This appears to occur because substrate limiting conditions lead to increased (p)ppGpp alarmone concentrations, which increase FtsH expression (Slominska *et al.*, 1980). The model could agree with these data as well, but only if the total FtsH count was increased roughly 25-fold to about 14,000 molecules (the model also used 250,000 UDP-GlcNAc, 650 β-

hydroxymyristoyl-ACP, and 7600 CMP-Kdo molecules, which are about 15 times higher than the single-substrate limitation values presented above). This modified model exhibited a 10 minute LpxC half-life and a 160 minute generation time, in close agreement with results presented in Schakermann *et al.* The cost of achieving this agreement was that the high FtsH concentration led to fast WaaA degradation which made WaaA catalysis of CMP-Kdo the rate-limiting step as observed by the fact that lipid IV_A accumulated rapidly. The large FtsH expression increase and the lipid IV_A accumulation suggest that this model is incorrect for substrate limiting conditions. In particular, achieving the combination of rapid LpxC degradation and relatively low lipid A disaccharide concentrations, without increasing the FtsH concentration 25-fold, requires additional LpxC degradation regulation.

2.5.2.6 Overexpression of lpxK stabilizes LpxC

As mentioned above, a preliminary model that did not include FtsH feedback regulation exhibited lipid A disaccharide accumulation (Fig. 2.2), which led to the proposition that this metabolite is the feedback source for LpxC degradation. If this is the case, then it follows that *lpxK* overexpression should reduce lipid A disaccharide concentration, which would down-regulate LpxC degradation and lead to higher LpxC levels. This hypothesis was tested experimentally. Fig. 2.4A indicates that this is indeed the case. LpxC levels increased substantially with *lpxK* overexpression, even under modest IPTG induction. This same perturbation was tested in the model, finding exactly the same results (Fig. 2.4B). These results are consistent with the assignment of lipid A disaccharide as the feedback source. In contrast, the opposite correlation between LpxC levels and *lpxK* overexpression would be expected if the feedback source were downstream of LpxK, so the experiments provide strong evidence against that

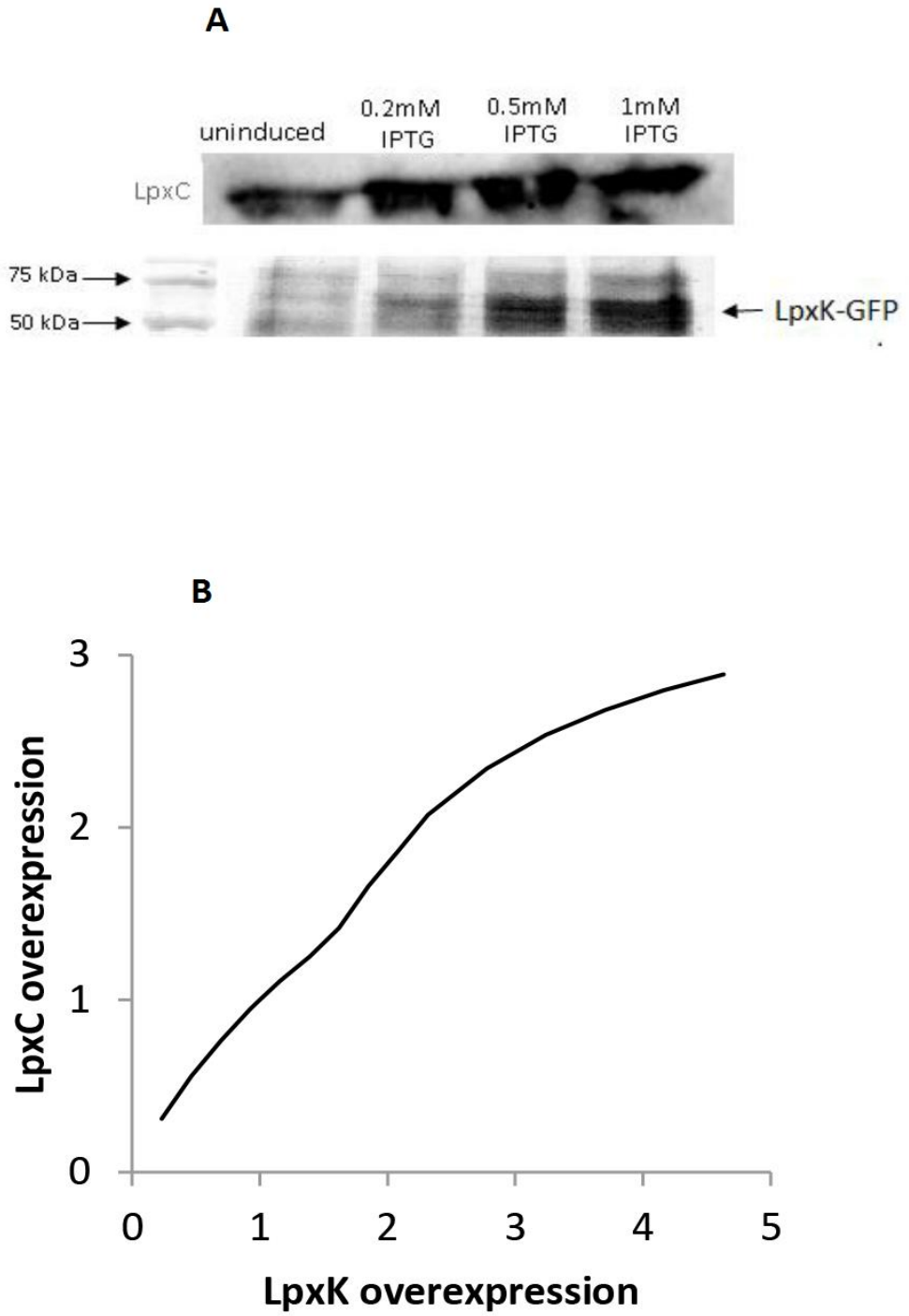

Figure 2.4. Overexpression of *lpxK* increases LpxC concentration. (A) Lower row represents LpxK bands on an SDS-PAGE gel, arising from overexpression induced with the amount of IPTG shown at the top of each column. The upper row represents the resultant LpxC bands on a Western blot for the same induction levels. (B) Model prediction of LpxC overexpression arising from *lpxK* overexpression. The model was that which was presented in Fig. 2.1 but with different LpxK enzyme counts at steady-state.

possibility. Similarly, only a very weak correlation would be expected if the feedback source were further upstream of LpxK, meaning at or before the lipid X metabolite, due to the near irreversibility of the LpxB enzyme, so the experiments provide strong evidence against those possibilities as well. Thus, the experiments presented here strongly indicate that lipid A disaccharide is the feedback source for activating FtsH for LpxC degradation.

2.5.3 Model predictions

2.5.3.1 Lipid A synthesis sensitivity on enzyme concentration

The sensitivity of lipid A synthesis on enzyme counts were investigated in several ways. First, the effect of small enzyme concentration variations were analyzed. Using the methods of metabolic control analysis (Fell and Sauro, 1985; Fell, 1992), flux control coefficient is defined as

$$C_i = \frac{\partial \ln J}{\partial \ln E_i} \times 100\% \tag{8}$$

where i represents one of the 10 pathway enzymes, J represents the biosynthesis rate of lipid A at the outer membrane, and E_i represents the count of enzyme i. The flux control coefficients were quantified by starting the model at steady-state, varying an enzyme count by 5%, and observing the effect on the lipid A production rate.

When the three pathway substrates were set to saturating concentrations and used the "open-loop", in which case, negative feedback through FtsH was removed but the wild-type enzyme counts were kept to values from Table 2.1, the pathway flux was solely controlled by LpxC (Fig. 2.5A black bars). This is consistent with the view that LpxC is

the rate-limiting step of lipid A synthesis (Fuhrer *et al.,* 2006; Mahalakshmi *et al.,* 2014). However, the "closed-loop" case, in which the feedbacks through FtsH were replaced and thus returned to a better model for the wild-type pathway, the model exhibited no sensitivity to LpxC concentration perturbations (Fig. 2.5A red bars). Instead, the feedback caused the LpxC enzyme count to return to its steady-state level, which meant that the perturbation did not affect the lipid A production rate. LpxK was the sole enzyme that controlled pathway flux in the closed-loop case.

Yet different enzymes controlled pathway flux when substrate concentrations were reduced. For each substrate, the concentration was set to the value that led to about 0.5 million lipid A molecules produced per generation and then computed flux control coefficients for each enzyme. Limiting UDP-GlcNAc shifted control to LpxA (Fig. 2.5B). This contrasts the view that LpxA does not affect pathway flux simply because it is reversible and has an unfavourable equilibrium constant (Anderson *et al.,* 1993). Limiting β-hydroxymyristoyl-ACP shifted control to LpxD, LpxH, and LpxB (60%, 20%, and 20%, respectively) (Fig. 2.5C). Finally, limiting CMP-Kdo shifted control to WaaA in the open-loop case (Fig. 2.5D black bars), and to MsbA in the closed-loop case (Fig. 2.5D red bars). These results suggest that control of pathway flux is typically localized to relatively few enzymes, but those which depend on the substrate concentrations.

Next, lipid A biosynthesis on enzyme counts for the case of large perturbations, assuming saturating substrate concentrations were examined. For each enzyme, the fraction of the wild-type count (Table 2.1) that would lead to 0.5 million lipid A molecules produced in 30 minutes was determined. In the open-loop case, the

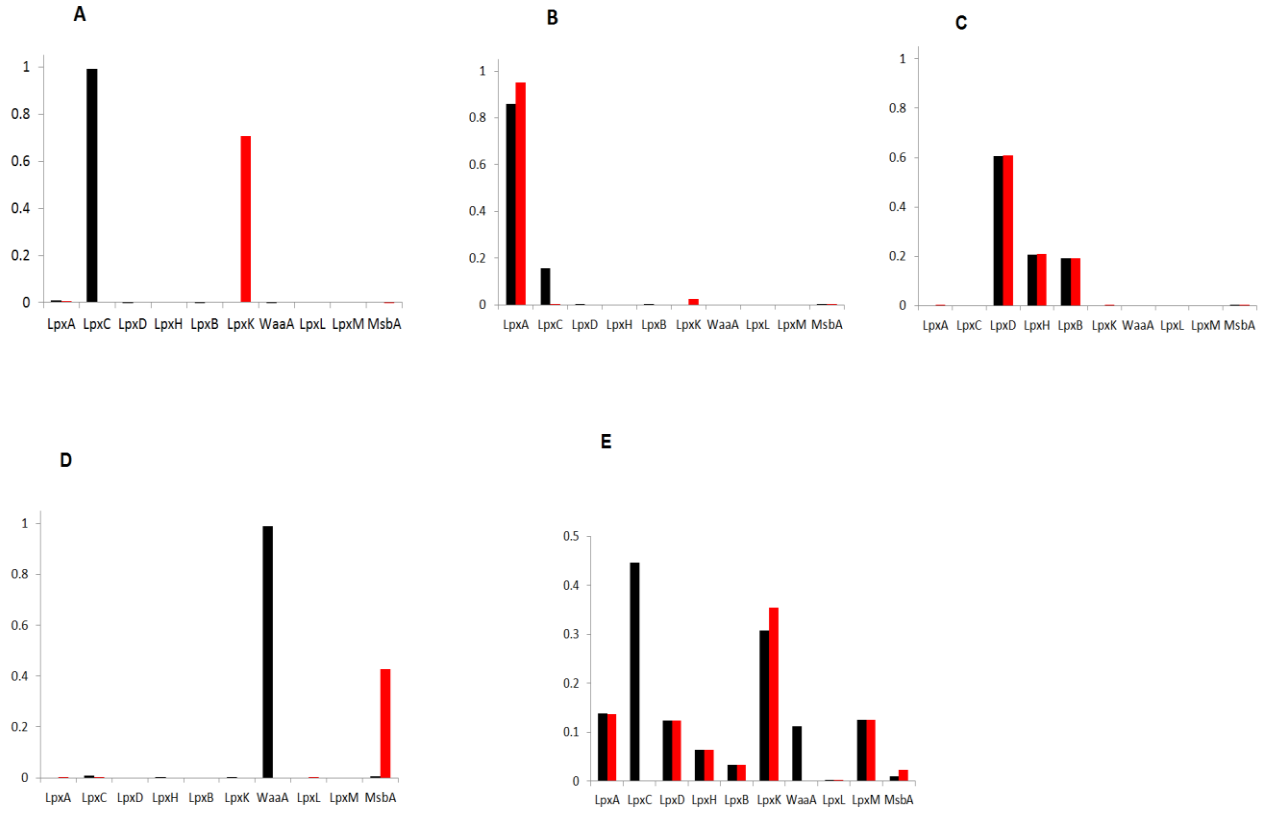

Figure 2.5. Sensitivity of lipid A production rate on enzyme abundance. (A) Black bars represents enzyme control coefficients for the open-loop case, in which wild-type enzyme counts were assumed but FtsH regulation was disabled. Red bars represents enzyme control coefficients for the closed-loop case, in which FtsH regulation was enabled. (B) The UDP-GlcNAc count was set to 50,000 molecules which represented substrate limiting conditions that led to approximately 0.5 million lipid A molecules produced per generation. As in 'A' above, black and red bars represent enzyme control coefficient for the open-loop and close-loop case respectively. (C) Enzyme control coefficient when β-hydroxymyristoyl-ACP count were limited at 200 molecules. Denotation for black and red bars are same as in 'A'. (D) Enzyme control coefficient when the CMP-Kdo count were limited at 5000 molecules. Black and red bars are same as in 'A'. (E) Enzyme abundance reductions that led the model to produce 0.5 million lipid A molecules per cell generation for the open-loop (black bars) and closed-loop (red bars) cases.

production rate was most sensitive to the LpxC and LpxK enzyme counts (Fig. 2.5E black bars). In the closed-loop case, as before, LpxC perturbations were ineffectual because its concentration was regulated through feedback. As a result, the pathway was most sensitive to LpxK (Fig. 2.5E red bars).

2.5.3.2 WaaA Regulation

Katz and Ron's finding that the concentration of WaaA is regulated through degradation by FtsH (Katz and Ron, 2008) leads to the obvious question of why it is regulated in addition to LpxC. From sensitivity analysis presented below, one answer may be that WaaA regulation is used to control pathway flux when the CMP-Kdo concentration is limiting (Fig. 2.6A). In this situation, the lipid A synthesis rate is insensitive to small changes in the LpxC concentration, making that less useful for regulation, but is controlled by the WaaA concentration instead. Also, reducing lipid A production when CMP-Kdo is limiting would conserve Kdo for other uses. For example, Kdo can be catalysed by Kdo aldolase to produce D-arabinose and pyruvate (Ghalambor and Heath, 1966). Although it has been suggested that CMP-Kdo synthesis is the rate-limiting step to lipid A synthesis (Ray *et al.*, 1981), the strong effects of LpxC and the other upstream enzymes discussed above, indicate that this is not the normal case. Additionally, the model observed that CMP-Kdo limitation leads to rapid lipid IV_A accumulation with no apparent correction mechanism. Together, these results point to the likelihood that WaaA regulation helps control the lipid A production rate when the CMP-Kdo concentration is low, but probably not so low as to be rate-limiting.

A second possible explanation for WaaA's regulation is that it might decrease reactions with undesirable substrates (Katz and Ron, 2008) due to the fact that WaaA has a low substrate specificity. As mentioned previously above, WaaA can glycosylate a wide

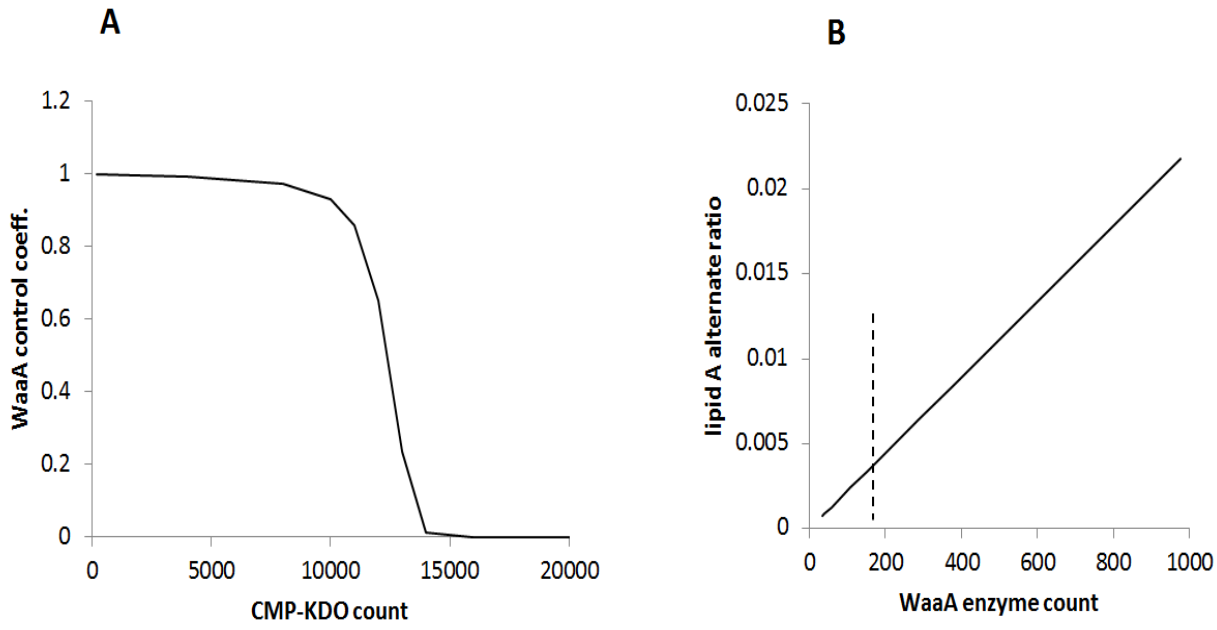

Figure 2.6. WaaA regulation. (A) The flux control coefficient of WaaA as a function of the CMP-Kdo substrate concentration. This is for the open-loop case, in which wild-type enzyme counts were assumed but FtsH regulation was disabled. (B) The ratio of alternate lipid A to normal lipid A (Kdo_2-lipid A) as a function of the number of WaaA proteins. All parameters are the same as in Table 2.1, except that the WaaA proteolysis rate constant was changed in order to alter the WaaA degradation rate and hence the WaaA steady-state copy number. The maximum enzyme count displayed arose from no FtsH mediated proteolysis. The dashed line indicates the wild-type count, from Table 2.1.

range of lipid acceptors, including Kdo_2-lipid A in particular (Brozek *et al.*, 1989; Belunis and Raetz, 1992), which was included in the model architecture as production of alternate lipid A. Simulations were run with different rate constants for WaaA degradation by FtsH. It was observed that slower WaaA degradation led to higher steady-state enzyme counts, which then led to higher relative amounts of alternate lipid A (Fig. 2.6B). Thus, the model agrees with suggestions that WaaA regulation might help regulate the lipid A molecule composition (Katz and Ron, 2008). This mechanism functions even if CMP-Kdo is in excess.

2.6 SUMMARY

A quantitative model of the nine enzyme-catalysed steps of *E. coli* lipid A biosynthesis has been developed, drawing parameters from the experimental literature. The model accounts for biosynthesis regulation, which occurs through regulated degradation of the LpxC and WaaA (also called KdtA) enzymes. The LpxC degradation signal appears to arise from the lipid A disaccharide concentration which was deduced from prior results, model results, and new *lpxK* overexpression results. The model agrees reasonably well with many experimental findings including the lipid A production rate, the behaviours of mutants with defective LpxA enzymes, correlations between LpxC half-lives and cell generation times, and the effects of *lpxK* overexpression on LpxC concentrations. Its predictions also differ from some experimental results which suggest modifications to the current understanding of the lipid A pathway, such as the possibility that LpxD can replace LpxA and that there may be metabolic channeling between LpxH and LpxB. The model results indicate that WaaA regulation may serve to regulate the lipid A production rate when the Kdo concentration is low and/or to control the number of Kdo residues that get attached to lipid A. Computation of flux control coefficients suggests

that LpxC is the rate-limiting enzyme if pathway regulation is ignored, but that LpxK is the rate-limiting enzyme if pathway regulation is present, as it is in real cells. Control also shifts to other enzymes if the pathway substrate concentrations are not in excess. Based on these results, LpxK may be a much better drug target than LpxC, which has been pursued most often.

Chapter 3

An integrated biosynthesis model for lipid A and phospholipids during outer membrane biogenesis in *E. coli*

3.1 OVERVIEW

This chapter builds upon the previous chapter which investigated the lipid A biosynthesis pathway. Although a large amount of research has been conducted on either LPS or phospholipids synthesis, our current understanding on the cross-talk between both pathways is limited at the moment. Since both pathways are synchronised in order to ensure a proper balance of membrane components, studies underpinning the underlying mechanisms would be invaluable. There are a number of experimental findings which indicate the existence of strong links between both biosynthetic pathways. Firstly, *E. coli* mutants which are resistant to an LpxC inhibitor (CHIR-090) harbour essential mutations in a gene involved in phospholipids synthesis called *fabZ* (Zeng *et al.,* 2013). In a similar manner, inactivation of the *ftsH* gene render cells non-viable apparently due to lack of controlled LPS synthesis (Narberhaus *et al.,* 2009). However, *ftsH* knockout mutants are viable when a suppressor mutation is present in the *fabZ* gene, making its protein product hyperactive (Ogura *et al.,* 1999; Schakermann *et al.,* 2013)**.** The fact that these two enzymes (i.e. LpxC and FabZ) in principle compete for a common substrate (the activity of LpxA is highly unfavourable), and sometimes harbour compensatory mutations underline a close regulatory relationship between both pathways. Secondly, the catalytic activity of LpxK is entirely dependent on the presence of phospholipids indicating there is a substrate level interaction between the two pathways (Ray and Raetz, 1987). Therefore, in the context of outer membrane biogenesis, the role of phospholipids cannot be ignored in the study of LPS biosynthesis and regulation.

Furthermore, during membrane synthesis, approximately 20 million molecules of fatty acids are synthesized in *E. coli* through the action of a series of enzymes as discussed earlier (Raetz *et al.,* 2009). Yu *et al.* (2011) reconstituted an *in vitro* steady state kinetic

system of fatty acid biosynthesis using purified enzymes and they observed that the maximum fatty acid production rate obtainable was 100 μM/min. This production rate falls way below the required amount of fatty acids required by a cell *in vivo* (if one assumes a cell volume of 6.7 x 10^{-16} L (Cayley *et al.*, 1991) and a generation time of 30 min (Mackie, 2013)). Thus, in order to test the consistency of reported *in vitro* parameters, and investigate the role of the biosynthetic enzymes on fatty acids turnover rate, a '*systems*' approach is necessary.

The aim of this chapter is to provide a first detailed integrated computational model of the LPS and phospholipids biosynthetic pathways. The model would examine interactions of all major enzymic components at the transcriptional, proteomic and metabolome level of detail. Such model would provide new insights into the complex biogenesis of the *E. coli* outer membrane.

3.2 MODEL ARCHITECTURE

Initiation of fatty acid biosynthesis begins with the condensation of malonyl-ACP with acetyl-CoA and this reaction is conducted exclusively by FabH (Heath and Rock, 1996a). Subsequent reaction steps are carried out by FabG, FabA/FabZ, and FabI respectively which ultimately completes a single cycle. At the expense of FabH, further elongation cycles begin with FabB and/or FabF by the condensation of malonyl-ACP to the growing fatty acyl chain. Yet again, FabG, FabA/FabZ, and FabI catalyse subsequent steps to complete the cycle (Fig. 1.6).

A schematic representation of the model is depicted in Fig. 3.1. The model commences at fatty acid initiation step with the FabH reaction (reaction involves 2-carbon substrate) which then leads to the formation β-hydroxydecenoyl-ACP (a 10-carbon substrate).

This meant that reaction intermediate steps between the actual product of FabH and β-hydroxydecenoyl-ACP were ignored (i.e. the 4-, 6-, and 8-carbon steps). Ignoring these steps were valid since β-hydroxydecenoyl-ACP is a direct substrate for *trans*-2-decenoyl-ACP production. *Trans*-2-decenoyl-ACP in turn, represents a key substrate in the metabolic junction of UFAs and SFAs synthesis. The distribution of SFAs and UFAs in membrane phospholipids is the most crucial aspect of phospholipids synthesis (Magnuson *et al.,* 1993). Amongt the components of phospholipids, fatty acids represent the only variable constituents. Furthermore, the relative distribution of SFAs and UFAs represent the key player in phospholipids and membrane regulation (Magnuson *et al.,* 1993; Zhu *et al.,* 2009). The consequence of ignoring these steps would have no significant effect on the model output since in reality, perturbation of steps prior to the formation of β-hydroxydecenoyl-ACP would directly affect the pool of *trans*-2-decenoyl-ACP which in turn, would affect both SFAs and UFAs levels proportionately.

The catalytic activity of FabH is regulated at the post-translational level (Heath and Rock, 1996a). This enzyme is known to be inhibited by acyl-ACPs especially palmitoyl-ACP (C16:0) and *cis*-vaccenoyl-ACP (C18:1) (Heath and Rock, 1996a).

FabA and FabZ dehydrates β-hydroxydecenoyl-ACP to produce *trans*-2-decenoyl-ACP. Under physiological conditions, this reaction step is unfavourable (Heath and Rock, 1996b). The *trans*-2-decenoyl-ACP synthesized can either be reduced to decanoyl-ACP (a SFA) by the action of FabI in an essentially irreversible reaction (Heath and Rock, 1995), or further isomerized by FabA to produce *cis*-3-decenoyl-ACP which is the first step in UFAs biosynthesis (Kass *et al.,* 1967). Thus, competition for *trans*-2-decenoyl-ACP between FabA and FabI influences the relative ratios of SFAs and UFAs.

Figure 3.1. Model of the *E. coli* LPS and phospholipids biosynthesis pathway. The figure herein is displayed on the next page. Enzymes and metabolites are displayed with three text styles: upright bold indicates that these concentrations are fixed, upright plain indicates that these concentrations vary, and italics indicates that these species are not included in the model explicitly. Black arrows with barbed heads represent chemical reactions in which reactants are converted to products. Red arrows with closed heads represent enzymatic influences on chemical reaction rates, and red arrows with T-bar heads represent inhibitory influences. Variables represent model parameters. Numbers next to black arrows for bi-substrate reactions indicate which substrate is designated number 1 and number 2. Blue arrows represents pathway interactions that are novel and derived from this work. The top right corner represents the transcriptional activation and repression of *fabA* and *fabB* genes. Both genes consist of two separate promoters; one which is constitutively expressed, and another which is activated by FadR and repressed by FabR.

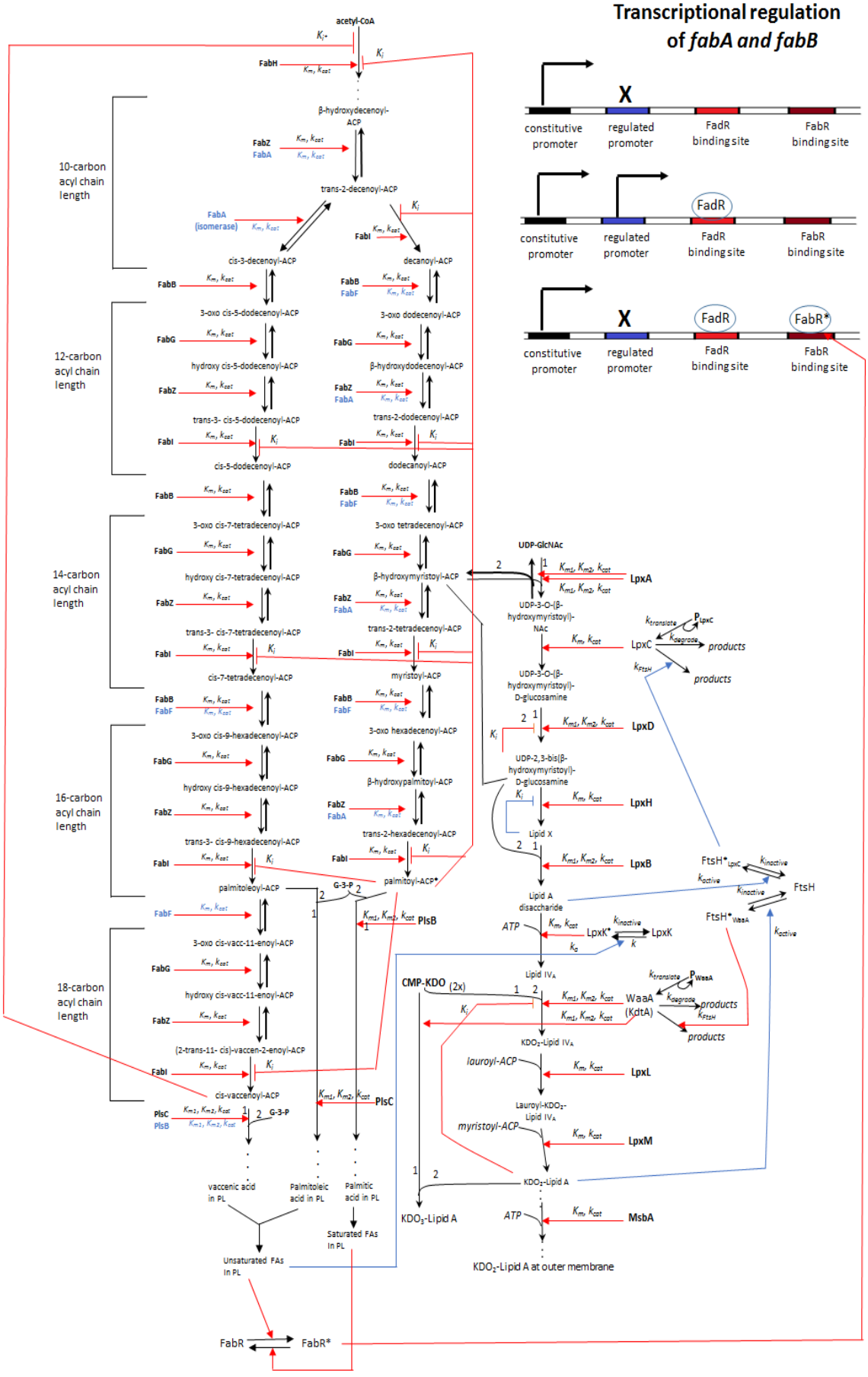
Transcriptional regulation of fabA and fabB
constitutive promoter
regulated promoter
FadR binding site
FabR binding site
FadR
FabR*
acetyl-CoA
FabH
β-hydroxydecenoyl-ACP
FabZ
FabA
trans-2-decenoyl-ACP
FabA (isomerase)
FabI
cis-3-decenoyl-ACP
decanoyl-ACP
FabB
FabF
3-oxo cis-5-dodecenoyl-ACP
3-oxo dodecenoyl-ACP
FabG
hydroxy cis-5-dodecenoyl-ACP
β-hydroxydodecenoyl-ACP
trans-3- cis-5-dodecenoyl-ACP
trans-2-dodecenoyl-ACP
cis-5-dodecenoyl-ACP
dodecanoyl-ACP
3-oxo cis-7-tetradecenoyl-ACP
3-oxo tetradecenoyl-ACP
hydroxy cis-7-tetradecenoyl-ACP
β-hydroxymyristoyl-ACP
trans-3- cis-7-tetradecenoyl-ACP
trans-2-tetradecenoyl-ACP
cis-7-tetradecenoyl-ACP
myristoyl-ACP
3-oxo cis-9-hexadecenoyl-ACP
3-oxo hexadecenoyl-ACP
hydroxy cis-9-hexadecenoyl-ACP
β-hydroxypalmitoyl-ACP
trans-3- cis-9-hexadecenoyl-ACP
trans-2-hexadecenoyl-ACP
palmitoleoyl-ACP
palmitoyl-ACP*
3-oxo cis-vacc-11-enoyl-ACP
hydroxy cis-vacc-11-enoyl-ACP
(2-trans-11- cis)-vaccen-2-enoyl-ACP
cis-vaccenoyl-ACP
G-3-P
PlsB
PlsC
vaccenic acid in PL
Palmitoleic acid in PL
Palmitic acid in PL
Saturated FAs in PL
Unsaturated FAs in PL
FabR
FabR*
10-carbon acyl chain length
12-carbon acyl chain length
14-carbon acyl chain length
16-carbon acyl chain length
18-carbon acyl chain length
UDP-GlcNAc
LpxA
UDP-3-O-[β-hydroxymyristoyl]-NAc
LpxC
products
UDP-3-O-[β-hydroxymyristoyl]-D-glucosamine
LpxD
UDP-2,3-bis[β-hydroxymyristoyl]-D-glucosamine
LpxH
Lipid X
LpxB
Lipid A disaccharide
ATP
LpxK*
LpxK
Lipid IVA
CMP-KDO (2x)
WaaA (KdtA)
KDO2-Lipid IVA
lauroyl-ACP
LpxL
Lauroyl-KDO2-Lipid IVA
myristoyl-ACP
LpxM
KDO2-Lipid A
KDO3-Lipid A
MsbA
KDO2-Lipid A at outer membrane
FtsH
FtsH*LpxC
FtsH*WaaA

However, overexpression of FabA does not increase UFAs yield because FabB limits UFAs synthesis in this case. In fact, FabA overexpression conditions increased the total cellular *SFAs* whilst the UFAs level remained the same (Clark *et al.,* 1983). This is because, overexpression would increase the concentration of *trans*-2-decenoyl-ACP, and subsequently result in faster production of SFAs; but UFAs synthesis rate remain unchanged. Unsurprisingly, overexpression of both FabA and FabB increased the total amount of cellular UFAs (Cao *et al.,* 2010). Decanoyl-ACP and *cis*-3-decenoyl-ACP are both utilized as substrates for further rounds of fatty acyl elongation catalysed by FabB/FabF, FabG, FabA/FabZ, and FabI respectively.

FabB and FabF differ only in some catalysed reactions. Both enzymes are capable of catalysing the elongation of saturated fatty acyl-ACP of chain length C6 to C14 (Janßen *et al.,* 2014). In the synthesis of UFA, FabB catalyses the condensation of *cis*-3-decenoyl-ACP and *cis*-5-dodecenoyl-ACP. Both FabB and FabF catalyses *cis*-7-tetradecenoyl-ACP, and the reaction involving palmitoleoyl-ACP is carried out exclusively by FabF (Edwards *et al.*, 1997). Deletion of FabB results in cells that are auxotrophic for UFAs (Cronan *et al.,* 1969). On the other hand, overexpression results in increased levels of UFAs (Cao *et al.,* 2010). FabF is not essential for growth in *E. coli;* however, FabF knockout mutants result in cells that are temperature-sensitive (Garwin *et al.,* 1980a). This is because *cis*-vaccenic acid produced from the condensation of palmitoleoyl-ACP is essential at maintaining membrane fluidity under low temperature conditions (Janßen *et al.*, 2014). Overexpression on the other hand, has been reported to be lethal to the cell (Subrahmanyam and Cronan, 1998).

One of the key regulation of fatty acid synthesis in *E. coli* is the transcriptional regulation of *fabA* and *fabB* genes (Nunn *et al.,* 1983; Zhang *et al.,* 2002; Feng and Cronan, 2012). Both genes have two set of promoters; one which is constitutively

expressed, and another which is activated by FadR and repressed by FabR (Campbell and Cronan, 2001; Zhang *et al.*, 2002; Feng and Cronan, 2009; Feng and Cronan, 2011). Transcription is repressed in the presence of sufficient UFAs which further highlights the dual role of FabA and FabB in UFAs synthesis (Zhu *et al.*, 2009). In addition to the activation of *fabA* and *fabB,* FadR is also a *repressor* of all genes that code for proteins involved in the β-oxidation cycle (Simons *et al.*, 1980).

The products of FabB and FabF are reduced by FabG which leads to the formation of a 3-hydroxyacyl ACP. Both unsaturated and saturated fatty acyl substrates[1] of varying chain-lengths are suitable substrates (Toomey and Wakil, 1966). Under physiological conditions, the reactions are readily reversible (Toomey and Wakil, 1966). Cells are non-viable under FabG knockout conditions which indicate its role cannot be substituted by other enzymes (Lai and Cronan, 2004).

Next, the 3-hydroxyacyl ACPs are dehydrated by the action of FabA and FabZ although, their substrate preferences differ. This reaction step is unfavourable under physiological conditions as well (Heath and Rock, 1996b). FabZ prefers fatty acyl substrates of short chain length whereas, FabA has a higher affinity for substrates of medium chain length (Heath and Rock, 1996b). Unlike FabZ, FabA is incapable of dehydrating fatty acyl-substrates with a *cis* configuration (i.e. UFAs substrates) (Heath and Rock, 1996b). One of the reaction substrates of FabA/FabZ, β-hydroxymyristoyl-ACP is also an essential precursor molecule in the biosynthesis of LPS (Ogura *et al.*, 1999) thus, phospholipids and LPS synthesis are regulated in response to perturbation in

[1] "*saturated acyl substrate*" was mentioned a number of times in this report for certain reactions of FabG, FabB, FabF, FabZ and FabA. Although, only substrates of FabF and FabB can be truly saturated, since all other acyl substrates catalysed by the enzymes mentioned above always contain at least a double-bond, the term "*saturated acyl substrate*" was utilized for simplicity to represent substrates that are consumed exclusively for SFAs synthesis.

this common substrate pool (Ogura *et al.,* 1999; Schakermann *et al.,* 2013). Co-ordinated regulation of both pathways is achieved through controlled FtsH-mediated proteolysis of LpxC, the second enzyme involved in LPS synthesis (Ogura *et al.,* 1999; Fuhrer *et al.,* 2006). Due to the highly unfavourable equilibrium constant of the first enzyme (LpxA), degradation of LpxC would increase the substrate pool of β-hydroxymyristoyl-ACP. As stated previously in Chapter 2 (Figs. 2.2 and 2.4), the feedback regulatory signal appear to arise from levels of lipid A disaccharide, a metabolite downstream of LpxC in the LPS pathway. Since compensatory mutations in the *fabZ* gene are crucial under *ftsH* inactivation (Ogura *et al.,* 1999) or LpxC inhibition conditions (Zeng *et al.,* 2013), this suggests that the activities of LpxC and FabZ are co-regulated in order to maintain an appropriate ratio of LPS and phospholipids.

The last step catalysed by FabI, is essentially the only irreversible step in fatty acyl elongation cycle. This enzyme is inhibited by one of its product, palmitoyl-ACP, presumably to prevent an unnecessary accumulation of acyl-ACPs due to the high energy requirement involved in fatty acid synthesis (Heath and Rock, 1996c). Inhibition of FabI is lethal to the cell (Egan and Russell, 1973); however, overexpression does not result in any growth defect (Xu *et al.,* 2006).

Fatty acid biosynthesis in *E. coli* usually ends when the acyl chain contains 16 or 18 carbon atoms which then serve as substrates for the synthesis of phospholipids (Heath *et al.,* 2002). The first step in the biosynthesis of phospholipids involves the transfer of two acyl moieties derived from acyl-ACPs to a single molecule of glycerol-3-phosphate (G3P). These acyl groups are attached to G3P by inner membrane proteins PlsB and PlsC (Goelz and Cronan, 1980; Rock *et al.,* 1981). Subsequent enzymic reaction steps occur leading to the formation of membrane phospholipids (Heath *et al.,* 2002). In the model, it was assumed that the reaction products of PlsB and PlsC would ultimately be

utilized for phospholipids synthesis so the model ignored subsequent steps. This is intuitively reasonable given that fatty acids of 16 and 18 carbon carbons are exclusively used in the production of phospholipids under optimum conditions (Heath *et al.,* 2002). Thus, the model focuses on the quantification of fatty acyl chains that are transferred to G3P. This was important to effectively study the SFAs/UFAs distribution in the membrane, rather than studying the phospholipid as a whole single molecule. Understanding the relative distributions of SFAs/UFAs is invaluable because as mentioned earlier, fatty acids are the only dynamic and variable component of phospholipids. Also, regulation of the fatty acid composition is crucial under varying environmental conditions.

PlsB attaches fatty acids to position-1 of G3P whereas, fatty acids found in position-2 result from reactions with PlsC (Goelz and Cronan, 1980; Rock *et al.,* 1981). Fatty acids located in position-2 are primarily UFAs while SFAs and *cis*-vaccenic acid are present in position-1 (Goelz and Cronan, 1980; Rock *et al.,* 1981). Although, myristic (C14:0) and stearic acids (C18:0) can also be detected at significant levels in some *E. coli* strains, the major fatty acids found in *E. coli* membranes are palmitic acid (C16:0), palmitoleic acid (C16:1), and *cis*-vaccenic acids (C18:1) and their ratios vary depending on the bacterial strain and growth conditions (Raetz, 1978).

The LPS pathway arm of the integrated model is similar to that which was described in Chapter 2 with some minor modifications. A brief summary is provided here. Biosynthesis of lipid A, the sole essential component of LPS involves nine enzyme catalysed reaction steps (Reatz *et al.,* 2009). The first enzyme LpxA, is characterized with an unfavourable equilibrium constant of approximately 0.01 which means that LpxC, the second enzyme catalyses the pathway committed step (Anderson *et al.,* 1993). Pathway regulation occurs through FtsH-mediated degradation of LpxC and

WaaA (Ogura *et al.*, 1999; Katz and Ron, 2008). In addition, the catalytic activity of LpxK is entirely dependent on the presence of phospholipids especially cardiolipins (Ray and Raetz, 1987). However, subsequent model findings indicated that the catalytic activation of LpxK is solely dependent on the abundance of UFAs moiety present in phospholipids as described below.

3.3 MODEL EQUATIONS AND PARAMETERS

The interactions between substrates and enzymes were modelled under steady-state conditions for an *E. coli* cell. A cell volume of 6.7×10^{-16} L and a doubling time of 30 min was assumed in the same manner as the lipid A model presented in Chapter 2. With the exceptions of FabA, FabB, LpxC and WaaA (whose regulation was being studied in the model), the concentration for other proteins were fixed. Thus, the model ignored protein synthesis and degradation, and cell volume growth. Such assumptions are adequate because enzyme concentrations remain relatively constant over the course of the cell cycle. Table 3.1 lists all parameters employed in the model.

Table 3.1: Abundance and kinetic parameters of integrated lipid A and phospholipids biosynthesis model.

Species	Species abundance (molec./cell)	Substrate	Substrate identity in COPASI file	K_{ms} *or* K_m (mM)	K_{mp} (mM)	k_{cat} *or* k_{catf} (s^{-1})	k_{catr} (s^{-1})	Notes and other parameters
UDP-GlcNAc	2,000,000							excess concentration
CMP-Kdo	2,000,000							excess concentration
G3P	1,000,000							excess concentration
Acetyl-CoA	2,000,000							excess concentration
ACP	1,024[a]							actual concentration
FabH	1,320[a]			0.04[g]		12		K_i = 0.1 mM K_{i*} = 0.067mM
FabB	14,300[a]	Decanoyl-ACP	C10	0.022	0.022	3.4	0.38	K_1 = 7.945 s^{-1}
		Dodecanoyl-ACP	C12	0.022[c]	0.022	3.4	0.38	K_{active} = 1.0 x 10^{-3} s^{-1}
		Myristoyl-ACP	C14	0.071[c]	0.071	2.1	0.23	$K_{inactive}$ = 0.1 s^{-1}
		cis-3-decenoyl-ACP	C10:1	0.012[d]	0.012	0.31	1.6	K_3 = 11.12 s^{-1}
		cis-5-dodecenoyl-ACP	C12:1	0.028[c]	0.028	3.9	0.43	K_{-4} = 2 s^{-1}
		cis-7-tetradecenoyl-ACP	C14:1	0.027[c]	0.027	4.14	0.46	K_{-5} = 2 s^{-1}
								$K_{degrade}$ = 5.556 x 10^{-4} s^{-1}
FabF	1,280[a]	Decanoyl-ACP		0.068	0.068	3	1.6	
		Dodecanoyl-ACP		0.068	0.068	2.7	1.45	
		Myristoyl-ACP		0.068[c]	0.068	0.83	0.45	
		cis-7-tetradecenoyl-ACP		0.06[c]	0.06	2.49	1.34	
		Palmitoleoyl-ACP	C16:1	0.017[d]	0.017	6.74[d]	3.6	
FabG	13,800[a]	3-oxo-dodecenoyl-ACP	Ketoacyl-12	0.01	0.01	1232	536	
		3-oxo tetradecenoyl-ACP	Ketoacyl-14	0.01	0.01	1232	536	
		3-oxo hexadecenoyl-ACP	Ketoacyl-16	0.01	0.01	1232	536	
		3-oxo-*cis*-5-dodecenoyl-ACP	Ketoacyl-12:1	0.01	0.01	1232	536	
		3-oxo-*cis*-7-tetradecenoyl-ACP	Ketoacyl-14:1	0.01	0.01	1232	536	
		3-oxo-*cis*-9-hexadecenoyl-ACP	Ketoacyl-16:1	0.01	0.01	1232	536	

		3-oxo-*cis*-vacc-11-enoyl-ACP	Ketoacyl-18:1	0.01	0.01	1232	536	
FabZ	3,330[a]	β-hydroxydecenoyl-ACP	B-OH-10	5.5×10^{-5}	5.5×10^{-5}	2.65	9.14	
		β-hydroxydodecenoyl-ACP	B-OH-12	5.5×10^{-5}	5.5×10^{-5}	1.59	1.59	
		β-hydroxymyristoyl-ACP	Beta-hydroxymyristoylACP	5.5×10^{-5}	5.5×10^{-5}	0.53	0.53	
		β-hydroxypalmitoyl-ACP	B-OH-16	5.5×10^{-5}	5.5×10^{-5}	1.06	1.06	
		β-hydroxy-*cis*-5-dodecenoyl-ACP	B-OH-12:1	5.5×10^{-5}	5.5×10^{-5}	1.59	1.59	
		β-hydroxy-*cis*-7-tetradecenoyl-ACP	B-OH-14:1	5.5×10^{-5}	5.5×10^{-5}	1.59	1.59	
		β-hydroxy-*cis*-9-hexadecenoyl-ACP	B-OH-16:1	5.5×10^{-5}	5.5×10^{-5}	3.18	3.18	
		β-hydroxy-*cis*-vacc-11-enoyl-ACP	B-OH-18:1	5.5×10^{-5}	5.5×10^{-5}	3.18	3.18	
FabA	23,400[a]	β-hydroxydecenoyl-ACP		1.7[e]	1.7	5.4	18.6	$K_1 = 5.2\ s^{-1}$
		β-hydroxydodecenoyl-ACP		1.7	1.7	4	4	$K_{activate} = 1.4 \times 10^{-3}\ s^{-1}$
		β-hydroxymyristoyl-ACP		1.7	1.7	0.53	0.53	$K_{inactivate} = 0.1\ s^{-1}$
		β-hydroxypalmitoyl-ACP		1.7	1.7	0.53	0.53	$K_3 = 31.2\ s^{-1}$
		trans-2-decenoyl-ACP	trans-10	1.0×10^{-4}	0.5[e]	1.65	11.75	$K_{-4} = 90\ s^{-1}$
								$K_{-5} = 90\ s^{-1}$
								$K_{degrade} = 5.556 \times 10^{-4}\ s^{-1}$
FabI	12,500[a]	*trans*-2-decenoyl-ACP		0.01		20.6		$K_i = 0.035$ mM
		trans-2-dodecenoyl-ACP	trans-12	0.0033[h]		15[h]		
		trans-2-tetradecenoyl-ACP	trans-14	0.0033		15		
		trans-2-hexadecenoyl-ACP	trans-16	0.0033		15		
		trans-3-*cis*-5-dodecenoyl-ACP	trans-12:1	0.0033		15		
		trans-3-*cis*-7-tetradecenoyl-ACP	trans-14:1	0.0033		15		
		trans-3-*cis*-9-hexadecenoyl-ACP	trans-16:1	0.0033		15		
		(2-*trans*-11-*cis*)-vaccen-2-enoyl-ACP	trans-18:1	0.0033		15		
FadR	295[a]							$K_2 = 0.054\ s^{-1}$
								$K_{-2} = 0.1\ s^{-1}$
FabR	295							
PlsB	1,400[b]	Palmitoyl-ACP	C16	0.015[b]		13.2		K_{m2} for G3P substrate is 0.14 mM estimated from **(b)**
		cis-vaccenoyl-ACP	C18:1	0.025[b]		11.76		
PlsC	4,200	Palmitoleoyl-ACP	C16:1	0.012		4.4		K_{m2} for G3P substrate is

	cis-vaccenoyl-ACP	0.025	7.6	0.7 mM estimated from **(f)**
LpxK				k = 0.0064 s^{-1} k_a = 0.0094 s^{-1} K_{inact} = 0.0034 s^{-1}

(a) Ishihama *et al.* (2008), **(b)** Green *et al.* (1981), **(c)** Garwin *et al.* (1980b), **(d)** D'Agnolo *et al.* (1975), **(e)** Kass *et al.* (1967), **(f)** Rock *et al.* (1981), **(g)** Heath and Rock (1996a), **(h)** Rafi *et al.* (2006) Parameters that do not have citations are discussed in the main text.

3.3.1 Substrate and enzyme abundance

The levels of UDP-GlcNAc and CMP-Kdo were kept constant at 2 million molecules (5 mM). The levels of acetyl-CoA and G3P were also maintained at 2 million and 1 million molecules respectively. This led to substrate saturation conditions throughout the simulations.

The FabA, FabB, FabF, FabG, FabH, FabI, FabZ, and FadR protein copy numbers were derived from mass spectrometry proteomic data collected on *E. coli* cytosolic fractions (Ishihama *et al.,* 2008). On the other hand, the PlsC count was estimated as 4200 molecules per cell from the reported PlsB count (Green *et al.,* 1981) as described below.

3.3.2 Enzyme kinetics

Most of the enzymes involved in fatty acid biosynthesis are involved in multiple reaction steps. This therefore suggests that accounting explicitly for enzyme-substrate complexation is essential. Unfortunately, accounting for complexation requires precise enzyme association/dissociation constant parameters; whereas, available information in the literature indicates the pathway is poorly parameterized. On the other hand, complexation in the model may not be crucial because acyl-ACPs could barely be detected experimentally in *E. coli* cells which indicate their levels are too low (Fig. 8 in Jiang and Cronan, 1994). Furthermore, there are a number of thioesterases in *E. coli* which cleave acyl-ACPs and thus, regulate their concentration; although the thioesterases are non-essential (Jiang and Cronan, 1994; Heath *et al.,* 2002). Finally, acyl-ACPs in the cytoplasm are toxic to the cell and they induce a strong inhibitory effect on a number of enzymes involved in fatty acid synthesis (Bergler *et al.,* 1996; Heath and Rock, 1996a; Heath and Rock, 1996c). All these indicate that substrate levels are extremely low and are likely below the K_m value for enzymes. Although, acetyl-

CoA which is a substrate for FabH is highly abundant in the cell, modelling complexation is unnecessary because FabH is involved in a single-reaction step as mentioned above.

All kinetic parameters for enzymes involved in the LPS biosynthesis arm of the model have been described previously in Chapter 2. The phospholipids pathway reactions were modelled using either single-substrate or bi-substrate Michaelis-Menten mechanisms. The integrated LPS/phospholipids model includes reversibility of reactions and several feedback loops which are essential for models to attain a steady-state (Cornish-Bowden and Cardenas, 2001).

A single-substrate reversible Michaelis-Menten kinetics was employed for FabG, FabB, FabF, FabZ, and FabA (Mendes *et al.*, 2009). Here the metabolic flux is

$$\frac{d[\mathrm{P}]}{dt} = -\frac{d[\mathrm{S}]}{dt} = \left(\frac{k_{cat_f}[\mathrm{E}][\mathrm{S}]}{K_{m_s}} - \frac{k_{cat_r}[\mathrm{E}][\mathrm{P}]}{K_{m_p}}\right)\left(\frac{1}{1+\frac{[\mathrm{S}]}{K_{m_s}}+\frac{[\mathrm{P}]}{K_{m_p}}}\right) \qquad (9)$$

where [S] is the substrate concentration, [P] is the product concentration, [E] is the total enzyme concentration, k_{catf} is the enzyme catalytic rate constant for the forward reaction, k_{catr} is the enzyme catalytic rate constant for the reverse reaction, K_{ms} and K_{mp} are the Michaelis constants for substrate and product respectively. The K_{mp} values were unavailable so the model assumes same values for K_{ms} and K_{mp} in all reversible reactions. This meant that the equilibrium constant for each reaction was implemented by adjusting the k_{catr} parameter as described below.

There were no specific FabG parameters with substrates of carbon chain lengths C10 to C18 so it was essential to make calculations. The specific activity of FabG whilst utilizing a 4-carbon ketoacyl substrate was reported as 2.9 µmol/min/µg (Zhang *et al.*,

2003) from which a k_{cat} value of 1232 s^{-1} was estimated assuming the MW of a FabG protein is 25.5 kDa (Sun *et al.,* 2008). This value was assigned to k_{catf} for all chain lengths in the model. Furthermore, a K_m value of 0.01 mM was utilized which is the K_m parameter for its second substrate (NADPH) (Sun *et al*., 2008). The absence of specific FabG parameters for any of its substrates studied in the model suggests that the model may be inadequate at investigating the effect of FabG perturbations on *E. coli* fatty acids profile. In Toomey and Wakil (1966), the FabG reaction led to 40% of product formation at a pH of 9.0 in comparison to its optimum pH in which all substrates were converted to product. The low product formation was as a result of the reaction becoming unfavourable at a pH of 9.0. However, the physiological pH of *E. coli* is about 7.5 (Wilks and Slonczewski, 2007), and this led to 70% of products being formed. This suggests that under physiological conditions, the reaction equilibrium constant is 2.3. Since the model assumes K_{ms} and K_{mp} to be same, this meant that the equilibrium constant equals the k_{catf} / k_{catr} ratio. Thus, k_{catr} was derived as 536 s^{-1}.

The K_m values for FabB with respect to dodecanoyl-ACP (C12:0), myristoyl-ACP (C14:0), *cis*-5-dodecenoyl-ACP (C12:1) and *cis*-7-tetradecenoyl-ACP (C14:1) substrates were derived from Table IV in Garwin *et al* (1980b). From the same source, the authors estimated the specific activity of FabB for myristoyl-ACP as 2.9 µmol/min/mg from which a k_{catf} value of 2.1 s^{-1} was estimated. The k_{catf} values for dodecanoyl-ACP, *cis*-5-dodecenoyl-ACP and *cis*-7-tetradecenoyl-ACP were further derived relative to the specific activity for myristoyl-ACP as reported in Garwin *et al.* (1980b). On the other hand, the catalytic activity of FabB with decanoyl-ACP (C10:0) and dodecanoyl-ACP substrates are similar (Edwards *et al.,* 1997) so the model uses same K_m and k_{catf} for both substrates. Although, a FabB k_{cat} value of 14.5 s^{-1} towards *cis*-3-decenoyl-ACP was initially estimated from the reported specific activity in D'Agnolo *et al.* (1975), this had to be modified to a k_{cat} of 0.31 s^{-1} as described below.

The FabF parameters for myristoyl-ACP and *cis*-7-tetradecenoyl-ACP were obtained from Table IV in Garwin *et al* (1980b) much as was done for FabB. According to Fig. 3 in Edwards *et al*. (1997), the catalytic activity of FabF whilst utilizing decanoyl-ACP and dodecanoyl-ACP substrates was 3.6 and 3.25 folds higher respectively relative to myristoyl-ACP. This fold increase was implemented in the model by adjusting the k_{catf} values relative to those of myristoyl-ACP while maintaining same K_m values. Furthermore, the equilibrium constants of the FabB and FabF reactions were derived as 9 and 1.86 respectively from Fig. 3 in D'Agnolo *et al* (1975) much as was done for FabG, which enabled the k_{catr} parameters to be estimated.

A k_{catf} value of 0.53 s^{-1} was estimated from the reported specific activity of FabZ towards β-hydroxymyristoyl-ACP (C14:0) (Zeng *et al.,* 2013). There were no available K_m parameters for FabZ thus, had to be estimated. In Zeng *et al* (2013), the authors found that in a 40 µl reaction volume, varying the concentration of FabZ from 12.75 to 25.5 nM resulted in a specific activity of 1.87 µmol/min/mg when the concentration of β-hydroxymyristoyl-ACP was 50 µM. Since the specific activity of a reaction equals the rate of reaction multiplied by reaction volume, divided by the mass of total protein, it is possible to estimate the reaction rate in their experiments and subsequently derive K_m. If one assumes an enzyme concentration of 12.75 nM, this amounts to 8.67 x 10^{-6} mg in 40 µl (the MW of FabZ is 17 kDa) thus, the reaction rate **R**, can be calculated as 6.75 x 10^{-3} µM/s. The K_m constant can then be derived from $\mathbf{R} = \frac{k_{cat}\,[\mathrm{E}][\mathrm{S}]}{K_m + [\mathrm{S}]}$. By inputting the necessary parameters ([E] = 12.75 nM, k_{cat} = 0.53 s^{-1}, [S] = 50 µM), a K_m value of 5.5 x 10^{-5} mM can be derived. This K_m value was utilized for all substrates of FabZ. Furthermore, the k_{catf} values for β-hydroxydecenoyl-ACP (C10:0), β-hydroxydodecenoyl-ACP (C12:0) and β-hydroxypalmitoyl-ACP (C16:0) were derived

relative to that of β-hydroxymyristoyl-ACP according to Fig. 5 in Heath and Rock (1996b).

The specific activity of FabZ whilst catalysing β-hydroxy-*cis*-7-tetradecenoyl-ACP (C14:1) is similar to that of β-hydroxymyristoyl-ACP (Fig. 6 in Heath and Rock, 1996b). Consequently, the parameters for FabZ were same for both substrates in the model (although this was modified as described below). There were no available information in the literature to estimate parameters for other unsaturated fatty acyl substrates of FabZ. Thus, the model assumed similar catalytic rates for both saturated and unsaturated fatty acyl substrates of the same chain length. This meant that parameters for 12-carbon and 16-carbon saturated substrates were assigned to 12-carbon and 16-carbon unsaturated substrates respectively.

The reaction affinity of FabA and FabZ towards β-hydroxymyristoyl-ACP is also similar (Heath and Rock, 1996b). Since they both have similar molecular weight, this indicates they also share similar k_{catf} values as well. The FabA k_{catf} values for β-hydroxydecanoyl-ACP, β-hydroxydodecenoyl-ACP and β-hydroxypalmitoyl-ACP relative to β-hydroxymyristoyl-ACP were calculated according to Fig. 5 in Heath and Rock (1996b). A FabA K_m value of 1.7 mM was obtained for β-hydroxydecenoyl-ACP from Kass *et al* (1967). This K_m value was assigned to other β-hydroxy substrates of FabA.

The equilibrium constant for the dehydratase activity (i.e both FabZ and FabA) has been reported to vary with substrate chain length. Under reactions involving short chain substrates (4-carbon chain), the ratio of substrates to products was 1:9 indicating the reverse reaction is more favourable (Heath and Rock, 1995). However, the ratio of substrates to product becomes 75:22 (the unaccounted 3% is the *cis*-product from the FabA isomerase reaction which indicates the equilibrium constant for the isomerase

reaction is 0.14) when utilizing β-hydroxydecenoyl-ACP as substrate indicating an equilibrium constant of 0.29 (Heath and Rock, 1996b). Therefore, the k_{catr} values of FabA and FabZ for this substrate can be calculated. Furthermore, the substrate/product ratio becomes 1:1 under reactions involving long chain substrates (Heath and Rock, 1995). This meant that k_{catf} equals k_{catr} for all other dehydratase reactions.

For the isomerase activity of FabA, the k_{catr} was estimated as 11.7 s^{-1} (i.e. *cis*-3-decenoyl-ACP was substrate) from Fig. 7 in Helmkamp and Bloch (1968) and the K_{mp} parameter obtained from Kass *et al.* (1967). The reaction equilibrium constant of 0.14 as mentioned above enabled k_{catf} to be derived. Although, the same values for K_{ms} and K_{mp} were initially assumed, the K_{ms} value was changed to 0.0001 mM as described below.

Bi-substrate Michaelis-Menten kinetics was used to model the transfer of fatty-acyl moieties to G3P by PlsB and PlsC. Here, the metabolic flux is

$$\frac{d[\mathrm{P}]}{dt} = -\frac{d[\mathrm{S}_1]}{dt} = -\frac{d[\mathrm{S}_2]}{dt} = \frac{k_{cat}[\mathrm{E}][\mathrm{S}_1][\mathrm{S}_2]}{\left(K_{m_1} + [\mathrm{S}_1]\right)\left(K_{m_2} + [\mathrm{S}_2]\right)} \qquad (10)$$

where $[S_1]$ and $[S_2]$ are the two substrate concentrations with respective Michaelis-Menten constants K_{m1} and K_{m2}. The phospholipids fatty acid composition in the model only includes the major fatty acids found in *E. coli* membranes (i.e. palmitic, palmitoleic, and *cis*-vaccenic acids). This is because, other minor fatty acids vary from strain-to-strain and sometimes, non-existent in some *E. coli* strains. As mentioned above, PlsB and PlsC attaches fatty acids to positions-1 and -2 of G3P respectively. Fatty acids found in position-1 are palmitic and *cis*-vaccenic acids while palmitoleic acids and, again, *cis*-vaccenic acids are present in position-2. Hence, PlsB and PlsC both utilize *cis*-vaccenoyl-ACP substrate.

The PlsB k_{cat} values were derived from the reported specific activities of 9.5 and 8.5 µmol/min/mg for palmitoyl-ACP and *cis*-vaccenoyl-ACP substrates respectively (Green *et al.,* 1981).

There were no available specific k_{cat} and K_m values for PlsC so estimates had to be made as well. Rock *et al.* (1981) reported a K_m value of 0.012 mM for the incorporation of palmitoleoyl-ACP into G3P whilst using inner membrane enzymic fractions. Since incorporation of palmitoleoyl-ACP is conducted exclusively by PlsC, one can assign this K_m value to PlsC with the assumption that there was no competition for this substrate with other membrane proteins. The authors also reported similar specific activities for the incorporation of palmitoyl-ACP and palmitoleoyl-ACP. The incorporation of palmitoyl-ACP is also performed exclusively by PlsB. This therefore suggests that 1 mg of inner membrane fraction (which contains PlsB) whilst utilizing palmitoyl-ACP would result in the same reaction rate as 1 mg of inner membrane fraction (containing PlsC) when catalysing palmitoleoyl-ACP. Since the molecular weight of PlsB is 3 times that of PlsC (Green *et al.,* 1981; Coleman, 1992), this indicates PlsC copy number in membrane extract is 3 times that of PlsB (hence, PlsC count per cell is about 4200 molecules). This also suggests that the k_{cat} value for PlsC towards palmitoleoyl-ACP would be 3 times less that for PlsB with palmitoyl-ACP substrate.

Additionally, Goelz and Cronan (1980) observed that 32% of fatty acids attached to position-1 of G3P were *cis*-vaccenic acids (i.e. by PlsB). A preliminary simulation for PlsB was run using COPASI (1400 copies per cell (Green *et al*., 1981) with saturated levels of palmitoyl-ACP and *cis*-vaccenoyl-ACP. It was observed that when there were no competition for *cis*-vaccenoyl-ACP (i.e. absence of PlsC), 37% of fatty acids attached to position-1 were *cis*-vaccenic acid instead of 32%. However, when

competition was included (i.e. presence of PlsC), it was observed the V_{max} for PlsC required to attain 32% of *cis*-vaccenic acid in position-1 was 1.94 folds greater than that of PlsB. Thus, with the knowledge of the PlsB k_{cat} value for *cis*-vaccenoyl-ACP, and protein counts for both PlsB and PlsC, the k_{cat} of PlsC towards *cis*-vaccenoyl-ACP substrate can be derived as 7.6 s^{-1}.

A single-substrate Michaelis-Menten kinetics with inhibition was used for the FabI enzyme for all substrates. In this case, the metabolite flux is

$$\frac{d[\mathrm{P}]}{dt} = -\frac{d[\mathrm{S}]}{dt} = \frac{k_{cat}[\mathrm{E}][\mathrm{S}]}{\left(K_m + [\mathrm{S}]\right)\left(1 + \frac{[\mathrm{P}]}{K_i}\right)} \qquad (11)$$

where K_i is the inhibition constant, [P] is the concentration of palmitoyl-ACP, and the other parameters are the same as in eq. 10.

The model used same parameters for *trans*-2-tetradecenoyl-ACP (C14:0) and *trans*-2-dodecenoyl-ACP (C12:0) since they both had similar affinities with FabI (Weeks and Wakil, 1968). There was no information available in the literature regarding FabI reactions with *trans*-2-hexadecenoyl-ACP (C16:0). The model assumed that the FabI reaction rate would not increase with increasing carbon-chain length for saturated substrates since the affinities of *trans*-2-dodecenoyl-ACP and *trans*-2-tetradecenoyl-ACP were same. Furthermore, in the absence of FabI parameters with unsaturated substrates, same parameters for saturated 12-carbon, 14-carbon and 16-carbon substrates were assigned to 12-carbon, 14-carbon and 16-carbon unsaturated substrates respectively. The FabI k_{cat} value for *trans*-2-decenoyl-ACP was estimated from Fig. 7 in Weeks and Wakil (1968) relative to that reported for *trans*-2-dodecenoyl-ACP (Rafi *et al.*, 2006) and its K_m parameter was derived from Fig. 6 of Weeks and Wakil (1968). Finally, Heath and Rock (1996c) observed that at a palmitoyl-ACP concentration of 400

μM, the FabI reaction rate was inhibited by 92%. If one assumes non-competitive inhibition and excess substrate conditions, a K_i value of 0.035 mM can be derived.

The FabH reaction step was modelled using an irreversible single-substrate Michaelis kinetics with dual acyl-ACP (palmitoyl-ACP and *cis*-vaccenoyl-ACP) inhibition. Here, the metabolite flux is

$$\frac{d[\mathrm{P}]}{dt} = -\frac{d[\mathrm{S}]}{dt} = \frac{k_{cat}[\mathrm{E}][\mathrm{S}]}{(K_m + [\mathrm{S}])\left(1 + \frac{[\mathrm{P}]}{K_i}\right)\left(1 + \frac{[\mathrm{P}^*]}{K_{i^*}}\right)} \quad (12)$$

where K_{i*} is inhibition constant arising from *cis*-vaccenoyl-ACP ([P*]) and other parameters are same as eq. 11.

Although, an initial FabH k_{cat} value of 3.28 s^{-1} was derived from the reported specific activity (Heath and Rock, 1996a), it was apparent that this parameter would be insufficient to produce the appropriate amount β-hydroxydecenoyl-ACP required for SFAs and UFAs synthesis (the FabH molecule count is 1320 per cell (Ishihama *et al.*, 2008) which suggests a maximum production of 8 million products whereas approximately 20 million fatty acids are generated *in vivo*). This is unsurprising as it has been suggested previously that there are other enzymes capable of replacing FabH (Yao *et al.*, 2012). Consequently, the k_{cat} value was increased to 12 s^{-1}. The inhibition constants for palmitoyl-ACP and *cis*-vaccenoyl-ACP inhibitors were estimated as 0.1 mM and 0.067 mM respectively from Heath and Rock (1996a) much as was done for FabI above.

3.3.2.1 LpxK catalytic activation and inactivation

The activation of LpxK from an inactive to an active state was modelled using mass action kinetics according to

$$\frac{d[\text{LpxK*}]}{dt} = k\left(1+\frac{[\text{activator}]}{K_a}\right)[\text{LpxK}] - K_{inact}[\text{LpxK*}] \qquad (13)$$

where k is the phospholipids-independent activation constant, K_a is the phospholipids-dependent activation constant, K_{inact} is the inactivation constant, [activator] is the phospholipids concentration (i.e. fatty acids), [LpxK*] and [LpxK] represent the concentrations of the activate and inactive forms of LpxK.

In Ray and Raetz (1987), the absence of phospholipids resulted in a maximum reaction rate which was 94% less than those with phospholipids stimulation. Since there are 432 copies of LpxK per cell, this means the absence of phospholipids would result in 406 copies of inactive LpxK, and 26 copies of active LpxK. By assuming K_{inact} as 0.1 s^{-1}, k value of 0.0064 s^{-1} can be derived.

When cells newly divide, LpxK would most likely be maximally activated quickly due to the essential need for LPS production. The model assumes that this maximal activation (which was arbitrarily defined as 95% of active proteins) would occur within 100 s. It was also assumed that about 1.1 x 10^6 fatty acids would have been produced in 100 s. This is because, there are approximately 1 million LPS in *E. coli* (Raetz *et al.*, 2009), and the LPS/phospholipids ratio is approximately 0.1 (Galloway and Raetz, 1990; Raetz *et al.*, 2009). Since 2 molecules of fatty acids make up a phospholipid molecule (with the exception of cardiolipins which occupy about 5% of total phospholipids), this suggest approximately 20 million fatty acids are produced for phospholipid biosynthesis per generation time. Thus, in 100 s, approximately 1.1 x 10^6 fatty acids would be synthesized given a cell generation time of 30 min. By Inputting

LpxK and LpxK* counts as 22 and 410 molecules respectively, coupled with the activator count, the K_a value can be calculated as 0.0094 mM.

3.3.2.2 Transcriptional regulation of fabA and fabB

The expression of *fabA* and *fabB* genes occur from two different promoters. One of them, which is usually regarded as the 'weak promoter' is constitutive while the dominant promoter is regulated through mediated transcriptional activation and repression by FadR and FabR proteins respectively.

Protein synthesis from the constitutive promoter was modelled according to the zeroth order reaction

$$\text{promoter}_{\text{const}} \xrightarrow{K_1} \text{promoter}_{\text{const}} + \text{protein} \qquad (14)$$

where $\text{promoter}_{\text{const}}$ represents the constitutive promoter and K_1 is the resulting protein translation rate constant. This approach combines transcription and translation into a single reaction step.

When *fadR* and *fabR* are inactivated, protein expression would occur solely from the constitutive promoter. Feng and Cronan (2011) observed that mRNA levels of *fabA* were 40% those of wild-type cells while those for *fabB* remained the same in a *fadR* and *fabR* double mutant. In the model, it was assumed that the relative fold-reduction in mRNA levels would result in a similar fold-reduction in protein levels. This is a reasonable assumption since neither FabA nor FabB are regulated at the post-transcription or post-translation level. Therefore, the transcript half-lives, protein translation and degradation rates would remain constant under *fabR* and *fadR*

inactivation conditions. In wild-type *E. coli*, the FabA count is 23,400 (Ishihama *et al.,* 2008) which indicates a *fadR/fabR* double mutant contains approximately 9,360 FabA proteins. Thus, the translation rate can be derived as the production of 9,360 proteins over the course of a cell generation which gives a K_1 of 5.2 molecules/s (assuming a generation time of 30 min). On the other hand, there are 14,300 FabB proteins per cell which enabled the K_1 to be calculated as 7.945 molecules/s.

In order to induce *fabA* and *fabB* expression, FadR is likely to be activated. The activation of FadR from an inactive to an active state was modelled using first order reaction kinetics

$$[\mathrm{FadR}] \underset{K_{-2}}{\overset{K_2}{\rightleftharpoons}} [\mathrm{FadR}^*] \tag{15}$$

where [FadR] and [FadR*] are the inactive and active forms of FadR , K_2 and K_{-2} are the resultant activation and inactivation constants respectively. The cellular count of FadR is about 295 (Ishihama *et al.,* 2008). The model assumes 100 copies of these would be used in the regulation of *fabA* and *fabB* (in which case, [FadR*] = 100) thereby leaving a reasonable FadR reservoir for other regulatory processes. This estimate may be inaccurate; however, they do not affect the model results at all. Thus, the estimate is only necessary to capture the activation of FadR. The model also assumed K_{-2} as 0.1 s^{-1} which then gave a K_2 value of 0.054 s^{-1}. Again, the accuracy of the K_2 and K_{-2} values are inconsequential provided their ratio is accurate.

The activated form of FadR can bind reversibly to a DNA sequence downstream the regulated promoter and induce protein expression.

$$\mathrm{promoter}_{\mathrm{reg}} \underset{K_{\mathrm{inactive}}}{\overset{K_{\mathrm{active}}[\mathrm{FadR}^*]}{\rightleftharpoons}} \mathrm{promoter}_{\mathrm{active}} \tag{16}$$

$$\mathrm{promoter}_{\mathrm{active}} \xrightarrow{K_3} \mathrm{promoter}_{\mathrm{active}} + \mathrm{protein} \tag{17}$$

where $promoter_{reg}$ is the regulated promoter, $promoter_{active}$ is the active promoter resulting from FadR binding to DNA sequence, K_{active} and $K_{inactive}$ are the resultant activation and inactivation constants. K_3 is the translation rate constant from the activated promoter.

As mentioned above, there are 23,400 FabA proteins in wild-type *E. coli*. This means that the sum of K_1 (i.e. from eq. 14) and $K_3[promoter_{active}]$ equals the synthesis of 23,400 proteins per cell generation time. There are four different states the regulated promoter can assume; *(i)* an inactive state resulting from lack of DNA binding by FadR or FabR; *(ii)* an active state from DNA binding by FadR; *(iii)* an inactive state arising from FabR bound to DNA; and *(iv)* an inactive state arising from DNA binding by FabR in addition to a bound FadR. Irrespective of FadR bound to DNA, binding of FabR would prevent expression (Zhu *et al.,* 2009)**.** The FabR and FadR concentrations are likely to be optimized for precise control, so it was assumed that their concentrations are about half of the binding constant values. This implies that the probability is 0.25 for each of the 4 states. This meant that $[promoter_{active}]$ count equals 0.25. Inputting this value with prior estimate of K_1 resulted in a K_3 value of 31.2 s^{-1}.

Furthermore, the transcript levels for *fabA* were increased by 1.8 folds in a *fabR* mutant which was estimated would result in 42,120 proteins. This indicates that there was continuous expression from the regulated promoter which meant the promoter can achieve only two possible states. Again, with prior knowledge of K_1 and K_3, a steady-state estimate for $[promoter_{active}]$ can be calculated as 0.583 molecules in a *fabR* mutant and subsequently derive $[promoter_{reg}]$ as 0.417 molecules. Next, by assuming $K_{inactive}$ as 0.1 s^{-1}, coupled with the [FadR*], $[promoter_{reg}]$, and $[promoter_{active}]$ values, one can derive K_{active} as 1.4 x 10^{-3} s^{-1}.

On the other hand, the expression rates of *fabB* were similar in both wild-type and *fadR* mutant (Feng and Cronan, 2011) which suggest FabR is the dominant regulator of *fabB* in agreement with prior propositions (Feng and Cronan, 2011). This indicates that in wild-type cell, expression occurs mainly from the constitutive promoter which gives the [$promoter_{active}$] count as approximately zero. However, in a *fabR* mutant, the mRNA levels were increased by 1.7 folds in comparison to wild-type which was calculated would lead to 24,310 FabB proteins. Yet again, only two possible promoter states exists under *fabR* inactivation conditions and the model assumes a steady state count for [$promoter_{reg}$] and [$promoter_{active}$] as both 0.5 molecules each. This enabled K_{active} to be derived as 1.0×10^{-3} s^{-1} much as was done for *fabA.*

The activation of FabR from an inactive to an active state is stimulated by the presence of UFAs (Zhu *et al.,* 2009). It is believed that the cell is able to detect the relative ratio of SFAs and UFAs which then determines if FabR is activated (Zhu *et al.,* 2009). The activated form of FabR then binds to an overlapping DNA sequence downstream of FadR (Zhu *et al.,* 2009). Prior binding of FadR does not prevent the binding of FabR. Therefore, an active form of FabR can bind to DNA with different promoter states of [$promoter_{reg}$] and [$promoter_{active}$] to give two different promoter inactive states.

$$[\mathrm{FabR}] \underset{[\mathrm{SFA}]}{\overset{[\mathrm{UFA}]}{\rightleftharpoons}} [\mathrm{FabR}^*] \tag{18}$$

$$\mathrm{promoter}_{\mathrm{reg}} \underset{K_{-4}}{\overset{[\mathrm{FabR}^*]}{\rightleftharpoons}} [\mathrm{inactive\_promoter}_1] \tag{19}$$

$$\mathrm{promoter}_{\mathrm{active}} \underset{K_{-5}}{\overset{[\mathrm{FabR}^*]}{\rightleftharpoons}} [\mathrm{inactive\_promoter}_2] \tag{20}$$

where [FabR] and [FabR*] are the inactive and active forms of FabR, [UFA] and [SFA] are the concentrations of UFAs and SFAs respectively, [$inactive\_promoter_1$] and [$inactive\_promoter_2$] are the different inactive promoter states, K_{-4} and K_{-5} are the FabR

dissociation rate constants from DNA of [inactive_promoter$_1$] and [inactive_promoter$_2$] respectively. There were no specific estimates of the FabR cellular count in the literature so the model assumed same count as FadR. Again, this estimate is inconsequential since K_{-4} and K_{-5} parameters were fitted as described below. It was also assumed that the affinity of active FabR for promoter$_{reg}$ and promoter$_{active}$ are similar which meant that the FabR dissociation constant is same irrespective of the promoter state. The K_{-4} and K_{-5} parameters were derived during model fitting.

Protein degradation was modelled with first order kinetics as well, with $K_{degrade}$ as the degradation rate constant. The steady-state protein abundance in a cell is (K_1 + [promoter$_{active}$]*K_3)/$K_{degrade}$. The $K_{degrade}$ value was calculated as 5.556 x 10^{-4} s^{-1} for FabA and FabB using [promoter$_{active}$], K_1 and K_3 parameters described above.

$$\text{protein} \xrightarrow{K_{\text{degrade}}} \varnothing \qquad (21)$$

3.4 SIMULATIONS

The integrated LPS and phospholipids synthesis model was simulated using deterministic methods using the COPASI software (Mendes *et al.*, 2009). Simulations represented an *E. coli* cell generation under optimal growth conditions which is 1800 s. As mentioned previously in Chapter 2, using stochastic simulations and accounting for stochasticity had negligible effect on the results due to the high copy numbers of all model components which justified the use of deterministic simulations. The COPASI file is available as a supplementary information.

3.5 MODEL ADJUSTMENT

Initial model parameters described above were unable to either achieve the appropriate SFAs/UFAs ratio or replicate some published experimental findings. This was as a result of limitations in the following areas;

3.5.1 FabA isomerase and FabZ kinetics

Initial simulations resulted in excess SFAs and little or no UFAs. This was solely due to FabI outcompeting FabA isomerase for *trans*-2-decenoyl-ACP substrate which led to an accumulation of SFAs substrates. This problem was solved in the model by reducing the K_{ms} value of FabA isomerase towards *trans*-2-decenoyl-ACP to 0.0001 mM which resulted in SFAs occupying 50% of total fatty acids. Indeed, there were no reported K_m parameters for the isomerization of *trans*-2-decenoyl-ACP in the literature as mentioned earlier; so it is unsurprising that the initial estimate was inadequate.

Although the model had obtained 50% SFAs yield, a bottleneck in the UFA arm of the pathway ensured an insufficient production of UFAs resulting from accumulation of substrates of FabZ. Again, this is understandable given there were also no reported parameters for unsaturated substrates of FabZ in the literature as mentioned earlier. This was resolved by increasing both the k_{catf} and k_{catr} parameters (so the equilibrium constant remained the same) for the 14, 16 and 18-carbon unsaturated substrates by 3 folds.

3.5.2 FabB activity towards *cis*-3-decenoyl-ACP

Initial parameters were unable to reproduce the roles of FabA and FabB in the synthesis and regulation of UFAs. For instance, overexpressing *fabA* in the model resulted in

increased levels of UFAs rather than the opposite effect. This was solely due to the high affinity of FabB for *cis*-3-decenoyl-ACP. This then suggests that the specific activity of FabB *in vivo* is far less than those reported *in vitro* by D'Agnolo *et al.* (1975). There are several pieces of evidence that supports the claim of FabB being the rate-limiting step in UFAs synthesis. Firstly, overexpression of FabA (which will theoretically increase the isomerisation of *cis*-3-decenoyl-ACP) does not increase nor decrease UFAs yield, although SFAs level are elevated (Clark *et al.,* 1993). Secondly, overexpression of FabB enhances UFAs yield (Cao *et al.,* 2010). In order to ensure FabB was the rate limiting step in UFAs synthesis, the k_{catf} parameter for *cis*-3-decenoyl-ACP substrate was chosen to be decreased. The proportion of SFAs in wild-type *E. coli* under optimum conditions can range from 50 – 70% of the total fatty acids (Zhu *et al.,* 2009; Oursel *et al.,* 2007). Whilst the levels of FabA and FabB were fixed to their steady-state counts, the k_{catf} value was reduced so that the model would produce 60% SFAs, which turned out to be a value of 0.31 s^{-1}.

3.5.3 LpxK catalytic activation

At first, when the role of fatty acid biosynthetic enzymes on LpxC regulation was investigated, the model results deviated from published datasets. For instance, model inhibition of FabZ did not result in LpxC degradation in contrast to experimental findings by Zeng *et al.* (2013). This was because, the model had sufficient amount of fatty acids (especially SFAs) to catalytically activate LpxK, which ensured that lipid A disaccharide (the feedback source for LpxC degradation) did not accumulate. However, when the catalytic activation of LpxK arose solely from UFAs, the model replicated the results in Zeng *et al.* (2013) and other published results. Thus, the activation of LpxK is

most likely sensitive to the SFAs/UFAs ratio. Eq. 13 was modified to ensure LpxK was catalytically activated by UFAs and inactivated by SFAs

$$\frac{d[\text{LpxK*}]}{dt} = k\left(1+\frac{[\text{UFA}]}{K_a}\right)[\text{LpxK}] - K_{inact}[\text{SFA}][\text{LpxK*}] \qquad (22)$$

where [UFA] and [SFA] are the concentrations of the activator and deactivators respectively and other parameters are same as in eq. 13. Here, it is assumed K_{inact}[SFA] equals 0.1 s^{-1}. As mentioned above, wild-type cells contain about 20 million fatty acids and 60% of these comprise of SFAs which is 12 million copies (29.7 mM). Using this concentration, K_{inact} can be derived as 0.0034 $mM^{-1}s^{-1}$.

Indeed, it was reported in Ray and Raetz (1987) that of all phospholipids species tested, cardiolipins had the most effect at activating LpxK. Although the authors did not provide a rationale for their observation, their use of bovine heart cardiolipins which are known to contain at least 94% UFAs of the total fatty acids, may have been implicated (Schlame *et al.,* 1993). Similarly, cardiolipins of *E. coli* are characterized with more UFAs relative to other phospholipids moieties (Yokota *et al.,* 1980). In this regard, the model strongly proposes that the activity of LpxK is dependent on the presence of UFA.

Finally the K_{-4} and K_{-5} values were fitted as 90 s^{-1} for *fabA*, and 2 s^{-1} for *fabB* which resulted in a protein steady-state count.

3.6 MODEL RESULTS

3.6.1 FabZ inhibition and overexpression

Zeng *at al.* (2013) isolated FabZ mutants with decreased specific activities that had low levels of LpxC. The authors also observed that overexpression of FabZ increased levels of LpxC in wild-type cells. Although, there were no specific LpxC fold-changes in

either case from Zeng *et al* to quantitatively make comparison, both perturbations were tested in the refined model by decreasing or increasing the FabZ counts by 100 folds. As seen in Fig. 3.2A, LpxC levels were decreased by 40% when FabZ was inhibited and consequently, the amount of LPS being produced was also reduced by 40%. It was observed the LpxK catalytic activation rate was reduced by 50% which enabled lipid A disaccharide to accumulate and negatively feedback on LpxC degradation. The model produced excess SFAs and could barely synthesize UFAs due to the absence of an essential FabZ role at dehydrating *cis*-containing β-hydroxyacyl-substrates. Despite this, it was also observed that no accumulation of FabZ substrates occurred due to the readily reversible nature of the FabZ reactions. The production of SFAs occurred from the activities of the bi-functional FabA enzyme. In contrast, the dehydratase role of FabZ in UFAs synthesis cannot be complemented by FabA (Heath and Rock, 1996b) hence the absence of UFAs. An upregulation in FabA and FabB concentrations were observed but these had no effect at elevating the concentrations of UFAs because FabZ became the rate-limiting step in UFAs synthesis.

On the other hand, the steady-state concentration of LpxC was increased by 2.6 fold when FabZ was overexpressed in the model (Fig. 3.2A). However, LPS levels were reduced by 70%. Since cells become non-viable when LPS amounts are reduced by more than 50% (Onishi *et al.,* 1996), overexpression of FabZ would result in a lethal effect to the cell in agreement with data presented in Zeng *et al.* (2013). Regarding the fatty acid profile, the production of SFAs was slightly enhanced while UFAs amounts remained the same. Although, Lee *et al.* (2013) had reported that overexpression of FabZ increases the proportion of UFAs, their data exhibited this phenomenon only after prolonged growth (i.e. stationary phase) whereas, the model represents the exponential or steady-state growth phase of *E. coli*. In fact, their results indicated that when the cells were harvested early, SFAs were increased and UFAs decreased. Thus, in this respect,

the FabZ model is compatible with their experiments. Despite the slight increase in SFAs amount in the model, an up-regulation in FabA or FabB was not observed.

3.6.2 The role of FabA and FabB in UFAs biosynthesis

As mentioned above, cellular requirement for UFAs result in an upregulation of both *fabA* and *fabB* genes which enhances UFAs yield. However, sole overexpression of FabA increases SFAs synthesis rather than UFAs synthesis (Clark *et al.,* 1983; Cao *et al.,* 2010). This phenomenon was tested in the model as presented in Fig. 3.2B. Model results agree qualitatively with experimental evidence presented in Clark *et al* (1983). The slight quantitative disparity may arise since the experimental results used for comparison were carried out at 42°C whereas the model parameters represent optimum conditions.

3.6.3 Overexpression of *fabH*

In Tsay *et al.* (1992), it was reported that overexpression of *fabH* increased the cellular concentration of SFAs by 16%. Testing this perturbation in the model was relatively straightforward. A 10% increase in SFAs level was observed when the FabH count was increased by 100 folds in close agreement with the experiments. Furthermore, the model displayed an increase in the expression levels of FabA and FabB; however, expression of the latter was not as pronounced as FabA.

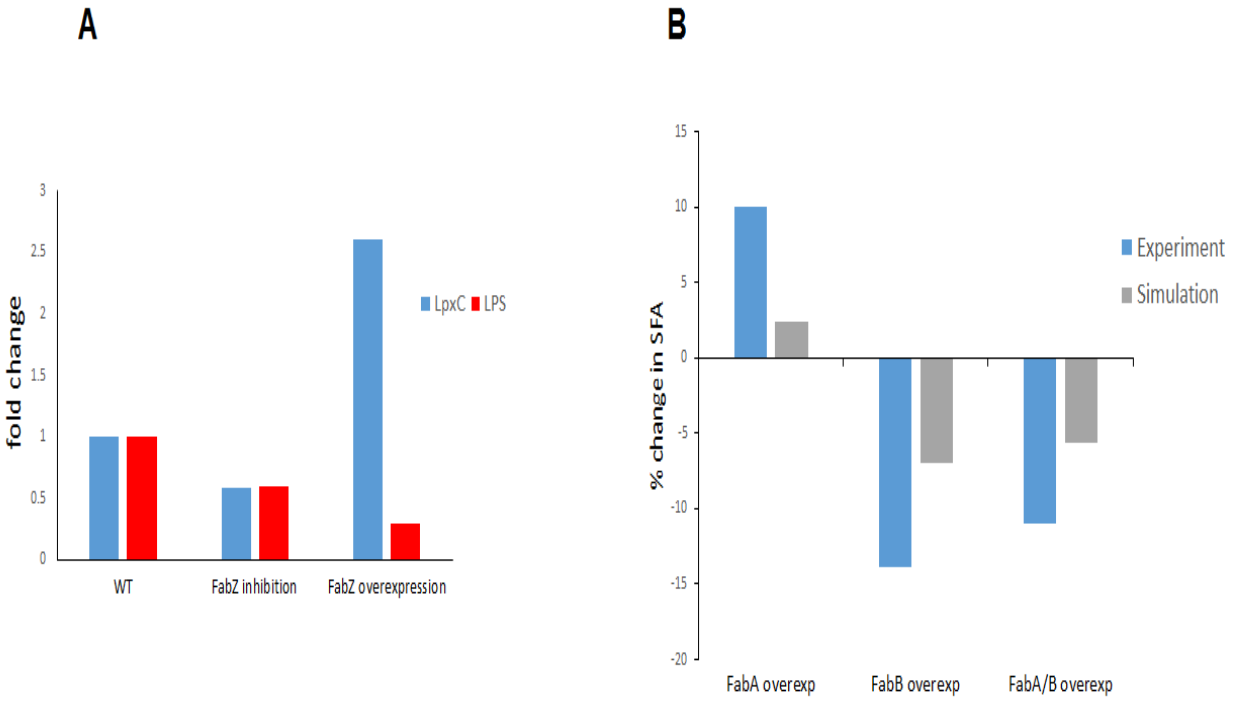

Figure 3.2. Model results. Model conditions were those depicted in Fig. 3.1 using paramters presented in Table 3.1. (A) Effect of FabZ inhibition and overexpression on LpxC and LPS levels. The FabZ molecule count were increased or decreased by 100 folds to represent FabZ overexpression and inhibition respectively. (B) The role of FabA and FabB on SFAs/UFAs ratio. The FabA and FabB counts were kept constant and increased by 100 folds to represent overexpression conditions. This meant that FadR/FabR regulation was disabled.

3.7 SUMMARY

A biosynthesis computational model of the outer membrane of *E. coli* was developed, drawing parameters from the literature, and making estimates when necessary. The model agrees qualitatively with experimental data and to some extent, quantitatively. The model findings indicate that the fatty acid enzymes have sufficient catalytic properties to produce approximately 20 million molecules required *in vivo.*

However, the model may be inadequate for testing certain pathway perturbations. For instance, there were no specific parameters for FabG involving any of the substrates studied in the model. Therefore, the estimates made may only be adequate under wild-type conditions where FabG does not limit pathway flux. Also, as stated above, FadR is a global regulator of certain genes involved in fatty acid biosynthesis and degradation. Apart from the transcriptional activation of *fabA* and *fabB,* the other roles of FadR are outside the scope of this work hence, the model may be inappropriate at studying the effect of FadR dynamics on fatty acid synthesis.

One of the interesting findings from the model was the observation that the catalytic activity of LpxK may be reliant on the concentration of UFAs. The significance of this finding suggest that LpxK plays a crucial role in outer membrane homeostasis than was previously envisaged. The resultant effect of a decrement in LpxK activity would lead to the accumulation of lipid A disaccharide which in turn will enhance the degradation of LpxC. In other words, LpxC is expected to be less stable under low UFAs conditions according to the model findings.

Chapter 4

Experimental methodology

4.1 OVERVIEW

The last two Chapters have discussed the development of an integrated biosynthetic pathway model of lipid A and phospholipids. Although, there are a number of published experimental datasets which could be used to further validate the model, they however, focus mainly on one arm of the integrated pathway. For instance, there is little available information to test the effects of perturbation of one synthetic pathway on the regulation of the other. This would appear important given both lipid A and phospholipids are synchronously produced as discussed previously. Furthermore, model reliability would be improved if its prediction can be validated experimentally.

This Chapter describes the experimental methodological approach aimed at model validation, and testing of its predictions.

4.2 PROCEDURES

4.2.1 Bacterial strains and growth conditions

The *E. coli* strains and plasmids used for these experiments along with their relevant characteristics are presented in Table 4.1. *E. coli* strains JP1111, CY53, CY288 and DC170 were obtained from the *E. coli* Genetic Stock Center (CGSC) at Yale, USA while strain AG1 was purchased from the National BioResource Project (NIG) Japan. Strains W3110, *ΔftsH*, and plasmid pBO110 were gifts from Prof. Franz Narberhaus. Unless stated otherwise, cells were grown in LB medium (10 g tryptone, 5 g yeast extract, 5 g NaCl per litre). When required, antibiotics were used at the following concentrations for selective pressure; 20 µg/ml chloramphenicol, 30 µg/ml kanamycin and 100 µg/ml ampicillin. Protein expression was induced with either L-arabinose (for

cells containing the pBAD plasmid), or IPTG (for cells containing plasmid with the *lac* operator) as appropriate when required.

4.2.2 Plasmid extraction

An overnight culture of strain AG1 containing the pCA24N plasmid bearing the *waaA* gene was centrifuged (1 ml) using a microcentrifuge at maximum speed (13,000 rpm) for 1 min. The pellets were washed with phosphate buffered saline (PBS) and re-suspended in 100 µl of a resuspension buffer (50 mM Tris-HCl, pH 7.5; 10 mM EDTA; 100 µg/ml RNase). 200 µl of lysis buffer (0.2 M NaOH; 1% SDS) was added and mixed by gently inverting the tube and immediately, 200 µl of Potassium acetate solution was added to precipitate the genomic DNA. After 5 min, the suspension was centrifuged at maximum speed for 5 min and the supernatant-containing plasmid DNA (about 400 µl) collected and transferred onto a fresh tube. Plasmid DNA was precipitated by adding 1 ml of absolute ethanol and placed in -20°C for 30 min prior to centrifugation. The pelleted plasmid DNA was air-dried and re-suspended in 30 µl of TE buffer (10 mM Tris-HCl pH 8.0, 1 mM EDTA) and subsequently used for bacteria transformation.

4.2.3 Preparation of chemically-competent cells and bacterial transformation

An overnight culture was grown in LB broth to mid-log phase (OD_{600} = 0.5). 1 ml of culture was aliquoted into Eppendorf tubes placed on ice, and harvested by centrifugation for 10 min at 3,000 rpm at 4°C. The pellets were re-suspended in 100 µl of ice-cold Transformation Storage Solution (TSS) buffer (Chung *et al.*, 1989) (5 g polyethylene glycol 8000 (PEG); 1.5 ml 1 M $MgCl_2$; 2.5 ml dimethyl sulfoxide (DMSO); LB broth added to 50 ml) and placed on ice.

Table 4.1: *E. coli* strains and plasmids used in this study and their relevant characteristics

Strains	Relevant characteristics[1]	Reference
W3110 (wild-type)	λ^-, *IN(rrnD-rrnE)1*, *rph-1*	Bachmann (1972)
JP1111	*galE45*(GalS), λ^-, ***fabI392*(ts)**, *relA1*, *spoT1*, *thiE1*	Egan and Russel (1973)
CY53	λ^-, ***fabA2*(ts)**, *relA1*, *rpsL118*(strR), *malT1*(λ^R), *xyl-7*, *mtlA2*, *thiE1*	Cronan *et al.* (1972)
CY288	*fhuA22*, ***fabF200***, *zcf 229::Tn10*, *gyrA220*(NalR), ***fabB15*(ts)**, *relA1*, *rpsL146*(strR), *pitA10*, *spoT1*, *T2R*	Garwin *et al.* (1980b)
ΔFtsH	W3110 *zad220*::Tn10 ***sfhC21ΔftsH3***::*kan*	Tatsuta *et al.* (1998)
DC170	F-, ***fabA203*(p)**, ***fadR16***, *tyrT58*(AS), *mel-1*	Clark *et al.* (1983)
AG1	*recA1*, *endA1*, *gyrA96*, *thi-1*, *hsdR17*(r_K^- m_K^+), *supE44*, *relA1*	Kitagawa *et al.* (2005)
Plasmids		
pBO110	P_{BAD}, araC, rrnBT, Amp^r, *lpxC*	Fuhrer *et al.* (2006)
pCA24N-*waaA*	$lacI_q$, T-rrnB, *cat*, *waaA*	Kitagawa *et al.* (2005)

1. Gene mutations highlighted in bold represent genes involved in fatty acid production/regulation. *sfhC* is a synonym for *fabZ*. The mutation *fabA203(p)* leads to the creation of a novel *fabA* promoter.

2 µl of plasmid DNA was added to the TSS cells and allowed to sit on ice. After 30 min, the cells were heat-shocked by incubating at 42°C for 30 s and immediately incubated on ice for 2 min. 1 ml of SOB (Super Optimal Broth) (0.5% yeast extract; 2% tryptone; 10 mM NaCl; 2.5 mM KCl; 20 mM $MgSO_4$; 20 mM glucose (Hanahan, 1983)) was added to the cells and incubated at 37°C for 1 h. 100 µl was spread onto LB agar plates with the appropriate antibiotics as selective marker and incubated overnight at 30 or 37°C.

4.2.4 Minimum inhibitory concentration (MIC) determination

The minimal inhibitory concentration was defined as the lowest antibiotic concentration at which no measurable bacterial growth was observed in LB medium. Cultures were inoculated at a starting OD_{600} of 0.01 and incubated overnight at 30°C in the presence of varying concentrations of antibiotics.

4.2.5 Preparation of cell extracts

In the case of the temperature-sensitive mutants, isogenic strains were harvested and re-suspended in TE buffer containing 1 mM of phenylmethanesulfonylfluoride (PMSF). The cells were lysed by sonication, centrifuged at maximum speed in a microcentrifuge for 1 min, and the protein concentration in the supernatant was determined using the Bradford assay and bovine serum albumin (BSA) as standard (Bradford, 1976). 1x Laemmli sample buffer was added to the supernatant and heated at 99°C for 5 min prior to Western blot analysis.

Unless specified otherwise, cell extracts for other strains were prepared as described previously (Sorenson *et al.*, 1996; Zeng *et al.*, 2013). Briefly, an overnight culture was

inoculated into fresh LB grown to mid-log phase (OD_{600} = 0.5). The respective cultures were normalized to the same OD_{600} of 0.5. 3 ml of normalized culture was centrifuged at maximum speed for 1 min and the cell pellets re-suspended in 100 µl of TE buffer containing 1x Laemmli sample buffer (Bio-Rad). The samples were heated for 10 min prior to centrifugation for 5 min. The supernatants were collected for Western blot analysis.

4.2.6 Western blot

20 µl of each normalized sample were loaded onto a 10% SDS-polyacrylamide gel. For samples subjected to the Bradford assay, equal amounts of protein were loaded onto each well. Following electrophoresis, proteins were transferred to a PVDF membrane using the Bio-Rad Trans-Blot Turbo system. An LpxC antiserum generated in rabbit (a kind gift from Prof. Franz Narberhaus) and a secondary anti-rabbit peroxidase-linked antibody (Sigma, UK) were used for immunodetection at dilutions of 1:20000 and 1:10000 respectively. The WaaA construct expressed from the plasmid contains a His-tag attached to its N-terminus. Consequently, WaaA was immunoblotted using a 6x-His epitope tag primary antibody (Pierce) generated in mouse (1:6000) and a secondary anti-mouse alkaline phosphatse-linked (AP) antibody (1:8000). Blots were developed using the ECL chemiluminiscent reagents (Bio-Rad) or AP substrate kit (Bio-Rad) as appropriate. Signals were detected using the ChemiDoc MP system (Bio-Rad).

4.2.7 LPS analyses

4.2.7.1 LPS extraction

LPS was extracted from the membrane according to the method described by Henderson *et al.* (2013). Bacterial cultures (3 ml) were harvested and washed with PBS, and re-suspended in 200 µl of PBS. 250 µl and 500 µl of chloroform and methanol were added respectively in order to form a single phase Bligh-Dyer mixture (chloroform, methanol, water, 1:2:0.8 v/v) (Bligh and Dyer, 1959)**.** The tubes were mixed by inversion and incubated at room temperature for 30 min to ensure complete cell lysis. The mixture was thereafter centrifuged at 2,000 x *g* for 20 min and the supernatant which contains phospholipids and other lipids was discarded. The LPS containing pellet was washed with 1 ml of a single phase Bligh-Dyer mixture followed by centrifugation at 2,000 x *g* for 20 min.

4.2.7.2 Kdo assay

LPS was quantified by measuring the concentration of Kdo in the membrane as described by Karkhanis *et al* (1978). The respective cultures were grown and normalized to the same density prior to harvesting. Harvested cells were washed with PBS and re-suspended in TE buffer containing 1 mg/ml lysozyme. Cells were sonicated and centrifuged for 20 min at maximum speed. The membrane fractions were re-suspended in 1 ml of 0.1 M H_2SO_4 and heated at 99°C for 30 min. After cooling and centrifugation for 5 min, 500 µl was pipetted into another test tube. 250 µl of 0.04M periodic acid was added, vortexed vigorously, and the mixture was left to stand at room temperature for 20 min. Next, 250 µl of 2.6% Sodium arsenate in 0.5M HCl was included in the mixture and vortexed vigorously. When the brown colouration that developed had disappeared, 500 µl of 0.6% thiobarbituric acid was added, vortexed and

heated for 15 min at 99°C. Whilst still hot, 1 ml of DMSO was added. The mixture was left to cool to room temperature and its optical density at 548 nm was read against a blank treated as above but without cell lysates.

4.2.7.3 Heptose assay

Heptose is a major constituent of the LPS core OS (Kneidinger *et al.,* 2002). Heptose levels were determined by the method described in Wright and Rebers (1972). Bacterial culture were normalized prior to harvesting and washed with PBS. LPS was extracted from the membrane as described above and then placed in an ice water bath. 1.125 ml of H_2SO_4 (6 vol. of conc. H_2SO_4 and 1 vol. of H_2O) was added, mixed vigorously, and left in the ice water bath for 3 min. Next, the tubes were transferred to a 25°C water bath for 3 min prior to the addition of 25 µl of 3% cysteine-HCl. The mixture was heated at 99°C for 20 min and absorbance readings were taken after 1 h at 505 nm and 545 nm. The difference in absorbance readings ($A_{505} - A_{545}$) were used for quantitative analyses. The blank was treated as above but with the exclusion of cysteine-HCl.

4.2.8 Phenotypic characterization on agar plates

E. coli strains containing the plasmid bearing the *waaA* gene were grown to an OD_{600} of 0.2 and serial dilutions from 10^{-1} to 10^{-4} were prepared. 2 µl of the dilutions were spotted on LB agar plates containing chloramphenicol and when required, IPTG was used to induce *waaA* expression. The plates were incubated at 30°C overnight.

4.2.9 Fatty acids analyses

4.2.9.1 Fatty acids extraction

Fatty acids extraction were performed essentially as described by Kurkiewicz *et al* (2003). 40 ml of bacteria cells harvested at an OD_{600} of approximately 0.5 were centrifuged and the pellets heated with 3M NaOH (1 ml) for 40 min at 90°C in a water bath. 2ml of 3.25M HCl was added and heated further for 10 min at the same temperature. After cooling, fatty acids were extracted 3 times using 1ml of hexane-diethyl ether mixture (1:1). The organic layers were separated by centrifugation for 5 min at 2400 x *g*. The obtained fatty acids were evapourated under vacuum prior to the derivation step.

4.2.9.2 Preparation of 3-pyridylcarbinol (picolinyl) ester derivatives

The derivatives were prepared as described previously (Harvey, 1998). The extracted fatty acids were heated with 20 µl of thionyl chloride for 10 min at 99°C. The residual thionyl chloride was evapourated under a stream of Nitrogen gas and a solution of 20% 3-(hydroxymethyl) pyridine in acetonitrile (10 µl) was added. The mixture was heated for 1 min at 99°C. 500 µl of hexane was added prior to gas chromatography-mass spectrometry (GCMS) analysis.

4.2.9.3 Gas chromatography-mass spectrometry

GCMS analyses were performed using an Agilent GC 7890A and EI/CI MSD 5975C models. Chromatographic separations were performed using a capillary column (30 m, 0.25 mm i.d., 0.25 µm film thickness) and helium was the carrier gas. The temperature program of the oven used were those previously described by Oursel *et al.* (2007);

initial temperature at 200°C, held for 1 min, raised to 240°C at 8°C min^{-1}, then ramped to 300°C at 2°C min^{-1}.

Peak identities were confirmed from their electron ionization (EI) mass spectra, and comparison with retention times of known standards.

Chapter 5

Experimental results

5.1 OVERVIEW

Whilst the model presented in Chapters 2 and 3 have provided insight into the complex regulation of LPS synthesis during outer membrane biogenesis, a number of the model findings required experimental evidence. This would further enhance model reliability and in addition, the experimental findings could further be used to constrain the simulation parameters which would ensure a more accurate representation of the model.

The regulation of fatty acids and phospholipids biosynthesis has been studied extensively; however, little information exists regarding the impact of fatty acids/phospholipids synthesis on LPS regulation in terms of metabolic cross-talk. Although, Ogura *et al.* (1999) had initially suggested that acyl-ACPs may affect the regulation pattern of LpxC, there are no studies to date to confirm or test this hypothesis. Similarly, since the regulation of WaaA by FtsH was first reported by Katz and Ron (2008), no study has investigated the underlying regulatory mechanism. This would appear important because WaaA catalyses the reaction step that provides lipid A with its antigenic properties (Meredith *et al.*, 2006).

Furthermore, because LPS is in direct contact with the external environment, it is intuitive that LPS synthesis and regulation would be sensitive to environmental and physiological changes. In addition to testing model predictions, this Chapter aims to investigate LPS regulation under varying environmental and physiological conditions, investigate the possible role of acyl-ACPs on LpxC stability, and underpin the possible rationale behind WaaA regulation using a range of experimental methods.

5.2 ROLE OF FATTY ACID BIOSYNTHESIS ENZYMES ON LPS REGULATION

Although, the model presented in Chapters 2 and 3 indicated that lipid A disaccharide is the feedback source for FtsH-mediated LpxC degradation, there are additional information which suggests there may be other FtsH feedback signals arising from the fatty acids biosynthesis pathway. For example, it was observed in Ogura *et al.* (1999) that LpxC levels were elevated in a *fabI* (ts) mutant. In order to understand the role of fatty acids synthesis on LpxC regulation, it was essential to analyse a number of fatty acid biosynthetic mutants as described below.

5.2.1 Excess substrate flux into the saturated fatty acid and LPS pathway stimulates LpxC degradation

Four *E. coli* strains were used to investigate the role of fatty acid synthesis on LPS regulation. The first was strain JP1111 which possesses a mutation in the *fabI* gene and consequently resulting in a temperature-sensitive FabI protein. In other words, when the cells are grown at low temperatures (such as 30°C), the effect of the mutation is not apparent and the FabI protein functions normally. However, when grown at higher temperatures (such as 42°C), growth ceases due to an inactive FabI protein. Higher temperatures are usually referred to as the "non-permissive temperatures". This phenomenon is the same for all temperature sensitive mutants in this study. The second strain CY288 possesses two relevant mutations; a mutation in the *fabF* gene which apparently reduces the FabF specific activity (this *fabF* mutation is active at all temperatures) (Garwin *et al.*, 1980b); and another mutation in the *fabB* gene leading to a temperature-sensitive FabB protein. The third *E. coli* strain was CY53 with a temperature sensitive FabA protein. Finally, strain DC170 has a mutation in the *fabA*

gene leading to the creation of a novel *fabA* promoter and thus, overexpressing the FabA protein by 13 folds (Clark *et al.*, 1983). The genetic characteristics of these strains are listed in Table 4.1.

The levels of LpxC in these mutants were used as an indicator of pathway activity. When *E. coli* strains JP1111 (*fabI* (ts)) and CY288 (*fabF*200, *fabB* (ts)) were grown at the non-permissive temperature, LpxC was highly stabilized whereas LpxC was rapidly degraded in strain CY53 (*fabA* (ts)) mutant (Fig. 5.1).

Next, the SFAs and UFAs distribution in these mutants were analysed to determine if the regulatory signal is driven by levels of lipid A disaccharide, or from sources outside of the LPS pathway. In other words, an increment of substrate flux into the SFAs pathway is an indirect indication of increased flux into the LPS pathway. This is because LPS substrates are derived from the SFAs pathway (i.e. β-hydroxymyristoyl-ACP) (Fig. 3.1).

When strain JP1111 (*fabI* (ts)) was grown at the non-permissive temperature, the proportion of UFAs were substantially increased (Fig. 5.2). Inhibition of FabI which catalyses the first committed step in SFAs synthesis (Heath and Rock, 1996b) enabled the isomerase activity of FabA to divert substrates towards UFAs synthesis (*see pathway description in Fig. 3.1).* This indicates a reduction of substrate influx into the SFAs synthesis arm and subsequently the LPS pathway. This was further confirmed using LPS quantification assay described below. Therefore, LpxC stability observed in strain JP1111 (*fabI* (ts)) at the non-permissive temperature is as a result of decreased levels of lipid A disaccharide.

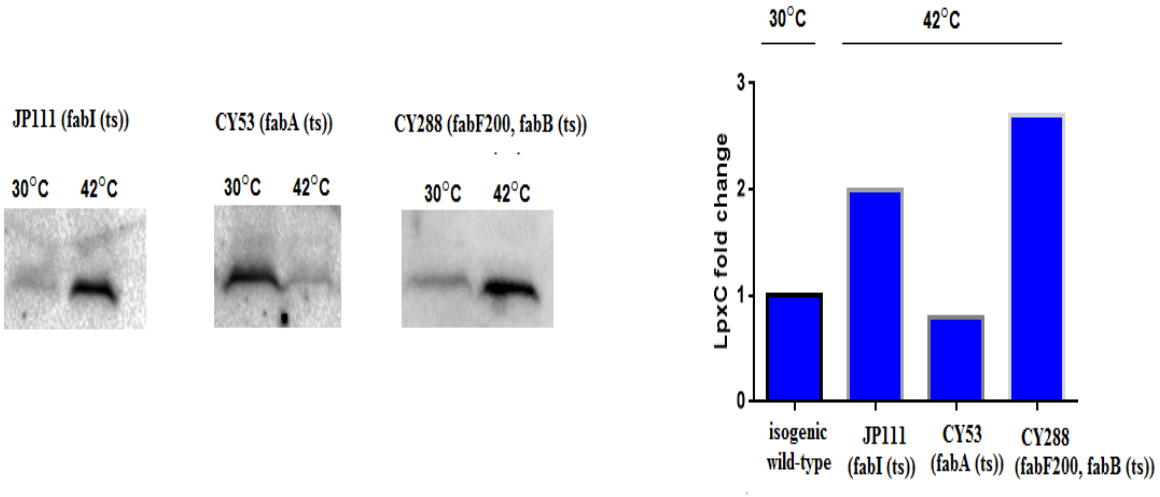

Figure 5.1. Effect of fatty acid biosynthetic enzyme inhibition on LpxC stability. *E. coli* strain JP1111 (*fabI* (ts)) cells were grown at 30°C to an OD_{600} of 0.15. Part of the culture was transferred to 42°C and grown for 150 min. Growth ceased after 2 generations at the non-permissive temperature. Strain CY288 (*fabB200*, *fabB* (ts)) cells were prepared as above except that cells were grown in a modified LB broth (5 g tryptone, 2.5 g yeast extract, 2.5 g NaCl). Growth ceased after 2 generations at 42°C. Overnight culture of strain CY53 (*fabA* (ts)) were grown directly either at 30°C or 42°C. At the latter temperature, growth ceased after 3 generations. Cell extracts and Western blotting were conducted as described in Chapter 4. Blue bars on the right represent computational simulations using the model described in Chapter 3 and parameters presented in Table 3.1. Here, model enzyme counts were reduced arbitrarily to mimic the non-permissive temperature because there were no available information in the literature on residual enzyme activity in these mutants. The FabF count was reduced by 10 folds, FabI and FabB by 100 folds, and FabA by 500 folds.

Similarly, fatty acids distribution were analysed in strain CY288 (*fabF200*, *fabB* (ts)). This strain had a lesion in the *fabF* gene in addition to having a temperature-sensitive FabB protein. When grown at 30°C, the fatty acid profile of the cells were characterised with significant levels of medium chain-length fatty acids (Fig. 5.2). This partial inhibition of fatty acid elongation occurred due to the lesion in FabF (Garwin *et al.*, 1980b); although, cells remain viable due to a functional FabB. However, when grown at 42°C, a further increment in medium chain fatty acids (especially pentadecanoic acid, an odd chain fatty acid) and reduction in long chain fatty acid moieties were observed (Fig. 5.2). This clearly indicates that fatty acid elongation has been halted. Since LPS precursor molecules are derived from fatty acyl-ACPs, halting fatty acid elongation would repress levels of lipid A disaccharide and stabilize LpxC. Although, increased levels of SFAs were generally observed at 42°C, these were mainly odd-chain fatty acids. Odd-chain fatty acyl-ACPs are unsuitable substrates for LPS synthesis due to a strict requirement of LpxA for β-hydroxymyristoyl-ACP (Anderson *et al.*, 1987) and therefore would not be expected to be shunted down the LPS pathway. Therefore LpxC stability in this strain can be attributed to low levels of the lipid A disaccharide. Again, this was confirmed by LPS quantification as described below.

Furthermore, a concomitant decrease in both long-chain SFA and UFA (stearic and *cis*-vaccenic acids) were observed in strain CY53 (*fabA* (ts)) when grown at the non-permissive temperature (Fig. 5.2). The only reasonable explanation from the pathway schematic in Fig. 3.1 is that the rate of synthesis of *trans*-2-decenoyl-ACP was reduced given FabA is the major dehydratase involved in this step (Heath and Rock, 1996b). Subsequently, limited substrates would be diverted into both SFAs and UFAs arm of the pathway resulting in reduced palmitoyl-ACP and palmitoleoyl-ACP concentrations. An

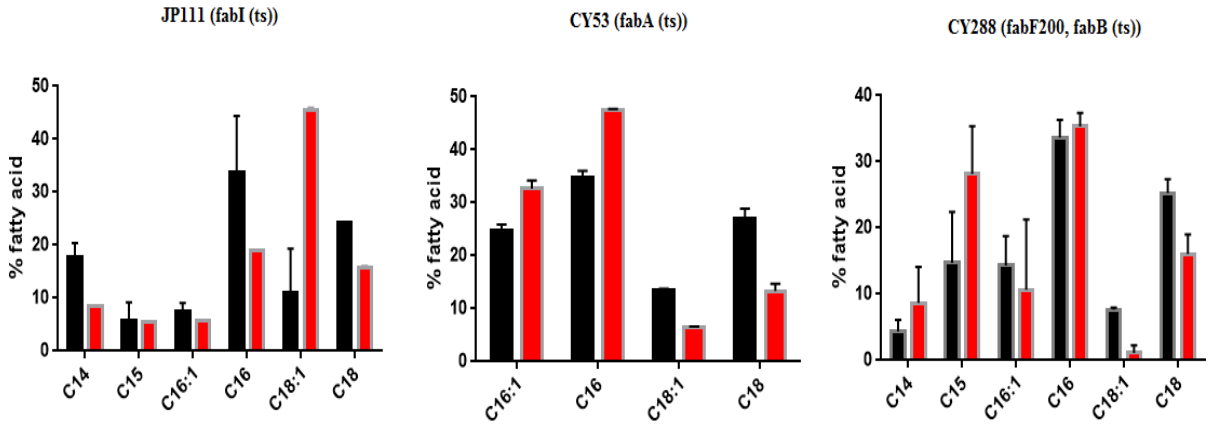

Figure 5.2. Effect of inhibiting fatty acid biosynthetic enzymes on fatty acid composition. Black and red bars represents growth conditions at 30°C and 42°C respectively. Cells were grown as described in Fig. 5.1 and their fatty acids content determined using GCMS analysis. Error bars represent standard error of mean. Fatty acids notation are C14, myristic acid; C15, pentadecanoic acid; C16:1, palmitoleic acid; C16, palmitic acid; C18:1, *cis*-vaccenic acid; C18, stearic acid.

increased competition for low levels of palmitoyl-ACP and palmitoleoyl-ACP by phospholipids acyltransferases (PlsB and PlsC) (Goelz and Cronan, 1980; Rock *et al.*, 1981) would further ensure that only a small proportion of these acyl pool are elongated to stearic and *cis*-vaccenic acids by FabB and FabF respectively (Edwards *et al.*, 1997). Although, substrate flux into the SFAs pathway would generally be reduced, inhibition of FabA resulted in increased LpxC degradation as presented in Fig. 5.1 due to an accumulation of lipid A disaccharide. Accumulation of lipid A disaccharide would occur under this condition because FabA plays a major role in the dehydration of β-hydroxymyristoyl-ACP due to a higher protein copy number (Ishihama *et al*., 2008) and similar catalytic activities with FabZ (Heath and Rock, 1996b). Therefore, a loss of FabA activity would increase the concentration of β-hydroxymyristoyl-ACP which is then shunted into the LPS pathway.

As a confirmation that strain CY53 (*fabA* (ts)) grown at 42°C was characterized with sufficient substrate flux into the LPS pathway, the concentration of LPS were identical to those grown at 30°C (Fig. 5.3). In contrast, reduction in LPS levels were observed in both strains JP1111 (*fabI* (ts)) and CY288 (*fabF200, fabB* (ts)) when grown at the non-permissive temperature which is indicative of low substrate availability (Fig. 5.3).

Together, these findings indicate that the FtsH-mediated LpxC degradation signal arises solely from lipid A disaccharide under fatty acids inhibition conditions.

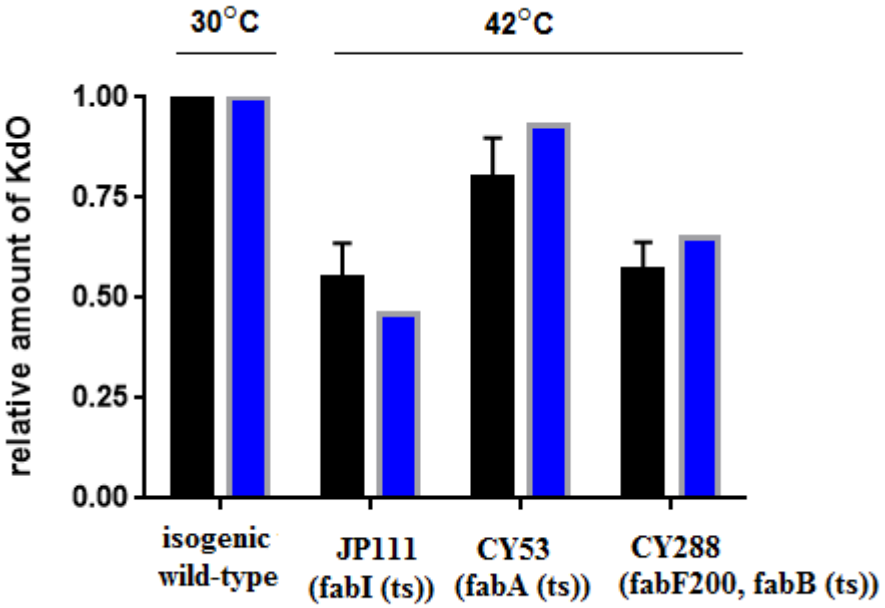

Figure 5.3. Quantification of LPS in fatty acid biosynthetic enzyme mutants. Black bars represents experimental results which were determined by measuring the amount of Kdo in the bacterial membrane. Error bars represent standard error of mean. The blue bars are simulations results using model conditions as described in Fig. 5.1 above.

5.2.1.1 Overexpression of FabA enhances LpxC degradation.

Up until now, the effect of fatty acyl enzymic inhibition on LpxC regulation has been analysed. It was also important to test the effect of fatty acyl enzymic overexpression on LpxC stability. This would confirm if the inhibition and overexpression data are compatible with conclusions above.

When strain DC170 (*fabAup*) which overexpresses *fabA* was grown at 30°C, there were no differences in LpxC levels relative to the control strain (W3110). However, at 42°C, LpxC was degraded more rapidly (Fig. 5.4A). Clark *et al.* (1983) had reported previously that strains overexpressing *fabA* at temperatures of 30°C or less, did not result in elevated level of SFAs whereas at optimum temperature, and especially 42°C, SFAs concentrations were significantly increased even though UFAs level remained constant. As stipulated above, excess flux of substrates into the SFA pathway arm and subsequently the LPS pathway enhances LpxC degradation which most likely explains the results presented in Fig. 5.4A. Furthermore, the amount of LPS synthesized at both temperatures were similar to those of wild-type (Fig. 5.4B). In particular, at 42°C in which pathway substrate flux was increased, an increment in LPS relative to wild-type (W3110) is not expected because LpxK becomes the rate-limiting step. Instead, lipid A disaccharide would accumulate leading to a rapid degradation of LpxC (Fig. 5.4A).

Furthermore, overexpression of LpxC was observed to be toxic in strain DC170 (*fabAup*) and under such condition, cells spend a significant length of time in the lag growth phase apparently to degrade excess LpxC prior to reproduction (Fig. 5.4C). This also supports the claim that LpxC levels must be lowered under FabA overexpression conditions.

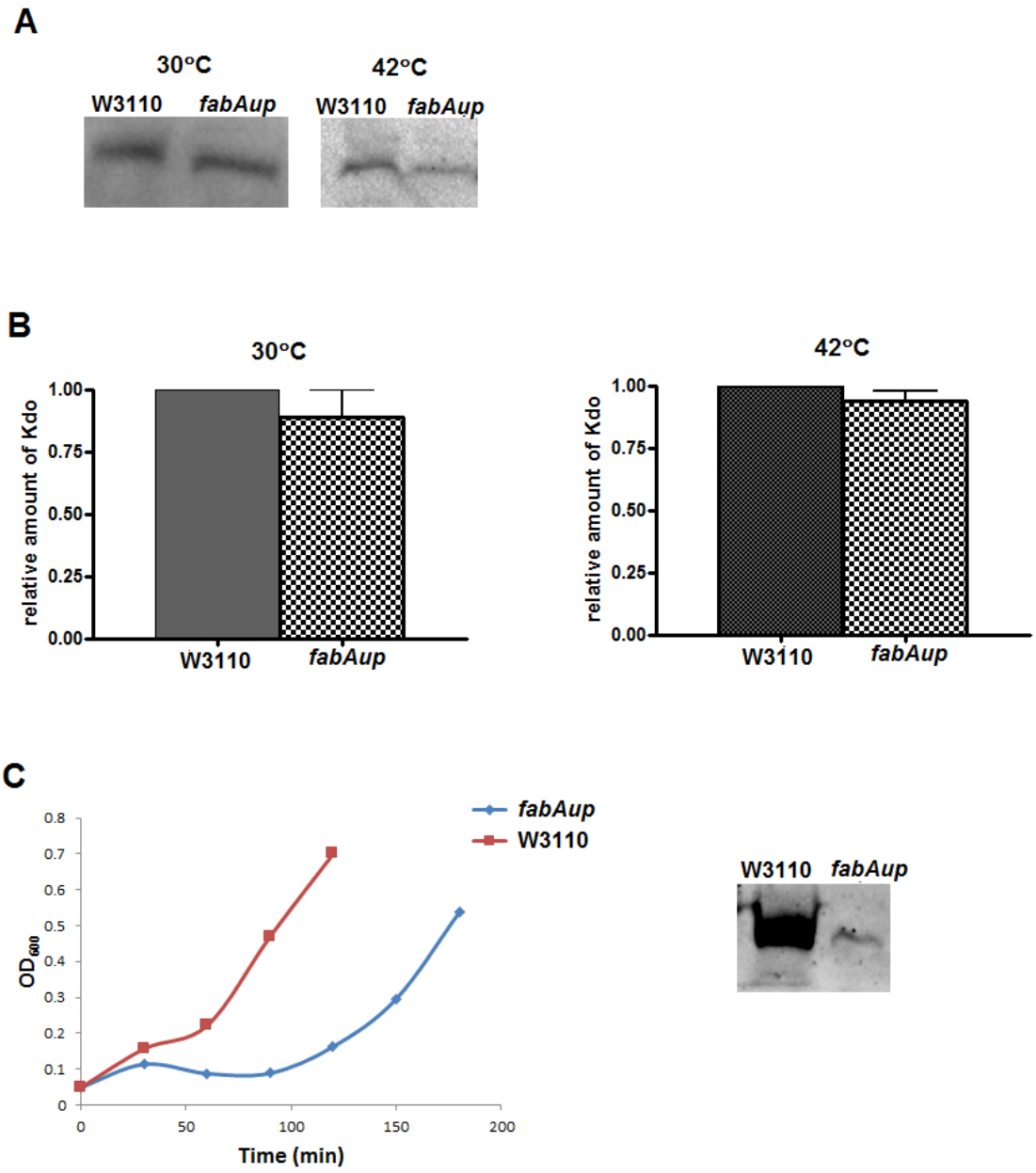

Figure 5.4. Effect of *fabA* overexpression on LPS regulation. Both wild-type (W3110) and DC170 (*fabAup)* cells were grown in LB broth at the given temperatures until mid-log phase. Cells were normalized prior to harvesting. (A) LpxC levels in W3110 and DC170 (*fabAup*). (B) LPS quantification in both W3110 and DC170 (*fabAup*) strains. Error bars represent standard error of mean. (C) Strains W3110 and DC170 (*fabAup*) were transformed with a plasmid bearing the *lpxC* gene (pBO110) and protein expression was induced using 0.1% L-arabinose overnight at 30°C. Overnight cells were transferred to fresh broth (without inducer) and incubated at 42°C. Growth rate was monitored (left) and after 90 min, part of the culture were harvested, and cell extracts subjected to the Bradford assay prior to Western blot analysis (right).

5.3 LPXC IS RAPIDLY DEGRADED UNDER TOXIC CELL CONDITIONS

Having established from above that mutations in the *fabI* and *fabF*/*fabB* genes stabilize LpxC, a similar study was conducted to observe the impact of specific inhibitors of these gene products on LpxC levels. When wild type cells (W3110) were treated with sub-MIC levels of irgasan (also called triclosan, an inhibitor of FabI (Rafi *et al.*, 2006)), LpxC was highly stabilized (Fig. 5.5A). A similar result was obtained in the presence of cerulenin, a specific inhibitor of FabF and FabB proteins (Price *et al.,* 2001). Thus, these results corroborates with the gene mutation studies presented in Fig. 5.1. It should be noted that under the drug treatment conditions in Fig. 5.5A, there were no differences in growth rates. However, under drug treatment conditions that led to differential growth rates, the LpxC regulation pattern deviated from those of the gene mutation studies (Fig. 5.5B). This therefore suggests that LpxC is rapidly degraded under toxic conditions.

Schakermann *et al.* (2013) had previously reported that FtsH-mediated LpxC degradation is correlated with growth rate under substrate limiting conditions resulting from an accumulation of the alarmone (p)ppGpp. This alarmone usually accumulates under amino acid starvation and/or environmental stress conditions (Janßen *et al.,* 2014). It is plausible that cellular toxicity induced by antibiotics leads to the accumulation of (p)ppGpp which activates LpxC degradation. Alternatively, (p)ppGpp accumulation is known to repress the expression of a wide range of genes including *lpxK* (Traxler *et al.,* 2008). In the latter scenario, repression of *lpxK* would cause lipid A disaccharide to accumulate and subsequently facilitate the rapid degradation of LpxC.

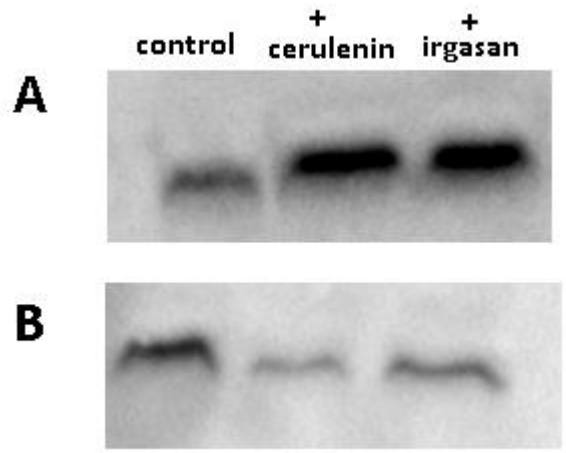

Figure 5.5. Effect of antibiotics that inhibit fatty acid enzymes on LpxC stability. Cerulenin is an inhibitor of FabF and FabB, while irgasan inhibits FabI at low concentrations. The antibiotics were used at the following concentrations; cerulenin, 10 µg/ml; irgasan, 0.01 µg/ml. (A) *lpxC* protein expression was induced in wild-type strain (W3110) overnight with 0.1% L-arabinose at 30°C. Overnight culture was inoculated into fresh broth (without inducer) at 42°C to an OD_{600} of about 0.1. The culture was split, antibiotics were added, and incubation was allowed to continue for another 90 min. There were no differences in growth rates prior to harvesting. Bradford assay was performed on the cell extracts and equal amount of protein was loaded onto a 10% SDS-PAGE gel for Western blot analysis. (B) Conditions were same as in 'A' above with the sole exclusion; *lpxC* expression was induced overnight with 0.2% arabinose. Cells treated with antibiotics grew more slowly than the control.

5.4 PROTEOLYTIC REGULATION OF LPXC IN AN FTSH KNOCKOUT MUTANT

Given that the results presented above indicate that excess flux of metabolites into the SFAs pathway enhances LpxC proteolysis, the next goal was to examine the likelihood of SFAs commonly found in membrane phospholipids to directly impact on LpxC instability. Under *in vitro* conditions, it was observed that the addition of excess palmitic acid to wild-type (W3110) cell lysates for 10 min resulted in an increased degradation rate of LpxC in a dose dependent manner (Fig. 5.6A). This phenomenon was not observed in the presence of myristic acid, a shorter chain fatty acid. Provided these findings are translatable *in vivo*, they prove interesting for a number of reasons. Firstly, and although highly unlikely, it points to a possibility of prior postulation of lipid A disaccharide being the feedback source for LpxC degradation as inaccurate. Secondly, and more plausible, it indicates the presence of an unidentified protease involved in the regulation of LpxC. In order to clarify these assumptions, further tests were required.

Next, cell lysates of an *ftsH* knockout mutant were treated with palmitic acid and LpxC degradation was also observed in a dose-dependent manner (Fig. 5.6B). This therefore indicate that under these *in vitro* conditions, an unidentified protease was responsible for the degradation of LpxC. Furthermore, proteolysis under palmitic acid condition was inhibited in the presence of EDTA which indicates the protease belonged to the class of metalloprotease, similar to FtsH (Fig. 5.6C).

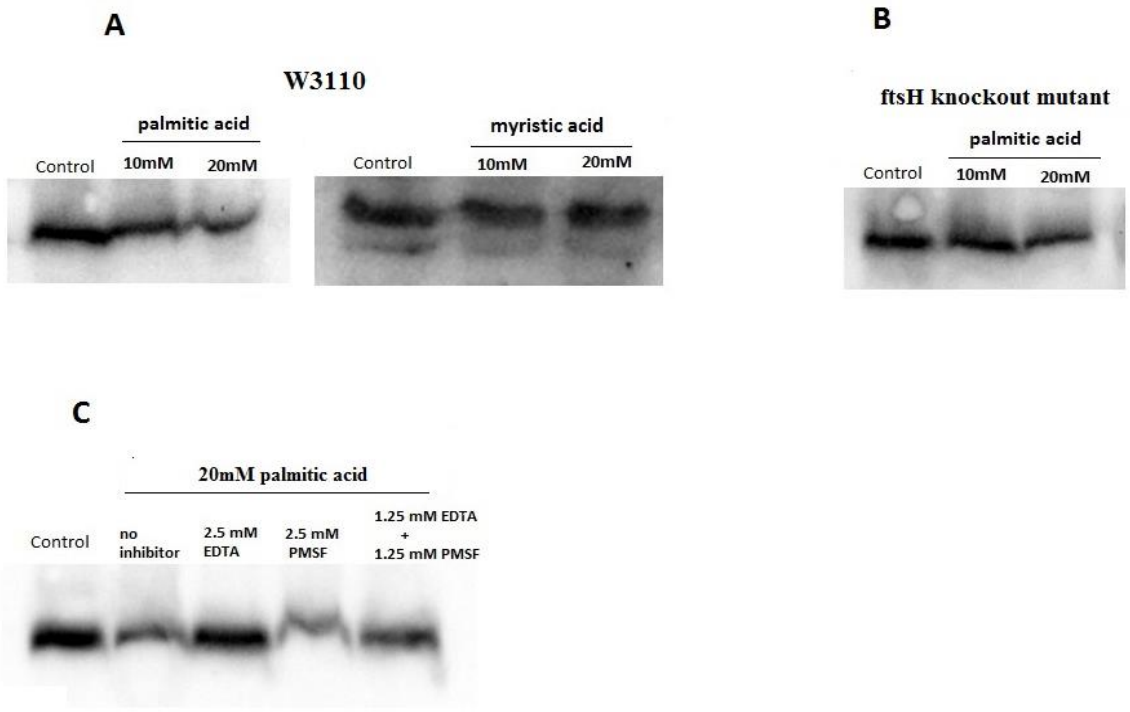

Figure 5.6. *In vitro* LpxC proteolysis in an *ftsH* knockout mutant. (A) Effect of fatty acids on LpxC stability *in vitro. E. coli* W3110 strain (wild-type) containing a plasmid bearing *lpxC* gene was grown at 30°C in the presence of 0.1% arabinose to induce protein expression. Cells were harvested at mid-log phase, re-suspended in Tris-HCl pH 8.0 (without EDTA) and lysed via sonication. The lysates were added to tubes containing various concentrations of fatty acids and incubated for 10 min at 30°C. Sample buffer was added immediately after incubation and heated for 5 min prior to Western blot analysis. (B) Effect of palmitic acid on LpxC stability in *ftsH* knockout mutant cells *in vitro.* Cells (without plasmid) were treated as in 'A' above. (C) Palmitic acid-induced LpxC degradation occurs via a metalloprotease *in vitro*. *E. coli* W3110 cells were prepared as in 'A' above but some samples contained EDTA and PMSF to inhibit metalloproteases and serine proteases respectively.

However, under normal physiological conditions, LpxC and palmitic acid are localized in separate cellular compartments (cytoplasm and outer membrane respectively) and may not be in direct contact with one another as it was in the *in vitro* assays. Since palmitic acid exists in the cytoplasm in the forms of palmitoyl-CoA and palmitoyl-ACP (Janßen *et al.,* 2014), it was essential to investigate the effect of both forms of palmitic acid on LpxC stability.

Palmitic acid is known to be actively transported across the membrane from the external environment by FadL (Kumar and Black, 1991) and immediately converted to palmitoyl-CoA by FadD (Weimar *et al.,* 2002). Interestingly, when palmitic acid was added to the growth medium of wild-type *E. coli* (W3110), the levels of LpxC were elevated (Fig. 5.7A). This observation is readily explainable from prior experimental data, and earlier results presented in Fig. 5.1. Palmitoyl-CoA induces a strong inhibitory effect on FabI with a K_i value of about 3 μM (Bergler *et al.,* 1996). Due to the inhibition of FabI, LpxC would be stabilized (Fig. 5.1). Thus, increment in cellular palmitoyl-CoA concentration has an opposite effect on LpxC stability than the free-form of palmitic acid.

On the other hand, under *in vivo* conditions, inhibiting substrate flux into the LPS pathway will increase the cellular concentration of palmitoyl-ACP (Zhu *et al.,* 2009). This is because when LPS substrate influx is inhibited, it leads to elevated levels of β-hydroxymyristoyl-ACP which is subsequently dehydrated by FabZ and shunted towards the production of palmitoyl-ACP. Cells were treated with sub-lethal concentrations of an LpxC inhibitor (CHIR-090) in order to reduce substrate flux into the LPS pathway. Under this condition, LpxC stability was observed in wild-type (W3110) cells (Fig. 5.7A). These results are also readily explainable; LpxC stability occurred due to decreased levels of lipid A disaccharide. Yet again, increment in cellular palmitoyl-ACP

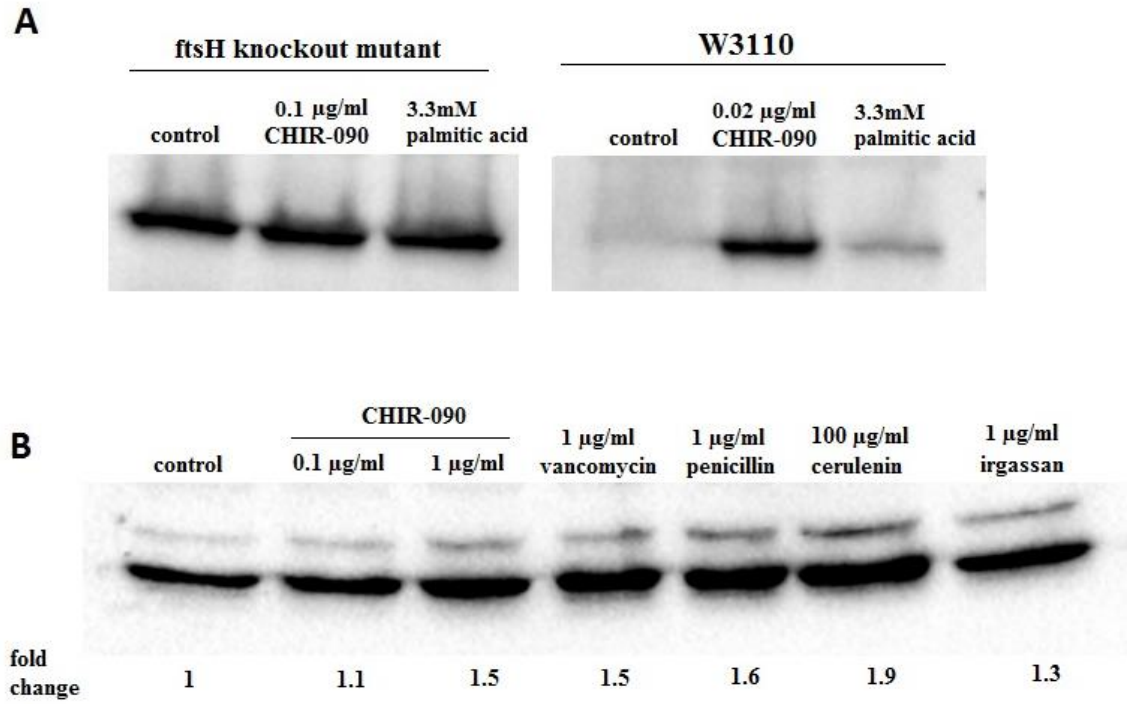

Figure 5.7. *In vivo* LpxC proteolysis in an *ftsH* knockout mutant. (A) Effect of increased palmitoyl-ACP and palmitoyl-CoA concentrations on LpxC stability *in vivo*. *E. coli* W3110 and *ftsH* knockout mutant cells were grown in LB broth at 30°C to an OD_{600} of 0.1. The cultures were split and CHIR-090 and palmitic were added and incubation continued until the OD_{600} reached 0.5. The cultures were normalized according to their density prior to Western blot analysis. (B) LpxC is less degraded *in vivo* in *ftsH* knockout cells in the presence of antibiotics that affect membrane synthesis/stability. Cells were grown to an OD_{600} of 0.5 and cultures were split into different tubes. The respective antibiotics were added for 5 min prior to the addition of 200 µg/ml of chloramphenicol to block protein expression. After 30 min, the cells were shock-frozen in liquid Nitrogen and thereafter, allowed to thaw on ice prior to Western blot analysis. Bands were quantified using the Chemi-Doc Imager software.

concentration has an opposite effect on LpxC stability than the free-form of palmitic acid. However, the presence of palmitic acid or sub-lethal concentration of CHIR-090 in the culture medium had no effect on LpxC stability in *ftsH* knockout mutant cells (Fig. 5.7A). Together, these findings indicate that the direct interaction of LpxC with long chain free-fatty acids (i.e. fatty acids not bound to ACP or CoA) facilitated FtsH-independent LpxC proteolysis as observed in the *in vitro* assays.

Interestingly, when the *in vivo* LpxC degradation rate was monitored in *ftsH* knockout cells that were treated with a higher concentration of CHIR-090 or other antibiotics that affected the bacterial membrane, an increment in LpxC level was observed (Fig. 5.7B). This indicates that in untreated cells, residual LpxC proteolysis occurred which confirms the presence of an additional regulatory protease. Additionally, it also indicates that LpxC regulation is crucial to the bacterial cells which must maintain the desired protein levels irrespective of an accumulation of lipid A disaccharide, or presence/absence of a functional FtsH protease.

5.5 WAAA REGULATION

In addition to LpxC, WaaA is regulated via FtsH-mediated degradation (Katz and Ron, 2008). The regulation of WaaA enzyme is poorly understood. In fact, only one study by Katz and Ron (2008) have investigated the regulatory role of WaaA to date. In Chapter 2, different rationales for WaaA regulation were postulated. Briefly, the model suggested that regulation of WaaA may influence LPS synthesis rate when CMP-Kdo is limiting. Alternatively, WaaA regulation may help to prevent reactions with undesirable substrates. As a result, it was important to investigate the exact role of WaaA degradation during LPS synthesis.

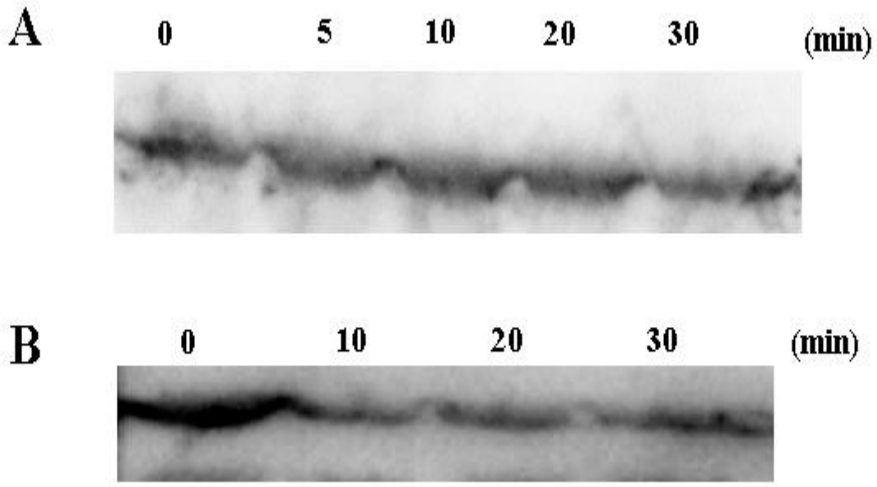

Figure 5.8. Proteolytic degradation of WaaA. (A) *E. coli* (W3110) cells containing a plasmid bearing the 6x-His-waaA gene were grown at 37°C in LB broth with the addition of 20 µg/ml of chloramphenicol for selective pressure. At an OD_{600} of 0.5, *waaA* expression was induced using 1 mM of IPTG for 10 min prior to the addition of 300 µg/ml of spectinomycin to block protein translation. 3 ml of culture were dispensed in various Eppendorf tubes and were shock frozen in liquid Nitrogen to stop all cellular processes. The indicated time points represent min after the addition of spectinomycin when the cells were frozen. The cells were allowed to thaw on ice and harvested prior to Western blot analysis. (B) The procedure was same as in 'A' above with the sole exclusion of *waaA* expression being induced with 0.1 mM IPTG.

An *E. coli* (W3110) strain was transformed with a plasmid bearing the *waaA* gene which had histidine (6x-His) tagged to its N-terminus region. Because gene fusions either to the N-or C- terminus region can prevent the proteolytic regulation of its protein product (Fuhrer *et al.*, 2006; Fuhrer *et al.*, 2007), it was crucial to ensure that the *waaA* plasmid construct was suitable for experimental investigations. In this regard, the WaaA half-life was monitored by inducing protein expression under different concentrations of IPTG. Under modest IPTG induction, the half-life of WaaA was approximately 10 min (Fig. 5.8B). This is in agreement with prior observations by Katz and Ron (2008) in which chromosomally expressed WaaA possessed a half-life of 10 min under optimum conditions. Therefore, the His-tag does not interfere with WaaA regulation. Although, under excessive IPTG induction, proteolysis of *waaA* was not observed after 30 min (i.e. half-life > 30 min) (Fig. 5.8A).

5.5.1 Overexpression of *waaA* is toxic to cells

When *waaA* was overexpressed, cell growth was inhibited (Fig. 5.9). A similar finding was observed previously for LpxC in studies by Fuhrer *et al.* in which overexpression of a functional *lpxC* gene resulted in cell toxicity (Fuhrer *et al.*, 2006). The authors also observed that overexpression of non-functional *lpxC* did not result in cell toxicity. Therefore, it is plausible that under unregulated WaaA conditions, such as during overexpression, increased metabolic activity occurs which is undesirable to the cell.

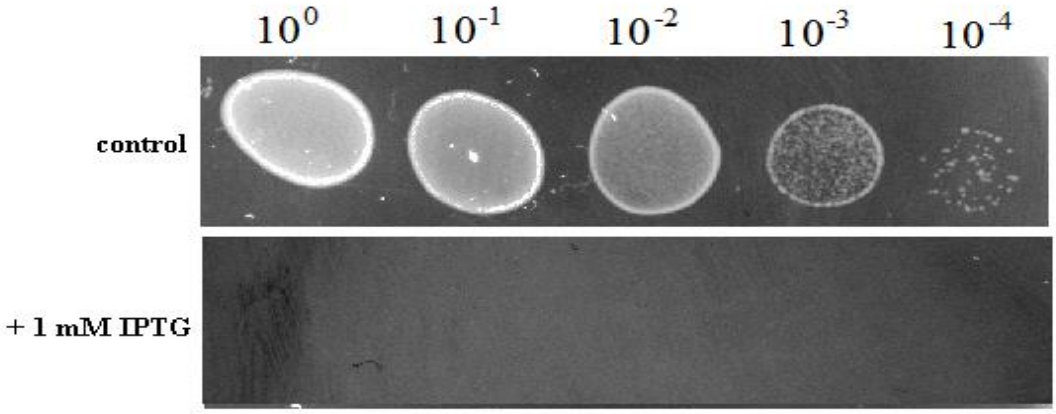

Figure 5.9. Overexpression of *waaA* is toxic to cells. *E. coli* strain W3110 containing a plasmid bearing 6x-His-WaaA gene was grown to an OD_{600} of 0.2, serially diluted, and spotted on agar plates containing either no sugar or 1 mM IPTG to induce protein expression. Plates were incubated overnight at 30°C.

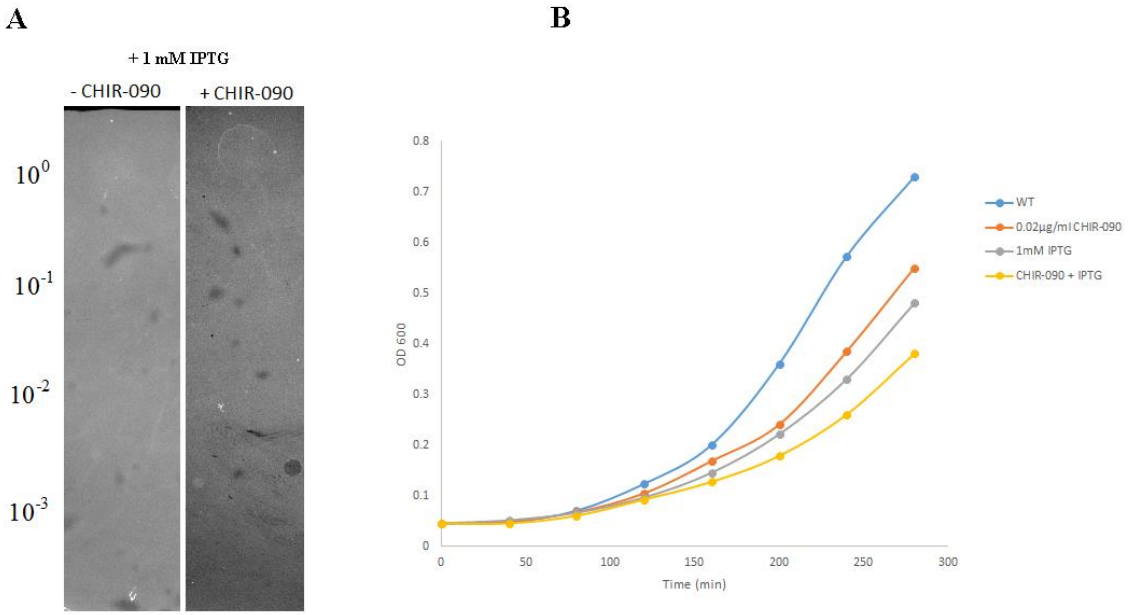

Figure 5.10. *waaA* overexpression under reduced LPS pathway flux conditions. (A) Cell growth was severely inhibited even under pathway flux inhibition with CHIR-090. Conditions are similar to Fig. 5.9 above. The concentration of CHIR-090 used was 0.02 µg/ml. (B) The combined toxicity resulting from *waaA* overexpression and CHIR-090 treatment is additive. The growth curve was monitored in LB broth.

The next step would be to determine if such an increase in metabolic activity correlates with an increment in LPS biosynthesis. If indeed LPS is increased, then it indicates that WaaA exerts some degree of control on LPS synthesis rate in contrast to model assumptions. To clarify this, LPS pathway flux was reduced by inhibiting LpxC using sub-MIC concentrations of CHIR-090. Yet, overexpression of *waaA* under this condition did not prevent cellular toxicity (Fig. 5.10A). This provided a first indication that unregulated production of WaaA would also result in increased metabolic activity which may be independent on LPS production rate. In fact, the toxicity induced by *waaA* overexpression and LpxC inhibition were additive (Fig. 5.10B). These results do not conclusively exclude the possibility of WaaA at influencing LPS synthesis rate. Therefore, further detailed analyses were required as described below.

5.5.2 Effect of *waaA* overexpression on LPS composition

In order to clarify if LPS levels were increased when *waaA* is overexpressed, LPS was quantified in cells overexpressing *waaA* by quantifying the amount of Kdo in the bacterial membrane. Under this condition, Kdo levels were elevated by approximately 20 % (Fig. 5.11). However, an increment in Kdo may not indicate increased LPS level under *waaA* overexpression. This is because, the role of WaaA is to add two Kdo residues to the LPS lipid precursor (lipid IV_A); therefore, the possibility still exists that overproduction of WaaA may result in multiple additions of Kdo to lipid IV_A (i.e. re-glycosylation) or alternatively, Kdo may be added to other undesirable lipid acceptors (other than lipid IV_A) (Brozek *et al.*, 1989; Belunis and Raetz, 1992) in the membrane. This also indicates that quantification of LPS using the Kdo assay may be inappropriate under *waaA* overexpression conditions. To further clarify these possibilities, substrate flux into the LPS pathway was inhibited using ½ MIC of CHIR-090. The rationale for

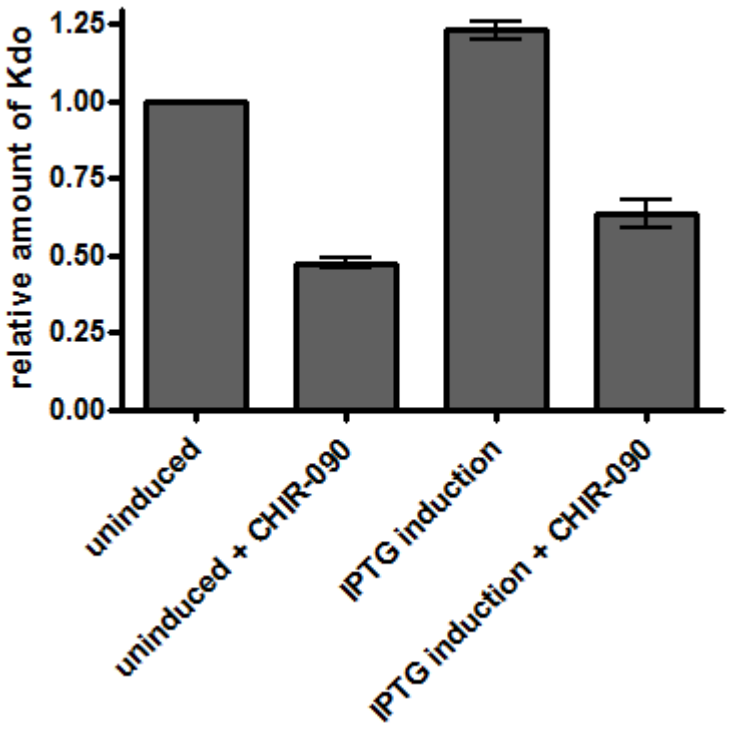

Figure 5.11. Kdo concentration under *waaA* overexpression. Cells were grown at 37°C to an OD_{600} of 0.1 and split. CHIR-090 was added to the appropriate culture for 30 min prior to addition of IPTG. Growth was allowed to continue for 45 min and the cultures were normalized according to their density prior to harvesting. Kdo in the membrane extract was quantified as described in Chapter 4. Error bars represent standard error of mean.

this was that by reducing the influx of substrates, the LPS synthesis rate would be dependent on substrate availability and not WaaA concentration. Similarly, overexpression of WaaA under this condition led to a 20 % increase in Kdo levels in comparison to cells that were solely treated with CHIR-090 (Fig. 5.11). Again, these findings indicate that the rate of glycosylation by WaaA is independent on lipid IV_A availability.

Furthermore, it was essential to investigate if the re-glycosylated lipid IV_A or other alternate lipids (i.e. lipids other than lipid IV_A) that could be glycosylated by WaaA are being consumed for LPS synthesis. Consequently, LPS was extracted from the membrane and the concentration of heptose sugar was quantified. Heptose sugars are primarily used in the synthesis of core OS of LPS. They are attached directly to the Kdo residues (Fig. 5.12A). In other words, they provide an alternative means to quantify LPS indirectly. The results obtained differed from those of the Kdo quantification. When *waaA* was overexpressed, the concentration of heptose was decreased in comparison to uninduced cells (Fig. 5.12B) which indicate that LPS levels are also decreased under *waaA* overexpression. Additionally, when pathway flux was inhibited (using CHIR-090) and *waaA* overexpressed, the concentration of heptose were slightly increased in comparison to cells solely treated with CHIR-090 (Fig. 5.12B). Altogether, these results indicate that unregulated *waaA* expression is undesirable under normal conditions.

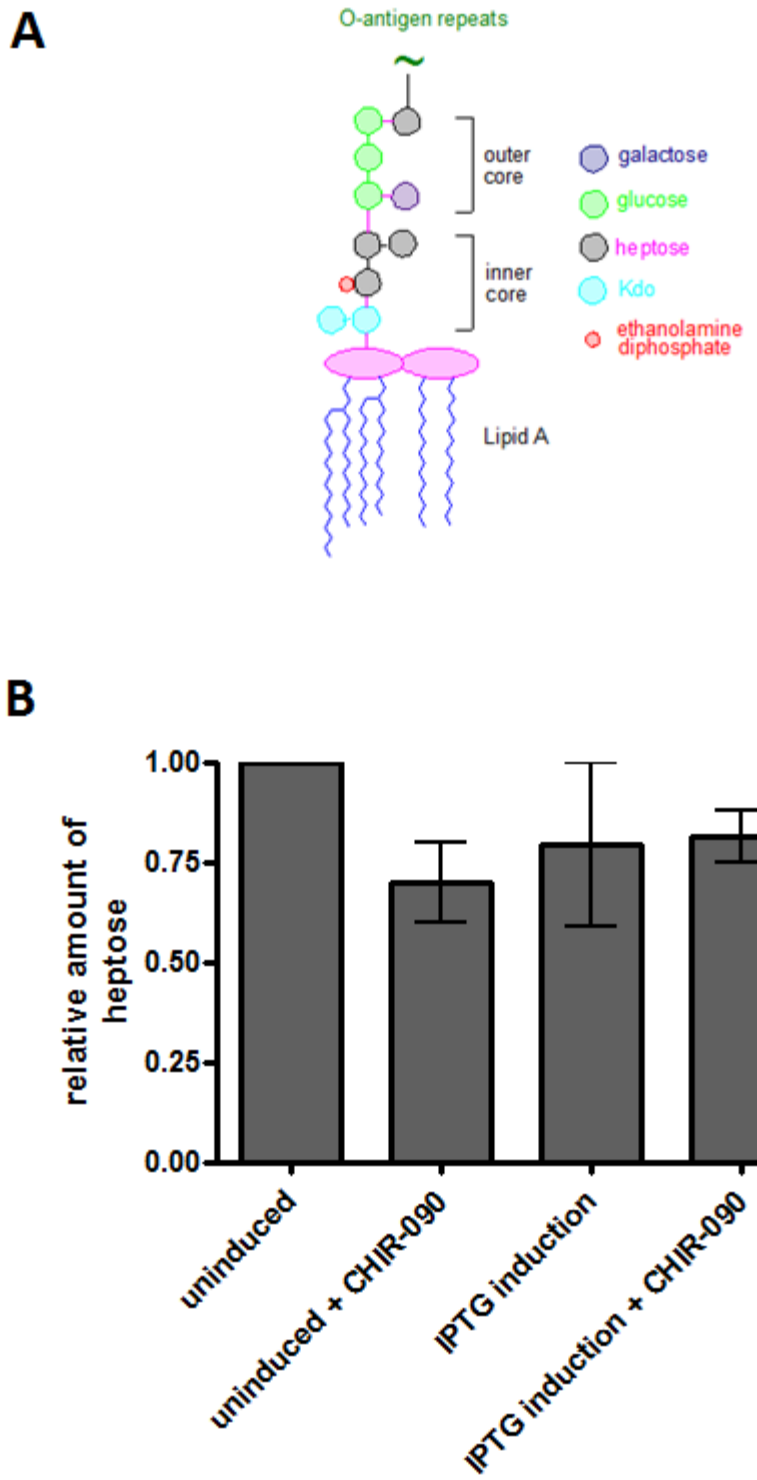

Figure 5.12. Heptose concentration under *waaA* overexpression. (A) Structure of LPS depicting the attachment of heptose residues to kdo in the core OS. *Source: http://lipidlibrary.aocs.org/Primer/content.cfm?ItemNumber=39339* [Accessed 17th September, 2015]. (B) Cells were prepared exactly as described in Fig. 5.11 above. LPS was extracted from the membrane prior to heptose quantification.

To further elucidate the effect of *waaA* overexpression on the structural stability of the bacterial outer membrane, the MICs of different antibiotics were determined for cells overexpressing *waaA.*

When *waaA* was overexpressed, the cells were more susceptible to colistin in comparison to uninduced cells (Table 5.1). Colistin is an antimicrobial peptide that selectively targets bacterial LPS (Warren *et al.,* 1985). Interestingly, at low levels of *waaA* overexpression, the MICs to erythromycin and kanamycin which are known to inhibit translation, were the same as uninduced cells. This indicate that overexpression of *waaA* results in cells with reduced LPS concentration or a defective LPS structure.

Table 5.1: MIC of different antibiotics under *waaA* overexpression

	Colistin (µg/ml)	Erythromycin (mg/ml)	Kanamycin (µg/ml)
Uninduced	1	0.125	8
IPTG induction	0.5	0.125	8

Cell preparation and growth conditions are same as in Fig. 5.11 with the exception; growth was allowed to continue for 2 h after IPTG induction. The cultures were normalized according to their density and MICs were determined as described in Chapter 4.

5.6 SUMMARY

The regulation of LPS biosynthesis is crucial to cell viability. Two of the key regulatory points previously reported are LpxC and WaaA which are both degraded by FtsH. Earlier studies have indicated that enzymes involved in fatty acid biosynthesis affect the regulation of LpxC which suggests the possibility of a regulatory signal arising from the fatty acids biosynthetic pathway. However, the results presented in this Chapter involving the analysis of cellular fatty acids composition and LPS quantification strongly indicate there are no additional FtsH feedback sources separately from lipid A disaccharide. Instead, excessive flux of metabolites into the SFAs pathway results in increased concentration of β-hydroxymyristoyl-ACP which subsequently shunts through the LPS pathway leading to elevated levels of lipid A disaccharide. Nevertheless, LpxC regulation appears to be independent on lipid A disaccharide under toxic cellular conditions. Interestingly, further investigation acknowledged the presence of an unidentified metalloprotease involved in LpxC regulation in *ftsH* knockout mutant cells. In this case, LpxC degradation was observed to be repressed *in vivo* under conditions that promote membrane vulnerability.

Although, overexpression of WaaA elevates the amount of Kdo in the bacterial membrane, this increment is independent of lipid IV_A availability and do not elevate the total LPS concentration. In fact, overexpression conditions resulted in cells that were more susceptible to colistin which is known to directly interact with the LPS structure. An increased susceptibility was not observed with antibiotics that target protein synthesis. Altogether, these suggest that the regulation of WaaA during LPS synthesis are for *qualitative* purposes and not *quantitative.*

Chapter 6

Discussion and conclusion

6.1 DISCUSSION

6.1.1 The lipid A model

This research began by constructing a model of the *E. coli* lipid A biosynthetic pathway, including its regulation, using parameters derived from published experimental data. After increasing the LpxM copy number and adding product inhibition to LpxH, the model agreed well with the observed lipid A production rate and exhibited steady-state metabolite concentrations. The model also agreed qualitatively with all published datasets that were tested, including ones in which LpxA was defective, LpxC was inhibited with an antibiotic, LpxC half-lives were compared with cell generation times, LpxC was overexpressed, and under substrate limiting conditions. The lipid A model also agreed well with experiments in which *lpxK* was overexpressed.

Findings from the model indicate that the lipid A biosynthesis rate is controlled by LpxC, but only if substrates are in excess and if feedback regulation is ignored. However, LpxK becomes the controlling enzyme if feedback regulation is included, as it is in living cells, and other enzymes gain control if substrate concentrations are below saturation levels. The lipid A model also strongly indicated that WaaA may be regulated in order to control the lipid A production rate when the CMP-Kdo concentration is limiting, and/or to control the ratio of normal to alternate lipid A that is produced.

Quantitative disagreements between metabolic models and experiments are particularly useful because they indicate which model assumptions are likely to be incorrect. These errors then enable new insights about the true system behaviour. Firstly, the initial lipid A model produced lipid A at 20% of the observed rate and exhibited LpxM substrate accumulation, which suggest that LpxM is actually present at a much higher concentration than was measured with proteomic methods (Ishihama *et al.,* 2008). Alternatively, it could indicate that other enzymes are capable of catalysing the

substrate of LpxM in agreement with prior postulations (Clementz *et al.,* 1997; Vorachek-Warren *et al.,* 2002b).

Secondly, high levels of lipid X during modelling suggest that the LpxH kinetics are regulated by product inhibition, and also that LpxH and LpxB may form a complex that performs metabolic channeling. The latter suggestion seems highly plausible because LpxB is immediately downstream of LpxH in the lipid A pathway, and both are peripheral membrane proteins. Since the LpxH substrate is localized in the cytoplasm, an absence of interaction between these proteins may result in a low LPS turnover rate because the catalytic product of LpxH may diffuse away from the membrane outside the reach of LpxB.

Thirdly, the model exhibited 4-fold increased LpxC when LpxA was made defective, instead of the observed 5-10 fold increase (Anderson *et al.,* 1993); this may arise from experimental differences, or due to unmodeled aspects of LpxC regulation, such as transcriptional regulation. There is recent evidence which suggests that LpxC could be regulated at the transcriptional level under sub-optimal conditions (Eraso *et al.,* 2014). Fourthly, the model exhibited a 98% reduction in the lipid A synthesis rate when LpxA was defective, instead of the 30% that was observed experimentally (Anderson *et al.,* 1993). This large discrepancy between the model and experiment suggests the presence of alternate metabolic routes around LpxA, such as the possibility of LpxD at catalysing the LpxA step. This is because both LpxA and LpxD are acyltransferases that utilize β-hydroxymyristoyl-ACP.

Fifth, the model underestimated cell generation times when LpxC had a very long half-life (Schakermann *et al.,* 2014) which suggest that the growth rates of fast growing cells are not limited by the lipid A production rate. Finally, the model could exhibit the experimentally observed LpxC half-life and cell generation time when substrates were

limited (Schakermann *et al.,* 2014), but only when the total FtsH concentration was increased 25-fold; this suggests that there are additional mechanisms that regulate LpxC degradation which was subsequently confirmed in this work. Not all of these speculations are proven by the model. Instead, they are possible solutions to situations in which the experiments that were used to create the model do not agree with experiments that were used to test the model. In this case, they provide hypotheses for further experimental investigation.

The combination of prior published data, model results, and LpxK overexpression experiments provide strong evidence for lipid A disaccharide being a primary feedback source for LpxC degradation (Figs 2.2 and 2.4). Furthermore, these same sources of information suggest that this is the only feedback source among the chemical species that are known to be present.

6.1.2 Integrated lipid A/phospholipids model

An integrated model for both lipid A and phospholipids pathways was developed with major emphasis at the transcriptome, proteome and metabolome level of detail. The refined model comprises of 81 reactions involving 90 reacting species. Yet again, the initial parameters for the phospholipids pathway were unable to replicate a number of published datasets. For instance, the model initially produced excess SFAs and little or no UFAs. This may indicate that in addition to palmitoyl-ACP, the activity of FabI is further repressed by other acyl-ACPs; or more still, the isomerase activity of FabA is much higher *in vivo.* Furthermore, accumulation of *cis*-substrates of FabZ were observed indicating that FabZ possesses a higher affinity for its unsaturated acyl-substrates than its saturated acyl substrates. The FabB activity for *cis*-3-decenoyl-ACP had to be reduced significantly which suggests that the first committed step in UFAs

synthesis may be regulated at the substrate level *in vivo*. Most importantly, the integrated model was able to replicate experimental results only when the catalytic activation of LpxK arose solely from UFAs.

Although Ray and Raetz (1987) had reported that LpxK catalysis is stimulated by phospholipids, the model strongly suggests that such stimulation is driven by the UFAs moiety in phospholipids, and inhibited by SFAs. There are a number of published dataset that supports this notion. The phospholipids utilized in Ray and Raetz (1987) were bovine heart cardiolipins which are known to consist almost entirely of UFAs (Schlame *et al.,* 1993). Furthermore, Roy and Coleman (1994) observed that when LpxD was inhibited, the specific activity of LpxK was decreased whereas the protein half-lives of LpxK were the same under normal and LpxD inhibition conditions. Further analysis by the authors indicated that overexpression of LpxD does not increase the specific activity of LpxK. This means that the decrease in LpxK activity is a secondary effect of the altered LpxD. These observations can readily be interpreted from the model. Because β-hydroxymyristoyl-ACP is a substrate utilized by LpxD, reduced LpxD activity would result in an accumulation of this substrate which is shunted towards SFAs production. This is because β-hydroxymyristoyl-ACP is derived from the SFAs pathway arm (Fig. 3.1). In return, excess SFAs would repress the catalytic activation of LpxK.

Since the ratio of UFAs/SFAs influences the activation of LpxK, this suggests that LPS synthesis rate is correlated with membrane fluidity. This is due to the fact that UFAs in the membrane increases fluidity while SFAs decreases fluidity (Mansilla *et al.,* 2004). It is also well documented that bacteria regulate their membrane composition in relation to fluidity (Mansilla *et al.,* 2004). It is probable that under conditions of low membrane fluidity (such as under high SFAs condition), a reduced LpxK activity may be essential

in order to reduce the amount of LPS produced which potentially would add an extra permeability barrier, and subsequently reduce the influx of metabolites from the external environment. The opposite effect seems to occur under conditions of high membrane fluidity. It was reported in Wahl *et al.* (2011) that *E. coli* grown in environments that had increased membrane fluidity through degradation of LPS, led to an induction of PlsB transcription which would ultimately enhance the production of phospholipids.

Nevertheless, more pathway regulation may take place around LpxK. Due to lipid A disaccharide being the feedback source for LpxC degradation, an increase in LpxK activity would lead to higher LpxC concentrations and hence faster lipid A production, which could help balance the phospholipid to LPS ratio. Thus, LpxK plays an essential role at maintaining LPS and phospholipids homeostasis.

In addition, the model can help elucidate which lipid A pathway enzymes are likely to be good or poor antibacterial targets. Most of the best known inhibitors of the LPS pathway to date have been directed at LpxC (Onishi *et al.,* 1996; McClerren *et al.*, 2005; Barb and Zhou, 2008), including the CHIR-090 antibiotic discussed above, presumably because most intracellular synthesis regulation takes place at LpxC. However, sensitivity analysis suggests that this intracellular regulation may actually make LpxC a poor drug target because it enables the cell to counteract external perturbations. Indeed, it was recently reported by Walsh and Wencewicz (2014) that the development of CHIR-090 has been hampered due to the ease of pathogen mutation to resistance. In contrast, the model suggests that LpxK would make a good target, as initially suggested by Emptage *et al.* (2012). LpxK is an essential enzyme without alternative synthetic routes, so strong inhibition would arrest lipid A production. More still, when the model accounted for feedback regulation, the lipid A production rate was

particularly sensitive to the LpxK concentration (Fig. 2.5A). Finally, inhibiting LpxK would lead to lipid A disaccharide accumulation. Lipid A disaccharide is cytotoxic (Garrett *et al.,* 1998) and its accumulation would lead to LpxC down-regulation, which would further repress lipid A production.

6.1.3 LpxC regulation

It is well documented that an appropriate ratio of LPS and phospholipids is crucial for cell viability (Galloway and Raetz, 1990; Ogura *et al.,* 1999) and this is achieved in part through controlled LpxC proteolysis by FtsH (Ogura *et al.,* 1999). Model and experimental results strongly indicate there are no separate FtsH feedback sources aside from lipid A disaccharide mediated towards LpxC degradation. There has been some uncertainties as to the role of acyl-ACPs in the regulation of LpxC. In the first scenario, since LPS and phospholipids biosynthesis pathways both derive their precursor molecules from β-hydroxymyristoyl-ACP, it was accepted that competition for this common substrate influences the regulation of LpxC (Ogura *et al.,* 1999). In other words, LpxC degradation would help conserve substrates for phospholipids synthesis. This initially seemed reasonable and is supported by the fact that FabZ inhibition enhances LpxC degradation (Zeng *et al.,* 2013), and FabZ overexpression results in LpxC stability (Ogura *et al.,* 1999). However, the model and experimental results disagree with this "*competition model*" regarding β-hydroxymyristoyl-ACP availability. As an example, LpxC would have been expected to be stabilized under conditions of FabA overexpression which invariably increases substrate flux into the SFAs pathway (Clark *et al.,* 1983), and subsequently elevate the pool of β-hydroxymyristoyl-ACP. This should lead to a reduced competition between LpxC and FabZ for substrates. On

the contrary, increased LpxC degradation was observed under this condition (Fig. 5.4A).

In support of the model's disagreement with the "*competition model*", Ogura *et al.* (1999) also observed that LpxC levels were elevated in *fabI (ts)* mutants. Although, the authors had initially suggested that increased concentration of *trans*-2-tetradecenoyl-ACP may enhance LpxC stability due to the observation that LpxC levels are also being elevated when FabZ is overexpressed, they also admitted the unlikelihood of *trans*-2-tetradecenoyl-ACP accumulation under *fabI (ts)* conditions (Heath and Rock, 1995). Thus, they were unable to explain the rationale for LpxC stability under FabI inhibition conditions. Clearly, the results of this research indicate that the increased levels of LpxC in *fabI (ts)* mutant occurred due to decreased flux of substrates into the SFAs and LPS pathways (Figs. 5.2 and 5.3) which ultimately depreciated the lipid A disaccharide concentration.

As mentioned above, a general contributing factor to the degradation of LpxC by FtsH is the excessive flux of substrates into the pathway arm of SFAs synthesis and subsequently the LPS pathway. The model presented in Chapter 3 provided a valuable tool at interpreting the observed cellular characteristics. There were two key factors from model interpretations which particularly influenced LpxC regulation; *(i)* competition between FabI and FabA isomerase for *trans*-2-decenoyl-ACP substrate. This competition determines substrate influx rate into SFAs and UFAs pathway arm; *(ii)* concentration of UFAs which is essential for the catalytic activation of LpxK. An increased concentration of UFAs would ensure lipid A disaccharide does not accumulate.

On the other hand, LpxC stability is not solely attributable to an increased concentration of UFAs. For instance, UFAs were increased at the non-permissive temperature in strain

JP1111 (*fabI* (ts)), and decreased in strain CY288 (*fabF200, fabB* (ts)). Yet, LpxC was stabilized under both conditions (Figs 5.1 and 5.2). In the latter case however, cells were characterized with more medium-chained fatty acids and less long-chain fatty acids (Fig. 5.2). This implies that fatty acids synthesis and elongation proceeded at a slow rate which also indicate that levels of lipid A disaccharide would be decreased. Furthermore, it also implies that cellular membrane fatty acids composition are connected with LpxC regulation. The latter phenomenon has been observed previously in studies investigating membrane fluidity where it was found that the presence of UFAs or shorter-chain SFAs increase fluidity (Royce *et al.,* 2013). Therefore, LpxC regulation may be correlated with membrane fluidity. Bacterial membrane fluidity is known to be increased at elevated temperatures (Mansilla *et al.,* 2004) and non-coincidentally, the half-life of LpxC is also increased under such conditions (although, it should be noted that the steady-state concentrations of LpxC are similar at both 30°C and 42°C) (Fig. S6 in Appendix)

The observation of FtsH-*dependent* LpxC proteolysis occurring under toxic cellular conditions (Fig. 5.5) indicate an essential role of LpxC in general cell metabolism**.** Under these sub-optimal conditions, cells tend to shut down growth which also involves halting the synthesis of membrane components (Traxler *et al.,* 2008). Schakermann *et al* (2013) observed that under stringent responses that led to the accumulation of the alarmone (p)ppGpp, the half-life of LpxC decreased and was dependent on FtsH. As mentioned earlier, their findings could be explained from the model based on prior results presented by Traxler *et al* (2008) in which the expression of *lpxK* is prominently deregulated under (p)ppGpp accumulation in comparison to other genes involved in LPS synthesis. This implies that LpxK would be present in low copies leading to increased concentration of lipid A disaccharide which enhances LpxC degradation. The correlation between LPS synthesis and growth rate is further supported by findings in

Zeng *et al.* (2013) whereby *E. coli* mutants resistant to CHIR-090 had decreased LpxC activity in addition to a suppressor mutation in the *thrS* gene. The mutation in the *thrS* gene leads to reduced protein production rate and slower cell growth (Zeng *et al.*, 2013). Alternatively, FtsH degradation of LpxC may be activated via an unidentified metabolite under sub-optimal growth conditions. Together, these point to substantial signal processing taking place at FtsH, which then controls LPS synthesis through LpxC.

The regulation of LpxC becomes more complicated by observations that an unidentified protease degrades LpxC. Although the *in vitro* results provided evidence that palmitic acid enhances LpxC proteolysis via another metalloprotease, this mechanism appears not to reflect the normal *in vivo* physiological setting (Fig. 5.6). In fact, an increase in the isoforms of palmitic acid usually found in the cytoplasm (i.e. palmitoyl-ACP and palmitoyl-CoA) stabilized LpxC levels (Fig. 5.7). Therefore, the observed *in vitro* results were possibly due to a direct interaction of the free-form of palmitic acid with LpxC. A possible implication is that during fatty acids biosynthesis, dissociation of the palmitic acid prosthetic group from its carrier protein (perhaps through the action of thioesterases) triggers LpxC proteolysis. Again, this mechanism may be linked to cellular toxicity as it is well documented that long chain free-fatty acids (i.e. fatty acids not bound to ACP or CoA) such as palmitic acid are toxic to cells (Lennen *et al.*, 2011)**.** An alternative explanation to the *in vitro* results could be due to palmitic acid binding to LpxC. Palmitic acid has also been reported to bind directly to the active site of LpxC *in vitro* (Barb and Zhou, 2008). Therefore, the actual LpxC substrate and excess palmitic acid possibly competes for the enzyme active site, in which case, palmitic acid may act as an inhibitor. Proteolysis under this condition could be directed at aberrant LpxC proteins. In support of this, Fuhrer *et al.* (2006) had initially suggested a possible involvement of other classes of proteases in the degradation of non-functional LpxC.

Irrespective of the *in vitro* results, residual degradation of LpxC still occurs under FtsH inactivation conditions (Fig. 5.7). Interestingly, treatment of bacterial cultures with compounds which reduced the levels of lipid A disaccharide and stabilized LpxC in wild-type cells, also led to LpxC stability in *ftsH* knockout mutants; although, much higher concentrations of those compounds were required. However, this does not indicate that lipid A disaccharide is the feedback source under those FtsH inactivation conditions since other antibiotics which directly targeted the membrane structure also resulted in LpxC stability (Fig. 5.7). Therefore, the regulatory signal for FtsH-*independent* LpxC proteolysis arises from an unidentified metabolite or pathway. Due to LpxC being localized in the cytoplasm, this unidentified protease would most likely be localized in the cytoplasm or inner membrane. Thus, under conditions of direct LPS attack from the environment (i.e. outer membrane), it is highly plausible that this protease functions in parallel with a separate adapter protein which senses the vulnerability of the outer membrane and translates such information to the protease. Indeed, in a similar pattern, FtsH-mediated LpxC degradation has been reported to be dependent on an adapter protein YciM (Mahalakshmi *et al.*, 2014). Due to LpxC being the first committed step in LPS synthesis, it is intuitively reasonable that when the bacterial membrane is under direct attack from the external environment, cells must attain the desired level of LPS through LpxC regulation irrespective of the concentration of lipid A disaccharide or presence of an active FtsH protein. It would be interesting to investigate whether the specific activity of LpxK are increased as well under such conditions.

6.1.4 WaaA regulation

The lipid A biosynthesis pathway in *E. coli* comprises of only nine enzymic reaction steps; yet, two of those enzymes are regulated by the same FtsH protease. One of many puzzles surrounding LPS regulation has been to underpin the exact rationale for WaaA regulation in addition to LpxC.

According to the model, there are several possible purposes for WaaA regulation. First, it may serve to regulate lipid A production, which the model proved is possible, but only if CMP-Kdo is at least partially limiting. Also, it may serve to regulate the relative production of lipid A and alternate lipid A, which the model also displayed is possible. This is because WaaA has a low substrate specificity (Katz and Ron, 2008).

Further experimental investigations suggest that under optimum conditions, WaaA regulation is more correlated with LPS composition. Although, the levels of Kdo in the membrane were elevated under WaaA overexpression, the overall LPS concentration was not elevated which suggests that WaaA degradation functions as a means to prevent an uncontrolled addition of Kdo residues to lipid precursors. In support of this, some of the precursors for other substrates that can be glycosylated by WaaA could not be detected in wild-type *E. coli* (Takayama *et al.*, 1983), suggesting that this step is tightly controlled. The situation changes at elevated temperatures where these alternate substrates accumulate (Nishijima and Raetz, 1979) and, probably not coincidentally, WaaA is degraded faster under these conditions (Katz and Ron, 2008). Furthermore, it is well established that the composition of lipids within bacterial membranes are altered as a response to temperature fluctuations and growth rate changes (de Mendoza *et al.*, 1983; Vigh *et al.*, 1998; Mansilla *et al.*, 2004), presumably to control membrane fluidity.

Nevertheless, since the alternate substrates that can be glycosylated by WaaA are absent under optimum conditions (Nishijima and Raetz, 1979; Takayama *et al.,* 1983), this suggests that WaaA possibly re-glycosylates lipid IV_A or alternatively, glycosylates other lipid A precursor molecules given that WaaA is rapidly degraded under optimum conditions. This also suggests that the activator is most likely downstream of LpxC within the LPS pathway.

Interestingly, when WaaA was overexpressed under CHIR-090 treatment, an increment in LPS (using the heptose assay) was observed in comparison with cells that were solely treated with CHIR-090 (Fig. 5.12). This is in contrast to observations in wild-type and WaaA overexpressed cells in which the latter condition led to less LPS. A first intuitive analogy would be to assume that when bacterial cells are characterized with reduced LPS synthesis rate, multiple or re-glycosylation pattern by WaaA could help compensate for a fluid outer membrane. However, this seems unlikely since a combination of CHIR-090 treatment and WaaA overexpression induces a highly toxic effect to the cells in comparison to either CHIR-090 treatment or WaaA overexpression only (Fig. 5.10). This indicates that WaaA overexpression is highly undesirable even under limited LPS substrate conditions.

From the arguments above, it can be concluded that WaaA does not control the rate of LPS synthesis under optimum conditions. Although, deletion of *waaA* has been reported to be lethal (Klein *et al.,* 2009), Reynolds and Raetz (2009) have provided evidence to suggest that the importance of WaaA is mainly to provide the right substrates for LpxL which make its role more of a *qualitative* one. Furthermore, findings by Meredith *et al.* (2006) have indicated that WaaA is not essential for LPS synthesis and assembly. In the study, the authors generated a *non-conditional E. coli* strain that lacks Kdo and remained viable. In furtherance, the authors also observed that a second Kdo knockout

strain that was auxotrophic for arabinose-5-phosphate (A5P) became viable in the absence of A5P under MsbA overexpression conditions. This indicate that rates of non-glycosylated lipid A transport can, in part, compensate for an absence of Kdo. Perhaps, previously observed correlation of cell viability and absence of Kdo arises due to a lethal pleiotropy resulting from the depletion of the carbohydrate, rather than an inherent need for the Kdo molecule itself as an indispensable component of LPS (Meredith *et al.,* 2006).

6.2 CONCLUSION

A central theme of cell biology modeling method development is that non-spatial, non-stochastic models are too simplistic (Ridgway *et al.,* 2006; Andrews *et al.,* 2009). In response, new software tools offer support for stochastic reaction dynamics and spatial localization of proteins. In this case, this research began by using the Smoldyn simulator (Andrews *et al.,* 2010), which accurately addresses stochasticity and spatial detail, but found that simulations ran too slowly and the spatial detail did not affect the results. Thus, simulations were switched to StochKit (Sanft *et al.,* 2011), which performs stochastic simulations but ignores spatial localization. Again though, the stochastic detail proved unnecessary (Fig. S8 in Appendix). Finally, the study settled on the use of non-spatial deterministic simulations. These simple simulations were appropriate in this case because the lipid A and phospholipids pathways are sufficiently poorly parameterized through experimental work. Therefore, including additional detail would have only complicated the model further. However, more detailed simulation methods will likely become useful as the lipid A and phospholipids syntheses become better characterized. For example, the model indicated that time-averaged intracellular CHIR-090 antibiotic count in cells was about 0.3 molecules, implying that it is present in

extremely low copy numbers. This could lead to strong stochastic effects. Also, the results suggest the presence of interesting dynamics between LpxH and LpxB, such as metabolic channeling. These might be best modeled using spatial simulation methods.

In conclusion, a first and comprehensive model for the biosynthesis of the outer membrane in *E. coli* was developed. The computational model agrees qualitatively with the presented experimental findings and to some degree, quantitatively. The regulatory elements presented in the model are largely new. The experimental results indicate a strong correlation between membrane fluidity and LpxC degradation. Furthermore, the results of this study indicate lipid A disaccharide is the sole feedback source for FtsH-mediated LpxC degradation. Interestingly, FtsH-independent LpxC proteolysis was observed *in vivo* which was independent on lipid A disaccharide accumulation. The results presented above also imply that the catalytic activation of LpxK is entirely dependent on the presence of UFAs. Additionally, the regulation of WaaA is unintended to control the LPS synthesis rate but rather, to prevent undesirable lipid glycosylation patterns.

The major points of control between LPS and phospholipid pathways lie with LpxC and LpxK. Both proteins sense interactions in the biosynthesis of phospholipids and co-ordinately regulate the amount of LPS produced accordingly. The fact that LpxC regulation occurs through multiple channels highlight an important role in bacterial metabolism. Also, cells could potentially adapt to perturbations in LpxC levels through multiple sources which subsequently makes LpxC undesirable as a drug target. On the other hand, because LpxK is not known to be regulated through multiple channels, in addition to its important role at maintaining LPS and phospholipids homeostasis, drug design directed towards LpxK would result in potent therapeutic agents. Altogether, the

findings of this work provide new insights into the complex biogenesis of the *E. coli* outer membrane.

6.3 FUTURE RECOMMENDATIONS

The model presented in this research represents the most complete model for the biosynthesis of the outer membrane components of *E. coli.* An extension of the model incorporating peptidoglycan synthesis would effectively result in the creation of a model representing the entire bacterial membrane. Such information would be invaluable at interrogating membrane permeability and invariably guide drug development process. Further expansion of the model would represent a key step towards achieving a whole-cell model.

Although the model agreed qualitatively with a wide range of experimental results, it also exhibited some quantitative differences. Thus, this model is not a final picture of lipid A and phospholipids biosynthesis, but instead represents the best understanding of the biosynthesis of the integrated pathway that is available to date. Nevertheless, the model present interesting findings which could not be validated in this research. For instance, a possibility that LpxH and LpxB could interact by forming a metabolic channel would be interesting for further investigation. The model also strongly indicates that the catalytic activity of LpxK is entirely dependent on the presence of UFAs. Again, this hypothesis would require further validation using *in vitro* enzyme kinetics assay.

Additionally, characterization of the unidentified protease involved in LpxC degradation would be invaluable. This would further enhance our understanding on the essentiality of such protease, and perhaps, result in the assignment of a function if previously

unannotated. Likewise, further studies are necessary to investigate the structural composition of LPS under WaaA overexpression conditions.

References

Abeyrathne, P. D., Daniels, C., Poon, K. K., Matewish, M. J. and Lam, J. S. (2005) 'Functional characterization of WaaL, a ligase associated with linking O-antigen polysaccharide to the core of Pseudomonas aeruginosa lipopolysaccharide', *J Bacteriol*, 187(9), pp. 3002-3012. doi: 10.1128/JB.187.9.3002-3012.2005.

Akiyama, Y. (2009) 'Quality control of cytoplasmic membrane proteins in Escherichia coli', *J Biochem.*, 146(4), pp. 449-54.

Alberts, B., Johnson, A., Lewis, J., Raff, M., Roberts, K. and Walter, P. (2002) *Molecular Biology of the Cell*. 4th ed. Garland Science New York.

Anderson, M. S. and Raetz, C. R. (1987) 'Biosynthesis of lipid A precursors in Escherichia coli. A cytoplasmic acyltransferase that converts UDP-N-acetylglucosamine to UDP-3-O-(R-3-hydroxymyristoyl)-N-acetylglucosamine', *J Biol Chem*, 262(11), pp. 5159-5169.

Anderson, M. S., Bull, H. G., Galloway, S. M., Kelly, T. M., Mohan, S., Radika, K. and Raetz, C. R. (1993) 'UDP-N-acetylglucosamine acyltransferase of Escherichia coli. The first step of endotoxin biosynthesis is thermodynamically unfavorable', *J Biol Chem*, 268(26), pp. 19858-19865.

Anderson, M. S., Robertson, A. D., Macher, I. and Raetz, C. R. (1988) 'Biosynthesis of lipid A in Escherichia coli: identification of UDP-3-O-[(R)-3-hydroxymyristoyl]-alpha-D-glucosamine as a precursor of UDP-N2,O3-bis[(R)-3-hydroxymyristoyl]-alpha-D-glucosamine', *Biochemistry*, 27(6), pp. 1908-1917.

Andrews, S. S. and Bray, D. (2004) 'Stochastic simulation of chemical reactions with spatial resolution and single molecule detail', *Phys Biol*, 1(3-4), pp. 137-151. doi: 10.1088/1478-3967/1/3/001.

Andrews, S. S., Addy, N. J., Brent, R. and Arkin, A. P. (2010) 'Detailed simulations of cell biology with Smoldyn 2.1', *PLoS Comput Biol*, 6(3), p. e1000705. doi: 10.1371/journal.pcbi.1000705.

Andrews, S.S., Tuan, D. and Arkin A. (2009) 'Stochastic models of biological processes' *Encyclopedia of Complexity and System Science*. Meyers, Robert (Ed.) 9: pp. 8730 - 8749.

Babinski, K. J., Ribeiro, A. A. and Raetz, C. R. (2002) 'The Escherichia coli gene encoding the UDP-2,3-diacylglucosamine pyrophosphatase of lipid A biosynthesis', *J Biol Chem*, 277(29),pp. 25937-25946. doi: 10.1074/jbc.M204067200.

Bachmann, B. J. (1972) 'Pedigrees of some mutant strains of Escherichia coli K-12', *Bacteriol Rev*, 36(4), pp. 525-557.

Band, V. I. and Weiss, D. S. (2015) 'Mechanisms of Antimicrobial Peptide Resistance in Gram-Negative Bacteria', *Antibiotics (Basel)*, 4(1), pp. 18-41. doi: 10.3390/antibiotics4010018.

Barb, A. W. and Zhou, P. (2008) 'Mechanism and inhibition of LpxC: an essential zinc-dependent deacetylase of bacterial lipid A synthesis', *Curr Pharm Biotechnol*, 9(1), pp. 9-15.

Barb, A. W., McClerren, A. L., Snehelatha, K., Reynolds, C. M., Zhou, P. and Raetz, C. R. (2007) 'Inhibition of lipid A biosynthesis as the primary mechanism of CHIR-090 antibiotic activity in Escherichia coli', *Biochemistry*, 46(12), pp. 3793-3802. doi: 10.1021/bi6025165.

Bartling, C. M. and Raetz, C. R. (2008) 'Steady-state kinetics and mechanism of LpxD, the N-acyltransferase of lipid A biosynthesis', *Biochemistry*, 47(19), pp. 5290-5302. doi: 10.1021/bi800240r.

Beard, D. A., Liang, S. D. and Qian, H. (2002) 'Energy balance for analysis of complex metabolic networks', *Biophys J*, 83(1), pp. 79-86. doi: 10.1016/S0006-3495(02)75150-3.

Belunis, C. J. and Raetz, C. R. (1992) 'Biosynthesis of endotoxins. Purification and catalytic properties of 3-deoxy-D-manno-octulosonic acid transferase from Escherichia coli', *J Biol Chem*, 267(14), pp. 9988-9997.

Bergler, H., Fuchsbichler, S., Högenauer, G. and Turnowsky, F. (1996) 'The enoyl-[acyl-carrier-protein] reductase (FabI) of Escherichia coli, which catalyses a key regulatory step in fatty acid biosynthesis, accepts NADH and NADPH as cofactors and is inhibited by palmitoyl-CoA', *Eur J Biochem*, 242(3), pp. 689-694.

Bernstein, J. A., Khodursky, A. B., Lin, P. H., Lin-Chao, S. and Cohen, S. N. (2002) 'Global analysis of mRNA decay and abundance in Escherichia coli at single-gene resolution using two-color fluorescent DNA microarrays', *Proc Natl Acad Sci U S A*, 99(15), pp. 9697-9702. doi: 10.1073/pnas.112318199.

Blattner, F. R., Plunkett, G., Bloch, C. A., Perna, N. T., Burland, V., Riley, M. *et al.* (1997) 'The complete genome sequence of Escherichia coli K-12', *Science*, 277(5331), pp. 1453-1462.

Bligh, E. G. and Dyer, W. J. (1959) 'A rapid method of total lipid extraction and purification', *Can J Biochem Physiol*, 37(8), pp. 911-917.

Bos, M. P., Tefsen, B., Geurtsen, J. and Tommassen, J. (2004) 'Identification of an outer membrane protein required for the transport of lipopolysaccharide to the bacterial cell surface', *Proc Natl Acad Sci U S A*, 101(25), pp. 9417-9422. doi: 10.1073/pnas.0402340101.

Bradford, M. M. (1976) 'A rapid and sensitive method for the quantitation of microgram quantities of protein utilizing the principle of protein-dye binding', *Anal Biochem*, 72,pp. 248-254.

Breitling, R. (2010) 'What is systems biology?', *Front Physiol*, 1, p. 9. doi: 10.3389/fphys.2010.00009.

Brinster, S., Lamberet, G., Staels, B., Trieu-Cuot, P., Gruss, A. and Poyart, C. (2009) 'Type II fatty acid synthesis is not a suitable antibiotic target for Gram-positive pathogens', *Nature*, 458(7234), pp. 83-86. doi: 10.1038/nature07772.

Brozek, K. A. and Raetz, C. R. (1990) 'Biosynthesis of lipid A in Escherichia coli. Acyl carrier protein-dependent incorporation of laurate and myristate', *J Biol Chem*, 265(26), pp. 15410-15417.

Brozek, K. A., Hosaka, K., Robertson, A. D. and Raetz, C. R. (1989) 'Biosynthesis of lipopolysaccharide in Escherichia coli. Cytoplasmic enzymes that attach 3-deoxy-D-manno-octulosonic acid to lipid A', *J Biol Chem*, 264(12), pp. 6956-6966.

Bush, K., Courvalin, P., Dantas, G., Davies, J., Eisenstein, B., Huovinen, P. *et al.* (2011) 'Tackling antibiotic resistance', *Nat Rev Microbiol*, 9(12), pp. 894-896. doi: 10.1038/nrmicro2693.

Campbell, J. W. and Cronan, J. E. (2001) 'Escherichia coli FadR positively regulates transcription of the fabB fatty acid biosynthetic gene', *J Bacteriol*, 183(20), pp. 5982-5990. doi: 10.1128/JB.183.20.5982-5990.2001.

Cao, Y., Yang, J., Xian, M., Xu, X. and Liu, W. (2010) 'Increasing unsaturated fatty acid contents in Escherichia coli by coexpression of three different genes', *Appl Microbiol Biotechnol*, 87(1), pp. 271-280. doi: 10.1007/s00253-009-2377-x.

Cayley, S., Lewis, B. A., Guttman, H. J. and Record, M. T. (1991) 'Characterization of the cytoplasm of Escherichia coli K-12 as a function of external osmolarity. Implications for protein-DNA interactions in vivo', *J Mol Biol*, 222(2), pp. 281-300.

Centers for Disease Control (2015a). *Antibiotic Resistance Threats in the United States, 2013* [online] Available from: **http://www.cdc.gov/drugresistance/threat-report-2013/**. [Accessed 21 July 2015]

Centers for Disease Control (2015b) *Facts about Antibiotic Resistance.* [online] Available from: **http://www.cdc.gov/getsmart/community/about/fast-facts.html**. [Accessed 21 July 2015]

Chang, Y. Y. and Cronan, J. E. (1999) 'Membrane cyclopropane fatty acid content is a major factor in acid resistance of Escherichia coli', *Mol Microbiol*, 33(2), pp. 249-259.

Chen, K. C., Calzone, L., Csikasz-Nagy, A., Cross, F. R., Novak, B. and Tyson, J. J. (2004) 'Integrative analysis of cell cycle control in budding yeast', *Mol Biol Cell*, 15(8), pp. 3841-3862. doi: 10.1091/mbc.E03-11-0794.

Choi-Rhee, E. and Cronan, J. E. (2003) 'The biotin carboxylase-biotin carboxyl carrier protein complex of Escherichia coli acetyl-CoA carboxylase', *J Biol Chem*, 278(33), pp. 30806-30812. doi: 10.1074/jbc.M302507200.

Chuang, H. Y., Hofree, M. and Ideker, T. (2010) 'A decade of systems biology', *Annu Rev Cell Dev Biol*, 26, pp. 721-744. doi: 10.1146/annurev-cellbio-100109-104122.

Chung, C. T., Niemela, S. L. and Miller, R. H. (1989) 'One-step preparation of competent Escherichia coli: transformation and storage of bacterial cells in the same solution',*Proc Natl Acad Sci U S A*, 86(7), pp. 2172-2175.

Clark, D. P., DeMendoza, D., Polacco, M. L. and Cronan, J. E. (1983) 'Beta-hydroxydecanoyl thio ester dehydrase does not catalyse a rate-limiting step in Escherichia coli unsaturated fatty acid synthesis', *Biochemistry*, 22(25), pp. 5897-5902.

Clementz, T. and Raetz, C. R. (1991) 'A gene coding for 3-deoxy-D-manno-octulosonic-acid transferase in Escherichia coli. Identification, mapping, cloning, and sequencing', *J Biol Chem*, 266(15), pp. 9687-9696.

Clementz, T., Bednarski, J. J. and Raetz, C. R. (1996) 'Function of the htrB high temperature requirement gene of Escherchia coli in the acylation of lipid A: HtrB catalysed incorporation of laurate', *J Biol Chem*, 271(20), pp. 12095-12102.

Clementz, T., Zhou, Z. and Raetz, C. R. (1997) 'Function of the Escherichia coli msbB gene, a multicopy suppressor of htrB knockouts, in the acylation of lipid A. Acylation by MsbB follows laurate incorporation by HtrB', *J Biol Chem*, 272(16), pp. 10353-10360.

Coleman, J. (1992) 'Characterization of the Escherichia coli gene for 1-acyl-sn-glycerol-3-phosphate acyltransferase (plsC)', *Mol Gen Genet*, 232(2), pp. 295-303.

Cornish-Bowden, A. (2004) *Fundamentals of Enzyme Kinetics.* 3rd ed. Portland Press, 2004.

Cornish-Bowden, A. and Cárdenas, M. L. (2001) 'Information transfer in metabolic pathways. Effects of irreversible steps in computer models', *Eur J Biochem*, 268(24), pp. 6616-6624.

Covert, M. W., Famili, I. and Palsson, B. O. (2003) 'Identifying constraints that govern cell behavior: a key to converting conceptual to computational models in biology?',*Biotechnol Bioeng*, 84(7), pp. 763-772. doi: 10.1002/bit.10849.

Cox, D. R. and Miller, H.D. (1977) *The Theory of Stochastic Processes.* Chapman & Hall, London.

Cronan, J. E. and Waldrop, G. L. (2002) 'Multi-subunit acetyl-CoA carboxylases', *Prog Lipid Res*, 41(5), pp. 407-435.

Cronan, J. E., Birge, C. H. and Vagelos, P. R. (1969) 'Evidence for two genes specifically involved in unsaturated fatty acid biosynthesis in Escherichia coli', *J Bacteriol*, 100(2), pp. 601-604.

Cronan, J. E., Silbert, D. F. and Wulff, D. L. (1972) 'Mapping of the fabA locus for unsaturated fatty acid biosynthesis in Escherichia coli', *J Bacteriol*, 112(1), pp. 206-211.

D'Agnolo, G., Rosenfeld, I. S. and Vagelos, P. R. (1975) 'Multiple forms of beta-ketoacyl-acyl carrier protein synthetase in Escherichia coli', *J Biol Chem*, 250(14), pp. 5289-5294.

Davis, M. S. and Cronan, J. E. (2001) 'Inhibition of Escherichia coli acetyl coenzyme A carboxylase by acyl-acyl carrier protein', *J Bacteriol*, 183(4), pp. 1499-1503. doi: 10.1128/JB.183.4.1499-1503.2001.

de Mendoza, D., Klages Ulrich, A. and Cronan, J. E. (1983) 'Thermal regulation of membrane fluidity in Escherichia coli. Effects of overproduction of beta-ketoacyl-acyl carrier protein synthase I', *J Biol Chem*, 258(4), pp. 2098-2101.

DebRoy, C., Roberts, E. and Fratamico, P. M. (2011) 'Detection of O antigens in Escherichia coli', *Anim Health Res Rev*, 12(2), pp. 169-185. doi: 10.1017/S1466252311000193.

Delcour, A. H. (2009) 'Outer membrane permeability and antibiotic resistance', *Biochim Biophys Acta*, 1794(5), pp. 808-816. doi: 10.1016/j.bbapap.2008.11.005.

Ditlevsen, S., and Samson, A. (2013) 'Introduction to Stochastic Models in Biology', in M. Bachar *et al.* (eds.), *Stochastic Biomathematical Models.* Springer-Verlag Berlin Heidelberg. pp. 3-35.

Doerrler, W. T. and Raetz, C. R. (2002) 'ATPase activity of the MsbA lipid flippase of Escherichia coli', *J Biol Chem*, 277(39), pp. 36697-36705. doi: 10.1074/jbc.M205857200.

Drake, T. A., Cheng, J., Chang, A. and Taylor, F. B. (1993) 'Expression of tissue factor, thrombomodulin, and E-selectin in baboons with lethal Escherichia coli sepsis', *Am J Pathol*, 142(5), pp. 1458-1470.

Edwards, P., Nelsen, J. S., Metz, J. G. and Dehesh, K. (1997) 'Cloning of the fabF gene in an expression vector and in vitro characterization of recombinant fabF and fabB encoded enzymes from Escherichia coli', *FEBS Lett*, 402(1), pp. 62-66.

Egan, A. F. and Russell, R. R. (1973) 'Conditional mutations affecting the cell envelope of Escherichia coli K-12', *Genet Res*, 21(2), pp. 139-152.

Emptage, R. P., Daughtry, K. D., Pemble, C. W. and Raetz, C. R. (2012) 'Crystal structure of LpxK, the 4'-kinase of lipid A biosynthesis and atypical P-loop kinase functioning at the membrane interface', *Proc Natl Acad Sci U S A*, 109(32), pp. 12956-12961. doi: 10.1073/pnas.1206072109.

Eraso, J. M., Markillie, L. M., Mitchell, H. D., Taylor, R. C., Orr, G. and Margolin, W. (2014) 'The highly conserved MraZ protein is a transcriptional regulator in Escherichia coli', *J Bacteriol*, 196(11), pp. 2053-2066. doi: 10.1128/JB.01370-13.

Erez, E., Stjepanovic, G., Zelazny, A. M., Brugger, B., Sinning, I. and Bibi, E. (2010) 'Genetic evidence for functional interaction of the Escherichia coli signal recognition particle receptor with acidic lipids in vivo', *J Biol Chem*, 285(52), pp. 40508-40514. doi: 10.1074/jbc.M110.140921.

Fange, D., Mahmutovic, A. and Elf, J. (2012) 'MesoRD 1.0: Stochastic reaction-diffusion simulations in the microscopic limit', *Bioinformatics*, 28(23), pp. 3155-3157. doi: 10.1093/bioinformatics/bts584.

Feigenbaum, J. and Schulz, H. (1975) 'Thiolases of Escherichia coli: purification and chain length specificities', *J Bacteriol*, 122(2), pp. 407-411.

Fell, D. (1971) *Understanding the Control of Metabolism*. Portland Press London.

Fell, D. A. (1992) 'Metabolic control analysis: a survey of its theoretical and experimental development', *Biochem J*, 286 (Pt 2), pp. 313-330.

Fell, D. A. and Sauro, H. M. (1985) 'Metabolic control and its analysis. Additional relationships between elasticities and control coefficients', *Eur J Biochem*, 148(3), pp. 555-561.

Feng, Y. and Cronan, J. E. (2009) 'Escherichia coli unsaturated fatty acid synthesis: complex transcription of the fabA gene and in vivo identification of the essential reaction catalysed by FabB', *J Biol Chem*, 284(43), pp. 29526-29535. doi: 10.1074/jbc.M109.023440.

Feng, Y. and Cronan, J. E. (2011) 'Complex binding of the FabR repressor of bacterial unsaturated fatty acid biosynthesis to its cognate promoters', *Mol Microbiol*, 80(1), pp. 195-218. doi: 10.1111/j.1365-2958.2011.07564.x.

Feng, Y. and Cronan, J. E. (2012) 'Crosstalk of Escherichia coli FadR with global regulators in expression of fatty acid transport genes', *PLoS One*, 7(9), p. e46275. doi: 10.1371/journal.pone.0046275.

Fiehn, O. (2001) 'Combining genomics, metabolome analysis, and biochemical modelling to understand metabolic networks', *Comp Funct Genomics*, 2(3), pp. 155-168. doi: 10.1002/cfg.82.

Fiers, W., Contreras, R., Duerinck, F., Haegeman, G., Iserentant, D., Merregaert, J. *et al.* (1976) 'Complete nucleotide sequence of bacteriophage MS2 RNA: primary and secondary structure of the replicase gene', *Nature*, 260(5551), pp. 500-507.

Führer, F., Langklotz, S. and Narberhaus, F. (2006) 'The C-terminal end of LpxC is required for degradation by the FtsH protease', *Mol Microbiol*, 59(3), pp. 1025-1036. doi: 10.1111/j.1365-2958.2005.04994.x.

Führer, F., Müller, A., Baumann, H., Langklotz, S., Kutscher, B. and Narberhaus, F. (2007) 'Sequence and length recognition of the C-terminal turnover element of LpxC, a soluble substrate of the membrane-bound FtsH protease', *J Mol Biol*, 372(2), pp. 485-496. doi: 10.1016/j.jmb.2007.06.083.

Fujita, Y., Matsuoka, H. and Hirooka, K. (2007) 'Regulation of fatty acid metabolism in bacteria', *Mol Microbiol*, 66(4), pp. 829-839. doi: 10.1111/j.1365-2958.2007.05947.x.

Funk, C. R., Zimniak, L. and Dowhan, W. (1992) 'The pgpA and pgpB genes of Escherichia coli are not essential: evidence for a third phosphatidylglycerophosphate phosphatase', *J Bacteriol*, 174(1), pp. 205-213.

Galloway, S. M. and Raetz, C. R. (1990) 'A mutant of Escherichia coli defective in the first step of endotoxin biosynthesis', *J Biol Chem*, 265(11), pp. 6394-6402.

Garrett, T. A., Kadrmas, J. L. and Raetz, C. R. (1997) 'Identification of the gene encoding the Escherichia coli lipid A 4'-kinase. Facile phosphorylation of endotoxin analogs with recombinant LpxK', *J Biol Chem*, 272(35), pp. 21855-21864.

Garrett, T. A., Que, N. L. and Raetz, C. R. (1998) 'Accumulation of a lipid A precursor lacking the 4'-phosphate following inactivation of the Escherichia coli lpxK gene', *J Biol Chem*, 273(20), pp. 12457-12465.

Garwin, J. L., Klages, A. L. and Cronan, J. E. (1980a) 'Beta-ketoacyl-acyl carrier protein synthase II of Escherichia coli. Evidence for function in the thermal regulation of fatty acid synthesis', *J Biol Chem*, 255(8), pp. 3263-3265.

Garwin, J. L., Klages, A. L. and Cronan, J. E. (1980b) 'Structural, enzymatic, and genetic studies of beta-ketoacyl-acyl carrier protein synthases I and II of Escherichia coli', *J Biol Chem*, 255(24), pp. 11949-11956.

Gaynes, R., Edwards, J. R. and System, N. N. I. S. (2005) 'Overview of nosocomial infections caused by gram-negative bacilli', *Clin Infect Dis*, 41(6), pp. 848-854. doi: 10.1086/432803.

Ghalambor, M. A. and Heath, E. C. (1966) 'The biosynthesis of cell wall lipopolysaccharide in Escherichia coli. V. Purification and properties of 3-deoxy-D-manno-octulosonate aldolase', *J Biol Chem*, 241(13), pp. 3222-3227.

Gibson, M. A., and E. Mjolsness. (1999) ‘Modeling the activity of single genes’, in J. M. Bower and H. Bolouri (eds), *Computational Modeling of Genetic and Biochemical Networks*. MIT Press, Cambridge, MA. pp. 3–48.

Gillespie, D. T., (1977) ‘Exact Stochastic Simulation of Coupled Chemical Reactions’, *The Journal of Physical Chemistry* 81(25), pp. 2340–2361

Gillespie, D. T. (2007) 'Stochastic simulation of chemical kinetics', *Annu Rev Phys Chem*, 58, pp. 35-55. doi: 10.1146/annurev.physchem.58.032806.104637.

Goelz, S. E. and Cronan, J. E. (1980) 'The positional distribution of fatty acids in Escherichia coli phospholipids is not regulated by sn-glycerol 3-phosphate levels', *J Bacteriol*, 144(1), pp. 462-464.

Goldman, R., Kohlbrenner, W., Lartey, P. and Pernet, A. (1987) 'Antibacterial agents specifically inhibiting lipopolysaccharide synthesis', *Nature*, 329(6135), pp. 162-164. doi: 10.1038/329162a0.

Golenbock, D. T., Hampton, R. Y., Qureshi, N., Takayama, K. and Raetz, C. R. (1991) 'Lipid A-like molecules that antagonize the effects of endotoxins on human monocytes', *J Biol Chem*, 266(29), pp. 19490-19498.

Green, P. R., Merrill, A. H. and Bell, R. M. (1981) 'Membrane phospholipid synthesis in Escherichia coli. Purification, reconstitution, and characterization of sn-glycerol-3-phosphate acyltransferase', *J Biol Chem*, 256(21), pp. 11151-11159.

Grogan, D. W. and Cronan, J. E. (1986) 'Characterization of Escherichia coli mutants completely defective in synthesis of cyclopropane fatty acids', *J Bacteriol*, 166(3), pp. 872-877.

Gronow, S. and Brade, H. (2001) 'Lipopolysaccharide biosynthesis: which steps do bacteria need to survive?', *J Endotoxin Res*, 7(1), pp. 3-23.

Güell, M., van Noort, V., Yus, E., Chen, W. H., Leigh-Bell, J., Michalodimitrakis, K., *et al.* (2009) 'Transcriptome complexity in a genome-reduced bacterium',*Science*, 326(5957), pp. 1268-1271. doi: 10.1126/science.1176951.

Guzman, L. M., Belin, D., Carson, M. J. and Beckwith, J. (1995) 'Tight regulation, modulation, and high-level expression by vectors containing the arabinose PBAD promoter', *J Bacteriol*, 177(14), pp. 4121-4130.

Hanahan, D. (1983) 'Studies on transformation of Escherichia coli with plasmids', *J Mol Biol*, 166(4), pp. 557-580.

Harvey, D. J. (1998) 'Picolinyl esters for the structural determination of fatty acids by GC/MS', *Mol Biotechnol*, 10(3), pp. 251-260. doi: 10.1007/BF02740846.

Heath, R. J. and Rock, C. O. (1995) 'Enoyl-acyl carrier protein reductase (fabI) plays a determinant role in completing cycles of fatty acid elongation in Escherichia coli', *J Biol Chem*, 270(44), pp. 26538-26542.

Heath, R. J. and Rock, C. O. (1996a) 'Inhibition of beta-ketoacyl-acyl carrier protein synthase III (FabH) by acyl-acyl carrier protein in Escherichia coli', *J Biol Chem*, 271(18),pp. 10996-11000.

Heath, R. J. and Rock, C. O. (1996b) 'Roles of the FabA and FabZ beta-hydroxyacyl-acyl carrier protein dehydratases in Escherichia coli fatty acid biosynthesis', *J Biol Chem*, 271(44), pp. 27795-27801.

Heath, R. J. and Rock, C. O. (1996c) 'Regulation of fatty acid elongation and initiation by acyl-acyl carrier protein in Escherichia coli', *J Biol Chem*, 271(4), pp. 1833-1836.

Heath, R. J. and Rock, C. O. (2004) 'Fatty acid biosynthesis as a target for novel antibacterials', *Curr Opin Investig Drugs*, 5(2), pp. 146-153.

Heath, R. J., Jackowski, S. and Rock, C. O. (1994) 'Guanosine tetraphosphate inhibition of fatty acid and phospholipid synthesis in Escherichia coli is relieved by overexpression of glycerol-3-phosphate acyltransferase (plsB)', *J Biol Chem*, 269(42), pp. 26584-26590.

Heath, R. J., Jackowski, S., and Rock, C. O. (2002) 'Fatty acid and phospholipid metabolism in prokaryotes', in D.E. Vance and J. E. Vance (eds), *Biochemistry of Lipids, Lipoproteins, and Membranes*, 4th Ed. Elsevier Science Publishing Co., Inc., New York. pp. 55-92.

Helmkamp, G. M., Brock, D. J. and Bloch, K. (1968) 'Beta-hydroxydecanoly thioester dehydrase. Specificity of substrates and acetylenic inhibitors', *J Biol Chem*, 243(12), pp. 3229-3231.

Henderson, J. C., O'Brien, J. P., Brodbelt, J. S. and Trent, M. S. (2013) 'Isolation and chemical characterization of lipid A from gram-negative bacteria', *J Vis Exp*, (79), p. e50623. doi: 10.3791/50623.

Hernick, M., Gennadios, H. A., Whittington, D. A., Rusche, K. M., Christianson, D. W. and Fierke, C. A. (2005) 'UDP-3-O-((R)-3-hydroxymyristoyl)-N-acetylglucosamine deacetylase functions through a general acid-base catalyst pair mechanism', *J Biol Chem*, 280(17), pp. 16969-16978. doi: 10.1074/jbc.M413560200.

Hoops, S., Sahle, S., Gauges, R., Lee, C., Pahle, J., Simus, N. *et al.* (2006) 'COPASI--a COmplex PAthway SImulator', *Bioinformatics*, 22(24), pp. 3067-3074. doi: 10.1093/bioinformatics/btl485.

Hucka, M., Finney, A., Sauro, H. M., Bolouri, H., Doyle, J. C., Kitano, H. *et al.* (2003) 'The systems biology markup language (SBML): a medium for representation and exchange of biochemical network models', *Bioinformatics*, 19(4), pp. 524-531.

Hwang, P. M., Bishop, R. E. and Kay, L. E. (2004) 'The integral membrane enzyme PagP alternates between two dynamically distinct states', *Proc Natl Acad Sci U S A*, 101(26), pp. 9618-9623. doi: 10.1073/pnas.0402324101.

Hyland, S. A., Eveland, S. S. and Anderson, M. S. (1997) 'Cloning, expression, and purification of UDP-3-O-acyl-GlcNAc deacetylase from Pseudomonas aeruginosa: a metalloamidase of the lipid A biosynthesis pathway', *J Bacteriol*, 179(6), pp. 2029-2037.

Icho, T. and Raetz, C. R. (1983) 'Multiple genes for membrane-bound phosphatases in Escherichia coli and their action on phospholipid precursors', *J Bacteriol*, 153(2), pp. 722-730.

Ideker, T., Galitski, T. and Hood, L. (2001) 'A new approach to decoding life: systems biology', *Annu Rev Genomics Hum Genet*, 2, pp. 343-372. doi: 10.1146/annurev.genom.2.1.343.

Ishihama, Y., Schmidt, T., Rappsilber, J., Mann, M., Hartl, F. U., Kerner, M. J. and Frishman, D. (2008) 'Protein abundance profiling of the Escherichia coli cytosol', *BMC Genomics*, 9, p. 102. doi: 10.1186/1471-2164-9-102.

Ito, K. and Akiyama, Y. (2005) 'Cellular functions, mechanism of action, and regulation of FtsH protease', *Annu Rev Microbiol*, 59, pp. 211-231. doi: 10.1146/annurev.micro.59.030804.121316.

Jackman, J. E., Fierke, C. A., Tumey, L. N., Pirrung, M., Uchiyama, T., Tahir, S. H. *et al.* (2000) 'Antibacterial agents that target lipid A biosynthesis in gram-negative bacteria. Inhibition of diverse UDP-3-O-(r-3-hydroxymyristoyl)-n-acetylglucosamine deacetylases by substrate analogs containing zinc binding motifs', *J Biol Chem*, 275(15), pp. 11002-11009.

Jackman, J. E., Raetz, C. R. and Fierke, C. A. (1999) 'UDP-3-O-(R-3-hydroxymyristoyl)-N-acetylglucosamine deacetylase of Escherichia coli is a zinc metalloenzyme', *Biochemistry*, 38(6),pp. 1902-1911. doi: 10.1021/bi982339s.

James, E. S. and Cronan, J. E. (2004) 'Expression of two Escherichia coli acetyl-CoA carboxylase subunits is autoregulated', *J Biol Chem*, 279(4), pp. 2520-2527. doi: 10.1074/jbc.M311584200.

Janßen, H. J. and Steinbüchel, A. (2014) 'Fatty acid synthesis in Escherichia coli and its applications towards the production of fatty acid based biofuels', *Biotechnol Biofuels*, 7(1), p. 7. doi: 10.1186/1754-6834-7-7.

Jayasekera, M. M., Foltin, S. K., Olson, E. R. and Holler, T. P. (2000) 'Escherichia coli requires the protease activity of FtsH for growth', *Arch Biochem Biophys*, 380(1), pp. 103-107. doi: 10.1006/abbi.2000.1903.

Jiang, P. and Cronan, J. E. (1994) 'Inhibition of fatty acid synthesis in Escherichia coli in the absence of phospholipid synthesis and release of inhibition by thioesterase action', *J Bacteriol*, 176(10), pp. 2814-2821.

Karkhanis, Y. D., Zeltner, J. Y., Jackson, J. J. and Carlo, D. J. (1978) 'A new and improved microassay to determine 2-keto-3-deoxyoctonate in lipopolysaccharide of Gram-negative bacteria', *Anal Biochem*, 85(2), pp. 595-601.

Karow, M. and Georgopoulos, C. (1993) 'The essential Escherichia coli msbA gene, a multicopy suppressor of null mutations in the htrB gene, is related to the universally conserved family of ATP-dependent translocators', *Mol Microbiol*, 7(1), pp. 69-79.

Karr, J. R., Sanghvi, J. C., Macklin, D. N., Gutschow, M. V., Jacobs, J. M., Bolival, B. *et al.* (2012) 'A whole-cell computational model predicts phenotype from genotype', *Cell*, 150(2), pp. 389-401. doi: 10.1016/j.cell.2012.05.044.

Kass, L. R., Brock, D. J. and Bloch, K. (1967) 'Beta-hydroxydecanoyl thioester dehydrase. I. Purification and properties', *J Biol Chem*, 242(19), pp. 4418-4431.

Katz, C. and Ron, E. Z. (2008) 'Dual role of FtsH in regulating lipopolysaccharide biosynthesis in Escherichia coli', *J Bacteriol*, 190(21), pp. 7117-7122. doi: 10.1128/JB.00871-08.

Kawasaki, K., Ernst, R. K. and Miller, S. I. (2004) '3-O-deacylation of lipid A by PagL, a PhoP/PhoQ-regulated deacylase of Salmonella typhimurium, modulates signaling through Toll-like receptor 4', *J Biol Chem*, 279(19), pp. 20044-20048. doi: 10.1074/jbc.M401275200.

Keating, D. H., Carey, M. R. and Cronan, J. E. (1995) 'The unmodified (apo) form of Escherichia coli acyl carrier protein is a potent inhibitor of cell growth', *J Biol Chem*, 270(38), pp. 22229-22235.

Kelly, T. M., Stachula, S. A., Raetz, C. R. and Anderson, M. S. (1993) 'The firA gene of Escherichia coli encodes UDP-3-O-(R-3-hydroxymyristoyl)-glucosamine N-acyltransferase. The third step of endotoxin biosynthesis', *J Biol Chem*, 268(26), pp. 19866-19874.

Kenanov, D., Kaleta, C., Petzold, A., Hoischen, C., Diekmann, S., Siddiqui, R. A. and Schuster, S. (2010) 'Theoretical study of lipid biosynthesis in wild-type Escherichia coli and in a protoplast-type L-form using elementary flux mode analysis', *FEBS J*, 277(4), pp. 1023-1034. doi: 10.1111/j.1742-4658.2009.07546.x.

Kim, H. U., Kim, T. Y. and Lee, S. Y. (2008) 'Metabolic flux analysis and metabolic engineering of microorganisms', *Mol Biosyst*, 4(2), pp. 113-120. doi: 10.1039/b712395g.

Kitagawa, M., Ara, T., Arifuzzaman, M., Ioka-Nakamichi, T., Inamoto, E., Toyonaga, H. and Mori, H. (2005) 'Complete set of ORF clones of Escherichia coli ASKA library (a complete set of E. coli K-12 ORF archive): unique resources for biological research', *DNA Res*, 12(5), pp. 291-299. doi: 10.1093/dnares/dsi012.

Kitano, H. (2002) 'Computational systems biology', *Nature*, 420(6912), pp. 206-210. doi: 10.1038/nature01254.

Klein, G., Lindner, B., Brabetz, W., Brade, H. and Raina, S. (2009) 'Escherichia coli K-12 Suppressor-free Mutants Lacking Early Glycosyltransferases and Late Acyltransferases: minimal lipopolysaccharide structure and induction of envelope stress response', *J Biol Chem*, 284(23), pp. 15369-15389. doi: 10.1074/jbc.M900490200.

Kneidinger, B., Marolda, C., Graninger, M., Zamyatina, A., McArthur, F., Kosma, P. *et al.* (2002) 'Biosynthesis pathway of ADP-L-glycero-beta-D-manno-heptose in Escherichia coli', *J Bacteriol*, 184(2), pp. 363-369.

Kühner, S., van Noort, V., Betts, M. J., Leo-Macias, A., Batisse, C., Rode, M. *et al.* (2009) 'Proteome organization in a genome-reduced bacterium', *Science*, 326(5957), pp. 1235-1240. doi: 10.1126/science.1176343.

Kumar, G. B. and Black, P. N. (1991) 'Linker mutagenesis of a bacterial fatty acid transport protein. Identification of domains with functional importance', *J Biol Chem*, 266(2), pp. 1348-1353.

Kumarasamy, K. K., Toleman, M. A., Walsh, T. R., Bagaria, J., Butt, F., Balakrishnan, R. *et al.* (2010) 'Emergence of a new antibiotic resistance mechanism in India, Pakistan, and the UK: a molecular, biological, and epidemiological study', *Lancet Infect Dis*, 10(9), pp. 597-602. doi: 10.1016/S1473-3099(10)70143-2.

Kurkiewicz, S., Dzierzewicz, Z., Wilczok, T. and Dworzanski, J. P. (2003) 'GC/MS determination of fatty acid picolinyl esters by direct curie-point pyrolysis of whole bacterial cells', *J Am Soc Mass Spectrom*, 14(1), pp. 58-62. doi: 10.1016/S1044-0305(02)00817-6.

Lachor, P., Puszynski, K., and Polanski, A. (2011) 'Deterministic models and stochastic simulations in multiple reaction models in systems biology', *Journal of Biotechnology, Computational Biology and Bionanotechnology*, 92(3), pp. 265-280.

Lai, C. Y. and Cronan, J. E. (2004) 'Isolation and characterization of beta-ketoacyl-acyl carrier protein reductase (fabG) mutants of Escherichia coli and Salmonella enterica serovar Typhimurium', *J Bacteriol*, 186(6), pp. 1869-1878.

Lander, E. S., Linton, L. M., Birren, B., Nusbaum, C., Zody, M. C., Baldwin, J. *et al.* (2001) 'Initial sequencing and analysis of the human genome', *Nature*, 409(6822), pp. 860-921. doi: 10.1038/35057062.

Langklotz, S., Baumann, U. and Narberhaus, F. (2012) 'Structure and function of the bacterial AAA protease FtsH', *Biochim Biophys Acta*, 1823(1), pp. 40-48. doi: 10.1016/j.bbamcr.2011.08.015.

Larson, T. J., Ludtke, D. N. and Bell, R. M. (1984) 'sn-Glycerol-3-phosphate auxotrophy of plsB strains of Escherichia coli: evidence that a second mutation, plsX, is required',*J Bacteriol*, 160(2), pp. 711-717.

Lee, H., Hsu, F. F., Turk, J. and Groisman, E. A. (2004) 'The PmrA-regulated pmrC gene mediates phosphoethanolamine modification of lipid A and polymyxin resistance in Salmonella enterica', *J Bacteriol*, 186(13), pp. 4124-4133. doi: 10.1128/JB.186.13.4124-4133.2004.

Lee, S., Jung, Y. and Lee, J. (2013) 'Correlations between FAS elongation cycle genes expression and fatty acid production for improvement of long-chain fatty acids in Escherichia coli',*Appl Biochem Biotechnol*, 169(5), pp. 1606-1619. doi: 10.1007/s12010-012-0088-8.

Lennen, R. M., Kruziki, M. A., Kumar, K., Zinkel, R. A., Burnum, K. E., Lipton, M. S. *et al.* (2011) 'Membrane stresses induced by overproduction of free fatty acids in Escherichia coli', *Appl Environ Microbiol*, 77(22), pp. 8114-8128. doi: 10.1128/AEM.05421-11.

Li, S. J. and Cronan, J. E. (1993) 'Growth rate regulation of Escherichia coli acetyl coenzyme A carboxylase, which catalyses the first committed step of lipid biosynthesis', *J Bacteriol*, 175(2), pp. 332-340.

Likić, V. A., McConville, M. J., Lithgow, T. and Bacic, A. (2010) 'Systems biology: the next frontier for bioinformatics', *Adv Bioinformatics*, p. 268925. doi: 10.1155/2010/268925.

Lu, H. and Tonge, P. J. (2008) 'Inhibitors of FabI, an enzyme drug target in the bacterial fatty acid biosynthesis pathway', *Acc Chem Res*, 41(1), pp. 11-20. doi: 10.1021/ar700156e.

Lu, Y. H., Guan, Z., Zhao, J. and Raetz, C. R. (2011) 'Three phosphatidylglycerol-phosphate phosphatases in the inner membrane of Escherichia coli', *J Biol Chem*, 286(7), pp. 5506-5518. doi: 10.1074/jbc.M110.199265.

Ma, B., Reynolds, C. M. and Raetz, C. R. (2008) 'Periplasmic orientation of nascent lipid A in the inner membrane of an Escherichia coli LptA mutant', *Proc Natl Acad Sci U S A*, 105(37), pp. 13823-13828. doi: 10.1073/pnas.0807028105.

Mackie, G. A. (2013) 'RNase E: at the interface of bacterial RNA processing and decay', *Nat Rev Microbiol*, 11(1), pp. 45-57. doi: 10.1038/nrmicro2930.

Magnuson, K., Jackowski, S., Rock, C. O. and Cronan, J. E. (1993) 'Regulation of fatty acid biosynthesis in Escherichia coli', *Microbiol Rev*, 57(3), pp. 522-542.

Magnuson, K., Oh, W., Larson, T. J. and Cronan, J. E. (1992) 'Cloning and nucleotide sequence of the fabD gene encoding malonyl coenzyme A-acyl carrier protein transacylase of Escherichia coli', *FEBS Lett*, 299(3), pp. 262-266.

Mahalakshmi, S., Sunayana, M. R., SaiSree, L. and Reddy, M. (2014) 'yciM is an essential gene required for regulation of lipopolysaccharide synthesis in Escherichia coli', *Mol Microbiol*, 91(1), pp. 145-157. doi: 10.1111/mmi.12452.

Majerus, P. W., Alberts, A. W. and Vagelos, P. R. (1965) 'Acyl carrier protein. An enoyl hydrase specific for acyl carrier protein thioesters', *J Biol Chem*, 240, pp. 618-621.

Maloy, S. R., Ginsburgh, C. L., Simons, R. W. and Nunn, W. D. (1981) 'Transport of long and medium chain fatty acids by Escherichia coli K12', *J Biol Chem*, 256(8), pp. 3735-3742.

Mamat, U., Meredith, T. C., Aggarwal, P., Kühl, A., Kirchhoff, P., Lindner, B. *et al.* (2008) 'Single amino acid substitutions in either YhjD or MsbA confer viability to 3-deoxy-d-manno-oct-2-ulosonic acid-depleted Escherichia coli', *Mol Microbiol*, 67(3), pp. 633-648. doi: 10.1111/j.1365-2958.2007.06074.x.

Mansilla, M. C., Cybulski, L. E., Albanesi, D. and de Mendoza, D. (2004) 'Control of membrane lipid fluidity by molecular thermosensors', *J Bacteriol*, 186(20), pp. 6681-6688. doi: 10.1128/JB.186.20.6681-6688.2004.

Marangoni, A.G. (2003) *Enzyme Kinetics: A Modern Approach*. John Wiley & Sons, New Jersey. doi: 10.1002/0471267295.ch7

Mattsby-Baltzer, I., Lindgren, K., Lindholm, B. and Edebo, L. (1991) 'Endotoxin shedding by enterobacteria: free and cell-bound endotoxin differ in Limulus activity', *Infect Immun*, 59(2),pp. 689-695.

May, R. M. (2004) 'Uses and abuses of mathematics in biology', *Science*, 303(5659), pp. 790-793. doi: 10.1126/science.1094442.

McClerren, A. L., Endsley, S., Bowman, J. L., Andersen, N. H., Guan, Z., Rudolph, J. and Raetz, C. R. (2005) 'A slow, tight-binding inhibitor of the zinc-dependent deacetylase LpxC of lipid A biosynthesis with antibiotic activity comparable to ciprofloxacin', *Biochemistry*, 44(50), pp. 16574-16583. doi: 10.1021/bi0518186.

Mendes, P., Hoops, S., Sahle, S., Gauges, R., Dada, J. and Kummer, U. (2009) 'Computational modeling of biochemical networks using COPASI', *Methods Mol Biol*, 500, pp. 17-59. doi: 10.1007/978-1-59745-525-1_2.

Meng, T. C., Somani, S. and Dhar, P. (2004) 'Modeling and simulation of biological systems with stochasticity', *In Silico Biol*, 4(3), pp. 293-309.

Mengin-Lecreulx, D., Flouret, B. and van Heijenoort, J. (1983) 'Pool levels of UDP N-acetylglucosamine and UDP N-acetylglucosamine-enolpyruvate in Escherichia coli and correlation with peptidoglycan synthesis', *J Bacteriol*, 154(3), pp. 1284-1290.

Meredith, T. C., Aggarwal, P., Mamat, U., Lindner, B. and Woodard, R. W. (2006) 'Redefining the requisite lipopolysaccharide structure in Escherichia coli', *ACS Chem Biol*, 1(1), pp. 33-42. doi: 10.1021/cb0500015.

Metzger, L. E. and Raetz, C. R. (2009) 'Purification and characterization of the lipid A disaccharide synthase (LpxB) from Escherichia coli, a peripheral membrane protein', *Biochemistry*, 48(48), pp. 11559-11571. doi: 10.1021/bi901750f.

Mohan, S., Kelly, T. M., Eveland, S. S., Raetz, C. R. and Anderson, M. S. (1994) 'An Escherichia coli gene (FabZ) encoding (3R)-hydroxymyristoyl acyl carrier protein dehydrase. Relation to fabA and suppression of mutations in lipid A biosynthesis', *J Biol Chem*, 269(52), pp. 32896-32903.

My, L., Rekoske, B., Lemke, J. J., Viala, J. P., Gourse, R. L. and Bouveret, E. (2013) 'Transcription of the Escherichia coli fatty acid synthesis operon fabHDG is directly activated by FadR and inhibited by ppGpp', *J Bacteriol*, 195(16), pp. 3784-3795. doi: 10.1128/JB.00384-13.

Narberhaus, F., Obrist, M., Führer, F. and Langklotz, S. (2009) 'Degradation of cytoplasmic substrates by FtsH, a membrane-anchored protease with many talents', *Res Microbiol*, 160(9),pp. 652-659. doi: 10.1016/j.resmic.2009.08.011.

Nikaido, H. (1996) 'Multidrug efflux pumps of gram-negative bacteria', *J Bacteriol*, 178(20), pp. 5853-5859.

Nikaido, H. (2003) 'Molecular basis of bacterial outer membrane permeability revisited', *Microbiol Mol Biol Rev*, 67(4), pp. 593-656.

Nishijima, M. and Raetz, C. R. (1979) 'Membrane lipid biogenesis in Escherichia coli: identification of genetic loci for phosphatidylglycerophosphate synthetase and construction of mutants lacking phosphatidylglycerol', *J Biol Chem*, 254(16), pp. 7837-7844.

Nunn, W. D. and Simons, R. W. (1978) 'Transport of long-chain fatty acids by Escherichia coli: mapping and characterization of mutants in the fadL gene', *Proc Natl Acad Sci U S A*, 75(7), pp. 3377-3381.

Nunn, W. D., Giffin, K., Clark, D. and Cronan, J. E. (1983) 'Role for fadR in unsaturated fatty acid biosynthesis in Escherichia coli', *J Bacteriol*, 154(2), pp. 554-560.

Ogura, T., Inoue, K., Tatsuta, T., Suzaki, T., Karata, K., Young, K. *et al.* (1999) 'Balanced biosynthesis of major membrane components through regulated degradation of the committed enzyme of lipid A biosynthesis by the AAA protease FtsH (HflB) in Escherichia coli', *Mol Microbiol*, 31(3), pp. 833-844.

Oliver, S. G., Winson, M. K., Kell, D. B. and Baganz, F. (1998) 'Systematic functional analysis of the yeast genome', *Trends Biotechnol*, 16(9), pp. 373-378.

O'Malley, M. A. and Dupré, J. (2005) 'Fundamental issues in systems biology', *Bioessays*, 27(12), pp. 1270-1276. doi: 10.1002/bies.20323.

Onishi, H. R., Pelak, B. A., Gerckens, L. S., Silver, L. L., Kahan, F. M., Chen, M. H. *et al.* (1996) 'Antibacterial agents that inhibit lipid A biosynthesis', *Science*, 274(5289), pp. 980-982.

Orth, J. D., Thiele, I. and Palsson, B. (2010) 'What is flux balance analysis?', *Nat Biotechnol*, 28(3), pp. 245-248. doi: 10.1038/nbt.1614.

Oursel, D., Loutelier-Bourhis, C., Orange, N., Chevalier, S., Norris, V. and Lange, C. M. (2007) 'Identification and relative quantification of fatty acids in Escherichia coli membranes by gas chromatography/mass spectrometry', *Rapid Commun Mass Spectrom*, 21(20), pp. 3229-3233. doi: 10.1002/rcm.3177.

Palsson, B.O. (2006) *Systems Biology: Properties of Reconstructed Networks.* Cambridge University Press New York, NY, USA.

Papp-Wallace, K. M., Endimiani, A., Taracila, M. A. and Bonomo, R. A. (2011) 'Carbapenems: past, present, and future',*Antimicrob Agents Chemother*, 55(11), pp. 4943-4960. doi: 10.1128/AAC.00296-11.

Parrillo, J. E. (1993) 'Pathogenetic mechanisms of septic shock', *N Engl J Med*, 328(20), pp. 1471-1477. doi: 10.1056/NEJM199305203282008.

Paterson, D. L. (2006) 'Resistance in gram-negative bacteria: Enterobacteriaceae', *Am J Infect Control*, 34(5 Suppl 1), pp. S20-28; discussion S64-73. doi: 10.1016/j.ajic.2006.05.238.

Patterson, S. D. and Aebersold, R. H. (2003) 'Proteomics: the first decade and beyond', *Nat Genet*, 33 Suppl, pp. 311-323. doi: 10.1038/ng1106.

Plank, L. D. and Harvey, J. D. (1979) 'Generation time statistics of Escherichia coli B measured by synchronous culture techniques', *J Gen Microbiol*, 115(1), pp. 69-77.

Poole, K. (2001) 'Multidrug resistance in Gram-negative bacteria', *Curr Opin Microbiol*, 4(5), pp. 500-508.

Price, A. C., Choi, K. H., Heath, R. J., Li, Z., White, S. W. and Rock, C. O. (2001) 'Inhibition of beta-ketoacyl-acyl carrier protein synthases by thiolactomycin and cerulenin. Structure and mechanism', *J Biol Chem*, 276(9), pp. 6551-6559. doi: 10.1074/jbc.M007101200.

Price, N. D., Thiele, I. and Palsson, B. (2006) 'Candidate states of Helicobacter pylori's genome-scale metabolic network upon application of "loop law" thermodynamic constraints', *Biophys J*, 90(11), pp. 3919-3928. doi: 10.1529/biophysj.105.072645.

Quinn, J. P. (1998) 'Clinical problems posed by multiresistant nonfermenting gram-negative pathogens', *Clin Infect Dis*, 27 Suppl 1, pp. S117-124.

Radika, K. and Raetz, C. R. (1988) 'Purification and properties of lipid A disaccharide synthase of Escherichia coli', *J Biol Chem*, 263(29), pp. 14859-14867.

Raetz, C. R. (1978) 'Enzymology, genetics, and regulation of membrane phospholipid synthesis in Escherichia coli', *Microbiol Rev*, 42(3), pp. 614-659.

Raetz, C. R. and Whitfield, C. (2002) 'Lipopolysaccharide endotoxins', *Annu Rev Biochem*, 71, pp. 635-700. doi: 10.1146/annurev.biochem.71.110601.135414.

Raetz, C. R., Guan, Z., Ingram, B. O., Six, D. A., Song, F., Wang, X. and Zhao, J. (2009) 'Discovery of new biosynthetic pathways: the lipid A story', *J Lipid Res*, 50 Suppl, pp. S103-108. doi: 10.1194/jlr.R800060-JLR200.

Raetz, C. R., Reynolds, C. M., Trent, M. S. and Bishop, R. E. (2007) 'Lipid A modification systems in gram-negative bacteria', *Annu Rev Biochem*, 76, pp. 295-329. doi: 10.1146/annurev.biochem.76.010307.145803.

Rafi, S. B., Cui, G., Song, K., Cheng, X., Tonge, P. J. and Simmerling, C. (2006) 'Insight through molecular mechanics Poisson-Boltzmann surface area calculations into the binding affinity of triclosan and three analogues for FabI, the E. coli enoyl reductase', *J Med Chem*, 49(15), pp. 4574-4580. doi: 10.1021/jm060222t.

Ray, B. L. and Raetz, C. R. (1987) 'The biosynthesis of gram-negative endotoxin. A novel kinase in Escherichia coli membranes that incorporates the 4'-phosphate of lipid A', *J Biol Chem*, 262(3), pp. 1122-1128.

Ray, P. H., Benedict, C. D. and Grasmuk, H. (1981) 'Purification and characterization of cytidine 5'-triphosphate:cytidine 5'-monophosphate-3-deoxy-D-manno-octulosonate cytidylyltransferase', *J Bacteriol*, 145(3), pp. 1273-1280.

Rees, D. C., Johnson, E. and Lewinson, O. (2009) 'ABC transporters: the power to change', *Nat Rev Mol Cell Biol*, 10(3), pp. 218-227. doi: 10.1038/nrm2646.

Resat, H., Petzold, L. and Pettigrew, M. F. (2009) 'Kinetic modeling of biological systems', *Methods Mol Biol*, 541, pp. 311-335. doi: 10.1007/978-1-59745-243-4_14.

Reynolds, C. M. and Raetz, C. R. (2009) 'Replacement of lipopolysaccharide with free lipid A molecules in Escherichia coli mutants lacking all core sugars', *Biochemistry*, 48(40), pp. 9627-9640. doi: 10.1021/bi901391g.

Ridgway, D., Broderick, G. and Ellison, M. J. (2006) 'Accommodating space, time and randomness in network simulation', *Curr Opin Biotechnol*, 17(5), pp. 493-498. doi: 10.1016/j.copbio.2006.08.004

Roberts, E., Magis, A., Ortiz, J. O., Baumeister, W. and Luthey-Schulten, Z. (2011) 'Noise contributions in an inducible genetic switch: a whole-cell simulation study', *PLoS Comput Biol*, 7(3), p. e1002010. doi: 10.1371/journal.pcbi.1002010.

Rock, C. O., Goelz, S. E. and Cronan, J. E. (1981) 'Phospholipid synthesis in Escherichia coli. Characteristics of fatty acid transfer from acyl-acyl carrier protein to sn-glycerol 3-phosphate', *J Biol Chem*, 256(2), pp. 736-742.

Roy, A. M. and Coleman, J. (1994) 'Mutations in firA, encoding the second acyltransferase in lipopolysaccharide biosynthesis, affect multiple steps in lipopolysaccharide biosynthesis', *J Bacteriol*, 176(6), pp. 1639-1646.

Royce, L. A., Liu, P., Stebbins, M. J., Hanson, B. C. and Jarboe, L. R. (2013) 'The damaging effects of short chain fatty acids on Escherichia coli membranes', *Appl Microbiol Biotechnol*, 97(18), pp. 8317-8327. doi: 10.1007/s00253-013-5113-5.

Ruiz, N., Gronenberg, L. S., Kahne, D. and Silhavy, T. J. (2008) 'Identification of two inner-membrane proteins required for the transport of lipopolysaccharide to the outer membrane of Escherichia coli', *Proc Natl Acad Sci U S A*, 105(14), pp. 5537-5542. doi: 10.1073/pnas.0801196105.

Rutten, L., Geurtsen, J., Lambert, W., Smolenaers, J. J., Bonvin, A. M., de Haan, A. *et al.* (2006) 'Crystal structure and catalytic mechanism of the LPS 3-O-deacylase PagL from Pseudomonas aeruginosa', *Proc Natl Acad Sci U S A*, 103(18), pp. 7071-7076. doi: 10.1073/pnas.0509392103.

Sanft, K. R., Wu, S., Roh, M., Fu, J., Lim, R. K. and Petzold, L. R. (2011) 'StochKit2: software for discrete stochastic simulation of biochemical systems with events', *Bioinformatics*, 27(17), pp. 2457-2458. doi: 10.1093/bioinformatics/btr401.

Schäkermann, M., Langklotz, S. and Narberhaus, F. (2013) 'FtsH-Mediated Coordination of Lipopolysaccharide Biosynthesis in Escherichia coli Correlates with the Growth Rate and the Alarmone (p)ppGpp', *J Bacteriol*, 195(9), pp. 1912-1919. doi: 10.1128/JB.02134-12.

Schena, M., Shalon, D., Davis, R. W. and Brown, P. O. (1995) 'Quantitative monitoring of gene expression patterns with a complementary DNA microarray', *Science*, 270(5235), pp. 467-470.

Schlame, M., Brody, S. and Hostetler, K. Y. (1993) 'Mitochondrial cardiolipin in diverse eukaryotes. Comparison of biosynthetic reactions and molecular acyl species', *Eur J Biochem*, 212(3), pp. 727-735.

Schomburg, I., Chang, A., Ebeling, C., Gremse, M., Heldt, C., Huhn, G. and Schomburg, D. (2004) 'BRENDA, the enzyme database: updates and major new developments',*Nucleic Acids Res*, 32(Database issue), pp. D431-433. doi: 10.1093/nar/gkh081.

Shih, Y. H. and Whitesides, G. M. (1977) 'Large-scale ATP-requiring enzymatic phosphorylation of creatine can be driven by enzymatic ATP regeneration', *J Org Chem*, 42(25), pp. 4165-4166.

Silhavy, T. J., Kahne, D. and Walker, S. (2010) 'The bacterial cell envelope', *Cold Spring Harb Perspect Biol*, 2(5), p. a000414. doi: 10.1101/cshperspect.a000414.

Simons, R. W., Egan, P. A., Chute, H. T. and Nunn, W. D. (1980) 'Regulation of fatty acid degradation in Escherichia coli: isolation and characterization of strains bearing insertion and temperature-sensitive mutations in gene fadR', *J Bacteriol*, 142(2), pp. 621-632.

Six, D. A., Carty, S. M., Guan, Z. and Raetz, C. R. (2008) 'Purification and mutagenesis of LpxL, the lauroyltransferase of Escherichia coli lipid A biosynthesis', *Biochemistry*, 47(33), pp. 8623-8637. doi: 10.1021/bi800873n.

Slomińska, M., Neubauer, P. and Wegrzyn, G. (1999) 'Regulation of bacteriophage lambda development by guanosine 5'-diphosphate-3'-diphosphate', *Virology*, 262(2), pp. 431-441. doi: 10.1006/viro.1999.9907.

Smallbone, K., Simeonidis, E., Broomhead, D. S. and Kell, D. B. (2007) 'Something from nothing: bridging the gap between constraint-based and kinetic modelling', *FEBS J*, 274(21), pp. 5576-5585. doi: 10.1111/j.1742-4658.2007.06076.x.

Sorensen, P. G., Lutkenhaus, J., Young, K., Eveland, S. S., Anderson, M. S. and Raetz, C. R. (1996) 'Regulation of UDP-3-O-[R-3-hydroxymyristoyl]-N-acetylglucosamine deacetylase in Escherichia coli. The second enzymatic step of lipid a biosynthesis', *J Biol Chem*, 271(42), pp. 25898-25905.

Sperandeo, P., Cescutti, R., Villa, R., Di Benedetto, C., Candia, D., Dehò, G. and Polissi, A. (2007) 'Characterization of lptA and lptB, two essential genes implicated in

lipopolysaccharide transport to the outer membrane of Escherichia coli', *J Bacteriol*, 189(1), pp. 244-253. doi: 10.1128/JB.01126-06.

Sperandeo, P., Lau, F. K., Carpentieri, A., De Castro, C., Molinaro, A., Dehò, G. *et al.* (2008) 'Functional analysis of the protein machinery required for transport of lipopolysaccharide to the outer membrane of Escherichia coli', *J Bacteriol*, 190(13), pp. 4460-4469. doi: 10.1128/JB.00270-08.

Stiles, J. R., Van Helden, D., Bartol, T. M., Salpeter, E. E. and Salpeter, M. M. (1996) 'Miniature endplate current rise times less than 100 microseconds from improved dual recordings can be modeled with passive acetylcholine diffusion from a synaptic vesicle', *Proc Natl Acad Sci U S A*, 93(12), pp. 5747-5752.

Subrahmanyam, S. and Cronan, J. E. (1998) 'Overproduction of a functional fatty acid biosynthetic enzyme blocks fatty acid synthesis in Escherichia coli', *J Bacteriol*, 180(17), pp. 4596-4602.

Sun, Y. H., Cheng, Q., Tian, W. X. and Wu, X. D. (2008) 'A substitutive substrate for measurements of beta-ketoacyl reductases in two fatty acid synthase systems', *J Biochem Biophys Methods*, 70(6), pp. 850-856. doi: 10.1016/j.jbbm.2007.10.005.

Sundararaj, S., Guo, A., Habibi-Nazhad, B., Rouani, M., Stothard, P., Ellison, M. and Wishart, D. S. (2004) 'The CyberCell Database (CCDB): a comprehensive, self-updating, relational database to coordinate and facilitate in silico modeling of Escherichia coli', *Nucleic Acids Res*, 32(Database issue), pp. D293-295. doi: 10.1093/nar/gkh108.

Székely, T. and Burrage, K. (2014) 'Stochastic simulation in systems biology', *Comput Struct Biotechnol J*, 12(20-21), pp. 14-25. doi: 10.1016/j.csbj.2014.10.003.

Takayama, K., Qureshi, N., Mascagni, P., Anderson, L. and Raetz, C. R. (1983) 'Glucosamine-derived phospholipids in Escherichia coli. Structure and chemical modification of a triacyl glucosamine 1-phosphate found in a phosphatidylglycerol-deficient mutant', *J Biol Chem*, 258(23), pp. 14245-14252.

Taneja, R., Malik, U. and Khuller, G. K. (1979) 'Effect of growth temperature on the lipid composition of Mycobacterium smegmatis ATCC 607', *J Gen Microbiol*, 113(2), pp. 413-416.

Taniguchi, Y., Choi, P. J., Li, G. W., Chen, H., Babu, M., Hearn, J. *et al.* (2010) 'Quantifying E. coli proteome and transcriptome with single-molecule sensitivity in single cells',*Science*, 329(5991), pp. 533-538. doi: 10.1126/science.1188308.

Tatsuta, T., Tomoyasu, T., Bukau, B., Kitagawa, M., Mori, H., Karata, K. and Ogura, T. (1998) 'Heat shock regulation in the ftsH null mutant of Escherichia coli: dissection of stability and activity control mechanisms of sigma32 in vivo', *Mol Microbiol*, 30(3), pp. 583-593.

Taylor, F. and Cronan, J. E. (1976) 'Selection and properties of Escherichia coli mutants defective in the synthesis of cyclopropane fatty acids', *J Bacteriol*, 125(2), pp. 518-523.

Taylor, F. R. and Cronan, J. E. (1979) 'Cyclopropane fatty acid synthase of Escherichia coli. Stabilization, purification, and interaction with phospholipid vesicles',*Biochemistry*, 18(15), pp. 3292-3300.

Toomey, R. E. and Wakil, S. J. (1966) 'Studies on the mechanism of fatty acid synthesis. XV. Preparation and general properties of beta-ketoacyl acyl carrier protein reductase from Escherichia coli', *Biochim Biophys Acta*, 116(2), pp. 189-197.

Traxler, M. F., Summers, S. M., Nguyen, H. T., Zacharia, V. M., Hightower, G. A., Smith, J. T. and Conway, T. (2008) 'The global, ppGpp-mediated stringent response to amino acid starvation in Escherichia coli', *Mol Microbiol*, 68(5), pp. 1128-1148. doi: 10.1111/j.1365-2958.2008.06229.x.

Trent, M. S., Ribeiro, A. A., Lin, S., Cotter, R. J. and Raetz, C. R. (2001) 'An inner membrane enzyme in Salmonella and Escherichia coli that transfers 4-amino-4-deoxy-L-arabinose to lipid A: induction on polymyxin-resistant mutants and role of a novel lipid-linked donor', *J Biol Chem*, 276(46), pp. 43122-43131. doi: 10.1074/jbc.M106961200.

Tsay, J. T., Oh, W., Larson, T. J., Jackowski, S. and Rock, C. O. (1992) 'Isolation and characterization of the beta-ketoacyl-acyl carrier protein synthase III gene (fabH) from Escherichia coli K-12', *J Biol Chem*, 267(10), pp. 6807-6814.

Tyson, J. J., Chen, K. and Novak, B. (2001) 'Network dynamics and cell physiology', *Nat Rev Mol Cell Biol*, 2(12), pp. 908-916. doi: 10.1038/35103078.

van Riel, N. A. (2006) 'Dynamic modelling and analysis of biochemical networks: mechanism-based models and model-based experiments', *Brief Bioinform*, 7(4), pp. 364-374. doi: 10.1093/bib/bbl040.

Vigh, L., Maresca, B. and Harwood, J. L. (1998) 'Does the membrane's physical state control the expression of heat shock and other genes?', *Trends Biochem Sci*, 23(10), pp. 369-374.

Vorachek-Warren, M. K., Carty, S. M., Lin, S., Cotter, R. J. and Raetz, C. R. (2002b) 'An Escherichia coli mutant lacking the cold shock-induced palmitoleoyltransferase of lipid A biosynthesis: absence of unsaturated acyl chains and antibiotic hypersensitivity at 12 degrees C', *J Biol Chem*, 277(16), pp. 14186-14193. doi: 10.1074/jbc.M200408200.

Vorachek-Warren, M.K., Ramirez, S., Cotter, R.J. and Raetz, C.R. (2002a) ‘A triple mutant of Escherichia coli lacking secondary acyl chains on lipid A’, *J Biol Chem.*, 277(16), pp. 14194-14205.

Wahl, A., My, L., Dumoulin, R., Sturgis, J. N. and Bouveret, E. (2011) 'Antagonistic regulation of dgkA and plsB genes of phospholipid synthesis by multiple stress responses in Escherichia coli', *Mol Microbiol*, 80(5), pp. 1260-1275. doi: 10.1111/j.1365-2958.2011.07641.x.

Walker, S. L., Redman, J. A. and Elimelech, M. (2004) 'Role of Cell Surface Lipopolysaccharides in Escherichia coli K12 adhesion and transport', *Langmuir*, 20(18), pp. 7736-7746. doi: 10.1021/la049511f.

Walsh, C.T. and Wencewicz, T.A. (2014) ‘Prospects for new antibiotics: a molecule-centered perspective’, *J Antibiot.*, 67(1), pp. 7-22. doi: 10.1038/ja.2013.49.

Wang, X. and Quinn, P. J. (2010) 'Lipopolysaccharide: Biosynthetic pathway and structure modification', *Prog Lipid Res*, 49(2), pp. 97-107. doi: 10.1016/j.plipres.2009.06.002.

Warren, H. S., Kania, S. A. and Siber, G. R. (1985) 'Binding and neutralization of bacterial lipopolysaccharide by colistin nonapeptide', *Antimicrob Agents Chemother*, 28(1),pp. 107-112.

Weeks, G. and Wakil, S. J. (1968) 'Studies on the mechanism of fatty acid synthesis. 18. Preparation and general properties of the enoyl acyl carrier protein reductases from Escherichia coli', *J Biol Chem*, 243(6), pp. 1180-1189.

Weimar, J. D., DiRusso, C. C., Delio, R. and Black, P. N. (2002) 'Functional role of fatty acyl-coenzyme A synthetase in the transmembrane movement and activation of exogenous long-chain fatty acids. Amino acid residues within the ATP/AMP signature motif of Escherichia coli FadD are required for enzyme activity and fatty acid transport', *J Biol Chem*, 277(33), pp. 29369-29376. doi: 10.1074/jbc.M107022200.

Whitfield, C. and Trent, M. S. (2014) 'Biosynthesis and export of bacterial lipopolysaccharides', *Annu Rev Biochem*, 83, pp. 99-128. doi: 10.1146/annurev-biochem-060713-035600.

Wilkinson, D. J. (2009) 'Stochastic modelling for quantitative description of heterogeneous biological systems', *Nat Rev Genet*, 10(2), pp. 122-133. doi: 10.1038/nrg2509.

Wilks, J. C. and Slonczewski, J. L. (2007) 'pH of the cytoplasm and periplasm of Escherichia coli: rapid measurement by green fluorescent protein fluorimetry', *J Bacteriol*, 189(15), pp. 5601-5607. doi: 10.1128/JB.00615-07.

Wright, B. G. and Rebers, P. A. (1972) 'Procedure for determining heptose and hexose in lipopolysaccharides. Modification of the cysteine-sulfuric acid method', *Anal Biochem*, 49(2), pp. 307-319.

Wu, T., McCandlish, A. C., Gronenberg, L. S., Chng, S. S., Silhavy, T. J. and Kahne, D. (2006) 'Identification of a protein complex that assembles lipopolysaccharide in the outer membrane of Escherichia coli', *Proc Natl Acad Sci U S A*, 103(31), pp. 11754-11759. doi: 10.1073/pnas.0604744103.

Wyckoff, T. J. and Raetz, C. R. (1999) 'The active site of Escherichia coli UDP-N-acetylglucosamine acyltransferase. Chemical modification and site-directed mutagenesis', *J Biol Chem*, 274(38), pp. 27047-27055.

Xu, H. H., Real, L. and Bailey, M. W. (2006) 'An array of Escherichia coli clones over-expressing essential proteins: a new strategy of identifying cellular targets of potent antibacterial compounds', *Biochem Biophys Res Commun*, 349(4), pp. 1250-1257. doi: 10.1016/j.bbrc.2006.08.166.

Yao, Z., Davis, R. M., Kishony, R., Kahne, D. and Ruiz, N. (2012) 'Regulation of cell size in response to nutrient availability by fatty acid biosynthesis in Escherichia coli', *Proc Natl Acad Sci U S A*, 109(38), pp. E2561-2568. doi: 10.1073/pnas.1209742109.

Yokota, K., Kanamoto, R. and Kito, M. (1980) 'Composition of cardiolipin molecular species in Escherichia coli', *J Bacteriol*, 141(3), pp. 1047-1051.

Yokoyama, K., Yamamoto, Y., Kudo, F. and Eguchi, T. (2008) 'Involvement of two distinct N-acetylglucosaminyltransferases and a dual-function deacetylase in neomycin biosynthesis',*Chembiochem*, 9(6), pp. 865-869. doi: 10.1002/cbic.200700717.

Yoshimura, M., Oshima, T. and Ogasawara, N. (2007) 'Involvement of the YneS/YgiH and PlsX proteins in phospholipid biosynthesis in both Bacillus subtilis and Escherichia coli', *BMC Microbiol*, 7, p. 69. doi: 10.1186/1471-2180-7-69.

Young, K., Silver, L. L., Bramhill, D., Cameron, P., Eveland, S. S., Raetz, C. R. *et al.* (1995) 'The envA permeability/cell division gene of Escherichia coli encodes the second enzyme of lipid A biosynthesis. UDP-3-O-(R-3-hydroxymyristoyl)-N-acetylglucosamine deacetylase', *J Biol Chem*, 270(51), pp. 30384-30391.

Yu, X., Liu, T., Zhu, F. and Khosla, C. (2011) 'In vitro reconstitution and steady-state analysis of the fatty acid synthase from Escherichia coli', *Proc Natl Acad Sci U S A*, 108(46), pp. 18643-18648. doi: 10.1073/pnas.1110852108.

Yus, E., Maier, T., Michalodimitrakis, K., van Noort, V., Yamada, T., Chen, W. H. *et al.* (2009) 'Impact of genome reduction on bacterial metabolism and its regulation', *Science*, 326(5957), pp. 1263-1268. doi: 10.1126/science.1177263.

Zeng, D., Zhao, J., Chung, H. S., Guan, Z., Raetz, C. R. and Zhou, P. (2013) 'Mutants resistant to LpxC inhibitors by rebalancing cellular homeostasis', *J Biol Chem*, 288(8), pp. 5475-5486. doi: 10.1074/jbc.M112.447607.

Zhang, F., Ouellet, M., Batth, T. S., Adams, P. D., Petzold, C. J., Mukhopadhyay, A. and Keasling, J. D. (2012) 'Enhancing fatty acid production by the expression of the regulatory transcription factor FadR', *Metab Eng*, 14(6), pp. 653-660. doi: 10.1016/j.ymben.2012.08.009.

Zhang, Y. and Cronan, J. E. (1998) 'Transcriptional analysis of essential genes of the Escherichia coli fatty acid biosynthesis gene cluster by functional replacement with the analogous Salmonella typhimurium gene cluster', *J Bacteriol*, 180(13), pp. 3295-3303.

Zhang, Y. M. and Rock, C. O. (2008) 'Membrane lipid homeostasis in bacteria', *Nat Rev Microbiol*, 6(3), pp. 222-233. doi: 10.1038/nrmicro1839.

Zhang, Y. M., Marrakchi, H. and Rock, C. O. (2002) 'The FabR (YijC) transcription factor regulates unsaturated fatty acid biosynthesis in Escherichia coli', *J Biol Chem*, 277(18), pp. 15558-15565. doi: 10.1074/jbc.M201399200.

Zhang, Y. M., White, S. W. and Rock, C. O. (2006) 'Inhibiting bacterial fatty acid synthesis', *J Biol Chem*, 281(26), pp. 17541-17544. doi: 10.1074/jbc.R600004200.

Zhang, Y. M., Wu, B., Zheng, J. and Rock, C. O. (2003) 'Key residues responsible for acyl carrier protein and beta-ketoacyl-acyl carrier protein reductase (FabG) interaction', *J Biol Chem*, 278(52), pp. 52935-52943. doi: 10.1074/jbc.M309874200.

Zhou, Z., White, K. A., Polissi, A., Georgopoulos, C. and Raetz, C. R. (1998) 'Function of Escherichia coli MsbA, an essential ABC family transporter, in lipid A and phospholipid biosynthesis', *J Biol Chem*, 273(20), pp. 12466-12475.

Zhu, K., Zhang, Y. M. and Rock, C. O. (2009) 'Transcriptional regulation of membrane lipid homeostasis in Escherichia coli', *J Biol Chem*, 284(50), pp. 34880-34888. doi: 10.1074/jbc.M109.068239.

Appendices

APPENDIX 1 – GCMS chromatograms

1.1 Fatty acids biosynthetic mutant strains

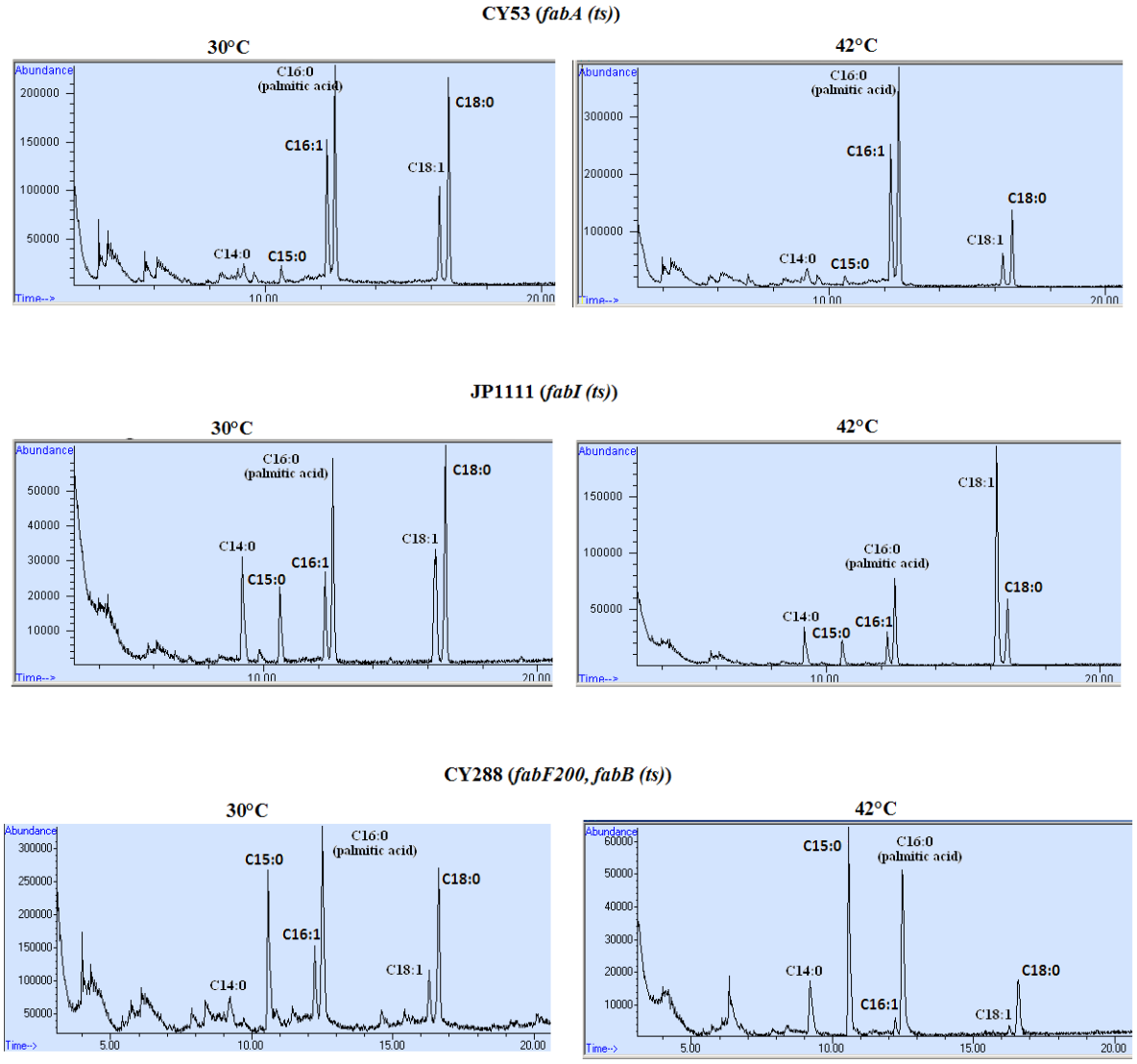

Figure S1. Chromatograms of temperature-sensitive *E. coli* mutants. Fatty acid extraction and analysis were conducted as described in Fig. 5.2. These chromatograms presented herein also formed part of the data used to generate Fig. 5.2. Fatty acids notation are C14:0, myristic acid; C15:0, pentadecanoic acid; C16:1, palmitoleic acid; C16:0, palmitic acid; C18:1, *cis*-vaccenic acid; C18:0, stearic acid.

In the chromatograms presented in Fig. S1, the values on the Y-axis scale differ substantially between isogenic strains grown at 30°C and 42°C. This is understandable given that varying amount of sample would be expected to be lost during the fatty acid extraction process. In this regard, researchers usually include internal standards during sample preparations. Nevertheless, internal standards are particularly important when absolute quantification (such as in microgram or nanogram units) of the metabolites are essential. However, for semi-quantitative or qualitative studies such as this research, representing the data as relative percentages are commonly adopted. These may include representing peaks relative to a another peak (Yu *et al.*, 2011), or representing a peak relative to the total peaks as was employed in this study (Goelz and Cronan, 1980; Clark *et al.*, 1983; Kurkiewicz *et al.*, 2003; Oursel *et al.*, 2007).

1.2 *ftsH* knockout mutant

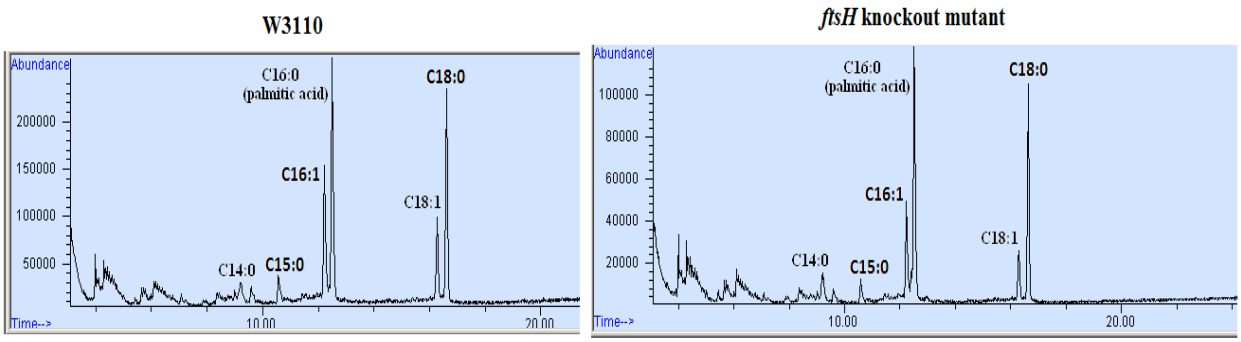

Figure S2. Fatty acids chromatogram of wild-tpye and *ftsH* knockout mutants. Cells were grown at 30°C to mid-log phase prior to harvesting. Fatty acids extraction and GCMS analysis were performed as described in Chapter 4. Fatty acids notation are same as Fig. S1.

As stated previously in the main text (section 3.1), *ftsH* knockout mutants are only viable when a suppressor mutation is present in the *fabZ* gene which subsequently leads to a hyperactive FabZ protein. Due to the lack of a functional FtsH protease, LpxC is stabilized. Results presented in Chapter 3 and Fig. 3.2 implies that when FabZ is overexpressed, SFAs are increased; however, the results in Fig. S2 above do not indicate a significant difference in SFAs level relative to wild-type (W3110). Thus, it is plausible that the increased concentration of LpxC effectively shunts β-hydroxymyristoyl-ACP into the LPS pathway which otherwise would have been used for SFAs synthesis. In support of this, *ftsH* knockout mutants are characterized with 20% increased LPS relative to wild-type (Ogura *et al.*, 1999).

1.3 Electron Ionization (EI) mass spectra

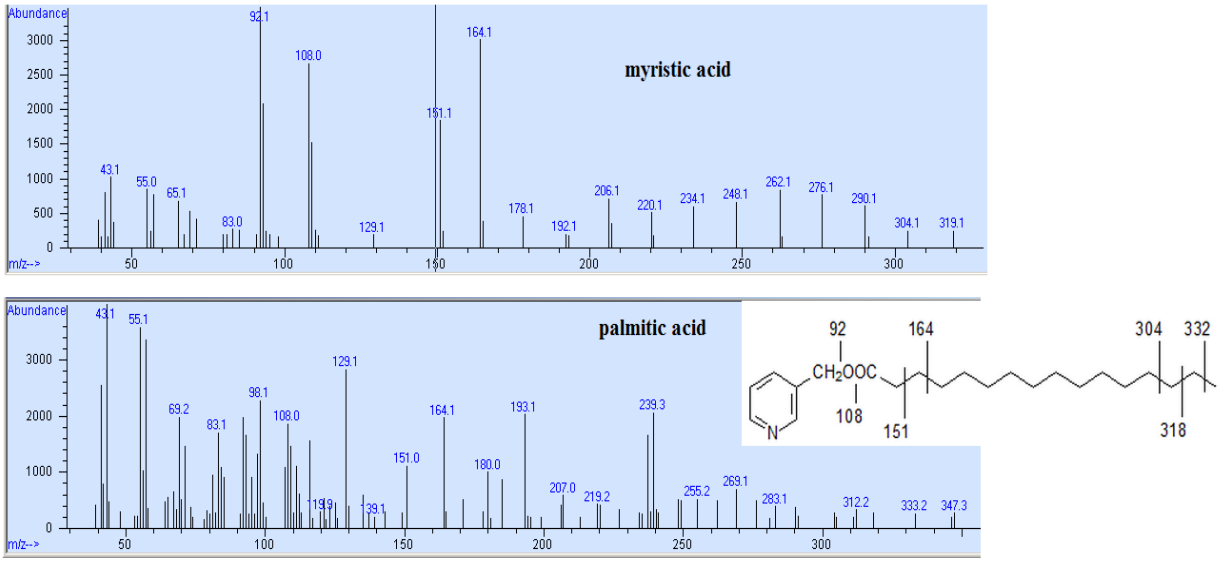

Figure S3. Mass spectra for myristic (C14:0) and palmitic acid (C16:0). This figure represents a typical spectra obtainable from picolinyl ester derivatives (Christie, 1989)[†]. The *inset* in the lower figure represents the points of cleavage in the picolinyl ester of palmitic acid that resulted in the ions of the spectra. In addition to identification using characteristic EI spectra, fatty acids were further confirmed using known standards.

Table S1: Retention time of picolinyl esters of fatty acids

Fatty acids	**Retention time (min)**
Myristic acid (C14:0)	9.2
Pentadecanoic acid (C15:0)	10.6
Palmitoleic acid (C16:1)	12.2
Palmitic acid (C16:0)	12.5
cis-vaccenic acid (C18:1)	16.3
stearic acid (C18:0)	16.6

[†] Christie, W.W. (1989) *Gas Chromatography and Lipids*. Oily Press Ltd., Ayr.

APPENDIX 2 – Lipid A regulation

2.1 LpxC proteolysis

As stated previously (Chapter 5, Fig. 5.6), LpxC was rapidly degraded when cell lysates were treated with palmitic acid. LpxC degradation did not occur when the reaction mixture contained 2.5 mM of EDTA which confirmed the protease responsible was a metalloprotease (Fig. 5.6). However, when the standard laboratory concentration of EDTA (1 mM) commonly used to inhibit metalloproteases was utilized, it had no effect on this protease under palmitic acid conditions (Fig. S4).

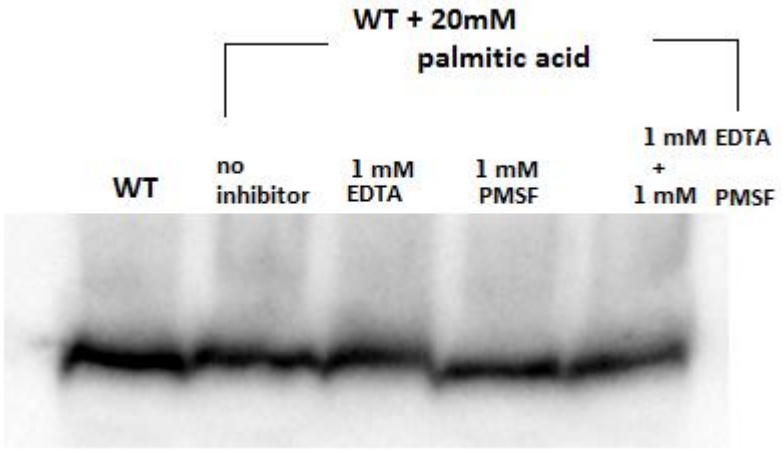

Figure S4. *In vitro* LpxC proteolysis under palmitic acid conditions. *E. coli* W3110 strain (wild-type) containing a plasmid bearing *lpxC* gene was grown at 30°C in the presence of 0.1% arabinose to induce protein expression. Cells were harvested at mid-log phase, re-suspended in Tris-HCl pH 8.0 (without EDTA) and lysed via sonication. The lysates were added to tubes containing various concentrations of palmitic acid and EDTA and PMSF were included to inhibit metalloproteases and serine proteases respectively. Samples were incubated for 10 min at 30°C. Sample buffer was added immediately after incubation and heated for 5 min prior to Western blot analysis.

Additional characterization of this protease was conducted *in vivo. E. coli ftsH* knockout mutant cells treated with either PMSF or sodium arsenate had no effect on LpxC stability (Fig. S5). Whilst PMSF is known to inhibit serine proteases, sodium arsenate inhibits ATP-dependent proteases *in vivo* (Katz and Ron, 2008).

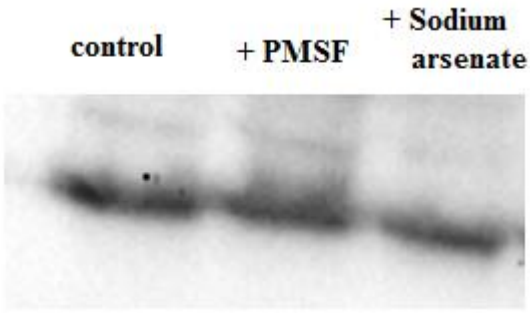

Figure S5. LpxC proteolysis in an *ftsH* knockout mutant *in vivo*. Cells were grown in LB broth to an OD_{600} of 0.5 and cultures were split into different tubes. 2.5 mM PMSF and 20 mM sodium arsenate were added for 5 min prior to the addition of 200 µg/ml of chloramphenicol to block protein expression. After 30 min, the cells were shock-frozen in liquid Nitrogen and thereafter, allowed to thaw on ice prior to Western blot analysis.

Although LpxC is rapidly degraded at lower temperatures (Schakermann *et al.,* 2013), the steady state concentrations remain the same at both low and high temperatures (Fig. S6). This indicates that the LpxC synthesis and degradation ratio is crucial in the bacterial metabolism.

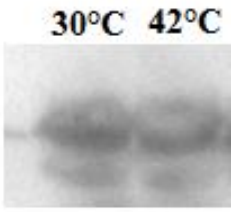

Figure S6. The steady-state concentrations of wild-type LpxC are similar at 30 and 42°C. Cells were prepared as described previously in Chapter 4.

2.1 WaaA regulation

Light microscopy data of cells overexpressing *waaA* did not provide any qualitative information regarding the structural integrity of the membrane or cell (Fig. S7). This is in contrast to *E. coli* overexpressing *lpxC* in which the cells were characterized with elongated cell filament which was observable under the light microscope (Fuhrer *et al.*, 2007). Therefore, the effect of uncontrolled *waaA* synthesis on the bacterial membrane would be best visualized using an electron microscope.

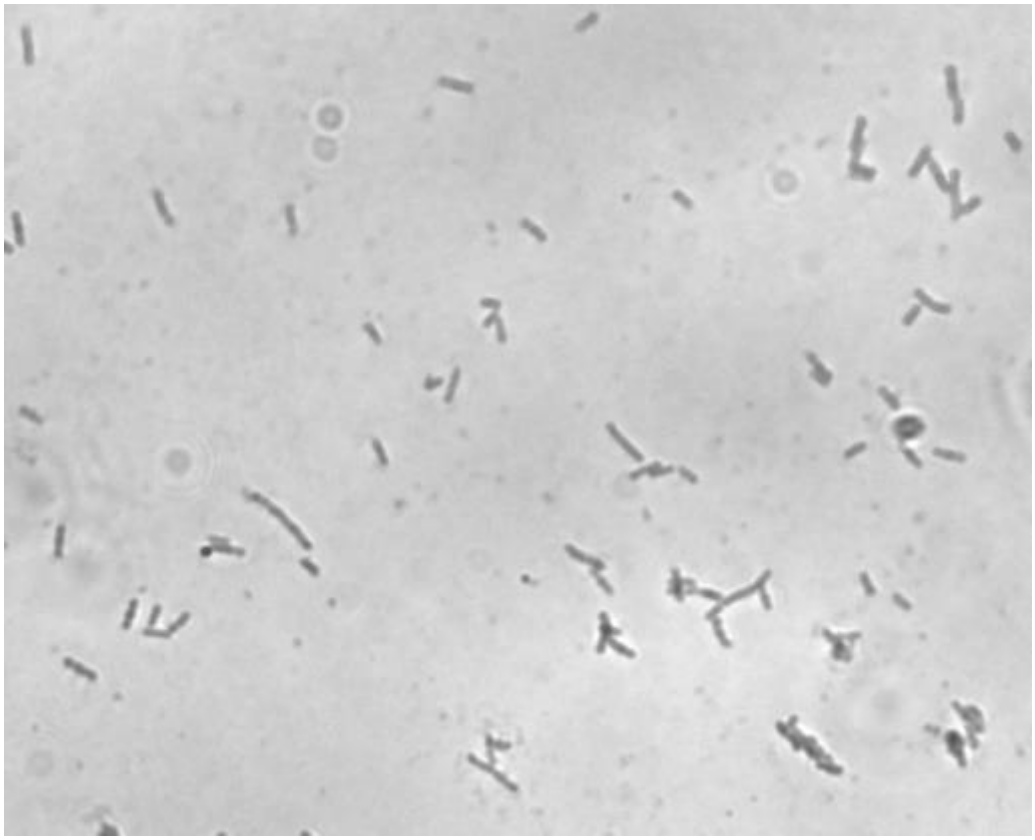

Figure S7. Microscopy of cells overexpressing *waaA*. Cells from an overnight culture were grown in fresh LB broth in the presence of 0.1 mM IPTG until an OD_{600} of 0.5. Cells were visualized using a Nikon microscope.

APPENDIX 3 – Model overview

Initial model created using stochastic methods (with Stochkit) indicated that including '*noise*' in the simulations were unnecessary due to the high copies of lipid A molecules produced per generation time (Fig. S8). As a result, the use of deterministic simulation throughout this research was justified.

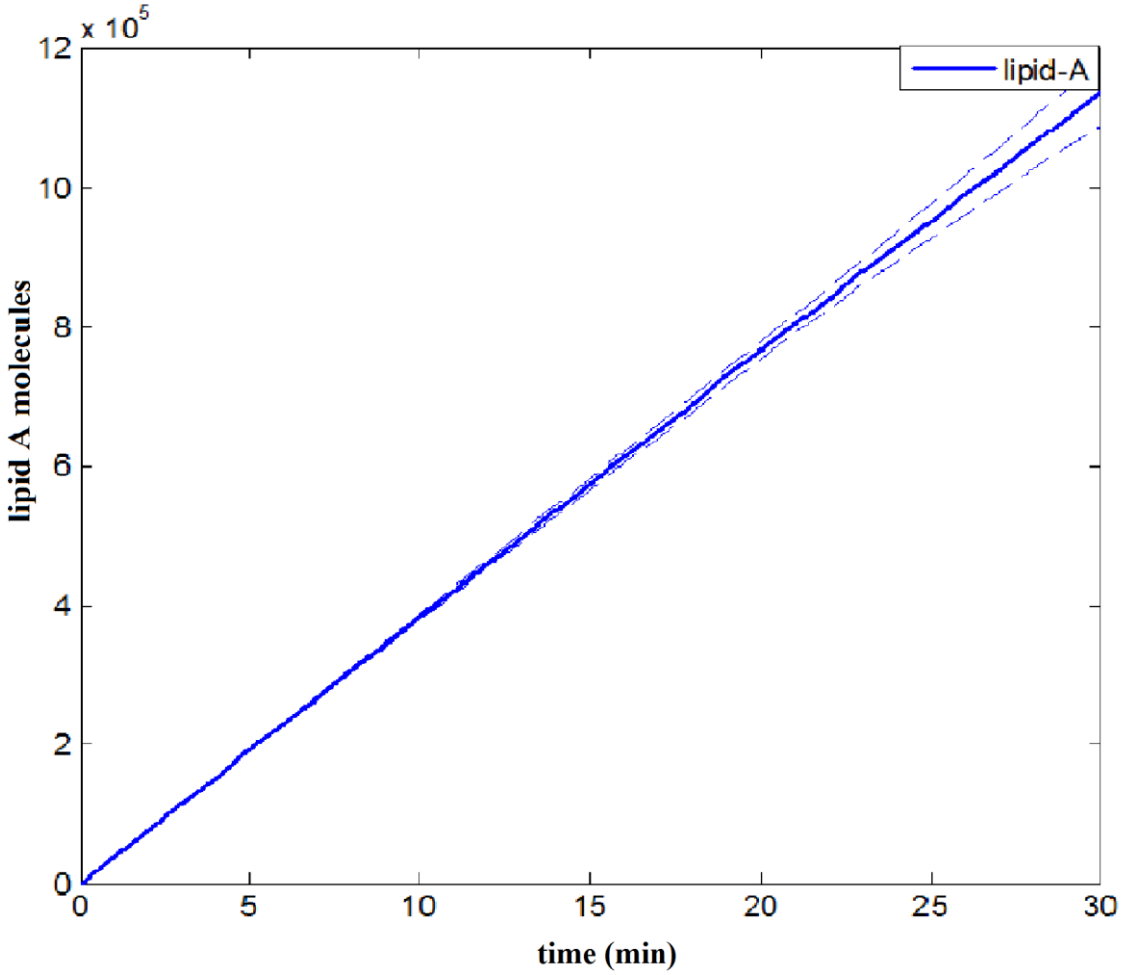

Figure S8. Stochastic simulation for lipid A biosynthesis in *E. coli* using Stochkit software. Simulation parameters were same as those described in Table 2.1. This figure is representative of 100 realizations or runs.

Table S2: Annotation/definition of species nomenclature used in the COPASI file

species name in COPASI file	actual scientific notation and/or definitions
acetyl-CoA	acetyl-CoA
ACP	Acyl-carrier protein (ACP)
Beta-hydroxymyristoylACP	β-hydroxymyristoyl-ACP
B-OH-10	β-hydroxydecenoyl-ACP
B-OH-12	β-hydroxydodecenoyl-ACP
B-OH-12:1	β-hydroxy-*cis*-5-dodecenoyl-ACP
B-OH-14:1	β-hydroxy-*cis*-7-tetradecenoyl-ACP
B-OH-16	β-hydroxypalmitoyl-ACP
B-OH-16:1	β-hydroxy-*cis*-9-hexadecenoyl-ACP
B-OH-18:1	β-hydroxy-*cis*-vacc-11-enoyl-ACP
C10	decanoyl-ACP
C10:1	*cis*-3-decenoyl-ACP
C12	dodecanoyl-ACP
C12:1	*cis*-5-dodecenoyl-ACP
C14	myristoyl-ACP
C14:1	*cis*-7-tetradecenoyl-ACP
C16	palmitoyl-ACP
C16:1	palmitoleoyl-ACP
C18:1	*cis*-vaccenoyl-ACP
CMP-KDO	CMP-Kdo
FabA	FabA
FabB	FabB
FabF	FabF
FabG	FabG
FabH	FabH

FabI	FabI
FabR	inactive FabR
FabR*	activated FabR
FabZ	FabZ
FadR	inactive FadR
FadR*	active FadR
FadR/proA	FadR that is bound to the *fabA* DNA i.e. active *fabA* promoter
FadR/proB	FadR that is bound to the *fabB* DNA i.e. active *fabB* promoter
FtsH	inactive FtsH
FtsH_act_kdta	activated FtsH for the degradation of WaaA
FtsH_act_lpxc	activated FtsH for the degradation of LpxC
G3P	glycerol-3-phosphate
inact_proA1	inactive *fabA* promoter resulting from FabR binding to DNA
inact_proA2	inactive *fabA* promoter resulting from FabR bound to DNA with prior FadR binding
inact_proB1	inactive *fabB* promoter resulting from FabR binding to DNA
inact_proB2	inactive *fabB* promoter resulting from FabR bound to DNA with prior FadR binding
KdtA	WaaA (formerly known as KdtA)
ketoacyl-12	3-oxo-dodecenoyl-ACP
ketoacyl-12:1	3-oxo-*cis*-5-dodecenoyl-ACP
ketoacyl-14	3-oxo tetradecenoyl-ACP
ketoacyl-14:1	3-oxo-*cis*-7-tetradecenoyl-ACP
ketoacyl-16	3-oxo hexadecenoyl-ACP

ketoacyl-16:1	3-oxo-*cis*-9-hexadecenoyl-ACP
ketoacyl-18:1	3-oxo-cis-vacc-11-enoyl-ACP
lipidA	Kdo_2-Lipid A (Lipid A in the inner membrane prior to being translocated by MsbA)
lipidA_OM	lipid A in the outer membrane
lipidA_un	undesirable lipid A resulting from additional glycosylation of lipid A by WaaA
lipidAdisaccharide	lipid A disaccharide
LpxA	LpxA
LpxB	LpxB
LpxC	LpxC
LpxD	LpxD
LpxH	LpxH
LpxK	inactive LpxK
LpxK_act	LpxK that has been catalytically activated by UFAs
LpxL	LpxL
LpxM	LpxM
MsbA	MsbA
P1	UDP-3-O-(β-hydroxymyristoyl)-Nac
P2	UDP-3-O-(β-hydroxymyristoyl)-D-glucosamine
P3	UDP-2,3-bis(β-hydroxymyristoyl)-D-glucosamine
P4	lipid X
P6	lipid IV_A
P7	Kdo_2-Lipid IV_A
P8	lauroyl-Kdo_2-Lipid IV_A
Palmitic	palmitic acid in phospholipids
Palmitoleic	palmitoleic acid in phospholipids
PlsB	PlsB

PlsC	PlsC
proA	regulated promoter of the *fabA* gene
proA_unreg	constitutive promoter of *fabA* gene
proB	regulated promoter of the *fabB* gene
proB_unreg	constitutive promoter of *fabB* gene
promoter-KdtA	the promoter of *waaA*
promoter-LpxC	the promoter of *lpxC*
trans-10	*trans*-2-decenoyl-ACP
trans-12	*trans*-2-dodecenoyl-ACP
trans-12:1	*trans*-3-*cis*-5-dodecenoyl-ACP
trans-14	*trans*-2-tetradecenoyl-ACP
trans-14:1	*trans*-3-*cis*-7-tetradecenoyl-ACP
trans-16	*trans*-2-hexadecenoyl-ACP
trans-16:1	*trans*-3-*cis*-9-hexadecenoyl-ACP
trans-18:1	(2-*trans*-11-*cis*)-vaccen-2-enoyl-ACP
UDP-GlcNac	UDP-N-acetylglucosamine
Vaccenic	*cis*-vaccenic acid in phospholipids

Table S3: Chemical reactions in the COPASI file and their definitions

No	Reaction name	Reaction	Definitions
1	LpxA_forward	UDP-GlcNac + Beta-hydroxymyristoylACP -> P1 + ACP	forward LpxA reaction
2	LpxA_reverse	P1 + ACP -> UDP-GlcNac + Beta-hydroxymyristoylACP	reverse LpxA reaction
3	LpxC	P1 -> P2	LpxC catalysis step which represents the committed reaction in lipid A synthesis
4	LpxC_translate	promoter-LpxC -> promoter-LpxC + LpxC	translation of LpxC from the promoter. This approach combines transcription, translation, and any translocation into a single reaction step
5	LpxC_degrade	LpxC ->	The degradation of LpxC that is not catalysed by FtsH
6	LpxH	P3 -> P4	LpxH catalytic step
7	LpxB	P3 + P4 -> lipidAdisaccharide	LpxB catalytic step
8	LpxK	lipidAdisaccharide -> P6	LpxK catalytic step
9	KdtA_translate	promoter-KdtA -> promoter-KdtA + KdtA	translation of WaaA from the promoter. This approach also combines transcription, translation, and any translocation into a single reaction step
10	KdtA_degrade	KdtA ->	The degradation of WaaA that is not catalysed by FtsH
11	KdtA	CMP-KDO + P6 -> P7	WaaA catalytic step
12	LpxL	P7 -> P8 + ACP	LpxL catalytic step
13	LpxM	P8 -> lipidA + ACP	LpxM catalytic step
14	MsbA	lipidA -> lipidA_OM	translocation of lipid A in the inner membrane by MsbA

15	LpxC_proteolysis	LpxC + FtsH_act_lpxc -> FtsH_act_lpxc	FtsH-dependent LpxC degradation
16	FtsH_activate_LpxC	FtsH + lipidAdisaccharide -> FtsH_act_lpxc + lipidAdisaccharide	activation of FtsH by lipid A disaccaharide towards LpxC degradation
17	FtsH_activate_KdtA	FtsH + lipidA -> FtsH_act_kdta + lipidA	activation of FtsH towards WaaA degradation. The activator is lipid A in the inner membrane prior to translocation by MsbA
18	KdtA_proteolysis	KdtA + FtsH_act_kdta -> FtsH_act_kdta	FtsH-dependent WaaA degradation
19	LpxD	P2 + Beta-hydroxymyristoylACP -> P3 + ACP	LpxD catalytic step
20	KdtA_alternate	CMP-KDO + lipidA -> lipidA_un	alternate glycosylation by WaaA of lipid A in the inner membrane prior to translocation by MsbA
21	FtsH_inactive_LpxC	FtsH_act_lpxc -> FtsH	inactivation of FtsH-mediated LpxC degradation
22	FtsH_inactive_KdtA	FtsH_act_kdta -> FtsH	inactivation of FtsH-mediated WaaA degradation
23	FabA_C10	b-oh-10 = trans-10	FabA catalysis of its 10-carbon substrate. Reversible reaction
24	FabZ_C10	b-oh-10 = trans-10	FabZ catalysis of its 10-carbon substrate. Reversible reaction
25	FabA_isomerase	trans-10 = C10:1	FabA isomerase reaction of *trans*-2-decenoyl-ACP which represents the first step in UFAs synthesis. Reversible reaction
26	FabI_C10	trans-10 -> C10	FabI catalysis of its 10-carbon substrate
27	FabI_C14	trans-14 -> C14	FabI catalysis of its 14-carbon saturated

			acyl substrate
28	FabB_C12:1	C12:1 = ketoacyl-14:1	FabB catalysis of its 12-carbon *cis*-unsaturated acyl substrate. Reversible reaction
29	FabG_C14:1	ketoacyl-14:1 = B-OH-14:1	FabG catalysis of its 14-carbon *cis*-unsaturated acyl substrate. Reversible reaction
30	FabZ_C14:1	B-OH-14:1 = trans-14:1	FabZ catalysis of its 14-carbon *cis*-unsaturated acyl substrate. Reversible reaction.
31	FabI_C14:1	trans-14:1 -> C14:1	FabI catalysis of its 14-carbon *cis*-unsaturated acyl substrate
32	FabB_C10	C10 = ketoacyl-12	FabB catalysis of its 10-carbon saturated acyl substrate. Reversible reaction
33	FabF_C10	C10 = ketoacyl-12	FabF catalysis of its 10-carbon saturated acyl substrate. Reversible reaction
34	FabG_C12	ketoacyl-12 = B-OH-12	FabG catalysis of its 12-carbon saturated acyl substrate. Reversible reaction
35	FabA_C12	B-OH-12 = trans-12	FabA catalysis of its 12-carbon saturated acyl substrate. Reversible reaction
36	FabZ_C12	B-OH-12 = trans-12	FabZ catalysis of its 12-carbon saturated acyl substrate. Reversible reaction
37	FabI_C12	trans-12 -> C12	FabI catalysis of its 12-carbon saturated acyl substrate
38	FabB_C10:1	C10:1 = ketoacyl-12:1	FabB catalysis of *cis*-3-decenoyl-ACP. Reversible reaction
39	FabG_C12:1	ketoacyl-12:1 = B-OH-12:1	FabG catalysis of its 12-carbon *cis*-unsaturated acyl substrate. Reversible reaction
40	FabZ_C12:1	B-OH-12:1 = trans-12:1	FabZ catalysis of its 12-carbon *cis*-unsaturated acyl substrate. Reversible

			reaction.
41	FabI_C12:1	trans-12:1 -> C12:1	FabI catalysis of its 12-carbon *cis*-unsaturated acyl substrate
42	FabB_C12	C12 = ketoacyl-14	FabB catalysis of its 12-carbon saturated acyl substrate. Reversible reaction
43	FabF_C12	C12 = ketoacyl-14	FabF catalysis of its 12-carbon saturated acyl substrate. Reversible reaction
44	FabG_C14	ketoacyl-14 = Beta-hydroxymyristoylACP	FabG catalysis of its 14-carbon saturated acyl substrate. Reversible reaction
45	FabA_C14	Beta-hydroxymyristoylACP = trans-14	FabA catalysis of its 14-carbon saturated acyl substrate. Reversible reaction
46	FabZ_C14	Beta-hydroxymyristoylACP = trans-14	FabZ catalysis of its 14-carbon saturated acyl substrate. Reversible reaction
47	FabB_C14	C14 = ketoacyl-16	FabB catalysis of its 14-carbon saturated acyl substrate. Reversible reaction
48	FabA_C16	B-OH-16 = trans-16	FabA catalysis of its 16-carbon saturated acyl substrate. Reversible reaction
49	FabZ_C16	B-OH-16 = trans-16	FabZ catalysis of its 16-carbon saturated acyl substrate. Reversible reaction
50	FabI_C16	trans-16 -> C16	FabI catalysis of its 16-carbon saturated acyl substrate
51	FabB_C14:1	C14:1 = ketoacyl-16:1	FabB catalysis of its 14-carbon *cis*-unsaturated acyl substrate. Reversible reaction.
52	FabF_C14:1	C14:1 = ketoacyl-16:1	FabF catalysis of its 14-carbon *cis*-unsaturated acyl substrate. Reversible reaction.
53	FabG_C16:1	ketoacyl-16:1 = B-OH-16:1	FabG catalysis of its 16-carbon *cis*-unsaturated acyl substrate. Reversible reaction.
54	FabZ_C16:1	B-OH-16:1 = trans-16:1	FabZ catalysis of its 16-carbon *cis*-

			unsaturated acyl substrate. Reversible reaction.
55	FabI_C16:1	trans-16:1 -> C16:1	FabI catalysis of its 16-carbon *cis*-unsaturated acyl substrate.
56	FabF_C14	C14 = ketoacyl-16	FabF catalysis of its 14-carbon saturated acyl substrate. Reversible reaction.
57	FabG_C16	ketoacyl-16 = B-OH-16	FabG catalysis of its 16-carbon saturated acyl substrate. Reversible reaction
58	FabF_C16:1	C16:1 = ketoacyl-18:1	FabF catalysis of its 16-carbon *cis*-unsaturated acyl substrate. Reversible reaction.
59	FabG_C18:1	ketoacyl-18:1 = B-OH-18:1	FabG catalysis of its 18-carbon *cis*-unsaturated acyl substrate. Reversible reaction.
60	FabZ_C18:1	B-OH-18:1 = trans-18:1	FabZ catalysis of its 18-carbon *cis*-unsaturated acyl substrate. Reversible reaction.
61	FabI_C18:1	trans-18:1 -> C18:1	FabI catalysis of its 18-carbon *cis*-unsaturated acyl substrate.
62	PlsB_C16	C16 + G3P -> palmitic	condensation of palmitoyl-ACP with glycerol-3-phosphate by PlsB
63	PlsB_C18:1	C18:1 + G3P -> vaccenic	condensation of *cis*-vaccenoyl-ACP with glycerol-3-phosphate by PlsB
64	PlsC_C16:1	C16:1 + G3P -> palmitoleic	condensation of palmitoleoyl-ACP with glycerol-3-phosphate by PlsC
65	PlsC_C18:1	C18:1 + G3P -> vaccenic	condensation of *cis*-vaccenoyl-ACP with glycerol-3-phosphate by PlsC
66	ACTIVATION_LpxK	LpxK = LpxK_act	catalytic activation and inactivation of LpxK by UFAs (*see screenshot in Fig. S9*)
67	FabA_constitutive_expression	proA_unreg -> proA_unreg + FabA	expresssion of *fabA* from the constitutive promoter

68	FabA_regulated_expression	FadR/proA -> FabA + FadR/proA	expresssion of *fabA* from the regulated promoter resulting from FadR binding to the DNA
69	FabA_repression_by_FabR_1	proA = inact_proA1	inactivation of the regulated *fabA* promoter by FabR
70	FabA_degradation	FabA ->	degradation of FabA
71	FabR_activation	FabR = FabR*	activation and inactivation of FabR
72	FabA_promoter_activation	proA = FadR/proA	binding of FadR to the *fabA* DNA to activate expression (*see screenshot in Fig. S10*)
73	FabA_repression_by_FabR_2	FadR/proA = inact_proA2	inactivation by FabR of the regulated *fabA* promoter already bound to FadR
74	FabH	acetyl-CoA -> b-oh-10	initiation of fatty acids synthesis by FabH
75	FadR_activation	FadR = FadR*	activation and inactivation of FadR
76	FabB_constitutive_expression	proB_unreg -> proB_unreg + FabB	expresssion of *fabB* from the constitutive promoter
77	FabB_degradation	FabB ->	degradation of FabB
78	FabB_promoter_activation	proB = FadR/proB	binding of FadR to the *fabB* DNA to activate expression (*see screenshot in Fig. S10*)
79	FabB_regulated_expression	FadR/proB -> FabB + FadR/proB	expresssion of *fabB* from the regulated promoter resulting from FadR binding to the DNA
80	FabB_repression_by_FabR1	proB = inact_proB1	inactivation of the regulated *fabB* promoter by FabR
81	FabB_repression_by_FabR_2	FadR/proB = inact_proB2	inactivation by FabR of the regulated *fabB* promoter already bound to FadR

Figure S9. Screenshots explaining reaction 66 in the COPASI file. (A) The catalytic activation of LpxK was modelled using reversible mass-action kinetics in which the forward and reverse rate constants represented the activation and inactivation rates respectively. The activation rate constant (B) and inactivation rate constant (C) were made pre-defined global quantities in COPASI using eq. 22 in Chapter 3. These global quantities were then recalled for use as rate constants as pictured in 'A'.

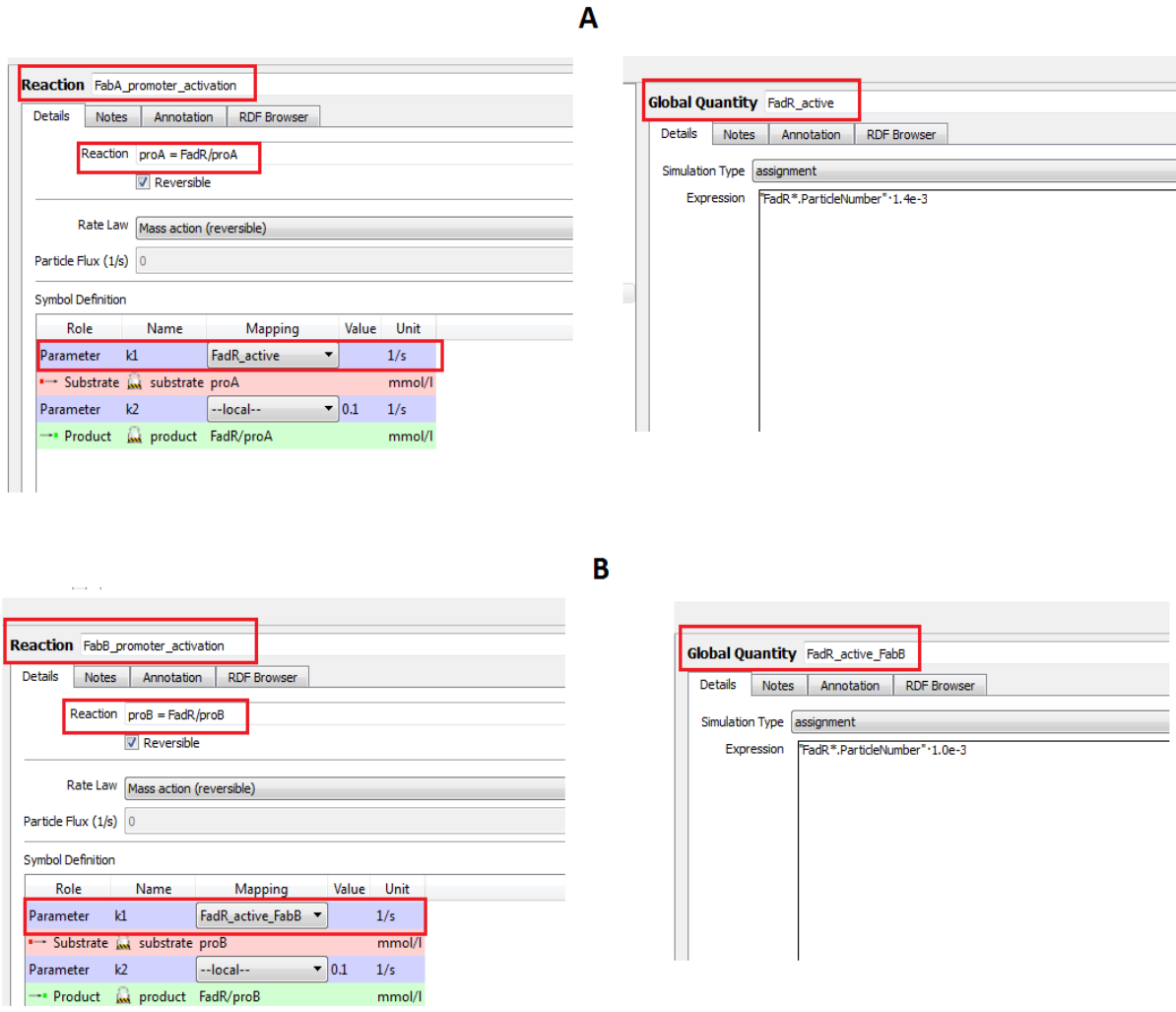

Figure S10. Screenshots explaining reactions 72 and 78 in the COPASI file. The rationale is same as in Fig. S9 above. (A) The activation of *fabA* promoter by FadR was modelled using reversible mass-action kinetics in which the forward and reverse rate constants represented the activation and inactivation rates respectively. The FadR activation rate was made a pre-defined global quantity in COPASI using eq. 16 in Chapter 3. As in Fig. S9, the global quantity was recalled for use as rate constant. (B) Activation of *fabB* promoter. Conditions are same as 'A' above.